TRANSLATION

JOURNAL OF APPLIED MECHANICS AND TECHNICAL PHYSICS

(COLLECTION OF ARTICLES)

FOREIGN TECHNOLOGY DIVISION

AIR FORCE SYSTEMS COMMAND

WRIGHT-PATTERSON AIR FORCE BASE

OHIO

EDITED MACHINE TRANSLATION

JOURNAL OF APPLIED MECHANICS AND TECHNICAL PHYSICS (COLLECTION OF ARTICLES)

English Pages: 339

Insert: TT-63-1033

S/0207/063/000/003

PREPARED BY:

TRANSLATION DIVISION
FOREIGN TECHNOLOGY DIVISION
WP-AFB, OHIO.

Akademiya Nauk SSSR – Sibirskoye Otdeleniye

PMTF

ZHURNAL PRIKLADNOY MEKHANIKI I TEKHNICHESKOY FIZIKI

No. 3

May – Iyun'

1963

Izdatel'stvo "Nauka"

Pages: 1-168

BLANK PAGE

TABLE OF CONTENTS

U. S. BOARD ON GEOGRAPHIC NAMES TRANSLITERATION SYSTEM

Block	Italic	Transliteration	Block	Italic	Transliteration
А а	*А а*	A, a	Р р	*Р р*	R, r
Б б	*Б б*	B, b	С с	*С с*	S, s
В в	*В в*	V, v	Т т	*Т т*	T, t
Г г	*Г г*	G, g	У у	*У у*	U, u
Д д	*Д д*	D, d	Ф ф	*Ф ф*	F, f
Е е	*Е е*	Ye, ye; E, e*	Х х	*Х х*	Kh, kh
Ж ж	*Ж ж*	Zh, zh	Ц ц	*Ц ц*	Ts, ts
З з	*З з*	Z, z	Ч ч	*Ч ч*	Ch, ch
И и	*И и*	I, i	Ш ш	*Ш ш*	Sh, sh
Й й	*Й й*	Y, y	Щ щ	*Щ щ*	Shch, shch
К к	*К к*	K, k	Ъ ъ	*Ъ ъ*	"
Л л	*Л л*	L, l	Ы ы	*Ы ы*	Y, y
М м	*М м*	M, m	Ь ь	*Ь ь*	'
Н н	*Н н*	N, n	Э э	*Э э*	E, e
О о	*О о*	O, o	Ю ю	*Ю ю*	Yu, yu
П п	*П п*	P, p	Я я	*Я я*	Ya, ya

* ye initially, after vowels, and after ъ, ь; e elsewhere. When written as ё in Russian, transliterate as yё or ё. The use of diacritical marks is preferred, but such marks may be omitted when expediency dictates.

FOLLOWING ARE THE CORRESPONDING RUSSIAN AND ENGLISH

DESIGNATIONS OF THE TRIGONOMETRIC FUNCTIONS

Russian	English
sin	sin
cos	cos
tg	tan
ctg	cot
sec	sec
cosec	csc
sh	sinh
ch	cosh
th	tanh
cth	coth
sch	sech
csch	csch
arc sin	$\sin^{-1}$
arc cos	$\cos^{-1}$
arc tg	$\tan^{-1}$
arc ctg	$\cot^{-1}$
arc sec	$\sec^{-1}$
arc cosec	$\csc^{-1}$
arc sh	$\sinh^{-1}$
arc ch	$\cosh^{-1}$
arc th	$\tanh^{-1}$
arc cth	$\coth^{-1}$
arc sch	sech^{-1}
arc csch	csch^{-1}
rot	curl
lg	log

MT-64-85
Journal of Applied Mechanics and
Technical Physics, Vol. 3,
May-June, 1963.
Pages: Cover-168.

ENERGY-MOMENTUM TENSOR OF RADIATION IN A MOVING MEDIUM UNDER CONDITIONS CLOSE TO EQUILIBRIUM

V. S. Imshennik and Yu. I. Morozov
(Moscow)

In a system of equations of hydrodynamics at high temperatures there must be included terms taking into account the role of radiation, and also an equation describing the transfer of radiation.

Thus, it is possible to arrive at equations of radiation hydrodynamics. Basic question, which is solved here consists in formulation of relativistics of the covariant kinetic equation of the transfer of radiation with a taking into account of the motion in the medium. The most important contribution to this question was made by Thomas [1] and Synge [2]. The system of equations of radiation hydrodynamics for a general relativistic case was written out by Prokof'yev [3] (in the same place there is given a list of the literature). Inherently, the equations describing the motion in medium include radiation in the form of a divergence of the energy-momentum tensor of radiation. In general, the form of this tensor is very complex and it is necessary to analyze jointly equations of the medium and the equation of transfer of radiation.

However, under conditions close to equilibrium it is possible to calculate this tensor by successive approximations and subsequently to analyze general equations being obtained from sum of tensors of the medium and of the radiation. Such a procedure very greatly simplifies problem of radiation hydrodynamics. If we were limited to the second approximation in calculating the energy-momentum tensor (to consider the linear terms according to gradients of the hydrodynamic magnitudes) then we shall have obtained a generalization of the well-known astrophysical approximation of the radiant thermoconductivity with the introduction of the Rosseland mean [4, 5]. In present work there is calculated the energy-momentum tensor of radiation in this approximation.

Previously, this tensor was calculated by Thomas [1], but the procedure of his calculation is nonstandard and results in very cumbersome integrals. The basis of our method of calculation will be the calculation of the energy-momentum tensor of radiation at first in the inherent system of reference and then its transformation to a fixed system of reference by formulas in the Calculus of Tensors. Preliminarily we shall present necessary formulas of relativistic transformations and the basic relativistically covariant equation of radiation transfer with brief conclusion.

§ 1. Relativistically Covariant Equation of Radiation Transfer Which Takes Into Account the Motion in the Medium

Let us assume that in a given system of coordinates S (it has the sense of being interpreted as fixed) the speed of motion of matter is arbitrary both in direction and also in magnitude at each point of space **r** and at each moment of time t. We shall write out the Lorentz transformation in vector form. Let us assume that as usual,

$$\mathbf{r}_{\parallel}' = \theta(\mathbf{r}_{\parallel} + \mathbf{q}t), \qquad \mathbf{r}_{\perp}' = \mathbf{r}_{\perp}, \qquad t' = \theta\left(t + \frac{\mathbf{q}\cdot\mathbf{r}}{c^2}\right). \tag{1.1}$$

Here

$$\mathbf{r}_{\parallel} = \frac{\mathbf{q}\cdot\mathbf{r}}{q^2}\mathbf{q}, \quad \mathbf{r}_{\perp} = \mathbf{r} - \mathbf{r}_{\parallel}, \quad \theta = \frac{1}{\sqrt{1-\beta^2}}, \quad \beta = \frac{q}{c}$$

System of reference S' is moved relative to system of reference S with a speed $-\mathbf{q}$. If we substitute $\mathbf{r}_{\parallel}$ and $\mathbf{r}_{\perp}$ in (1.1) then we shall obtain the sought form:

$$\mathbf{r}' = \mathbf{r} + (\theta - 1)\frac{\mathbf{q}\cdot\mathbf{r}}{q^2}\mathbf{q} - \theta\mathbf{q}t, \qquad t' = \theta\left(t - \frac{\mathbf{q}\cdot\mathbf{r}}{c^2}\right) \tag{1.2}$$

From the invariance of the phase $2\pi i(\mathbf{k}\cdot\mathbf{r} - \nu t)$ it follows that

$$\mathbf{K} = \left\{\mathbf{k}; i\frac{\nu}{c}\right\} = \left\{\frac{\nu}{c}\mathbf{l}; i\frac{\nu}{c}\right\}$$

will be a 4-vector which is transformed by the formulas $K_i' = (\partial x_i'/\partial x_l)K_l$, where elements of matrix of the transformation $\partial x_i'/\partial x_l$ are from (1.2) with replacement of t for $\tau = ict$. Thus, we shall obtain

$$\frac{\nu'}{\nu}\mathbf{I}' = \frac{\nu}{\nu}\left[\mathbf{I} + (\theta - 1)\frac{\mathbf{q}\cdot\mathbf{I}}{q^2}\mathbf{q} + \frac{\mathbf{q}}{c}\theta\right], \quad i\frac{\nu'}{c} = i\frac{\nu}{c}\eta\left[1 - \frac{\mathbf{q}\cdot\mathbf{I}}{c}\right] \tag{1.3}$$

We introduce the designation

$$L = \theta\left[1 + \frac{\mathbf{q}\cdot\mathbf{I}}{c}\right] \tag{1.4}$$

Then equality (1.3) will acquire the form,

$$\nu' = \nu L, \quad \mathbf{I}' = \frac{1}{L}\left[\mathbf{I} + (\theta - 1)\frac{\mathbf{q}\cdot\mathbf{I}}{q^2}\mathbf{q} + \frac{\mathbf{q}}{c}\eta\right]. \tag{1.5}$$

By means of these formulas we find that in system of reference S'

$$L = \frac{1}{\theta(1 - \mathbf{q}\cdot\mathbf{I}'/c)} \tag{1.6}$$

The relationship between elements of solid angles and frequencies in both systems of reference is established by differentiation (1.6) with q = const and (1.5) with L = const respectively:

$$d\omega' = \frac{1}{L^2}d\omega, \qquad d\nu' = Ld\nu \tag{1.7}$$

We shall express the intensity of radiation $I'_{\nu'}$ in system of reference S' in terms of intensity of radiation I_ν in system of reference S, proceeding from corpuscular interpretation of radiation transfer theory. Let us assume that in S' the quiescent area dS' is located perpendicular to **q**. The number of quanta of radiation with frequency from ν' to $\nu' + d\nu'$, passing through this area during the time dt' at an angle φ' to the normal within the solid angle $d\omega'$, is proportional to

$$\frac{I'_{\nu'}}{\nu'}dS'd\nu'dt'd\omega'\frac{\mathbf{I}'\cdot\mathbf{q}}{q} \tag{1.8}$$

This must coincide with number of quanta calculated in the system S:

$$\frac{I_\nu}{\nu}dS\,d\nu\,dt\,d\omega\frac{\mathbf{I}\cdot\mathbf{q}}{q} = \frac{I_\nu}{\nu}\frac{q}{c}dS\,d\nu\,dt\,d\omega \tag{1.9}$$

Here the element of the area dS is perpendicular to q and rests in system of reference S', where dS' = dS; the second term is the number of quanta of given type included in the volume dS q dt. Equating (1.9) and (1.8) by means of (1.4)-(1.7) and the equation of the inherent time $dt' = \theta^{-1}dt$ in S' (the latter may be obtained from (1.2) with dr' = 0), we find:

$$I'_\nu = L^2 I_\nu \tag{1.10}$$

Using (1.5), it is possible to present (1.10) in the form of the invariant

$$\frac{I'_\nu}{\nu'^3} = \frac{I_\nu}{\nu^3} = \text{inv}. \tag{1.11}$$

Hence it is evident that I_ν/ν^3 with an accuracy up to a constant factor is the Lorentz- invariant function of the distribution of photons [2, 3].

The equation of radiation transfer may be immediately written in system of reference S. On the basis of balance of energy

$$(1/c)\dot{I}_\nu + \mathbf{l}\cdot\nabla I_\nu = -\rho k_\nu I_\nu - \rho\sigma_\nu I_\nu + \rho\varepsilon_\nu - \\ + \int_0^\infty \rho\sigma_{\nu_1}\frac{d\nu_1}{\nu_1^3}\int_{(4\pi)} I_{\nu_1}(r, \mathbf{l}_1, t)\,\Omega(\nu_1, \nu; \mathbf{l}_1, \mathbf{l}, r, t)\,d\omega_1 \tag{1.12}$$

In this equation there are considered processes of absorption, scattering and emission of radiation (mass coefficients of absorption, scattering and radiation respectively are equal to k_ν, σ_ν and ε_ν; Ω is the nucleus of integral term of scattering into a given beam reverting to unity with the coherence and isotropism of the scattering).

We shall establish the relation between the phenomenological coefficients k_ν, σ_ν ε_ν and Ω with atomic constants of interaction of radiation with matter. For this purpose first of all we shall analyze the transformation properties of the operator

$$\frac{1}{c}\frac{\partial}{\partial t} + \mathbf{l}\cdot\nabla$$

There is readily calculated from (1.2):

$$\frac{1}{c}\frac{\partial}{\partial t} + \mathbf{q}\left[\frac{1}{c}\frac{\partial}{\partial t'} + \frac{\mathbf{q}\cdot\nabla'}{c}\right], \mathbf{l}\cdot\nabla = \mathbf{l}\cdot\left[\nabla' + (\mathbf{q}-\mathbf{l})\frac{\mathbf{q}}{q^2}\,\mathbf{q}\cdot\nabla' + \frac{1}{c}\left[\mathbf{q}\,\frac{\partial}{\partial t'}\right]\right] \qquad (1.13)$$

If then in the right hand side of these formulas we substitute $\mathbf{l}$ in terms of $\mathbf{l}'$ using for this purpose the inversion of formula (1.5) (the simultaneous substitution of $\mathbf{l}$ for $\mathbf{l}'$ and $\mathbf{q}$ for $-\mathbf{q}$, including also in L), and then add both operator ratios, then we shall find

$$\frac{1}{c}\frac{\partial}{\partial t} + \mathbf{l}\cdot\nabla = L\left[\frac{1}{c}\frac{\partial}{\partial t'} + \mathbf{l}'\cdot\nabla'\right] \qquad (1.14)$$

or, according to (1.5), in invariant form:

$$\nu\left[\frac{1}{c}\frac{\partial}{\partial t} + \mathbf{l}\cdot\nabla\right] = \nu'\left[\frac{1}{c}\frac{\partial}{\partial t'} + \mathbf{l}'\cdot\nabla'\right] = \mathrm{inv} \qquad (1.15)$$

By means of the invariants (1.11)-(1.15) we shall transform the equation of transfer (1.12) into the system of reference S'. For this purpose we shall multiply it by $1/\nu^2$ and form the already obtained invariants:

$$\nu\left[\frac{1}{c}\frac{\partial}{\partial t} + \mathbf{l}\cdot\nabla\right]\frac{I_\nu}{\nu^3} = -(\rho k,\nu)\frac{I_\nu}{\nu^3} - (\rho\sigma,\nu)\frac{I_\nu}{\nu^3} +$$
$$+\left(\frac{\rho\varepsilon_\nu}{\nu^2}\right) + \frac{1}{4\pi}\int_0^\infty\int_{(4\pi)}(\rho\sigma_{\nu_1},\nu_1)\frac{I_{\nu_1}}{\nu_1^3}\left(\frac{\nu_1\Omega(\nu_1,\nu,\mathbf{l}_1,\mathbf{l},r,t)}{\nu^2}\right)\nu_1 d\nu_1 d\omega_1, \qquad (1.16)$$

Under integral here there also is separated the invariant $\nu_1 d\nu_1 d\omega_1$, ensuing from (1.5) and (1.7). Equation (1.16) has a relativistically covariant form. In parentheses there are included the new invariant expressions which are evident from the invariance of the left-hand side of (1.16) and the co-factors of these expressions. Thus, in system of reference S' we have,

$$\nu'\left[\frac{1}{c}\frac{\partial}{\partial t'}+\mathbf{l}'\cdot\nabla'\right]\frac{I'_{\nu'}}{\nu'^3}=-(\rho'k'_{\nu'}\nu')\frac{I'_{\nu'}}{\nu'^3}-(\rho'\sigma'_{\nu'}\nu')\frac{I'_{\nu'}}{\nu'^3}$$
$$+\left(\frac{\rho'\varepsilon'_{\nu'}}{\nu'^3}\right)+\frac{1}{4\pi}\int_0^{\infty}\int_{(4\pi)}(\rho'\sigma'_{\nu'}\nu'_1)\frac{I'_{\nu'_1}}{\nu'^3_1}\frac{\nu'_1\Omega'(\nu'_1,\nu';\mathbf{l}'_1,\mathbf{l}',\mathbf{r}',t')}{\nu'^3}\nu'^2_1\,d\nu'_1\,d\omega'_1 \qquad (1.17)$$

We note that it no longer is possible to take $1/\nu'^3$ out from the sign of the differentiation if by S' we infer the inherent system of reference at each point of space and at any moment of time. We shall write out the four new invariant expressions :

$$\rho k_{\nu}\nu=\rho'k'_{\nu'}\nu'=\text{inv},\qquad \rho\frac{\varepsilon_{\nu}}{\nu^3}=\rho'\frac{\varepsilon'_{\nu'}}{\nu'^3}=\text{inv}$$
$$\rho\sigma_{\nu}\nu=\rho'\sigma'_{\nu'}\nu'=\text{inv},\qquad \frac{\nu_1\Omega(\nu_1,\nu;\mathbf{l}_1,\mathbf{l},\mathbf{r},t)}{\nu^3}=\frac{\nu'_1\Omega'(\nu'_1,\nu';\mathbf{l}'_1,\mathbf{l}',\mathbf{r}',t')}{\nu'^3}=\text{inv} \qquad (1.18)$$

Then, if S' is the inherent system of reference, we shall assume $\mathbf{q} = -\mathbf{v}$, where $\mathbf{v}$ is the local macroscopic speed of matter, and we shall replace the primes by the subsscript zero. Then by means of (1.18) we shall express phenomenological coefficients of equation (1.12) in terms of atomic constants of the interaction of radiation with matter

$$\rho k_{\nu}=L\rho_0 k_{\nu_0}^{\circ},\qquad \rho\varepsilon_{\nu}=\frac{L}{L_1}\rho_0\varepsilon_{\nu_0}^{\circ},\qquad \rho\sigma_{\nu}=L\rho_0\sigma_{\nu_0}^{\circ}$$
$$\Omega(\nu_1,\nu;\mathbf{l}_1,\mathbf{l},\mathbf{r},t)=\frac{L_1}{L^3}\Omega_0(\nu_{10},\nu_0;\mathbf{l}_{10},\mathbf{l}_0,\mathbf{r}_0,t_0) \qquad (1.19)$$

Expressions L in (1.19) may be written out according to (1.4) and (1.6) (for L_1 the expressions are analogous):

$$L=\frac{1}{\delta(1+\mathbf{v}\cdot\mathbf{l}/c)}=\delta\left(1-\frac{\mathbf{v}\cdot\mathbf{l}}{c}\right) \qquad (1.20)$$

Thus, in the most general case the process of radiation transfer in a moving medium may be described in fixed system of reference by the equation of transfer (1.12) together with relationships (1.19).

In the inherent system of reference S', designated as S_0, there occurs the equation (1.17). Here it must be specified that ν' ($= \nu_0$) depends on $\mathbf{r}'$ ($= \mathbf{r}_0$) and t' ($= t_0$).

§ 2. Energy-Momentum Tensor of Radiation in the Inherent System of Reference

We shall write out the system of equations of an ideal medium taking into account the interaction with radiation [1, 6, 7]

$$\frac{\partial T_{ik}}{\partial x_k} = F_i, \quad T_{ik} = (p+\varepsilon)u_i u_k + p\delta_{ik}, \quad \frac{\partial(\rho_0 u_i)}{\partial x_i} = 0 \tag{2.1}$$

Here p is the scalar pressure in medium, ε is the internal energy taking into account energy of rest relative to unit of volume in the inherent system of reference, ρ_0 is the density of medium in the inherent system of reference.

The first of equations (2.1), which constitutes the law of conservation of the energy-momentum of a medium which takes radiation into account, contains on the right-hand side the 4-vector F_i, describing the exchange with radiation by the energy-momentum. The energy-momentum tensor of medium T_{ik} is expressed in terms of the 4-speed

$$u_\alpha = \frac{v_\alpha}{c\sqrt{1-v^2/c^2}} \quad (\alpha = 1, 2, 3), \qquad u_4 = \frac{i}{\sqrt{1-v^2/c^2}} \tag{2.2}$$

The latter equation (2.1) constitutes the law of conservation of number of particles in a medium. It is readily understood that the 4-vector F_i may be in following manner expressed in terms of characteristics of the radiation:

$$F_\alpha = \frac{1}{c}\int\int (\rho k_\nu I_\nu - \rho\varepsilon_\nu) l_\alpha d\nu d\omega, \qquad F_4 = -\frac{1}{ic}\int\int (\rho k_\nu I_\nu - \rho\varepsilon_\nu) d\nu d\omega \tag{2.3}$$

Here intensity of radiation I_ν satisfies the equation of transfer (1.12) in fixed system of reference; l_α is the direction cosine of beam. Henceforth, we shall be limited to the case, when scattering of

radiation in the medium can be ignored. Coefficients of absorption and emission of radiation are determined from relationships (1.19) with a consideration of (1.20). On the other hand, F_i by means of equation of transfer (1.12) may be presented as the divergence of energy-momentum tensor of radiation :

$$F_i = -\frac{\partial W_{ik}}{\partial x_k} \tag{2.4}$$

$$W_{\alpha\beta} = \frac{1}{c}\iint l_\alpha l_\beta I_\nu \, d\nu \, d\omega, \quad W_{\alpha 4} = \frac{i}{c}\iint l_\alpha I_\nu \, d\nu \, d\omega, \quad W_{44} = -\frac{1}{c}\iint I_\nu \, d\nu \, d\omega \tag{2.5}$$

The proof of tensor character of magnitude W_{ik} is made very simply and directly, if there are used the matrix of the transformation $\partial x_i'/\partial x_k$ and relationships (1.5), (1.7) and (1.10). However, even without this by determining I_ν the magnitudes

$$K_{\alpha\beta} = \frac{1}{c}\iint l_\alpha l_\beta I_\nu \, d\nu \, d\omega, \quad S_\alpha = \iint l_\alpha I_\nu \, d\nu d\omega, \quad U = \frac{1}{c}\iint I_\nu \, d\nu \, d\omega$$

are components of momentum flow of radiation, components of the flux of energy of radiation and the density of energy of radiation respectively.

According to general properties of an energy momentum tensor valid for an arbitrary physical system [6]

$$W_{\alpha\beta} = K_{\alpha\beta}, \quad W_{\alpha 4} = (i/c)S_\alpha, \quad W_{44} = -U.$$

The magnitudes of W_{ik} from (2.5) satisfy these relationships. Law of conservation of energy-momentum of medium with the radiation (2.1) can be presented in the form

$$\frac{\partial}{\partial x_k}(T_{ik} + W_{ik}) = 0 \tag{2.6}$$

Now let us turn to calculation of tensor of W_{ik} under almost equilibrium conditions, i.e., when characteristic length of range of radiation in a medium is less than the scale of variation of

thermodynamic magnitudes p, ε, ρ_0 and speed of medium **v**. At first we shall calculate W_{ik} in the inherent system of reference S_0, which is significantly simpler. From equation (1.12) as a second approximation, ignoring the scattering and taking into consideration (1.19) we shall obtain

$$I_\nu = \frac{\varepsilon_\nu}{k_\nu} - \frac{1}{\rho k_\nu}\left[\frac{1}{c}\frac{\partial}{\partial t} + \mathbf{l}\cdot\nabla\right]\frac{\varepsilon_\nu}{k_\nu} = \frac{1}{L^3}B_\nu - \frac{1}{L\rho k_\nu c}\left[\frac{1}{c}\frac{\partial}{\partial t} + \mathbf{l}\cdot\nabla\right]\frac{1}{L^3}B_\nu \qquad (2.7)$$

In the inherent system of reference Kirchhoff's law $\varepsilon_{\nu_0}{}^{\circ}/k_{\nu_0}{}^{\circ} = B_{\nu_0}$ is assumed valid [4, 5]. In order to find I_ν in the inherent system of reference it is necessary to identify the fixed system of reference with the inherent system of reference at a given point of space **r** and at given moment of time t. For this purpose (2.7) we shall assume **v** = 0, with the exception of expressions, subject to differentiation (here we take into consideration that ν_0 depends on **v**). Then from (2.7) substituting from (1.20) and remembering that

$$B_{\nu_0} \sim \frac{\nu_0^3}{\exp(h\nu_0/kT) - 1}$$

we shall find

$$I_{\nu_0} = B_{\nu_0} - \frac{1}{\rho k_{\nu_0}} \cdot \frac{\partial B_{\nu_0}}{\partial T}\left\{\left[\frac{1}{c}\frac{\partial}{\partial t_0} + \mathbf{l}_0\cdot\nabla_0\right]T - \frac{T}{c}\left[\mathbf{l}_0\left(\frac{1}{c}\frac{\partial}{\partial t_0} + \mathbf{l}_0\cdot\nabla_0\right)\mathbf{v}_0\right]\right\} \qquad (2.8)$$

Here there is used the circumstance that under the sign of differentiation the given constant is $\nu = \nu_0/L$ (see (1.5)). This formula for intensity of radiation I_{ν_0} can be obtained otherwise proceeding from equation of transfer (1.17) pertaining to the inherent system of reference (scattering will be ignored). As a second approximation from (1.17) we have

$$I_{\nu_0} = B_{\nu_0} - \frac{\nu_0^3}{\rho k_{\nu_0} c}\left[\frac{1}{c}\frac{\partial}{\partial t_0} + \mathbf{l}_0\cdot\nabla_0\right]B_{\nu_0} \qquad (2.9)$$

This again results in (2.8), if we assume $\nu_0 = \nu L$ and in expression for L we assume $\mathbf{v} = 0$ outside the sign of differentiation. Thus, $I^{\circ}_{\nu_0} = I_{\nu_0}$ which is natural, inasmuch as both systems of reference are identical to each other. It must be noted that magnitude $\mathbf{v}_0$ in (2.8) pertains to the inherent system of reference. Then the expression I_{ν_0} we shall substitute in (2.5) and shall calculate by means of integration over the frequency and directions the tensor of W°_{ik} in the inherent system of reference. We shall introduce the designation of Rosselands' mean

$$\frac{1}{\varkappa} = \left(\frac{dB_0}{dT}\right)^{-1} \int_0^{\infty} \frac{1}{k_{\nu_0}} \frac{\partial B_{\nu_0}}{\partial T} d\nu_0, \qquad B_0 = \int_0^{\infty} B_{\nu_0} d\nu_0 \tag{2.10}$$

By means of this formula in all elements of W_{ik}° there is made an integration of I_{ν_0} from (2.8) with respect to frequency

$$\int_0^{\infty} I_{\nu_0} d\nu_0 = B_0 - \frac{1}{\rho\varkappa} \frac{dB_0}{dT} \left[\left(\frac{1}{c} \frac{\partial}{\partial t_0} + \mathbf{l}_0 \cdot \nabla_0 \right) T + \frac{T}{c} \mathbf{l}_0 \left(\frac{1}{c} \frac{\partial}{\partial t_0} + \mathbf{l}_0 \nabla_0 \right) \mathbf{v}_0 \right] \tag{2.11}$$

The remaining integration over the solid angle gives

$$\begin{aligned} W_{\alpha\beta}^{\circ} &= \delta_{\alpha\beta} \frac{4\pi}{3c} B_0 - \frac{4\pi}{c\rho\varkappa} \frac{dB}{dT} \left[\frac{1}{3c} \delta_{\alpha\beta} \frac{\partial T}{\partial t_0} + \frac{T}{15c} \left(\frac{\partial v_{0\alpha}}{\partial x_{0\beta}} + \frac{\partial v_{0\beta}}{\partial x_{0\alpha}} + \delta_{\alpha\beta} \nabla_0 \cdot \mathbf{v}_0 \right) \right] \\ W_{\alpha 4}^{\circ} &= -i \frac{4\pi}{c\rho\varkappa} \frac{dB}{dT} \left[\frac{1}{3} \frac{\partial T}{\partial x_{0\alpha}} + \frac{T}{3c^2} \frac{\partial v_{0\alpha}}{\partial t_0} \right] \\ W_{44}^{\circ} &= -\frac{4\pi}{c} B_0 + \frac{4\pi}{c\rho\varkappa} \frac{dB_0}{dT} \left[\frac{1}{c} \frac{\partial T}{\partial t_0} + \frac{T}{3c} \nabla_0 \cdot \mathbf{v}_0 \right] \end{aligned} \tag{2.12}$$

Thus, in (2.12) there are obtained expressions of the energy-momentum tensor of radiation in the inherent system of reference S_0 for an arbitrary point in space and moment of time.

To avoid a misunderstanding, here it must be noted that in the calculation of the tensor of W_{ik}° it is impossible to substitute in integrals (2.5) $I_{\nu_0}^{\circ}$ from the solution of equation (1.17) with $\mathbf{v} \neq 0$. A formal construction of such magnitudes on the basis of the formulas,

of course, can be made. But their aggregate in this case no longer will be a tensor. The difference from a tensor arises only in terms of the second approximation, where the dependence of $\mathbf{v}$ on $\mathbf{r}_0$, t_0, is essential. In the noted circumstance there is reflected the nontrivial character of direct proof of the tensor character of magnitudes of W_{ik} from (2.5), when I_ν satisfies the equation of transfer (1.12) in the fixed system of reference S. In calculating I_{ν_0} by (2.8) there was used the intensity I_ν determined in (2.7) by means of (1.12).

§ 3. Energy-Momentum Tensor of Radiation in a Fixed System of Reference

The equations (2.6) include the tensor of W_{ik} calculated in a fixed system of reference S. The obtained tensor of W^0_{ik} in preceding section may be used now by means of well known formulas of the transformation of tensors [6] to find W_{ik}:

$$W_{ik} = \frac{\partial x_i}{\partial x_i'} \frac{\partial x_k}{\partial x_m'} W^0_{lm} \tag{3.1}$$

System of reference S is moved relative to system of reference S_0 at a speed $-\mathbf{v}$. Therefore, from the formulas of transformation (1.2) we shall obtain expressions for $\mathbf{r}$ and t, replacing $\mathbf{q}$ by $\mathbf{v}$ and replacing the primed magnitudes with nonprimed (except, instead of primes in the inherent system of reference we shall substitute zero subscripts)

$$\mathbf{r} = \mathbf{r}_0 + (\beta - 1)\frac{\mathbf{v}\cdot\mathbf{r}_0}{v^2}\mathbf{v} - \frac{l}{c}\beta\mathbf{v}t_0, \quad t = \beta\left[t_0 + l\frac{\mathbf{v}\cdot\mathbf{r}_0}{c^2}\right] \tag{3.2}$$

From formulas (3.2) we shall find matrix of the transformation

$$|\alpha_{ik}| = \left|\frac{\partial x_i}{\partial x_k'}\right| = \begin{vmatrix} \delta_{ik} + (\beta - 1)\frac{v_i v_k}{v^2} & -\beta l v_i / c \\ \beta l v_k / c & \beta \end{vmatrix} \tag{3.3}$$

We shall emphasize in particular that the problem under consideration of the Lorentz transformations are used in a vector form (3.3),

since field of speeds v in the fixed system of reference S is assumed to arbitrary.

As a first approximation, in which tensor $W_{ik}^{\circ} = W_{ik}^{\circ(1)}$ has a diagonal form, after the transformation (3.1) we obtain the well known expression [1]:

$$|W_{\alpha\beta}^{(1)}| = \begin{vmatrix} \frac{4\pi B_0}{3c}\delta_{\alpha\beta} + \frac{4\pi B_0}{3c}\frac{\partial^2}{\partial^2}v_\alpha v_\beta & i\frac{4\pi B_0}{3c}\frac{\partial^2}{\partial}v_\alpha \\ i\frac{4\pi B_0}{3c}\frac{\partial^2}{\partial}v_\beta & \frac{4\pi B_0}{3c} - \frac{4\pi B_0}{3c}\partial^2 \end{vmatrix} \qquad (3.4)$$

Subsequently, there will be calculated the additional part in tensor of W_{ik}, which appears as the second approximation. We shall introduce the designation

$$W_{ik} = W_{ik}^{(1)} + W_{ik}^{(2)} \qquad (3.5)$$

According to (3.1)

$$W_{ik}^{(2)} = a_{il}a_{km}W_{lm}^{(2)} = Aa_{il}a_{km}F_{lm}, \quad A = -\frac{1}{c}\frac{4\pi}{\rho_{00}}\frac{dB_0}{dT} \qquad (3.6)$$

$$F_{\alpha\beta} = i\frac{1}{3}\delta_{\alpha\beta}\frac{\partial T}{\partial v_0} + \frac{T}{15}\left[\frac{\partial \tau_{\alpha\beta}}{\partial x_{\alpha\beta}} + \frac{\partial \tau_{\alpha\alpha}}{\partial x_{\alpha\beta}} + \delta_{\alpha\beta}\nabla_0\cdot\tau_0\right]$$
$$F_{\alpha 4} = i\left[\frac{1}{3}\frac{\partial T}{\partial x_{\alpha\alpha}} + i\frac{T}{3}\frac{\partial \tau_{\alpha\alpha}}{\partial v_0}\right], \quad F_{44} = -\left[i\frac{\partial T}{\partial v_0} + \frac{T}{3}\nabla_0\cdot\tau_0\right], \quad \tau_0 = \frac{v_0}{c} \qquad (3.7)$$

Using (3.3), from formulas (3.7) we shall obtain expressions for elements of tensor of $W_{ik}^{(2)}$ in terms of F_{lm}, presented in a somewhat different form in work [3]

$$\frac{1}{A}W_{\alpha\beta}^{(2)} = F_{\alpha\beta} + \frac{\theta-1}{\beta^2}\beta_\alpha(\beta_\gamma F_{\gamma\beta} + \beta_\gamma F_{\gamma\alpha}) + \frac{(\theta-1)^2}{\beta^4}\beta_\alpha\beta_\gamma\beta_\delta\beta_\nu F_{\gamma\nu} -$$
$$-\theta^2\beta_\alpha\beta_\gamma F_{\gamma 4} - \theta\left[\beta_\gamma F_{\gamma\alpha} + \beta_\alpha F_{\gamma 4} + 2\frac{\theta-1}{\beta^2}\beta_\alpha\beta_\gamma\beta_\delta F_{\delta 4}\right] \qquad (3.8)$$

$$\frac{1}{A}W_{\alpha 4}^{(2)} = \theta\left[i\frac{\theta-1}{\beta^2}\beta_\alpha\beta_\gamma\beta_\delta F_{\gamma\delta} + \beta_\gamma F_{\gamma\alpha} + F_{\alpha 4} + \frac{\theta(1+\beta^2)-1}{\beta^2}\beta_\alpha\beta_\gamma F_{\gamma 4} - \beta_\alpha\theta F_{44}\right] \qquad (3.9)$$

$$\frac{1}{A}W_{44}^{(2)} = \theta^2(-\beta_\gamma\beta_\delta F_{\gamma\delta} + 2\beta_\gamma F_{\gamma 4} + F_{44}) \qquad (3.10)$$

Substitutions of F_{lm} from (3.7) in equations of $W_{ik}^{(2)}$ (3.8)-(3.10) are still insufficient for obtaining the sought expression. In (3.7) it is necessary to change to coordinates of the time and speed of medium in system of reference S. Here there must be used the following operator relationships from (3.2):

$$i\frac{\partial}{\partial t_0} = \theta\left[i\frac{\partial}{\partial t} + \beta\cdot\nabla\right], \qquad \nabla_0 = \nabla + i\theta\beta\frac{\partial}{\partial t} + \frac{(\theta-1)\beta}{\beta^2}\beta\cdot\nabla \tag{3.11}$$

and also relativistic law of addition of speeds in vector form

$$\gamma_0 = \frac{1}{\theta(1-\beta\cdot\gamma)}\left[\gamma + \frac{(\theta-1)\beta}{\beta^2}\beta\cdot\gamma - \beta\theta\right] \tag{3.12}$$

At any given universal point $\gamma = \beta$ and after carrying out the differentiation also it is assumed $\gamma = \beta$. From (3.12) it is evident that in such case the effect of any differential operator D on γ_0 reduces to the following:

$$D\gamma_0 = \theta\left[D\gamma + \frac{(\theta-1)\beta}{\beta^2}\beta\cdot D\gamma\right] \equiv \theta\left[D\beta + \frac{(\theta-1)\beta}{\beta^2}\beta\cdot D\beta\right] \tag{3.13}$$

Substituting F_{ik} from (3.7) in (3.8)-(3.10) with the use of relationships (3.11), (3.13) and introducing the 4-speed (2.2), we shall obtain

$$\frac{1}{\lambda}W_{\mu\nu}^{(2)} = \frac{1}{3}(\delta_{\mu\nu}+6u_\mu u_\nu)\left[u_\alpha\frac{\partial}{\partial x_\alpha} + u_\alpha\frac{\partial}{\partial x_\alpha}\right]T + \frac{1}{3}\left[u_\mu\frac{\partial}{\partial x_\alpha} + u_\nu\frac{\partial}{\partial x_\mu}\right]T + \tag{3.14}$$
$$+\delta_{\mu\nu}\frac{T}{15}\left[\frac{\partial u_\alpha}{\partial x_\alpha} + \frac{\partial u_\alpha}{\partial x_\alpha}\right] + \frac{T}{15}\left[\frac{\partial u_\nu}{\partial x_\mu} + \frac{\partial u_\mu}{\partial x_\nu}\right] + \frac{2}{5}T\left[\frac{\partial}{\partial t}(u_\mu u_\nu u_\alpha) + \frac{\partial}{\partial x_\alpha}(u_\mu u_\nu u_\alpha)\right]$$

$$\frac{1}{\lambda}W_{\mu 4}^{(2)} = \left[2u_\mu u_4^2 + \frac{1}{3}u_\mu\right]\frac{\partial T}{\partial t} + 2u_\mu u_\alpha u_\alpha\frac{\partial T}{\partial x_\alpha} + \tag{3.15}$$
$$+\frac{1}{3}u_\alpha\frac{\partial T}{\partial x_\mu} + \frac{T}{15}\left[\frac{\partial u_\mu}{\partial t} + \frac{\partial u_4}{\partial x_\mu}\right] + \frac{2}{5}T\left[\frac{\partial}{\partial t}(u_\mu u_4^2) + \frac{\partial}{\partial x_\alpha}(u_\alpha u_\mu u_4)\right]$$

$$\frac{1}{\lambda}W_{44}^{(2)} = (2u_4^2 + u_4)\frac{\partial T}{\partial t} + \left(2u_4^2 + \frac{1}{3}\right)u_\alpha\frac{\partial T}{\partial x_\alpha} + \tag{3.16}$$
$$+\frac{T}{5}\left[\frac{\partial u_4}{\partial t} + \frac{1}{3}\frac{\partial u_\alpha}{\partial x_\alpha}\right] + \frac{2}{5}T\left[\frac{\partial}{\partial t}(u_4^2) + \frac{\partial}{\partial x_\alpha}(u_\alpha u_4^2)\right]$$

It is readily verified that expression $W_{ik}^{(2)}$ coincides with formula (8) in [1], if we take into consideration the small difference in factors of components of the tensors.

In conclusion we shall present $W_{ik}^{(2)}$ in the simplest Galilean one-dimensional , two-dimensional case

$$u_\alpha = \begin{cases} \beta & (\alpha = 1), \\ 0 & (\alpha = 2,3), \end{cases} \qquad u_4 = i, \qquad \frac{\partial}{\partial x_\alpha} = \begin{cases} \partial/\partial x & (\alpha = 1) \\ 0 & (\alpha = 2,3) \end{cases} \tag{3.17}$$

We shall ignore all the terms $\sim\beta^2$ and shall obtain from (3.14)-(3.16)

$$\frac{1}{\lambda} W_{11}^{(2)} = -\frac{1}{3\varkappa}\frac{\partial T}{\partial x} + \beta\frac{\partial T}{\partial x} + \frac{T}{3}\frac{\partial \beta}{\partial x} \tag{3.18}$$

$$\frac{1}{\lambda} W_{12}^{(2)} = -\frac{1}{3}\frac{\partial T}{\partial z}, \quad \frac{1}{\lambda} W_{44}^{(2)} = -\frac{4}{3}\beta\frac{\partial T}{\partial x} - \frac{T}{3}\frac{\partial \beta}{\partial x} - \frac{1}{c}\frac{\partial T}{\partial t} \tag{3.19}$$

In comparison to the non-relativistic analysis [4, 5] here a new result will be appearance of terms of viscosity of radiation in (3.18).

Thus, the solution of very broad class of problems of radiation hydrodynamics may be obtained on the basis of equations (2.6) with substitution of W_{ik} from (3.4) and (3.14)-(3.16), and in the simplest Galilean one-dimensional case from (3.18)-(3.19).

Submitted
14 March 1963

Literature

1. L. H. Thomas. The radiation field in a fluid in motion. The Quarterly Journal of Mathematics, Oxford series, 1930, Vol 1.

2. J. L. Synge. The relativestic gas. Moscow, IL, 1960.

3. V. A. Prokof'yev. Equation of transfer in relativistic radiation hydrodynamics. DAN SSSR, 1961, 140, p. 1033.

4. S. Chandrasekhar. An introduction to the study of stellar structure. Moscow, Foreign Lit. Publ. House, 1950.

5. D. A. Frank-Kamenetskiy. Physical processes within stars, Moscow, State Publ. House of Physics and Mathematical Lit., 1959.

6. L. D. Landau and Ye. M. Lifshits. Field theory. 2nd edition, Moscow-Leningrad, State Press for Technical and Theoretical Literature, 1948.

7. L. D. Landau and Ye. M. Lifshits. Mechanics of continuous media. 2nd edition revised and enlarged. Moscow, State Press for Technical and Thoeretical Literature, 1953.

THE SPEED OF WEAK WAVES IN A RADIATING GAS

V. A. Prokof'yev
(Moscow)

In the article proceeding from relativistic equations of radiation hydrodynamics [1-4] of an inviscid and nonheat conducting fluid, in ignoring the effects of the interaction of particles of high energies (formation of vapors meson fields et cetera), there is studied the propagation of small flat harmonic perturbations in a quiescent equilibrium medium; this study takes into account its own radiation field created by thermal emission and absorption of electromagnetic waves by particles of medium. Here a priori there are not imposed the conditions of smallness of the ratios of speed of sound and velocity of light and radiation pressure to pressure of the gas under which there are valid the conclusions of previously conducted investigations of this problem [5, 6] on the basis of Jeans and Vogt's equations [7, 8]. Relativistic effects may be noted at small macroscopic speeds of the medium when microscopic speeds of individual particles are close to the velocity of light (very high temperatures). Differences in the values of the parameters describing radiation field in a fixed and in local systems of reference will be not only in the terms having as a factor $1/c^2$ (c – is the velocity of light), but also in terms containing $1/c$, owing to the Doppler effect and aberration.

§ 1. Linearized Equations

As a result of the perturbation parameters of medium we shall obtain small relative increments (denoted by primes)

$$P = P_0(1 + P'), \quad H_\nu = 2\pi B_{\nu 0} H_\nu', \quad H = 2\pi B_0 H', \quad u = c_0 u' \equiv c_0 M \qquad (1.1)$$

where P is any of following parameters: p, ρ, T, ϑ are pressure, density, temperature, internal thermal energy of gas; B_ν, I_ν, ε_ν, π_ν – Planck's function, the intensity of radiation, volume density of radiation energy, radiation pressure of the optical frequency ν; B, I, ε, π_1 are the corresponding integral parameters obtained from preceding spectral parameters by integrating over all frequencies; H_ν, H are the spectral and integral fluxes of radiation (subsequently along the axis Ox); u is the macroscopic velocity of the perturbed motion, c_0 is the nonrelativistic speed of sound (without radiation). The little zeroes pertain to parameters of an equilibrium medium at rest, so that ρ_0, ϑ_0 are the residual density and residual internal thermal energy of the gas.

Then there is investigated the motion with plane waves (along Ox-axis); the squares of small perturbations, and of their derivatives will be ignored. The motion developed will be related to the fixed system of reference, however, some of the parameters will be determined also in the inherent system (which is marked by asterisks), where in an undisturbed medium both systems coincide and the corresponding parameters in both systems will be identical as a consequence of which asterisks next to magnitudes with a zero subscript are omitted. Since the motion is one-dimensional, then the inherent radiation field will be axially symmetric and from determinations of the parameters it is evident

$$\varepsilon' = \frac{1}{3}E(1), H' = E(\mu), \pi'_1 = \frac{3}{5}E(\mu^2), \quad E(\mu^k) \equiv \int_0^\infty B_\nu d\nu \int_{-1}^{1} I'_\nu \mu^k d\mu \Big/ \int_0^\infty B_\nu d\nu \qquad (1.2)$$

A linearized equation of radiation transfer has the form

$$\frac{1}{c}\frac{\partial I'_\nu}{\partial t} + \cos\phi \frac{\partial I'_\nu}{\partial x} = \omega_\nu \left[(T' + Mc^2)\left(\frac{\partial \ln B_\nu}{\partial \ln T}\right)_0 - I'_\nu \right] \qquad (1.3)$$

if we assume the radiation as quasi-equilibrium and use Kirchhoff's law. Here $\varkappa_\nu = \rho\alpha_\nu$ is the volumetric coefficient of absorption, φ is the angle between Ox-axis and direction of the beam along which there propagates radiation $c^\circ = c_0/c$. Variations of the radiation flux along the Ox-axis in the fixed and in local systems of reference are connected thus [4]:

$$H' = H^{\circ\prime} + \tfrac{5}{3} Mc^\circ \qquad (1.4)$$

Relativistic equations of a one-dimensional motion of gas taking into account radiation field [4] after their linearization near the state of rest will be written out in a fixed system of reference in the following form:

$$\rho_0\left(1 + \frac{a_0}{c^2} + \frac{p_0}{\rho_0 c^2}\right)\frac{\partial u}{\partial t} + p_0\frac{\partial p'}{\partial x} + \varkappa_{10}\frac{\partial \pi'_1}{\partial x} + \frac{2\pi B_0}{c^3}\frac{\partial H'}{\partial t} = 0$$
$$\rho_0 a_0\frac{\partial \sigma'}{\partial t} - p_0\frac{\partial p'}{\partial t} + 2\pi B_0\frac{\partial H'}{\partial x} + \varepsilon_0\frac{\partial \sigma'}{\partial t} = 0, \quad \frac{\partial p'}{\partial t} + \frac{\partial u}{\partial x} = 0 \qquad (1.5)$$

We shall supplement system (1.3), (1.5) with equations of state of gas

$$p = f_1(\rho, T), \quad \varepsilon = f_2(\rho, T), \quad p' = h_1\rho' + h_2 T', \quad \varepsilon' = h_3\rho' + h_4 T'$$
$$h_1 = \lambda_\rho(p), \quad h_2 = \lambda_T(p), \quad h_3 = \lambda_\rho(\varepsilon), \quad h_4 = \lambda_T(\varepsilon), \lambda_x(y) \equiv (\partial \ln y / \partial \ln x)_\varepsilon \qquad (1.6)$$

In the linearization of equations essentially there occurs a transition from the relativistic case to the classical which satisfies principle of Galileo's relativity taking into account the Doppler effect and aberration; however, the equations of state have remained at the same time relativistic.

§ 2. The Frequency Equation

The system (1.3), (1.5), (1.6) has a solution of the type

$$P'(x, t) = P'(0, 0)\exp[i(kx + \omega t)] \qquad (k, \omega = \text{const}) \qquad (2.1)$$

which describes, in particular, in an infinite medium the propagation of forced harmonic oscillations of infinitesimally small amplitude with a frequency ω. The real parts (2.1) have a physical meaning.

Substituting expression of the type (2.1) in (1.3) and then, in (1.2), we shall obtain

$$I_\nu' = \lambda_T (B_\nu) \frac{T' + Mc^2 \cos\Phi}{1 + ic^2 v_\nu + m v_\nu \cos\Phi} \left(m = \frac{ikc_0}{\omega} \right) \tag{2.2}$$

$$\varepsilon' = g_1 T' + \frac{1}{2} Mc^2 g_3, \quad H' = g_2 T' + \frac{2}{3} Mc^2 g_3, \quad \pi_1' = g_3 T' + Mc^2 g_4 \tag{2.3}$$

$$g_1 = \frac{2}{m} S\left\{ \ln \frac{1+q_\nu}{1-q_\nu} \right\}, \qquad g_2 = \frac{8}{m} S\left\{ 1 - \frac{1}{2q_\nu} \ln \frac{1+q_\nu}{1-q_\nu} \right\}$$

$$g_3 = -\frac{12}{m} S\left\{ \frac{1}{q_\nu} \left(1 - \frac{1}{2q_\nu} \ln \frac{1+q_\nu}{1-q_\nu} \right) \right\} \qquad \left(q_\nu = \frac{m}{w_\nu + ic^2} \right)$$

$$g_4 = \frac{4}{m} S\left\{ 1 + \frac{3}{q_\nu^2} \left(1 - \frac{1}{2q_\nu} \ln \frac{1+q_\nu}{1-q_\nu} \right) \right\} \tag{2.4}$$

$$S(y) = \int_0^\infty \left(\frac{\partial B_\nu}{\partial T} \right)_0 w_\nu y d\nu \Big/ \int_0^\infty \left(\frac{\partial B_\nu}{\partial T} \right)_0 d\nu \qquad \left(w_\nu = \frac{1}{v_\nu} = \frac{\omega_0 w_0}{\omega} \right) \tag{2.5}$$

After substituting (2.1) in the system of equations (1.5), (1.6) there is obtained together with (2.3) a system of linear homogeneous equations, the condition of existence of whose nontrivial solution with respect to variations of parameters is the frequency equation

$$\left(h_3 m + \xi m g_3 + \frac{3}{2} ic^2 \xi g_3 \right) \left(e_1 m + e_3 \xi m g_3 + \frac{3}{2} e_3 ic^2 \xi g_3 \right) +$$
$$+ \left(h_4 + 3 e_3 \xi g_1 - \frac{i}{\beta} h_4 Z m g_3 \right) \left(e_2 + h_1 m^2 - ic^2 \xi m g_4 + c^{0*} \xi g_3 \right) = 0 \tag{2.6}$$

where all relative variations of the parameters are expressed in terms of one of them, for example, in terms of T' in the following manner:

$$M = iLT', \quad \rho' = -mLT', \quad p' = (h_2 - h_1 mL)\, T', \quad s' = (h_4 - mL)\, T'$$
$$\varepsilon' = (g_1 + \tfrac{1}{2} c^2 L g_3)\, T', \quad H' = (g_2 + \tfrac{2}{3} ic^2 L g_3)\, T', \quad \pi_1' = (g_3 + ic^2 L g_4)\, T' \tag{2.7}$$

$$L \equiv \frac{h_3 m + \xi m g_3 + {}^3/_2 ic^2 \xi g_3}{e_2 + h_1 m^2 - ic^2 \xi m g_4 + c^{0*} \xi g_3}, \qquad Z = \frac{12 e_3 \xi}{h_4 c^2}, \qquad \gamma = \frac{\rho_0 c_0^2}{h_1 p_0}$$
$$\xi = \frac{\varkappa_0}{p_0}, \quad e_2 = \gamma h_1 + e_4 c^{0*}, \quad e_4 = 1 + \frac{1}{e_3}, \quad e_3 = \frac{p_0}{\rho_0 \varepsilon_0} \tag{2.8}$$

Here γ is the ratio of the specific heats of the gas. On the basis of well-known thermodynamic relationships

$$\gamma = 1 + \frac{a_0 a_1}{k_0 k_1}, \qquad a_1 \equiv a_0 - k_0 \tag{2.9}$$

The general investigation of the attenuation and dispersion of waves of infinitesimally small amplitude reduces to an investigation of the roots of the frequency equation. In subsequent sections there are made certain derivations from an analysis of this equation.

From characteristic equation (2.6) it follows that there may exist two types of attenuating waves: compression waves and thermal radiation waves. Compression waves are a modification of nonattenuating sonic waves in a nondissipative medium, and thermal radiation waves are a modification of radiation waves generating under the effect of a pulsating source of radiation at the origin of coordinates.

System of equations for determining the radiation transfer of the frequencies does not have the solution $q_\nu = 1$, since this case corresponds to the propagation of radiation in a nonradiating medium from a flat source at the origin of coordinates with velocity of light in a vacuum altenuating under effect of absorption of medium according to the Bouguer law which does not correspond to conditions of the problem being considered here.

In nonrelativistic case at $c^0 = 0$ and $\xi = 0$ equation (2.6) will acquire the form

$$\gamma \frac{1+m^2}{\gamma+m^2} = iZS\left\{1 - \frac{m}{2m}\ln\frac{m_0+m}{m_0-m}\right\} \tag{2.10}$$

For an illustration of obtained derivations below there will be used in addition to general equations (1.6), equations of state of an ideal relativistic nondegenerated gas of particles and the gas of particles with constant heat capacities.

§ 3. Relativistic Ideal Gas

The internal energy of the relativistic gas of particles in a calculation for a unit of inherent volume is the expression $E = \rho c^2 + \rho\varepsilon$, where $\rho = nm_p$ is the residual density of mass of gas, m_p is the average rest mass of an individual particle, n is the number of particles per unit of inherent volume, $\rho\varepsilon$ is the thermal internal energy of gas per unit of inherent volume. Equations of state of a nondegenerated ideal gas will be written out in the form [9, 10]:

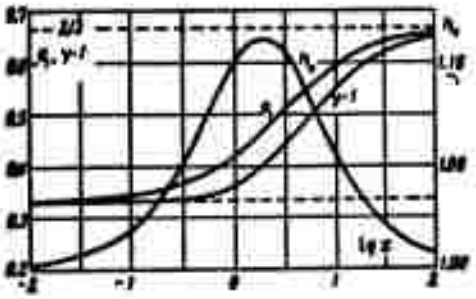

Fig. 1.

$$p = \frac{k}{m_p}\rho T, \quad \varepsilon = \frac{p}{\rho}\varphi(x), \quad \varphi(x) = 3 - x + xG, \quad G = \frac{K_1}{K_2}, \quad x = \frac{m_p c^2}{kT} \tag{3.1}$$

where k is the Boltzmann's constant, $K_n(x)$ are the modified Bessel functions.

In accordance with this we shall obtain (Figs. 1 and 2)

$$h_1 = h_2 = 1, \quad h_4 = c_{v0}T_0/E_0 = f/\varphi, \quad \gamma = 1 + 1/f, \quad e_1 = e_2 = 1/\varphi$$
$$h_3 = 0, \quad c^{*2} = \gamma/x = (1+f)/(fx), \quad f(x) = 3 + x^2 - xG(3 + xG) \tag{3.2}$$

In an ideal gas with constant heat capacities

$$h_1 = h_2 = h_4 = 1, \quad h_3 = 0, \quad Z = 12(\gamma - 1)\xi/c^2$$
$$e_1 = e_2 = \gamma - 1, \quad c^{*2} = \gamma/x, \quad e_3 = \gamma + \gamma c^{*2}/(\gamma - 1) \tag{3.3}$$

A relativistic gas in a general case does not obey these relationships, but within the limit of very high and low temperatures they approximately are realized where the ratio of the specific heats will be equal to 4/3 and 5/3 respectively.

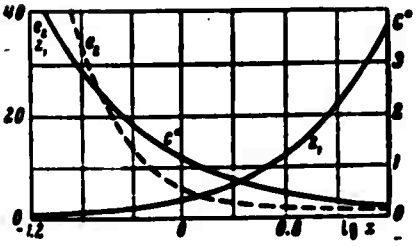

Fig. 2.

In an ideal relativistic gas

$$x = 1.082 \cdot 10^{12} \mu_H T^{-1}$$

$$c^0 = 3.040 \cdot 10^{-7} (\gamma T)^{1/2} \mu_H^{-1/2}$$

$$(\mu_H = m_p / m_H) \qquad (3.4)$$

$$\xi = \frac{8}{45} \frac{\pi^3 c^3 m_p^3 c^{*6}}{h^3 n_0 T^3} = 18.28 \frac{T^3}{n_0} = \frac{2.384 \cdot 10^{20}}{\gamma^3 n_0} c^{*6} \mu_H^3 \qquad (3.5)$$

Here m_H is the atomic mass of hydrogen, h is Planck's constant, n_0 is the number of particles in 1 cm^3. Hence there are evident the limiting values c^0, ξ, Z, consistent with concept about medium as about a material continuum.

If energy in unit of volume is equal to the pressure [11], then

$$p\rho = p, \quad h_1 = h_2 = h_4 = e_1 = e_2 = 1, \quad h_3 = 0, \quad e_3 = 2(1 + c^{*2}), \quad \gamma = 2 \qquad (3.6)$$

In case of an ultrarelativistic gas of particles we have

$$p\rho = 3p, \quad h_1 = h_2 = h_4 = 1, \quad h_3 = 0, \quad e_1 = e_2 = 1/3$$
$$e_3 = 4(1/3 + c^{*2}), \quad \gamma = 4/3 \qquad (3.7)$$

§ 4. Waves of Large Optical Length

At small numbers of v_ν for determining the radiation transfer of energy of optical frequencies the conditional wave length $l_0 = 2\pi c_0/\omega$ expressed in lengths of free path of photons, is large (large optical length of conditional adiabatic wave). The lifetime of a photon $t_\nu = 1/(c\omega_{\nu 0})$ is small in comparison to period of oscillations in wave. This will take place, if the frequencies of the oscillations are small, or if coefficients of absorption of radiation are large for determining optical frequencies. The radiation field within the wave under these conditions may be assumed as equilibrium.

Within the limit while $\nu_\nu \to 0$ the waves will be nonattenuating and will be propagated at a constant speed independent of the frequency. The square of this speed is equal to

$$c_{\infty}^2 = c_0^2 \frac{\gamma A_0 A_0 + 4\xi (a_0 + A_0 b_0 + 3A_1 a_0 - A_0) + 16 a_0 \xi^2}{(a_0 + 4\xi c^{(0)})(A_0 + 12 a_0 \xi)} \qquad (4.1)$$

and may be determined by equality (the derivative is taken with a constant entropy)

$$c_0^2 = \left(\frac{\partial (p+\varepsilon)}{\partial \rho}\right)_{s_0} \qquad (4.2)$$

from equations (1.5), (1.6), if in them we substitute the equilibrium values of the radiation parameters. The speed of waves (4.1) is the low-frequency adiabatic speed of sound; it, in particular, takes place during very low frequencies where the influx of heat to a unit of inherent volume in this case is lacking. At $c^{(0)} \ll 1$ formula (4.1) will determine the speed of sound in a gas, being in equilibrium with the black radiation [12]. For an ideal relativistic gas there follows the formula obtained by Guess [13] from a consideration of the Rankine-Hugoniot relations in a weak shock wave in a thermally ideal relativistic gas; if we assume still $\xi = 0$, then we shall obtain the speed of sound calculated by Synge [2] in relativistic ideal gas of particles without radiation. In the case of an ideal gas with constant heat capacities

$$\frac{c_{\infty}^2}{c_0^2} = \frac{\gamma + 20(\gamma - 1)\xi + 16(\gamma - 1)\xi^2}{[\gamma + 4\xi c^{(0)} + \gamma c^{(0)}/(\gamma - 1)][1 + 12(\gamma - 1)\xi]} \qquad (4.3)$$

which at $c^{(0)} = 0$ reverts to Sach's formula [14]. At large ξ from (4.1) there is obtained speed of sound in a photon gas [15]

$$c_{\infty} = c/\sqrt{3} \qquad (4.4)$$

At large values of c^0 (4.1) is replaced by formula

$$\frac{c_{a0}^2}{c^2} = \frac{\gamma h_0 h_1 + 4\xi (a_0 + h_0 a_0 + 3h_1 a_0 - h_0) + 16 a_0 \xi^2}{(a_0 + 4\xi)(h_1 + 12 a_0 \xi)} \qquad (4.5)$$

which for $\xi \gg 1$ again gives (4.4). If the gas is an ideal relativistic gas or a gas with constant heat capacities, then from (4.5) it is evident

$$\frac{c_{a0}^2}{c^2} = \frac{1 + f + 20\xi + 16\xi^2}{(1 + \varphi + 4\xi)(f + 12\xi)}, \quad \frac{c_{a0}^2}{c^2} = \frac{(\gamma - 1)[\gamma + 20(\gamma - 1)\xi + 16(\gamma - 1)\xi^2]}{\gamma + 4\xi(\gamma - 1)[3\gamma + 1 + 12(\gamma - 1)\xi]} \qquad (4.6)$$

Formula (4.5) for one only real gas ($\xi \ll 1$) in a general case and in case of an ideal relativistic gas will be transformed respectively, to the form

$$\frac{c_{a0}^2}{c^2} = \frac{\gamma h_1 a_0}{1 + a_0}, \qquad \frac{c_{a0}^2}{c^2} = \frac{1}{f}\frac{1 + f}{1 + \varphi} \qquad (4.7)$$

and for gas with constant heat capacities there is obtained Taub's formula [16]. At large c^0 with higher accuracy $f = \varphi = 3$, as a consequence of which formulas (4.6) and (4.7) are transformed into (4.4). To this same formula there will be transformed equality (4.5) for an ideal gas at $\gamma = 4/3$.

The ratios $c_{a0}/c_0 \leq 1$, if as is evident from (4.1) and (2.8)

$$\xi^0 < \frac{3 a_0 \xi}{h_0^2} \frac{(1 + a_0 + 4a_0\xi)(h_1 + 12 a_0 \xi)}{a_0 [1 + h_1 - 3(\gamma - 1) h_1 + 4\xi] - h_0} \qquad (4.8)$$

In the case of a nonrelativistic real gas being in equilibrium with a photon gas in accordance with (4.1) and as was pointed out in article [12], the ratio c_{a0}/c_0 with an increase of ξ monotonically increases from unity to infinity. In the case of a relativistic gas (Figs. 3 and 4, on the curves there are indicated the values ξ) this ratio does not exceed the magnitude

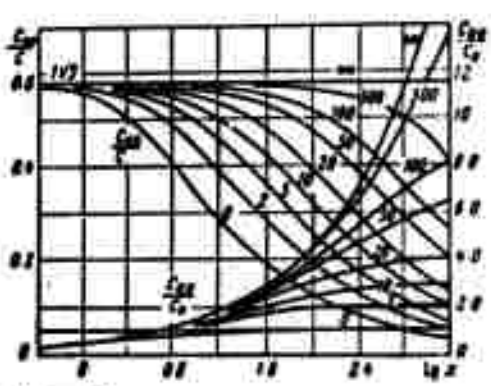

Fig. 3.

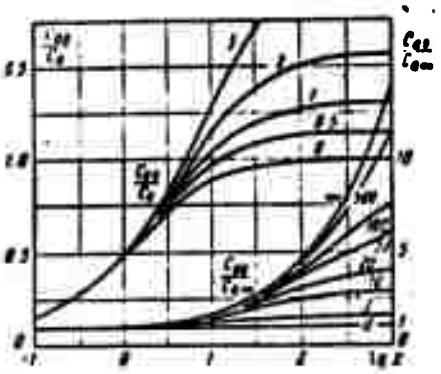

Fig. 4.

$c^{\circ}/\sqrt{3}$, as is evident from (4.1), where it may be depending on relationship between basic thermodynamic parameters of the gas, be either greater than or also less than unity, even if the ratio of the specific heats of the gas are constant.

At small values of v_ν

$$H' = {}^{2}/_{3} Mc^{\circ}, \quad H^{\circ\prime} = 0 \tag{4.9}$$

Owing to the transfer of the radiation energy within the element of the inherent volume an accumulation of energy does not occur.

Equation (2.6) at small values of v_ν, in addition to the root

$$m \approx \pm ic_0/c_\infty \tag{4.10}$$

also has the root

$$\pm m \approx \frac{1+i}{\sqrt{2v_R}} \left\{ \frac{3}{2} \left[\gamma + \frac{4\xi}{h_3 h_4} (e_1 + h_2 h_3 + 3h_1 e_3 + 4e_3 \xi) \right] \right\}^{1/4}, \quad v_R = S(v, s) \tag{4.11}$$

At small and large values of ξ (in the latter case we consider as previously, that the order of any term is determined by order of magnitude v_ν) we shall obtain respectively

$$m \approx \pm (1+i) \left(\frac{3\gamma}{2Zv_R} \right)^{1/4}, \quad \xi < 1; \quad m \approx \pm 2(1+i) \left(\frac{6e_3}{h_3 h_4 Zv_R} \right)^{1/4} \xi, \quad \xi > 1 \tag{4.12}$$

Thus, simultaneously there exist two categories of waves: pressure waves described by root of (4.10), and thermal radiation waves described by root of (4.11). The thermal radiation waves are propagated in the considered case of small values of v_ν with a speed by far lower than both the ordinary speed of sound c_0 without taking into account the radiation and also velocity of the propagation of the pressure waves. These are the slow waves attenuating by far more intensely

than the pressure waves. Therefore, the prevailing waves will be the pressure waves. Waves of second category possess strong dispersion, their speed is proportional to the square root of the frequency of oscillations in the wave.

Coefficient of absorption over the length of thermal radiation waves

$$a_a^{(2)} = 2\pi \frac{m_r}{m_i} \approx 2\pi \tag{4.13}$$

is a constant. The shape of the wave is not maintained since $\alpha_a^{(2)}$ is not a small magnitude. Coefficient of absorption in unit of length is proportional to the square root of the frequency. The length of thermal radiation waves is a large magnitude, inversely proportional to the square root of the frequency. These waves are by far much longer than sound waves and pressure waves.

The existence in an emitting and absorbing gas in addition to pressure waves in an ideal gas also of pressure waves and of viscosity waves in a viscous and heat-conducting fluid and of even thermal radiation waves was ascertained previously [17-19].

In conclusion we shall compute the speed of waves in a Zel'dovich gas (3.6). If $\nu_\nu \to 0$, then

$$\frac{c_{a0}^2}{c_0^2} = \frac{1 + 2\xi(5 + 4\xi)}{(1 + 12\xi)(1 + c^{o2} + 2\xi c^{o2})} \tag{4.14}$$

At large ξ we shall obtain the ultrarelativistic speed of sound (4.4), and at small $c_{a0} = c_0(1 + c^{o2})^{-1/2}$, which in case of small c^o gives the adiabatic speed of sound in a nonrelativistic gas. In the case of large or small c^o (leaving aside here the applicability of the equation of state (3.6)), we shall obtain

$$\frac{c_{a0}^2}{c^2} = \frac{1 + 2\xi(5 + 4\xi)}{(1 + 12\xi)(1 + 2\xi)} < 1, \quad c^o > 1; \quad \frac{c_{a0}^2}{c_0^2} = \frac{1 + 2\xi(5 + 4\xi)}{1 + 12\xi}, \quad c^o < 1 \tag{4.15}$$

§ 5. Waves of Small Optical Length

Suppose now the numbers $v_\nu \gg 1$. This means that either the infrequencies responsible for the heat transfer the coefficients of radiation absorption are small, or frequencies of the forced mechanical oscillations are large, the life-duration of the photon greatly exceeds period of oscillations in the wave and during the period of one oscillation the radiation field can not change: the propagation of waves occurs during a "frozen" radiation field. Within the limit at $v_\nu \to \infty$ the only one of the dissipative processes being taken into account here disappears; the waves become nonattenuating and are propagated with the high-frequency speed of sound which can be calculated by formula (4.2) from equations (1.5), (1.6), if in them we substitute the frozen values H, ε, π_1, i.e., $H' = \varepsilon' = \pi'_1 = 0$, absolutely not involving the equation of radiation transfer. As a result there is obtained following value of the square of speed of the waves:

$$c_{a\infty}^2 = c_0^2 \frac{\gamma h_1 c_3}{\gamma h_1 c_3 + (1 + c_3) c^{*2}} \qquad (5.1)$$

This formula coincides with the expression of the speed of waves of low frequencies, if in expression (4.1) we assume $\xi = 0$. In a nonrelativistic gas, in an ultrarelativistic, in an ideal ultrarelativistic gas and in gas with constant heat capacities

$$c_{a\infty} = c_0, \quad c_{a\infty}^2 = \gamma h_1 c_3 c^{*2}/(1 + c_3), \quad c_{a\infty}/c\sqrt{3}, \quad c_{a\infty}^2 = (\gamma - 1)c^2$$

The speed of propagation of high-frequency waves c_a always is less than the adiabatic speed of sound c_0. The speed of low-frequency waves in a given medium is higher or is equal to speed of high-frequency waves, if

$$\gamma h_1 e_0 [(1 + h_0) e_0 - 3 (\gamma - 1) h_1 e_0 - h_0] + \\ + c^{o2} \{(1 + e_0) [(1 + h_0) e_0 - h_0] - 3 [(\gamma - 1) (1 + e_0) + \gamma h_0] h_1 e_0\} + \\ + 4 e_0^2 [\gamma h_1 e_0 + (1 + e_0 - 3\gamma h_1 e_0) c^{o2}] > 0 \qquad (5.2)$$

Condition (5.2) for an ideal relativistic gas always is realized, i.e., at any value of c° and ξ in a relativistic ideal gas the low-frequency speed of sound is greater than the high-frequency. In a gas with constant heat capacities from a comparison of the speeds of sound of very high and very low frequencies it is evident that: 1) these speeds are equal, if $\xi = 0$; 2) $c_{a0} > c_{a\infty}$, if $\gamma \leq 4/3$, 3) $c_{a0} > c_{a\infty}$ at $5/3 \geq \gamma \geq 4/3$, if

$$x^2 > \frac{144 (\gamma - 1)^2 (3\gamma - 4) (1 + 4\xi) \xi^2}{5 - 3\gamma + 4(\gamma - 1)\xi} \qquad (5.3)$$

The relation between adiabatic low-frequency and high-frequency speeds of sound in an ideal relativistic gas at different values of x and ξ is shown in Fig. 4. It tends towards unity at $\xi \to 0$ at any value x and at $x \to 0$ with any ξ, at $x \to \infty$ and finite ξ its square tends to $0.4\ (5/3 + 20\xi + 16\xi^2)/(1 + 8\xi)$, and at $\xi \to \infty$, but at finite x – to $1/3f(1 + x + \varphi)/(1 + f)$.

From an analysis of the frequency equation, it is evident that formula (5.1) is true also in the more general case when simultaneously there are realized the inequalities

$$e^{\circ} v_{\nu} > 1, \qquad Z S (1) < 1 \qquad (5.4)$$

At large values of v_{ν} the radiation flux through the fixed area is a constant magnitude: in any stationary volume in a fixed system of reference the heat flux owing to radiation is equal to zero. In the inherent system of reference the radiation flux $H^{*\prime} = -8/3c^{\circ}M$ is different from zero, however, the heat influx owing to radiation in each given element of gas (in element of the given particles of

the gas) is absent.

In case of a gas (3.6) from (2.6) it follows that at $v_\nu \to \alpha$ and any finite ξ, c^o, and also at $c^o \to \infty$ then at any limited v_ν, ξ the speed of the waves is equal to velocity of light. If $\xi \to \alpha$, then at any limited v_ν, c^o the speed of waves is equal to the ultrarelativistic speed of sound.

§ 6. Isothermal Waves

Low-frequency speed of sound is equal to isothermal $c_T = c_0/\sqrt{\gamma}$ under the condition that

$$c^{o2} = \frac{\gamma a_0 [(\gamma-1) h_1 h_3 + 4\xi (a_3 + h_3 a_3 - h_3) + 16 a_3 \xi^2]}{(h_3 + 12 a_3 \xi)(1 + a_3 + 4 a_3 \xi)} \qquad (6.1)$$

If c^{o2} is less or larger than the right-hand side of (6.1), then the low-frequency speed of sound is higher or lower than the isothermal. The right-hand side of (6.1) for an ideal relativistic gas and a gas with constant heat capacities is less than unity. The high-frequency speed of sound is equal to the isothermal, if

$$c^{o2} = (\gamma - 1)\gamma h_1 a_3 (1 + a_3)^{-1} \qquad (6.2)$$

In case of an ideal relativistic gas this occurs at $x \approx 5.6$ and in the case of a gas with constant heat capacities at $c^o = \gamma - 1$.

A simultaneous equality of the low-frequency, high-frequency and isothermal speeds of sound is impossible. Returning to the investigation of the general case of not very large and not very small values of the numbers v_ν in the spectral interval determining the motion it is possible to point out a broad class of conditions when the waves (as a first approximation) will move with the Newtonian speed of sound. Such conditions are

$$2|a_0^{(0)}| \gg 1, \quad a_0^{(0)} = S(1 - w, \operatorname{arc\,ctg} w), \quad \xi < 0(1) \qquad (6.3)$$

which must be realized simultaneously. From an evaluation of modulus $a_{00}^{(0)}$ it follows that here there must be $Z \gg 1$, and consequently, $c^{0} \ll 1$, since ξ must not be a larger magnitude, Therefore, the gas here is close to the nonrelativistic.

From equations of hydromechanics of an inviscid and nonheat-conducting gas radiating and absorbing radiation energy within the framework of a special theory of relativity there is obtained the dispersion equation of the propagation of weak perturbations in a quiescent gas. The formation of vapors, meson fields and other effects pertaining to the interaction of particles of high energies in all cases has been ignored. It was assumed that state of radiation is determined by Kirchhoff's law. Some of these limitations can be removed; it is too laborious to generalize the discussed theory into more general equations of the state of radiation. There is established the existence of two terminal velocities of propagation of waves: the adiabatic speed of sound of low frequencies and adiabatic speed of sound of high frequencies. These results were obtained earlier [6] from Jeans-Vogt's nonrelativistic equations of the hydrodynamics of a radiating gas where there was not considered the difference between their graphic representation in fixed and in inherent systems of reference. The consideration of the latter circumstance made it possible to establish the correct formula (5.1) for an adiabatic speed of high-frequency waves (instead of formula (3.8) in article [6]). There has been pointed out the possibility of propagation of pressure waves with isothermal speed of sound. There is demonstrated the possibility of the existence of thermal radiation waves in addition to the pressure waves.

Submitted
26 December 1962

Literature

1. L. H. Thomas. The radiation field in a fluid in motion. Quarterly Journal Mathem., Oxford ser., 1930, Vol 1, pp. 239-251.

2. J. L. Synge. The relativistic gas. Amsterdam, Noth-Holland Publishing Company, 1957. (Russian translation, Moscow, Atomizdat, 1960).

3. J. Halzlehurst and W. L. W. Sargent. Hydrodynamics in a radiation field — a covariant treatment. The Astrophysical Journal, 1959, Vol. 130, No. 1, pp. 276-285.

4. V. A. Prokof'yev. Equations of relativistic radiation hydrodynamics. Reports of the Academy of Sciences of USSR, 1961, Vol. 140, No. 5, pp. 1033-1036, Corrected in: Reports of Academy of Sciences of USSR, 1962, Vol. 143, No. 1, p. 8.

5. V. A. Prokof'yev. Weak waves in a compressible fluid taking into account radiation. PMM, 1957, Vol 21, No. 6, pp. 775-782. Corrected in: PMM, Vol. 22, No. 3, p. 424.

6. V. A. Prokof'yev. Propagation of forced plane compression waves of small amplitude in viscous gas with a consideration of the inherent radiation field. News. Academy of Sciences of USSR, Department of Technological Sciences. Mechanics and machine building, 1960, No. 2. pp. 18-33.

7. J. H. Jeans. A theory of stellar evolution. Monthly Notices RAS, 1925, Vol. 85, pp. 914-933.

8. H. Vogt. Die Stabilität der Sterne. Astronomische Nachrichten, 1928, Bd. 232, No. 5545, SS. 1-4.

9. V. Pauli. Theroy of relativity. Moscow, State Technical Press, 1947.

10. S. Chandrasekhar. An introduction to the study of stellar structure. Chicago, Illinois, The University of Chicago Press, 1939. (Russian transl: Moscow, Foreign Lit. Pub. House, 1950.)

11. Ya. B. Zel'dovich. Equation of state with super-high density and relativistic limitations. ZhETF, 1961, Vol. 41, No. 5, pp. 1609-1615.

12. V. A. Prokof'yev. On speed of small perturbations and the existence of weak shock waves in a radiating gas taking into account the radiation pressure. Herald of Moscow University, Series 1, Mathematics and Mechanics, 1960, No. 1, pp. 43-59.

13. A. W. Guess. Density compression ratio across relativistic — strong — shock waves. The Physics of Fluids, 1960, Vol. 3, No. 3, pp. 697-705.

14. R. G. Sachs. Some properties of very intense shock waves. The Physical Review, 1946, Vol. 69, No. 9-10, pp. 514-522.

15, L. D. Landau and M. Ye. Lifshits. Mechanics of continuous media. 2nd ed., Moscow State Technical Press, 1953, p. 604.

16. A. H. Taub. Relativistic Rankine – Hugoniot equations. The Phsyical Review, 1958, Vol. 74, No. 3, pp. 328-334.

17. V. A. Prokof'yev. Influence of radiation on the propagation of small perturbationsin a viscous and heat-conducting fluid (hydrodynamic theory). News of Academy of Sciences of USSR. Dept of Technological Science, 1957, No. 7, pp. 94-102.

18. V. A. Prokof'yev. Calculation of radiation in hydrodynamic theory of propagation of plane forced waves of infinitesimal amplitude. Herald of Moscow Universkity, series of mathematics, mechanics, astronomy, physics, chemistry, 1957, No. 6, pp. 7-16.

19. V. A. Prokof'yev. Infinitesimally small forced waves in a radiating barotropic medium. Questions of mechanics. No. 193, Collection of articles, Ed. L. N. Sretenskiy. Publishing House of Moscow Universkity, 1961, pp. 93-130.

ON THE HIGH TEMPERATURE INTERNAL FRICTION DURING LONGITUDINAL VIBRATIONS

S. I. Meshkov and T. D. Shermergor

(Voronezh)

There is solved the boundary value problem of longitudinal vibrations of a uniform isotropic rod whose one end is secured and on other there acts a pulse force. The volumetric part of tensor of stresses is described by A. Yu. Ishlinskiy's medium with the time of relaxation τ_2 (standard linear body), and the shear part by Maxwell's medium with the time of relaxation τ_1. It is shown that temperature function of the internal friction of such medium gives during longitudinal vibrations a relaxation peak and background where the latter increases up to infinity, after which the vibrations alternate with an aperiodic process. The solution of boundary value problem is compared with the calculation of corresponding rheological model. For the region not adjoining the point of transition to aperiodicity the results of both methods coincide, except the region of relaxation peak where rehological model gives a result somewhat too low.

In the region adjoining the aperiodicity when the frequency begins to decrease sharply the rheological model is not suitable for the calculation, since it does not take into consideration the change in frequency of the vibrations. It is shown that at $\Delta K/K_\infty = 0.1$ (K is the modulus of hydrostatic stress, $\Delta K = K(\omega = \alpha) - K(\omega = 0)$; ω is the frequency) peak, caused by volumetric relaxation, is manifested only at $\tau_1/\tau_2 \sim 10^3$. For $\tau_1/\tau_2 \sim 1$ volumetric relaxation does not appear and the temperature curves of the internal friction during longitudinal vibrations must be the same as for torsional vibrations.

Application of thermodynamics of irreversible processes to solid body which is in a nonequilibrium state leads to the conclusion that in a linear approximation and in the presence of one relaxation mechanism the tensor of stresses of uniform isotropic body is characterized by two relaxation times, one of which – τ_1 characterizes relaxation of the shear stresses, and the other – τ_2 the volumetric. The expression of tensor of stresses σ_{ik} of such a medium in ignoring the relaxation of the heat flow can be written as [1, 2]

$$\sigma_{ik} = K_0 \varepsilon_{ll} \delta_{ik} + 2\mu \int_{-\infty}^{t} \exp \frac{t'-t}{\tau_1} \dot{e}_{ik}(t')\, dt' + (K_\infty - K_0)\delta_{ik} \int_{-\infty}^{t} \exp \frac{t'-t}{\tau_2} \dot{\varepsilon}_{ll}(t')\, dt' \qquad (1)$$

Here e_{ik} is the deviator of tensor of deformations ε_{ik}, the dot designates the time derivative; K_0 and K_α are respectively the relaxed and nonrelaxed adiabatic moduli of the m hydrostatic stress. Since at high temperatures the shear stresses thermodynamically are unstable, in (1) the equilibrium value of shear modulus is assumed equal to zero [3] and therefore, μ is the nonrelaxed shear modulus μ_0.

One of the methods of determining times of relaxations τ_1 and τ_2 is the method of internal friction. For determining the relaxation time of the shear stresses τ_1 there are used forced or free attenuating vibrations of a torsion pendulum [4]. From equation (1) it is evident that for torsional vibrations when there exist only shear deformations the internal friction with a rise in temperature must monotonically increase [5], since for majority of relaxation mechanisms $\tau = \tau_0 \exp(H/RT)$, where H is the activation energy, R is a gas constant. Such a temperature function of internal friction is observed experimentally for single crystals of pure metals [6], where the mechanism of internal

friction is the diffusion of voids [7].

On the other hand, the same relaxation mechanism must result in a peak of the internal friction for purely volumetric deformations. Since there have been no experiments in a direct study of purely volumetric relaxation, then it is of interest to examine the possibility of determining the relaxation time of the volumetric stresses τ_2 by the attenuating of longitudinal vibrations, when there must take place relaxation of both the shear and also the volumetric stresses.

We shall consider attenuating longitudinal vibrations of a rod, whose one end is secured and on free end there acts pulse force. For solution of the posed problem we shall express tensor of deformations in terms of the tensor of stresses by means of equality (1), analogous to what was done for the calculation of elastic vibrations [8]

$$\dot{e}_{ik} = \frac{1}{9K_\infty}\delta_{ik}\dot{\sigma}_{ll} + \frac{1}{9\tau}\left(\frac{1}{K_0} - \frac{1}{K_\infty}\right)\delta_{ik}\int_{-\infty}^{t}\dot{\sigma}_{ll}\exp\frac{t'-t}{\tau}\,dt' +$$
$$+\frac{1}{2\mu_\infty}\left(\dot{\sigma}_{ik} - \frac{1}{3}\delta_{ik}\dot{\sigma}_{ll}\right) + \frac{1}{2\mu_\infty\tau_1}\left(\sigma_{ik} - \frac{1}{3}\delta_{ik}\sigma_{ll}\right) \qquad \left(\tau \equiv \tau_0\frac{K_\infty}{K_0}\right) \qquad (2)$$

We shall assume that the deformation of rod located along the z-axis is uniform, i.e., the tensor of deformations ε_{ik} is constant along the z-axis. Then also tensor of the stresses everywhere is constant, and it can be found from the condition that on the free lateral surface forces are lacking ($\sigma_{ik}n_k = 0$). Since the component n_z of the unit vector on lateral surface is equal to zero, then all the components σ_{ik} with the exception of σ_{zz} must be equal to zero.

Remembering this from formula (2) we shall obtain the relationship

$$e_{zz} + \frac{1}{\tau}\dot{e}_{zz} = \left(\frac{1}{3\mu_\infty} + \frac{1}{9K_\infty}\right)\dot{\sigma}_{zz} + \left[\frac{1}{\tau}\left(\frac{1}{9K_0} + \frac{1}{3\mu_\infty}\right) + \frac{1}{3\mu_\infty\tau_1}\right]\dot{\sigma}_{zz} + \frac{1}{3\mu_\infty\tau_1\tau}\sigma_{zz} \qquad (3)$$

Since

$$\left(\frac{1}{E_0}+\frac{1}{9K}\right)=\frac{1}{E} \quad (E \text{ is Young's modulus}) \tag{4}$$

then expressions in parentheses are respectively the nonrelaxed and intermediate (nonrelaxed shear and relaxed volumetric stresses) values of the magnitude inverse to Young's modulus, i.e., of compliance.

Function (3) is equivalent to the expression

$$\sigma_{zz}=A\int_{-\infty}^{t}\dot{\varepsilon}_{zz}\exp\frac{t'-t}{\tau_1^0}\,dt'+B\int_{-\infty}^{t}\dot{\varepsilon}_{zz}\exp\frac{t'-t}{\tau_2^0}\,dt' \tag{5}$$

where

$$\tau_{1,2}^0=\frac{1}{2}\left[\left(1+\frac{\mu_\infty}{3K_0}\right)\tau_1+\frac{1}{K_0}K_\infty\tau_2\right]\pm\left\{\frac{1}{4}\left[\left(1+\frac{\mu_\infty}{3K_0}\right)\tau_1+\frac{1}{K_0}K_\infty\tau_2\right]^2-\frac{\tau_1\tau_2(3K_\infty+\mu_\infty)}{3K_0}\right\}^{1/2},\qquad A=E_\infty\frac{\tau_2^0(\tau_1^0-\tau)}{\tau(\tau_1^0-\tau_2^0)},\qquad B=E_\infty\frac{\tau_1^0(\tau-\tau_2^0)}{\tau(\tau_1^0-\tau_2^0)} \tag{6}$$

Substituting expression (5) in general equation of the motion

$$\rho\ddot{u}_z=\frac{\partial\sigma_{zz}}{\partial z} \tag{7}$$

we shall obtain equation of longitudinal vibrations of rod being considered

$$\rho\ddot{u}_z=A\int_{-\infty}^{t}\frac{\partial^2\dot{u}_z}{\partial z^2}\exp\frac{t'-t}{\tau_1^0}\,dt'+B\int_{-\infty}^{t}\frac{\partial^2\dot{u}_z}{\partial z^2}\exp\frac{t'-t}{\tau_2^0}\,dt' \tag{8}$$

which in accordance with the posed problem we solve with the following threshold and initial conditions:

$$u_z|_{t=-\infty}=0\qquad \sigma_{zz}|_{t=-L}=F\delta(t) \tag{9}$$

where F is the constant stress impulse; $\delta(t)$ is the Dirac δ-function describing instantaneous action of the applied force. For the solution of equation (8) under conditions (9) we shall use integral

Laplace transform; in space of the transforms we shall obtain the following expressions:

$$\frac{d^2U_z}{dz^2} = \lambda^2 U_z, \qquad \lambda^2 \equiv \frac{p^2\rho}{A\rho\tau_1^2(p\tau_1^2+1)^{-1} + B\rho\tau_2^2(p\tau_2^2+1)^{-1}} \tag{10}$$

$$U_z|_{z=0} = 0, \qquad \left.\frac{dU_z}{dz}\right|_{z=L} = \frac{F\lambda^2}{p^2\rho} \tag{11}$$

where U_z is the Laplace transform of the z-th component of vector of displacement **u**.

The solution of equation (10) under conditions (11) has the form

$$U_z = \frac{\lambda F}{p^2\rho}\frac{\operatorname{sh}\lambda z}{\operatorname{ch}\lambda L} \tag{12}$$

In order to change in expression (12) to the original we shall use Cauchy theorem on the expansion of the meromorphic function U_z into a series, as a result of which we shall obtain

$$U_z = \frac{2F}{\rho L}\sum_{n=0}^{\infty}(-1)^n \sin\left[\pi\left(n+\frac{1}{2}\right)\frac{z}{L}\right]\Phi_n(p), \qquad \Phi_n = \frac{Q_1(p)}{Q_2(p)} \tag{13}$$

$$Q_1(p) = (p\tau_1^2+1)(p\tau_2^2+1) \tag{14}$$

$$\begin{gathered} Q_2(p) = p^2(p\tau_1^2+1)(p\tau_2^2+1) + \\ + a_n^2 p\left[A\tau_1^2(p\tau_2^2+1) + B\tau_2^2(p\tau_1^2+1)\right] \end{gathered} \qquad \left(a_n = \pi\left(n+\frac{1}{2}\right)\frac{1}{L\sqrt{\rho}}\right) \tag{15}$$

where L is the length, ρ is the density of the rod.

Passing to expressions (13) from the transform to the original, we shall obtain

$$\begin{gathered} u_z(z,t) = \frac{2F}{\rho L}\sum_{n=0}^{\infty}(-1)^n \sin\left[\pi\left(n+\frac{1}{2}\right)\frac{z}{L}\right]\times \\ \times \sum_{\nu=1}^{6}\left((p_\nu\tau_1^2+1)(p_\nu\tau_2^2+1)\frac{1}{\tau_1^2\tau_2^2}\left[\prod_{\nu\neq i}^{6}(p_\nu - p_i)\right]^{-1}\exp(p_\nu t)\right) \end{gathered} \tag{16}$$

where p_ν, p_i are roots of equation $Q_2(p) = 0$. The form of these

roots depends on the sign of the discriminant

$$D_n = m_n^2 + q_n^3 \tag{17}$$

where

$$m_n = \frac{1}{3} s_1^* s_2^* + \frac{1}{3} E_{cm} a_n^2 - \left[\frac{1}{3}(s_1^* + s_2^*)\right]^2 \tag{18}$$

$$q_n = \left[\frac{1}{3}(s_1^* + s_2^*)\right]^3 - \frac{1}{6} s_1^* s_2^* (s_1^* + s_2^*) + \frac{1}{3} a_n^2 \left[s_1^* \left(B - \frac{1}{3} A\right) + s_2^* \left(A - \frac{1}{3} B\right)\right] \tag{19}$$

and in terms of $s_{1,2}^* = 1/\tau_{1,2}^*$ there are designated the frequencies of the relaxation [9].

If $D_n > 0$, then from formula (16) we obtain the following expression:

$$u_z(z, t) = \frac{F z\, s_1^* s_2^*}{A s_2^* + B s_1^*} + \frac{2F}{\rho L} \sum_{n=0}^{\infty} \frac{(-1)^n \sin[\pi (n + 1/2)\, z / L]}{(9\varkappa_n^2 + \omega_n^2)\beta_n} \{-[s_1^* s_2^* - \beta_n (s_1^* + s_2^*) + \beta_n^2] \exp(-\beta_n t) + \frac{(I_n^2 + h_n^2)^{1/2} \beta_n}{(\gamma_n^2 + \omega_n^2)\omega_n} s_1^* s_2^* \exp(-\gamma_n t) \sin(\omega_n t + \psi_n)\} \tag{20}$$

where

$$\beta_n = -2\left[\varkappa_n - \frac{1}{3}(s_1^* + s_2^*)\right], \quad \gamma_n = \varkappa_n + \frac{1}{3}(s_1^* + s_2^*)$$
$$I_n = (s_1^* s_2^*)^{-1} (\gamma_n^2 + \omega_n^2)(9\varkappa_n^2 + \omega_n^2 - 6\gamma_n \varkappa_n) + 3\gamma_n \varkappa_n - \omega_n^2$$
$$h_n = \omega_n \{3\varkappa_n + \gamma_n [1 - 2 (s_1^* s_2^*)^{-1} (\omega_n^2 + \gamma_n^2)]\}$$
$$\psi_n = \operatorname{arctg} \frac{h_n}{I_n} \tag{21}$$

Condition $D_n > 0$ is realized in two cases.

1) At $m_n > 0$. Then the magnitudes $\varkappa_n$ and ω_n are determined by the formulas

$$\omega_n = \sqrt{3}\, r_n \operatorname{ch} \theta_n, \qquad \varkappa_n = -r_n \operatorname{sh} \theta_n$$
$$r_n = \pm \sqrt{|m_n|}, \qquad \theta_n = \frac{1}{3} \operatorname{arcsh}(q_n r_n^{-3}) \tag{22}$$

Here the sign of r_n must be identical with the sign of q_n.

2) At $m_n < 0$, but $q_n^2 > |m_n|^3$. In this case the magnitudes $\varkappa_n$ and ω_n are equal to

$$\omega_n = \sqrt{3}\, r_n \operatorname{sh}\theta_n, \qquad \varkappa_n = -r_n \operatorname{ch}\theta_n$$
$$r_n = \pm\sqrt{|m_n|}, \qquad \theta_n = \frac{1}{3}\operatorname{arcch}\left(q_n r_n^{-3}\right) \tag{23}$$

If $D_n < 0$, then all roots of p_ν are real, and expression (16) describes the aperiodic motion.

Thus, from expression (20) it is evident that dependence of vector of displacement on time is given by three components. The first component describes the new position of equilibrium near which the attenuating vibrations occur, second characterizes elastic after-effect and, finally, third constitutes infinite sum of the attenuating harmonic vibrations in time and the logarithmic attenuating decrement for the n-th harmonic, which is taken as measure of the internal friction, is equal to

$$\Delta_n = \left[\varkappa_n + \frac{1}{3}\left(s_1^{\circ} + s_2^{\circ}\right)\right]\frac{2\pi}{\omega_n} \tag{24}$$

where ω_n is the angular frequency, calculated by formulas (22) or (23), depending upon sign of m_n.

For a numerical evaluation of the obtained results we shall be limited to a consideration of the zero harmonic (n = 0). Then, using mechanical characteristics of aluminum: shear modulus $\mu = 2.4 \cdot 10^{11}$ d/cm^2, Poisson's ratio $\nu = 0.34$, the density $\rho = 2.7$ g/cm^3 — and adopting for the relative relaxation of the bulk modulus $\Delta K/K_\alpha = 0.1$, we shall obtain the relationship shown in Fig. 1 between $\ln \tau_1$ of the internal friction $\tan \delta = \Delta_0/\pi$ and square of frequency according to which usually there is experimentally evaluated

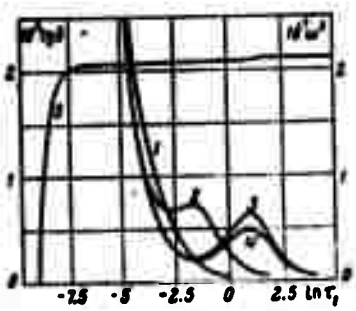

Fig. 1. Relationship between internal friction tan δ and logarithm of relaxation time ln τ_1; curves 1, 2 and 3 correspond to the values τ_1/τ_2 = = 10^2, 30^3 and 10^4 curve 4 is calculated on basis of rheological model for $\tau_1 = \tau_2 = 10^4$; curve 5 is the dependence of square of frequency the rods vibrations ω_2^0 for $\tau_1/\tau_2 = 10^4$.

the dynamic Young' modulus [6, 10], in the function ln τ_1.

Since ln τ_1 = ln τ_0 + H/RT, then the magnitude plotted along the axis of abscissas is proportional to 1/T, i.e., in Fig. 1 actually there is represented temperature relationship between the internal friction and the square of frequency. In the construction of the graphs as parameters there were selected the following relaxation time ratios $\tau_1/\tau_2 = 10^2$, 10^3, 10^4. As is evident in Fig. 1, peak caused by relaxation of volumetric stresses at $\Delta K/K_\infty = 0.1$, appears only beginning from $\tau_1/\tau_2 \sim 10^3$. However, the volumetric relaxation may be ascertained also at smaller ratios of τ_1/τ_2, if there are used double logarithmic coordinates ln tg δ –ln τ_1. The corresponding curves for the same values of parameters τ_1/τ_2 are given in Fig. 2, where region of relaxation for $\tau_1/\tau_2 = 10^2$ manifests itself as a sector of the bend in the region of the linear dependence.

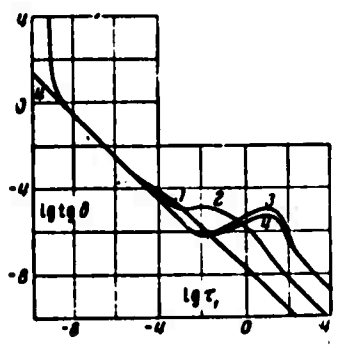

Fig. 2. Relationship between internal friction and relaxation time in double logarithmic coordinates. Designations of curves are the same as in Fig. 1.

By means of the double logarithmic scale it is convenient also to trace temperature dependence of internal friction in the entire region of vibrations up to the point of transition. As might have been expected immediately before the point of transition to

aperiodicity, the internal friction sharply increases, where it is identical for all τ_1/τ_2 values under consideration.

At the selected value $\Delta K/K_\infty = 0.1$ relaxation of square of frequency caused by relaxation of volume stresses, will be insignificant ~0.95%. Basic role in relaxation of square of frequency up to zero is played by the relaxation of the shear stresses.

From the evaluation made it follows that the relaxation time of volume stresses τ_2 may be found from experiments on the study of longitudinal attenuating vibrations under the condition that $\tau_2 \ll \tau_1$. In case, if $\tau_2 \sim \tau_1$ or $\tau_2 > \tau_1$, the relaxation of volume stresses with a minor defect of bulk modulus does not manifest itself and internal friction of such medium will give a clear background caused by the relaxation of shear stresses, analogous to that, which such a medium gives for torsional vibrations.

We shall compare the obtained results with the calculation of corresponding rheological model. Since relaxation processes during longitudinal vibrations are described by complex Young's modulus E*, for the derivation of formula of internal friction we shall express E* in terms of complex shear moduli and the hydrostatic stresses μ^* and K*, using, according to formula (1), for μ^* Maxwell's model and for K* — the model of standard linear body. Then for the tangent of the shear angle of phases between the stress and deformation we shall obtain the formula

$$\operatorname{tg}\delta = -\frac{\operatorname{Im} 1/E^*}{\operatorname{Re} 1/E^*} = \left(\frac{1}{\mu_\infty \omega\tau_1} + \frac{1}{3}\frac{\Delta K \omega\tau_0}{K_0^2 + K_\infty^2\omega^2\tau_0^2}\right)\left(\frac{1}{\mu_\infty} + \frac{1}{3}\frac{K_0 + K_\infty\omega^2\tau_0^2}{K_0^2 + K_\infty^2\omega^2\tau_0^2}\right)^{-1} \qquad (26)$$

The curve constructed by formula (26) for $\tau_1/\tau_2 = 10^4$, is shown in Figs. 1 and 2 from which it is evident that rheological model gives a value of internal friction somewhat too low in the region of the relaxation peak.

For a discussion of this deviation we shall evaluate the contribution of zero harmonic to the total motion. This can be done after taking the ratio of squares of amplitudes at t = 0 which are found in formula (20) before sin $(\omega_n t + \psi_n)$. In the region of peak at $\tau_1/\tau_2 = 10^4$ for the first and zero harmonics this ratio is equal to 0.11 which in accuracy coincides with the determined evaluation of first harmonic during free torsional vibrations of a rod whose shear stresses are described by Maxwell's rheological equation, where for the evaluation of contribution of harmonics there is obtained the formula $\nu_n = 8/\pi^2(2n + 1)^2$ [5]. Thus, contribution of higher harmonics during vibrations of free rod is not very small. However, higher harmonics can be practically removed by attaching an inertial suspension to the rod [11, 12]. Nevertheless, also after suppression of higher harmonics for torsional vibrations the indicated deviation will take place [12], therefore, it may be assumed that it is not the result of ignoring the higher harmonics. But taking into consideration that the difference between results of calculating the internal friction in region of peak by rheological model and the solution of boundary value problem is comparatively small, and calculations in latter case are very cumbersome for an approximate description of peak of internal friction it is possible to use the rheological model.

However, in region, adjoining the point of transition to aperiodicity, the rheological model gives an incorrect result. This is associated with the fact that during the calculation by rheological model the frequency and the temperature are considered as independent variables whereas in reality the heating up of a specimen changes the frequency of vibrations where the change is very great near the point of transition to aperiodicity.

The authors thank V. S. Postnikov and D. D. Ivlev for their discussion of the obtained results.

Submitted
24 December 1962

Literature

1. B. N. Finkel'shteyn and N.S. Fastov. To the theory of relaxation phenomena in solid bodies. DAN SSSR, 1950, Vol. 71, No. 5, p. 875.

2. T. D. Shermergor and V. S. Postnikov. Temperature relaxation in solid bodies. Collection: Transactions of the Third All-Union Conference on Relaxation Phenomena in Metals and Alloys (in press).

3. N. S. Fastov. On the thermodynamics of irreversible processes in elastically-deformed bodies. Fifth collection: "Problems of phsyical metallurgy and physics of metals." Metallurgy Publishing House, 1958, p. 550.

4. A. S. Novik. Internal friction in metals and alloys. Collection: Progress in physics of metals," Metallurgy Publishing House, 1956, Vol. 1, p. 7.

5. T. D. Shermergor and S. I. Meshkov. On describing the background of internal friction during torsional vibrations. Physics of metals and metal science, 1962, Vol 13, No. 6, p. 817.

6. V. S. Postnikov. The temperature function of internal friction of pure metals and alloys. Progress in Physical Sciences, 1958, Vol. 66, No. 1, p. 43.

7. V. T. Shmatov and A. V. Grin'. High-temperature internal friction in metals. Physics of metals and physical metallurgy, 1961, Vol 12, No. 4, p. 600.

8. L. D. Landau and Ye. M. Lifshits. Mechanics of solid media. State Technical Press, 1954.

9. B. Gross. Mathematical structure of the theories of viscoelasticity. Paris, 1953.

10. K'o Ting-Sui. Experimental proof of the viscous behavior of edges of grains in metals. Collections: Elasticity and nonelasticity of metals." IL, 1954, p. 198.

11. V. S. Postnikov. Concerning the question of damping of oscillations of a cylindrical model. Physics of metals and physical metallurgy 1958, Vol. 6, Issue 3, p. 523.

12. S. I. Meshkov and T. D. Shermergor. On temperature function of internal friction of torsion pendulum. PMTF, 1962, No. 6, p. 98.

INVARIANT GROUP SOLUTIONS OF EQUATIONS OF A SPATIAL STATIONARY BEAM OF CHARGED PARTICLES

V. A. Syrovoy

(Moscow)

In works [1, 2] there was introduced the concept of an invariant group solution (H-solution) and there is worked out a general method of obtaining such solutions. In a number of works [2-6] this method was applied to systems of partial differential equations in partial derivatives describing different physical phenomena. Below there have been investigated the group properties of equations of stationary normal beam of analogously charged particles in an arbitrarily oriented external magnetic field both during nonrelativistic speeds and also in a relativistic case when the radiation of moving charges can be ignored.

§ 1. Fundamental Equations

A normal [7] nonrelativistic charged-particle beam in stationary case in an arbitrarily oriented external magnetic field **H** is described by system of differential equations, which in tensor form has the form

$$(S)\qquad \begin{gathered} v^k\left(\frac{\partial v^l}{\partial x^k}+\Gamma^l_{pk}v^p\right)=g^{ll}\left(\frac{\partial \varphi}{\partial x^l}+\sqrt{g}\,e_{mnl}v^m H^n\right)\\ \frac{\partial}{\partial x^l}\left(\sqrt{g}\,g^{lk}\rho v_k\right)=0,\qquad \frac{1}{\sqrt{g}}\frac{\partial}{\partial x^l}\left(\sqrt{g}\,g^{lk}\frac{\partial \varphi}{\partial x^k}\right)=\rho \end{gathered} \tag{1.1}$$

Equations (1.1) are written out in dimensionless form [6]; all indices pass through the values 1, 2, 3; here there are adopted the following designations: v^k, H^n – contravariant component of speed and magnetic field strength; φ is the scalar potential; ρ is the density of the space charge; Γ^i_{pk} is the Christoffel symbol of second kind; e_{mnl} is the covariant isotropic pseudotensor of weight 1 and, finally g^{ik} is the contravariant meteric tensor ($g = |g_{ik}|$).

As will be evident from further discussion the H-solutions are obtained in four orthogonal systems of coordinates: cartesian x, y, z; cylindrical R, ψ, z; spiral cylindrical q_1, q_2, z; spherical r, θ, ψ. Equations of the beam can be written out in each of these coordinate systems. Equations of motion have the integral

$$2\varphi - g_{ik}v^i v^k = \text{const} \tag{1.2}$$

External magnetic field H satisfies the equation

$$\frac{\partial}{\partial z}(\sqrt{g}\,g^{ik}H_k) = 0 \tag{1.3}$$

For magnetic fields, which can exist without special supporting devices in the beam there is still another equation

$$e^{ikl}\frac{\partial H_k}{\partial x^l} = \rho \tag{1.4}$$

§ 2. Group Properties of Equations of a Beam

The solution of the determining equations for the coordinates of infinitesimal operators of basic group G of equations of the beam (1.1) shows that Lie algebra of basic group is generated by following linearly independent operators:

$$
\begin{aligned}
X_1 &= r\nabla + a\left(V\nabla_r + 2\rho\frac{\partial}{\partial\rho}\right) + (z-1)\left(2\rho\frac{\partial}{\partial\rho} + H\nabla_H\right)\\
X_2 &= r\nabla - 2\rho\frac{\partial}{\partial\rho} - H\nabla_H \qquad (z=0)\\
X_3 &= -y\frac{\partial}{\partial z} + z\frac{\partial}{\partial y} - v\frac{\partial}{\partial u} + u\frac{\partial}{\partial v} - H_y\frac{\partial}{\partial H_z} + H_z\frac{\partial}{\partial H_y}\\
X_4 &= -z\frac{\partial}{\partial x} + x\frac{\partial}{\partial z} - w\frac{\partial}{\partial u} + u\frac{\partial}{\partial w} - H_z\frac{\partial}{\partial H_x} + H_x\frac{\partial}{\partial H_z}\\
X_5 &= -x\frac{\partial}{\partial y} + y\frac{\partial}{\partial x} - w\frac{\partial}{\partial v} + v\frac{\partial}{\partial w} - H_x\frac{\partial}{\partial H_y} + H_y\frac{\partial}{\partial H_x}\\
X_6 &= \frac{\partial}{\partial x}, \quad X_7 = \frac{\partial}{\partial y}, \quad X_8 = \frac{\partial}{\partial z}
\end{aligned}
\tag{G}
\tag{2.1}
$$

Here ∇, ∇_V, ∇_H are Hamiltonian operators in space of the coordinates, speeds and components of magnetic field strength, respectively. To the enumerated infinitesimal operators there correspond the following finite transformations maintaining the system (1.1): operator X_1 is an extension with the arbitrary parameter α; operator X_2 is an extension with $\alpha = 0$; operators X_3, X_4, X_5 – the simultaneous turn by an identical angle in one of planes of coordinate space x, y, z and corresponding planes of space of speeds u, v, w corresponding to it, and of the space of components of magnetic field H_x, H_y, H_z; finally the operators X_6, X_7, X_8 are transfers along axes x, y, z. Optimum system of two-parametric subgroups assuring the ascertaining of all essentially different H-solutions of rank 1, has the form

$$
\begin{array}{lll}
1^\circ.\ X_7, X_8 & 4^\circ.\ X_1 - X_2 + X_3, X_8 & 7^\circ.\ X_1 - X_2 + X_3, X_8\\
2^\circ.\ X_3, X_6 & 5^\circ.\ X_1 - X_2 + X_7, X_8 & 8^\circ.\ X_1 - X_2 + X_3, X_1 - X_2 + X_8\\
3^\circ.\ X_1 + aX_2, X_8 & 6^\circ.\ X_1, X_3 & 9^\circ.\ X_1 - X_2 + X_3, X_1, \qquad 10^\circ.\ X_3, X_6
\end{array}
$$

(a is an arbitrary constant)

(2.2)

§ 3. Invariant Group Solutions of Rank 1

If the magnetic field is directed along the z-axis, then the H-solutions obtained in subgroups 1°-5° of system (2.2), correspond to two-dimensional flows considered in [6]. In case of an arbitrary orientation of magnetic field the form of solution does not change,

however, the flow becomes spacial. It must be noted that the analytic solutions presented below for flows with two components of speed are obtained under assumptions, reducing to the system (S/H) for corresponding H-solution to equation of form (3.1), from which there were obtained analytic solutions for two-simensional flows [6]

$$y'' + a^2 y = y^{-3} \qquad (0 < a < 1) \tag{3.1}$$

1°. For the subgroup H $\langle X_7, X_8 \rangle$ the solution has the form

$$V = J^{(1)}(x), \qquad \varphi = J_4(x), \qquad \rho = J_5(x), \qquad H = J^{(2)}(x) \tag{3.2}$$

Here

$$V = (v_x, v_y, v_z), \quad H = (H_x, H_y, H_z), \quad J^{(1)} = (J_1, J_2, J_3), \quad J^{(2)} = (J_6, J_7, J_8)$$

A uniform magnetic field satisfied equations (1.3), (1.4).

2°. For the subgroup H $\langle X_3, X_8 \rangle$ we obtain

$$V = J^{(1)}(R), \qquad \varphi = J_4(R), \qquad \rho = J_5(R), \qquad H = J^{(2)}(R) \tag{3.3}$$

The common solution (1.3), (1.4) determines the following magnetic field:

$$H_R = H_{01}/R, \qquad H_\varphi = H_{02}/R, \qquad H_z = H_{03} \tag{3.4}$$

$3^\circ.1$. For the subgroup H $\langle X_1 + aX_3, X_8 \rangle$ the investigation naturally is made in the spiral cylindrical system of coordinates q_1, q_2, z; here

$$V = e^{\gamma q_2} J^{(1)}(q_1), \qquad \varphi = e^{2\gamma q_2} J_4(q_1) \qquad (\gamma = ab_1)$$
$$\rho = \frac{1}{b_1^2 + b_2^2} e^{2(\gamma - b_1)q_2 - 2b_1 q_1} J_5(q_1), \qquad H = \frac{1}{\sqrt{b_1^2 + b_2^2}} e^{(\gamma - b_1)q_2 - b_1 q_1} J^{(2)}(q_1) \tag{3.5}$$

Let us consider the case, when $J_2 \equiv 0$. Assuming in addition

$$J_1 = \varkappa e^{-b_1 q_1} J_4^{-3} \qquad (0 < \varkappa < 1) \tag{3.6}$$

we shall obtain the following solution:

$$J_4 = \left[\frac{j_0}{2\varkappa(1-\sigma)\gamma^2}\right]^{\frac{1}{1+\sigma}} \{\sin[\gamma(1+\sigma)(q_1-q_0)]\}^{\frac{2}{1+\sigma}}, \qquad J_1 J_3 = j_0 e^{-b_1 q_1}$$

$$J_4 = \left[\frac{j_0(1+\sigma)^2}{2\varkappa(1-\sigma)}\right]^{\frac{1}{1+\sigma}} (q_1-q_0)^{\frac{2}{1+\sigma}} \quad (\gamma=0), \qquad J_3 = (2J_4 - J_2^2)^{1/2}$$

$$J_6 = -\gamma J_3, \qquad J_7 = J_3', \qquad J_8 = (\gamma + b_2) J_3 \tag{3.7}$$

The possible values of $\varkappa$ in (3.6) are determined by the inequality

$$\varkappa < \sqrt{2} e^{b_1 q} \quad (a \le q_1 \le b; \quad q = a, \quad b_1 < 0; \quad q = b, \quad b_1 > 0) \tag{3.8}$$

In approaching the emitter the tangential component of the magnetic field increases without limit; J_6, $J_8 \to 0$ at $q_1 \to q_0$. Particles, abandoning spiral cylindrical emitter $q_1 = q_0$, move along the surface of spiral cylinder $q_2 = \text{const}$; at $\sigma = 1/2$ the trajectories will be

$$s = \frac{\sqrt{b_1^2 + b_2^2}}{2b_1} e^{b_1 q_1} \left[e^{b_1 q_1} \sqrt{2e^{2b_1 q_1} - \varkappa^2} - \frac{\varkappa^2}{\sqrt{2}} \ln\left(e^{b_1 q_1} + \sqrt{e^{2b_1 q_1} - \varkappa^2/2} \right) + C \right] \tag{3.9}$$

In this case, as everywhere later there are satisfied the conditions of emission limited by the space charge.

The following magnetic field satisfies equations (1.3), (1.4)

$$H_{q_1} = -H_{01} e^{(\gamma - b_2) q_1 - b_1 q_2} \sin(\gamma q_1 + \delta), \qquad H_{q_2} = H_{01} e^{(\gamma - b_2) q_1 - b_1 q_2} \cos(\gamma q_1 + \delta),$$
$$H_z = H_{03} \qquad (H_{01}, H_{03}, \delta \text{ are arbitrary constants}) \tag{3.10}$$

Here H_{03} may be different from zero only at $\alpha = 1$.

$3^0.2$. For the subgroup H $\langle X_1, X_8 \rangle$ we have

$$\mathbf{V} = R^{\alpha} \mathbf{J}^{(1)}(\psi), \quad \varphi = R^{2\alpha} J_4(\psi), \quad \rho = R^{2(\alpha-1)} J_5(\psi), \quad \mathbf{H} = R^{\alpha-1} \mathbf{J}^{(2)}(\psi) \tag{3.11}$$

Assuming $J_1 \equiv 0$, $J_2 = \varkappa J_4^{\sigma}$ $(0 < \sigma < 1.0 < \varkappa \le \sqrt{2})$, we obtain

$$J_4 = \left[\frac{j_0}{2\varkappa(1-\sigma)\alpha^2}\right]^{\frac{1}{1+\sigma}} \{\sin[\alpha(1+\sigma)\psi]\}^{\frac{2}{1+\sigma}}, \quad J_4 = \left[\frac{j_0(1+\sigma)^2}{2\varkappa(1-\sigma)}\right]^{\frac{1}{1+\sigma}} \psi^{\frac{2}{1+\sigma}} \quad (\alpha = 0)$$

$$J_3 J_5 = j_0, \quad J_3 = (2J_4 - J_2^2)^{1/2}, \quad J_6 = -J_3', \quad J_7 = \alpha J_3 + a$$

$$J_8 = -(\alpha+1) J_3 + a \frac{J_3}{J_5} \tag{3.12}$$

At $\sigma = 1/2$ and $\varkappa = \sqrt{2}$ the given solution described a two-dimensional flow with circular trajectories [6]. At $\varkappa < \sqrt{2}$ trajectories are located on surface of the cylinder R = const. The emitter is the half-plane $\psi = 0$. At $\sigma = 1/2$ the trajectoreis are determined by the equations

$$R = \text{const}, \qquad z = \frac{\sqrt{2-\varkappa^2}}{\varkappa} R\psi + \text{const} \tag{3.13}$$

The following magnetic field satisfies equations (1.3), (1.4):

$$\begin{aligned} &H_R = H_{01}R^{\alpha-1}\sin(\alpha\psi+\delta), \quad H_\psi = H_{01}R^{\alpha-1}\cos(\alpha\psi+\delta), \quad H_z \equiv 0 \\ &H_R = H_{01}\sin(\psi+\delta), \quad H_\psi = H_{01}\cos(\psi+\delta), \quad H_z = H_{03} \quad (\alpha = 1) \end{aligned} \tag{3.14}$$

At $\alpha = 1$ we obtain the uniform magnetic field $\mathbf{H} \equiv \mathbf{H}_0$. It is readily seen that $\delta = \pi/2 - \beta$, where β is the angle between projection of vector $\mathbf{H}$ onto the plane z = const and the emitter $\psi = 0$.

4°. For the subgroup H $\langle X_1 - X_2 + X_3, X_8\rangle$ we have

$$\mathbf{V} = e^{\alpha\phi}\mathbf{J}^{(1)}(\xi), \quad \varphi = e^{2\alpha\phi}J_4(\xi), \quad \rho = e^{2\alpha\phi}J_5(\xi), \quad \mathbf{H} = e^{\alpha\phi}\mathbf{J}^{(2)}(\xi) \tag{3.15}$$

Assuming $J_2 \equiv 0$ and $J_1 = \varkappa e^{-1/R}J_4^\sigma (0 < \sigma < 1)$, we shall obtain

$$\begin{aligned} &J_4 = \left[\frac{J_0}{2\varkappa(1-\sigma)\alpha^2}\right]^{\frac{1}{1+\sigma}} (\sin[\alpha(1+\sigma)\xi])^{\frac{2}{1+\sigma}}, \qquad J_1 J_3 = J_0 \exp\left(-\frac{1}{R}\right) \\ &J_3 = (2J_4 - J_1^2)^{1/2}, \quad I_6 = -\alpha J_3 + a, \quad I_7 = J_3', \quad I_8 = \alpha J_1 + a\frac{J_3}{J_1} \end{aligned} \tag{3.16}$$

Here

$$\xi = \ln R, \qquad \mathbf{I}^{(2)} = R\mathbf{J}^{(2)}, \quad I_5 = R^2 J_5, \quad a = \text{const}$$

The given solution describes a flow, in which the particles are emitted from surface of cylinder R = 1. Particles move in planes, passing through the axis of emitter along the curves ($\sigma = 1/2$)

$$\psi = \text{const}, \qquad z = \int\left(\frac{2}{\varkappa^2}\exp\frac{2}{R} - 1\right)^{1/2} dR \tag{3.17}$$

The magnetic field of the following form satisfies equations (1.3),

BLANK PAGE

At $\sigma = 1/2$ and $\varkappa = \sqrt{2}$ the given solution described a two-dimensional flow with circular trajectories [6]. At $\varkappa < \sqrt{2}$ trajectories are located on surface of the cylinder R = const. The emitter is the half-plane $\psi = 0$. At $\sigma = 1/2$ the trajectoreis are determined by the equations

$$R = \text{const}, \qquad z = \frac{\sqrt{2-\varkappa^2}}{\varkappa} R\psi + \text{const} \tag{3.13}$$

The following magnetic field satisfies equations (1.3), (1.4):

$$\begin{aligned} &H_R = H_{01} R^{\alpha-1} \sin(\alpha\psi + \delta), \quad H_\psi = H_{01} R^{\alpha-1} \cos(\alpha\psi + \delta), \quad H_z \equiv 0 \\ &H_R = H_{01} \sin(\psi + \delta), \quad H_\psi = H_{01} \cos(\psi + \delta), \quad H_z = H_{02} \quad (\alpha = 1) \end{aligned} \tag{3.14}$$

At $\alpha = 1$ we obtain the uniform magnetic field $\mathbf{H} \equiv \mathbf{H}_0$. It is readily seen that $\delta = \pi/2 - \beta$, where β is the angle between projection of vector $\mathbf{H}$ onto the plane z = const and the emitter $\psi = 0$.

4°. For the subgroup H $\langle X_1 - X_2 + X_3, X_8 \rangle$ we have

$$\mathbf{V} = e^{\alpha\phi} \mathbf{J}^{(1)}(\xi), \quad \varphi = e^{\alpha\phi} J_4(\xi), \quad \rho = e^{2\alpha\phi} J_5(\xi), \quad \mathbf{H} = e^{\alpha\phi} \mathbf{J}^{(2)}(\xi) \tag{3.15}$$

Assuming $J_2 \equiv 0$ and $J_1 = \varkappa e^{-1/R} J_4^{\sigma} (0 < \sigma < 1)$, we shall obtain

$$\begin{aligned} &J_4 = \left[\frac{I_0}{2\varkappa(1-\sigma)\alpha^2}\right]^{\frac{1}{1+\sigma}} \left(\sin\left[\alpha(1+\sigma)\frac{\xi}{2}\right]\right)^{\frac{2}{1+\sigma}}, \qquad J_1 I_3 = I_0 \exp\left(-\frac{1}{R}\right) \\ &J_3' = (2J_4 - J_1^2)^{1/2}, \quad I_0 = -\alpha J_3 + a, \quad I_1 = J_3', \quad I_2 = \alpha J_1 + a\frac{J_3}{J_1} \end{aligned} \tag{3.16}$$

Here

$$\xi = \ln R, \qquad \mathbf{I}^{(2)} = R\mathbf{J}^{(2)}, \qquad I_3 = R^{\alpha} J_3, \qquad a = \text{const}$$

The given solution describes a flow, in which the particles are emitted from surface of cylinder R = 1. Particles move in planes, passing through the axis of emitter along the curves ($\sigma = 1/2$)

$$\psi = \text{const}, \qquad z = \int \left(\frac{2}{\varkappa^2} \exp\frac{2}{R} - 1\right)^{1/2} dR \tag{3.17}$$

The magnetic field of the following form satisfies equations (1.3),

(1.4)

$$H_R = -\frac{H_0}{R} e^{\alpha\psi} \sin(\alpha\xi + \delta), \quad H_\theta = \frac{H_0}{R} e^{\alpha\psi} \cos(\alpha\xi + \delta), \quad H_z \equiv 0 \qquad (3.18)$$

5°. For the subgroup H $\langle X_1 - X_2 + X_7, X_8 \rangle$ we obtain

$$V = e^{\alpha\psi} J^{(1)}(x), \quad \varphi = e^{\alpha\psi} J_4(x), \quad \rho = e^{\alpha\psi} J_5(x), \quad H = e^{\alpha\psi} J^{(2)}(x) \qquad (3.19)$$

Assuming $J_2 \equiv 0$, $J_1 = \varkappa\omega J_4^{\sigma}$ $(0 < \sigma < 1.0 < \varkappa \leq \sqrt{2})$, we shall obtain

$$J_4 = \left[\frac{J_0}{2\varkappa(1-\sigma)\alpha^2}\right]^{\frac{1}{1+\sigma}} (\sin[\alpha(1+\sigma)x])^{\frac{2}{1+\sigma}}, \quad J_1 J_5 = J_0$$
$$J_3 = (2J_4 - J_1^2)^{1/2}, \quad J_6 = -\alpha J_3 + a, \quad J_7 = J_3', \quad J_8' = \alpha J_1 + a\frac{J_3}{J_1} \qquad (3.20)$$

Solution (3.20) is a generalization of earlier considered solution [6]. At $\sigma = 1/2$ the particles move along straight lines, inclined to emitter $x = 0$ at an angle Φ $(\tan\Phi = \varkappa/\sqrt{2 - \varkappa^2})$.

The magnetic field of following form satisfies equations (1.3), (1.4)

$$H_x = -H_0 e^{\alpha y} \sin(\alpha x + \delta), \quad H_y = H_0 e^{\alpha y} \cos(\alpha x + \delta), \quad H_z \equiv 0 \qquad (3.21)$$

Thus, there are considered those subgroups in which in the case, when magnetic field is directed along the z-axis there is possible the construction of the H-solutions describing two-dimensional flows [6]. Only a uniform magnetic field which is admitted by first four of the considered subgroups satisfies equations (1.3), (1.4). For the last two of them the magnetic field may be uniform at $\alpha = 1$. Magnetic fields of form $e^{\alpha\psi}J(R)$ and $e^{\alpha y}J(x)$, where $J \neq 0$, are not realized without certain additional measures.

Let us assume that we have a two-dimensional flow in a uniform magnetic field. We shall change the direction of the vector **H**. Here the flow becomes spatial. As is evident from the above discussion the form of the solution will not be changed except only for the subgroups

H $\langle X_7, X_8 \rangle$ and H $\langle X_1, X_8 \rangle$.

6°. For the subgroup H $\langle X_1, X_3 \rangle$ we have

$$V = r^{\alpha} J^{(1)}(\theta), \quad \varphi = r^{\alpha} J_4(\theta), \quad \rho = r^{\alpha(\alpha-1)} J_5(\theta), \quad H = r^{\alpha-1} J^{(2)}(\theta) \qquad (3.22)$$

Let us consider the case, when

$$J_1 = kJ_2, \quad J_2 = \varkappa e^{-\alpha k \theta} \sqrt{J_4}, \quad J_4 = (J_2/\varkappa)^{1/2} J \qquad (3.23)$$

The solution of the system (S/H) reduces here to the solution of the equation

$$J'' + \operatorname{ctg}\theta J' + 2\alpha(2\alpha+1) J = J^{-1/2} \csc\theta \qquad (3.24)$$

At $\alpha(2\alpha + 1) = 1$ equation (3.24) coincides with equation, obtained in [8] for azimuthal electrostatic flow from a conical emitter (single-component flow in θ-direction). The function J for this case has been tabulated [8]. Thus, we obtain prepared numerical solutions for the two following flows:

$$V = \frac{1}{r} J^{(1)}(\theta), \quad \varphi = \frac{1}{r^2} J_4(\theta), \quad \rho = \frac{1}{r^2} J_5(\theta), \quad H = \frac{1}{r^2} J^{(2)}(\theta) \qquad (\alpha = -1)$$

$$V = \sqrt{r} J^{(1)}(\theta), \quad \varphi = r J_4(\theta), \quad \rho = \frac{1}{r} J_5(\theta), \quad H = \frac{1}{\sqrt{r}} J^{(2)}(\theta) \qquad (\alpha = 1/2)$$

The corresponding magnetic field and the ψ-component of the speed are determined by expressions

$$J_5 = -J_2' - \operatorname{ctg}\theta J_2 + ak\varkappa e^{-(\alpha+1)k\theta}, \qquad J_7 = (\alpha+1) J_2 + a\varkappa e^{-(\alpha+1)k\theta} \csc\theta$$

$$J_2 = kJ_1' - (\alpha+1) J_3 + a\varkappa e^{-(\alpha+1)k\theta} \csc\theta \frac{J_3}{J_2}, \qquad J_3 J_5 = J_4 e^{-2\alpha k\theta} \csc\theta$$

$$J_3 = [2 - (1+k^2)\varkappa^2 e^{-2\alpha k\theta}]^{1/2} \sqrt{J_4} \qquad (3.25)$$

It is evident that the ψ-component of speed vanishes at a $\varkappa$ value equal to $\sqrt{2/(1+k^2)}$, and if α (or k) is equal to zero. Particles abandoning conical emitter $\theta = \theta_0$, move along the surface $\ln r - k\theta =$ = const, being obtained from rotation of spiral around the z-axis.

At $\varkappa$ equal to the indicated value, and $\alpha = 0$ the trajectories are flat spirals, since here $\psi = \text{const}$ for a particle. It is of interest that equipotential surfaces in this case will be the cones $\theta = \text{const}$. At $k = 0$ a particle abandoning the emitter at point with coordinates r_0, θ_0, ψ_0, moves along a sphere of radius r_0, where its coordinates θ, ψ are associated by the relationship

$$\psi - \psi_0 = \frac{\sqrt{2-\varkappa^2}}{\varkappa}\left(\ln \operatorname{tg}\frac{\theta}{2} - \ln \operatorname{tg}\frac{\theta_0}{2}\right) \tag{3.26}$$

At $k = 0$ and $\varkappa = \sqrt{2}$ we obtain single-component flows in the θ-direction. The solution given in [8] is a particular case of this series of solutions when $\alpha = -1$ and magnetic field is lacking. Assuming

$$3\alpha J_1 + \operatorname{ctg}\theta J_2 = 0, \qquad J_3 = \varkappa \sqrt{J_4}\sin\theta \tag{3.27}$$

we shall obtain the equation (3.24) for the potential. Furthermore, we have

$$\begin{gathered}
J_1 = -\frac{\varkappa}{3\alpha}\sqrt{J_4}\cos\theta, \quad J_2 = \left[2 - \varkappa^2\left(\sin^2\theta + \frac{\cos^2\theta}{9\alpha^2}\right)\right]^{1/2}\sqrt{J_4} \\
J_2 = -J_2' - \operatorname{ctg}\theta J_2 - \frac{\varepsilon}{3\alpha}\frac{\operatorname{ctg}\theta}{(\sin\theta)^2}, \quad J_2 J_3 = J_0 \left(\chi = \frac{2\alpha - 1}{3\alpha}\right) \\
J_4 = (\alpha + 1) J_2 + \frac{\varepsilon}{(\sin\theta)^2}, \quad J_4 = J_4' - (\alpha + 1) J_2 + \frac{\varepsilon}{(\sin\theta)^2}\frac{J_2}{J_4}
\end{gathered} \tag{3.28}$$

The trajectories are located on surface of the figures of rotation

$$r^{3\alpha}\sin\theta = \text{const} \tag{3.29}$$

At $\varkappa = \sqrt{2}$ and $\alpha^2 = 1/9$ the speed in ψ-direction v_ψ becomes zero. At $\alpha = 1/3$ the particles from conical emitter $\theta = \theta_0$ move in straight lines parallel to the z-axis. At $\alpha = -1.1/2$ again we have at our disposal prepared numerical solutions. At $H \equiv 0$ the flows from conical emitter were investigated in work [9], in which there are given

numerical results for a number of α and θ_0 values. The flow in this case is potential: $v_i = \partial W/\partial x^i$, where W is the action pertaining to the mass of the particle.

We examined what magnetic fields satisfy the equations (1.3), (1.4). For the radial component J_6 of the magnetic field we obtain Legendre's equation whose solution is the Legendre functions of first and second kind $P_\alpha(\xi)$ and $Q_\alpha(\xi)$. Inasmuch as $J_6' = \alpha J_7$, then the θ-component H may be expressed in terms of the associated Legendre functions $P_\alpha^1(\xi)$ and $Q_\alpha^1(\xi)$ of the first and second kind of degree α and of order 1. Here $\xi = \cos\theta$.

For J_8 we have the following alternative:

$$J_\theta = H_{0\theta}\csc\theta \quad (\alpha = 0), \qquad J_\theta = 0 \quad (\alpha \neq 0) \tag{3.30}$$

At $\alpha = 0$ and $\alpha = -1$ the solution of equations (1.3), (1.4) is determined by the formulas

$$H_r = \frac{H_{01}}{r} = \frac{H_{01}}{r} P_0(\xi), \quad H_\theta = \frac{1}{r}\left(H_{01}\operatorname{ctg}\theta + \frac{H_{0\theta}}{\sin\theta}\right), \quad H_\phi = \frac{H_{0\theta}}{r\sin\theta} \quad (\alpha = 0)$$
$$H_r = \frac{H_0}{r^2}\ln\operatorname{tg}\frac{\theta}{2} = -\frac{H_0}{r^2}Q_0(\xi), \quad H_\theta = \frac{H_0}{r^2\sin\theta}, \quad H_\phi \equiv 0 \quad (\alpha = -1) \tag{3.31}$$

At $\alpha = 1$ and $J_6 = H_0 P_1(\xi)$ we have

$$H_r = H_0\cos\theta, \qquad H_\theta = -H_0\sin\theta, \qquad H_\phi \equiv 0 \tag{3.32}$$

Formulas (3.32) determine a uniform magnetic field directed along the z-axis, i.e., along the axis of conical emitter $\theta = \theta_0$.

Thus, a flow of the form (3.22) in a uniform magnetic field is possible when this field is directed along the z-axis. In the deviation of H from this direction the flow parameters do not satisfy formulas (3.22).

7°. For the subgroup $H \langle X_1 - X_2 + X_8,\ X_3\rangle$ we obtain

$$V = e^{\alpha z} f^{(1)}(R),\quad \varphi = e^{\alpha z} f_4(R),\quad \rho = e^{\alpha z} f_5(R),\quad H = e^{\alpha z} f^{(2)}(R) \qquad (3.33)$$

At $H \equiv 0$ flows of the form (3.33) from cylindrical emitter in case of emission limited by a space charge, were investigated in [9]. The flow in this case is potential, the action is determined by expression

$$W = e^{\alpha z} f(R) \qquad (3.34)$$

The common solution of equations (1.3), (1.4) has the form

$$H_R = e^{\alpha z} Z_1(\alpha R),\quad H_\varphi \equiv 0,\quad H_z = e^{\alpha z} Z_0(2\alpha\sqrt{R})\quad (Z_\alpha = c_1 J_\alpha + c_2 Y_\alpha) \qquad (3.35)$$

Here J_α and Y_α are cylindrical functions of first and second kind; c_1, c_2 are arbitrary constants.

8°. For the subgroup $H \langle X_1 - X_2 + X_3,\ X_1 - X_2 + X_8\rangle$ we obtain

$$\begin{aligned} V &= e^{\alpha\varphi+\beta z} f^{(1)}(R), & \varphi &= e^{\beta(\alpha\varphi+\beta z)} f_4(R) \\ \rho &= e^{\beta(\alpha\varphi+\beta z)} f_5(R), & H &= e^{\alpha\varphi+\beta z} f^{(2)}(R) \end{aligned} \qquad (3.36)$$

At $H \equiv 0$ the solution of the form (3.36) was considered in [10]. Form of solution was established by method of separation of the variables.

Equations (1.3), (1.4) result in the following equation:

$$\frac{d^2 J_0}{d\xi^2} + \frac{1}{\xi}\frac{dJ_0}{d\xi} + \left(1 - \frac{\nu^2}{\xi^2}\right) J_0 = 0 \qquad (3.37)$$

Cylindrical functions of first and second kind are the solution of (3.37). In the considered case $\xi = \alpha R$ and $\nu = i\alpha/\beta$.

9°. For the subgroup $H \langle X_1 - X_2 + X_3,\ X_1\rangle$ we have

$$\begin{aligned} V &= r^\alpha e^{\alpha\varphi} f^{(1)}(\theta), & \varphi &= r^{\alpha z} e^{\alpha\varphi} f_4(\theta) \\ \rho &= r^{\alpha(\alpha-1)} e^{\alpha\varphi} f_5(\theta), & H &= r^{\alpha-1} e^{\alpha\varphi} f^{(2)}(\theta) \end{aligned} \qquad (3.38)$$

The solution of the system (S/H) for a given H-solution can be replaced by integrating an equation of the form (3.1) for $\alpha = 0$ and $\alpha = -1/2$. Assuming $\alpha = 0$, $J_3 \equiv 0$ and $J_2 = kJ_4^{\sigma} \sin\theta (0 < \sigma < 1.0 \leq k \leq \sqrt{2})$, we shall obtain

$$J_4 = \left[\frac{J_0}{2k(1-\sigma)\beta^{\sigma}}\right]^{\frac{1}{1+\sigma}} (\sin[\beta(1+\sigma)(\xi - \xi_0)])^{\frac{\sigma}{1+\sigma}} \quad \left(\xi = \ln \operatorname{tg}\frac{\theta}{2}\right) \tag{3.39}$$

At $\sigma = 1/2$ and $k = \sqrt{2}$ we obtain the simplest expressions for the components V and H

$$J_1 = \pm\sqrt{2J_4}\cos\theta, \quad J_2 = \sqrt{2J_4}\sin\theta, \quad J_3 = (2\beta J_4 \csc\theta + J_1 J_2)/J_2$$
$$J_2 = -\beta\csc^2\theta\left[J_1\sin\theta + \int\cos\theta(\csc\theta - 1)J_1 d\theta\right], \quad J_3 = J_1' - J_2 \tag{3.40}$$

The trajectories as is evident from (3.40) will be the plane curves

$$r\sin\theta = \text{const} \quad (J_1 = \sqrt{2J_4}\cos\theta), \quad r\csc\theta = \text{const} \quad (J_1 = -\sqrt{2J_4}\cos\theta) \tag{3.41}$$

If there occurs the first formula (3.41), then particles from emitter $\theta = \theta_0$ move in straight lines parallel to z-axis.

Equations (1.3), (1.4) results in the equation

$$(1-\xi^2)\frac{d^2 I_\beta}{d\xi^2} - 2\xi\frac{dI_\beta}{d\xi} + \left[\alpha(\alpha+1) - \frac{\mu^2}{1-\xi^2}\right]I_\beta = 0 \tag{3.42}$$

whose solutions are associated Legendre function of the first and second kind. In the considered case

$$I^{(m)} = \sin\theta J^{(m)}, \quad \xi = \cos\theta, \quad \mu = i\beta$$
$$\text{At } \alpha = 0 \text{ и } \alpha = -1 \text{ we find } (\xi = \ln \operatorname{tg}^{1}/_{2}\theta)$$
$$J_\theta = \frac{aH_0}{\beta}\sin\theta\cos(\beta\xi + \delta), \quad J_r = -H_0\sin(\beta\xi + \delta), \quad J_\theta = H_0\cos(\beta\xi + \delta) \tag{3.43}$$

10°. For the subgroup H $\langle X_3, X_4\rangle$ we obtain

$$a_r = J_3(r), \quad \varphi = J_4(r), \quad \rho = J_5(r), \quad H_r = J_6(r) \tag{3.44}$$

The radial magnetic field in no way affects the flow described by formulas (3.44). The series solution of the system (S/H) determining a given H-solution is given in work [11] for case of emission limited by space charge. In works [12-14] solution of system (S/H) is expressed in terms of Airy functions for different conditions of emission.

Thus, there are considered all the essentially different invariant group solutions of rank 1 equations of stationary charged-particle beam. In work [4] there were given examples of H-solutions of rank 2, which are constructed of one-parameter subgroups, but are determined in the final analysis from a system of ordinary differential equations. At the same time such solutions are not invariant with respect to any two-parametric subgroups of the basic group G of the system of partial differential equations (S) being investigated. In our case, etc, such examples can not be constructed. This is explained by the difference between the space coordinate and time.

§ 4. Certain Remarks

In this work there have been investigated group properties of equations of a normal nonrelativistic charged-particle beam in stationary case in arbitrarily oriented external magnetic field. There was found a common solution of system of determining equations for coordinates of infinitesimal operators, determining basic group of G equations of the beam (S). The construction of optimum system of two-parametric subgroups has assured the finding of all essentially different H-solutions of rank 1. The invariant-group solutions were obtained in four orthogonal systems of coordinates: Cartesian x, y, z; cylindrical R, ψ, z; spiral cylindrical q_1, q_2, z; spherical r, θ, ψ. The Cartesian and cylindrical system of coordinates are limiting cases of spiral cylindrical system of coordinates [6].

Clarification of question about those coordinate systems, in which there are possible single-component flows [15], i.e., a flow in direction of one of coordinate axes, at $H \equiv 0$ was the thesis of a number of works [16-22]. In works [16-18, 20, 21] there was made an attempt to formulate the conditions necessary and sufficient for possibility of single-component flow in the x^1-direction in the given system of coordinates x^1 ($i = 1, 2, 3$).

The sufficient conditions are formulated both as conditions under which equation (4.1) is transformed into an ordinary differential equation with respect to w

$$h\sqrt{w}\frac{d^2w}{dx_1^2} + \frac{\partial f_1}{\partial x_1}\sqrt{w}\frac{dw}{dx_1} + f_1 f_2 \sqrt{w} w = F(x_2, x_3)$$
$$f_1(x_1, x_2, x_3) = \frac{h_2 h_3}{h_1}, \quad f_2(x_1, x_2, x_3) = h_1^6 \Delta\left(\frac{1}{h_1^2}\right), \quad w(x_1) = \left(\frac{dW}{dx_1}\right)^2 \qquad (4.1)$$

Here $h_\alpha = \sqrt{g_{\alpha\alpha}}$ are the Lamé coefficients; W is the action; $F(x_2, x_3)$ is a certain function. In work [20] the question about reduction of equation (4.1) to an ordinary equation in fact reduces to the same question for a linear homogeneous equation

$$G(x_1, x_2, x_3)\frac{d^2w}{dx_1^2} + H(x_1, x_2, x_3)\frac{dw}{dx_1} + K(x_1, x_2, x_3) = 0 \qquad (4.2)$$

Finally sufficient conditions were written out only in case of the two variables ξ, η, [22]. Question about number of coordinate systems in which there are possible single-component flows has remained open.

The investigation of group properties of equations of a beam conducted in present work makes it possible to corroborate that single-component flows are possible only in the four indicated systems of coordinates. In connection with this, the results of work [20] become understandable; in this work there was investigated a large

number of coordinate systems and it was shown that single-component flows in these systems are impossible. The separation of variables in the equations of beam are possible, apparently, only in these four systems of coordinates.

Thus, the particles can be emitted from following surfaces:

1) planes x = const; 2) circular cylinders R = const; 3) half-planes ψ = const; 4) spiral cylinders q_1 = = corst (q_2 = const); 5) spheres r = const; 6) cones θ = const.

In work [22] there were written general expressions for potential in case of the two variables ξ, η, at H = 0 in the finite form or in quadratures where the potential completely was determined by assignment of metrics in system being considered to the ordinates. In the case, when f_1 may be presented as

$$f_1(\xi, \eta) = X(\xi) Y(\eta) \tag{4.3}$$

final expression for potential was determined by the formula

$$\varphi = \varphi_0 [L(\xi)]^{-n} \tag{4.4}$$

Function $L(\xi)$ followed from the expression

$$\frac{\partial}{\partial \eta} \frac{h_0}{Y} = L(\xi) M(\eta) \tag{4.5}$$

We note that for the four above-indicated systems of coordinates there occurs precisely this case. Unfortunately, formula (4.4) cannot be used. Owing to the fact that $f_2 \equiv 0$ in all these systems, $L(\xi)$ remains indeterminate. All relationships obtained in [22] including the expression for proportionality factor in the 3/2 law for an arbitrary single-component flow have sense only for solutions of the type (4.6) leaving a degenerated character and the validly contrasted [16, 17] to solutions describing single-component flows from a surface on which there are realized conditions of a thermo-emission.

It must be mentioned that all the solutions known to author describing flows having their beginning from a thermo-emissional cathode are invariant-group solutions. Only certain solutions not satisfying conditions of a thermo-emission represent an exception.

1°. A two-dimensional electrostatic flow along hyperbolic trajectories with vector of speed V = {ax, by} and with constant density of space charge [23]. At a = -b the flow becomes irrotational and the action has the form

$$W = \frac{a}{2}(x^2 - y^2) \tag{4.6}$$

The solution (4.6) is a unique solution obtained on the assumption on constant density of space charge [24]. Under this assumption the number of equations does not decrease and therefore, (4.6) is solution of an overdetermined system. Actually, for the function w in this case there is obtained two second order differential equations [20] instead of one equation. Just by this is there explained the fact that solution (4.6) is not invariant.

2°. The generalization of solution in Paragraph 1° in a spatial case [25]. Here, the vector of the speed and the trajectories are determined by the expressions

$$\mathbf{V} = (ax, by, -(a+b)z), \quad xyz = \text{const}, \quad x^b y^{-a} = \text{const} \tag{4.7}$$

The density of space charge is constant.

3°. The solution [26, 27] for a two-dimensional flow in uniform magnetic field perpendicular to the plane of flow on hyperbolic or elliptic trajectories is

$$(\omega + a)x^2 + (\omega - a)y^2 = \text{const} \qquad (\omega = eH/mc) \tag{4.8}$$

The density of the space charge is constant. The potential is determined by expression

$$2\varphi\varphi + (\varphi + a)^2\varphi^2 + (\varphi - a)^2\varphi^2 = 0 \qquad (4.9)$$

4°. Two-dimensional electrostatic periodic flow [26, 19]. The trajectories of particles and potential are determined by formulas

$$\cos 2x + \operatorname{ch} 2y = \text{const}, \qquad \frac{\varphi}{\varphi_0} = \frac{\operatorname{ch} 2x \pm \cos 2y}{\operatorname{ch} 2x - \cos 2y} \qquad (4.10)$$

An investigation of group properties of equations of a nonrelativistic beam makes it possible to make certain conclusions also for case of relativistic speeds when radiation of moving charges can be ignored.

Owing to the manifestation in the equations of motion of additional nonlinearity $\sqrt{1 - V^2}$ (in the reduction to a dimensionless form as characteristic speed the velocity of light c is selected) the basic group of equations of relativistic beam will be less extensive than in a nonrelativistic case. It is readily seen that this nonlinearity does not make it possible to make an extension of the speed. Therefore, the H-solutions of equations of relativistic beam have the same form as H-solution in the nonrelativistic case corresponding to zero value of the arbitrary parameter α. In a strict calculation of the inherent magnetic field and for the case when through each point of space there passes only one line of flow, single component flows beginning from a thermo-emission cathode are impossible. In the class of flows with $v_n = 0$, where v_n is the component of speed normal to the equipotential surfaces there are possible the following single-component flows: flow in the z-direction when the equipotential surfaces are spiral and circular cylinders parallel and passing through the z-axis of the plane; flow in ψ-direction when equipotential surfaces are

circular cylinders [28]; flows in the r- and ψ-directions when the equipotential surfaces are coaxial cones. For a flow in r-direction there can be obtained an analytic solution. For the potential we obtain

$$J_0 = \frac{1 + b^2 (\operatorname{tg}^2 \tfrac{1}{2}\theta)^{2a}}{2b (\operatorname{tg}^2 \tfrac{1}{2}\theta)^a} \tag{4.11}$$

Here a, b are arbitrary constants. At a = b = 1 the solution has the form

$$v_r = \pm \cos\theta, \quad v_\theta = v_\psi = 0, \quad \varphi = \frac{1}{\sin\theta}, \quad \rho = \frac{1}{r^2 \sin^2\theta}$$
$$H_r = H_\theta = 0, \quad H_\psi = \mp \frac{1}{r \sin^2\theta} \tag{4.12}$$

Relativistic flow having its source from a surface, on which there are realized conditions of a thermo-emission is possible only in a diode with spiral electrodes q_1 = const and in diode with electrodes in which there are the inclined half-planes ψ = const. These flows may be either two-dimensional or three-dimensional.

We note in conclusion that from all enumerated solutions of equations of a relativistic beam only the solution for single-component flow in z-direction is not invariant with all the functions f

$$v_z = \omega f(x, y) \qquad (\Delta f = 0) \tag{4.13}$$

It will be the H-solution at $f = q_1$, $f = q_2$ and their limiting expressions ($b_1, b_2 \to 0$; $b_1 \to 0$, $b_2 \to 1$).

Submitted
6 February 1963

Literature

1. L. V. Ovsyannikov. Groups and invariant-group solutions of differential equations. Reports of the Academy of Sciences of USSR, 1958, Vol. 118, No. 3.

2. L. V. Ovsyannikov. Group properties of equation of a nonlinear thermal conduction. Reports of the Academy of Sciences of USSR, 1959, Vol. 125, No. 3.

3. L. V. Ovsyannikov. Group properties of differential equations. Siberian Department, Academy of Sciences of USSR, 1962.

4. V. V. Pukhnachev. Group properties of equations of Navier-Stokes in a two-dimensional case. PMTF, 1960, No. 1.

5. Yu. N. Pavlovskiy. Investigation of certain invariant solutions of boundary-layer equations. Journal of computer math. and mathematical physics, 1961, Vol. 1, No. 2.

6. V. A. Syrovoy. Invariant-group solutions of equations of a two-dimensional stationary charged-particle beam. PMTF, 1962, No. 4.

7. R. J. Lomax. Single Component Relativistic Space Charge Flow. J. Electronics and Control, 1958, Vol. 5, No. 6.

8. W. E. Waters. Azimuthal Electron Flow in a Spherical Diode. J. Appl. Phys., 1959, Vol. 30, No. 3.

9. P. T. Kirstein and G. S. Kino. Solution to the Equations of Space – Charge Flow by the Method of the Separation of Variables. J. Appl. Phys., 1958, Vol. 29, No. 12.

10. P. T. Kirstein. Curvilinear Space-Charge Flow for Convergent Electron Guns. Techn. Rep., M. L. Report No. 440, Microwave Laboratory, Stanford Universkty, Stanford, California.

11. I. Langmuir and K. Blodgett. Currents Limited by Space Charge Between Concentric Spheres. Phys. Rev., 1924, Vol. 24, pp. 49-59.

12. V. L. Kan. Exact solution of Langmuir's problem for a spherical capacitor. Journal of tech. physics, 1948, Vol. 18, No. 4.

13. R. P. Poplavskiy. Distribution of potential in spherical capacitor in the ease of a saturation current. Journal of tech. physics, 1950, Vol. 20, No. 2.

14. I. Itzkan. Solutions of the Equations of Space Charge Flow for Radial Flow Between Concentric Spherical Electrodes. J. Appl. Phys., 1960, Vol 31, No. 4.

15. B. Meltzer. Single-Component Stationary Electron Flow Under Space Charge Conditions. J. Electronics, 1956, Vol 2, No. 2.

16. W. M. Mueller. Electronics Research Laboratory Report, Series No. 60, Issue No. 143, 1957, Universkty of California, Berkley, California.

17. A. R. Lucas, B. Meltzer, and G. A. Stuart. A General Theorem for Dense Electron Beams. J. Electronics and Control, 1958, Vol. 4, No. 2.

18. B. Meltzer and A. R. Lucas. Sufficient and Necessary Trajectory Conditions for Dense Electron Beams. J. Electronics and Control, 1958, Vol. 4, No. 5.

19. P. T. Kirstein. Comments on "A General Theorem for Dense Electron Beams" by A. R. Lucas, B. Meltzer, and G. A. Stuart. J. Electronics and Control, 1958, Vol. 4, No. 5.

20. W. M. Mueller. Necessary and Sufficient Trajectory Conditions for Dense Electron Beams. J. Electronics and Control, 1959, Vol. 5, No. 6.

21. W. M. Mueller. Comments on Necessary and Sufficient Trajectory Conditions for Dense Electron Beams. J. Electronics and Control, 1960, Vol. 8, No. 2.

22. J. Rosenblatt. Three-Dimensional Space Charge Flow. J. Appl. Phys., 1960, Vol. 31, No. 8.

23. B. Meltzer. Electron Flow in Curved Paths Under Space-Charge Conditions. Proc. Phys. Soc. B, 1949, Vol. 62, No. 355.

24. G. B. Walker. Congruent Space Charge Flow. Proc. Phys. Soc. B, 1950, Vol. 63, No. 372.

25. B. Meltzer. Electron Flow in Curved Paths Under Space — Charge Conditions. Proc. Phys. Soc. B, 1949, Vol. 62, No. 360.

26. P. T. Kirstein. The Complex Formulation of the Equations of Two-Dimensional Space-Charge Flow. J. Electronics and Control, 1958, Vol. 4, No. 5.

27. L. R. Walker. Generalization of Brillouin Flow. J. Appl. Phys., 1955, Vol. 26, No. 6.

28. O. Buneman. Self-Consistent Electrodynamics. Proc. Cambridge Philos. Soc., 1954, Vol. 50, No. 1.

INTEGRAL-MOMENT METHOD OF SOLVING THE BOLTZMANN KINETIC EQUATION

by

M. N. Kogan (Moscow)

A method is proposed which enables one to compute the flow of a gas, in principle, with an arbitrary Knudsen number. This method is convenient practically for solving problems where the knudsen numbers are not too small ($a \ll K \ll \infty$, where $0 < a < 1$).

Sec. 1. The motion of a rarefied gas with random Knudsen numbers is described by Boltzmann's equation which for a single-atom gas in the absence of mass forces has the form

$$\frac{df}{dt} = \frac{\partial f}{\partial t} + \xi_i \frac{\partial f}{\partial x_i} = J(t, x_i, \xi_i) \tag{1.1}$$

Here $f(t, x_i, \xi_i)$ is the function of the distribution standardized in such a way that the integral

$$\int f d\xi_1 d\xi_2 d\xi_3 \equiv \int f d\xi$$

is equal to the number of molecules in a unit of volume, t is the time, x_i is the Descartes coordinates, ξ_i is the components of the velocity vector of the molecule, and

$$J(t, x_i, \xi_i) = \int [f(\xi') f(\eta') - f(\xi) f(\eta)] g b db d\theta d\eta \tag{1.2}$$
$$(d\eta = d\eta_1 d\eta_2 d\eta_3, \quad g = |\eta - \xi|)$$

is the integral of collisions. Here $\eta = \{\eta_1, \eta_2, \eta_3\}$ is the vector of velocity of the molecules, b is the sighting distance of the molecules in the collision process, θ is the angle reckoned from the random direction in the plane perpendicular to the vector g, and ξ' and η' are the vectors of velocity after collision of the molecules which have up to the collision respectively the velosicies ξ and η.

The function $f(\xi)$ does not depend on the variable of the integration of η; therefore the integral of the collisions can be represented in the form

$$J(t, x_i, \xi_i) = L(t, x_i, \xi_i) - f(t, x_i, \xi_i) G(t, x_i, \xi_i) \tag{1.3}$$

The integrals L and G are finite only for molecules with a finite radius of interaction.

Boltsmann's equation is often written in the integral. Apparently for any differential equation it is possible to juxtapose an endless number of integral equations equivalent to it. Considering, for example, J to be an unknown, Boltsmann's equation can be considered as an ordinary differential equation, the general solution of which has the form [1, 2]

$$f(t, x_i, \xi_i) = f(t_0, x_i - \xi_i(t - t_0), \xi_i) + \int_{t_0}^{t} J(\tau, x_i - \xi_i(t - \tau), \xi_i)\, d\tau \qquad (1.4)$$

By considering L and G as given we will get another integral form of the equation (see, for example [3—4])

$$f(t, x_i, \xi_i) = f(t_0, x_i - \xi_i(t - t_0), \xi_i) \exp\left\{-\int_{t_0}^{t} G(\tau, x_i - \xi_i(t - \tau), \xi_i)\, d\tau\right\} + \qquad (1.5)$$

$$+ \int_{t_0}^{t} L(s, x_i - \xi_i(t - s), \xi_i) \exp\left\{-\int_{s}^{t} G(\tau, x_i - \xi_i(t - \tau), \xi_i)\, d\tau\right\} ds$$

Ordinarily, where the Knudsen numbers are small one gets by one or another expansion the functions of the distribution along the length of the run near the Maxwell distribution [2].

Where $K \gg 1$ the function of distribution is expanded in accordance with the magnitude K^{-1}, or one makes use of the method of successive approximations which is equivalent to this expansion. In the report [2] it is shown with definite limitations, that this process converges for the times less than the time of relaxation or areas less than the length of the run, i. e., for numbers $K \gg 1$. Ordinarly (see, for example, [2, 5—7]) for f_c one uses the solution for free molecular flow and the integration is carried out from the boundaries of the area.

Sec. 2. Stationary and nonstationary problems for Boltsmann's equation are solved in qhite distinct ways. Therefore one can consider f_0 as some initial state, and instead of the successive approximations one can solve

the corresponding nonstationary problems:

$$f(t_n, x_i, \xi_i) = f(t_{n-1}, x_i - \xi_i \Delta t, \xi_i) + \int_{t_{n-1}}^{t_n} J_{n-1}(t_{n-1}, x_i - \xi_i (t_n - \tau), \xi_i) d\tau \quad (2.1)$$

where J_{n-1} is calculated in accordance with the value of the function f at the moment of time t_{n-1} and $t_n = t_0 + n\Delta t$. Let t be the full interval of time over the course of which one considers the process. If one selects intervals of time Δt so small that during this time J changes only by an amount of the order of Δt then after N number of steps ($\Delta t = T / N$). The solution obtained will differ from the precise one by a value of the order of Δt (just so as in the case of the numerical solution of an ordinary differential equation). In the equality (2.1) the integration is carried out along the trajectory of the molecules. Therefore the integrals J are obtained at the expense of change in f in accordance with the time and the coordinates.

Two processes lead to change of the function of distribution. From one side to a given point of space there come molecules from different areas of flow. If L is characteristic of the dimensions of the flow, and ξ characteristic of the velocity of the molecules, then a characteristic time of this process will be $T_1 = L/\xi$. On the other hand the function of the distribution changes as a result of the collision of the molecules. The characteristic time of this process proves to be the time of the relaxation or the time between the collisions of the molecules $T_2 = \lambda/\xi$, where λ is the characteristic length of the run[1].

For flows with Knudsen numbers of the order of unity the two characteristic times have identical orders $T_1 \sim T_2 \sim T$, so that by selecting sufficient-large N we can rewrite (2.1) in a different form

$$f(t_n, x_i, \xi_i) = f(t_{n-1}, x_i - \xi_i \Delta t, \xi_i) + J_{n-1}(t_{n-1}, x_i, \xi_i) \Delta t \quad (\Delta t = T/N) \quad (2.2)$$

[1] Speaking generally the flow can encompass several characteristic lengths of run and several characteristic velocities of the molecules (see, for example, [8]).

With small Knudsen number $T_2 \ll T_1$. In this case if one takes $\Delta t \ll T_2$ very many steps are necessary. Therefore here it is essential to consider that at each point during a time of the order of T_2 equilibrized distribution is accomplished, or close to it, which is also done in the methods used for low Knudsen numbers.

For high Knudsen numbers, on the other hand, the transfer of molecules from some areas into others is a more rapid process than the change of the function of distribution as a result of collisions. Here Δt should be less than T_1.

If the state is known close to the one sought, then the number of steps naturally is reduced. Thus if one is researching the stationary flow close to the free-molecular one, and for the initial state one takes one takes the solution for the free-molecular flow, then the procedure (2.1) practically coincides with the successive approximations (1.4) or (1.5).

In this case it is possible to take large sections of time $\Delta t \sim L/\xi = T_1$, since the function of distribution at any point can change at the most to a magnitude of the order of $f_0 K^{-1}$ and the integral $J \sim f_0/T_2$. Consequently, the error with $\Delta t \sim T$ will be of the order of $f_0 K^{-2}$.

Practically in the finding of the first correction to the free molecular flow the integration is done between the boundaries, and the correction to the free-molecular function of the distribution occurs only on the boundaries of the area (for example, on the surface of the body [5—7]).

For computing the following approximation it is necessary to find and keep in mind the function of the distribution of the first approximation in the inner points of the flow, which makes the problem too complicated for modern computing machines.

Therefore the flow which requires the computation of the second and following approximations will be computed best in line with the point sought

by the integral-moment method proposed below.

Sec. 3. In accomplishing the numerical process (2.2) two difficulties crop up. In the first place the integral the integral J_n possesses a complicated structure, which requires not only squaring but also the computation of the velocities of the molecules after collision, i. e., accompanying repeated solution of the problem of collision. In the second place at each step one is required to keep in mind too many values (at each point of space at a given moment of time the function of distribution depends on the three components of velocity). Therefore the operating memory of modern computing machines with difficulty can suffice for solving the most simple (single-dimension) problems that come up. These difficulties are overcome in the following way with the aid of the introduction of moments from the function of distribution. As is known moments from the function of distribution is the term used for the expression in the form

$$n(t, x_i) = \int f(t, x_i, \xi_i)\,d\xi, \qquad u_i(t, x_i) = \frac{1}{n}\int \xi_i f(t, x_i, \xi_i)\,d\xi$$
$$P_{ij}(t, x_i) = \int c_i c_j f(t, x_i, \xi_i)\,d\xi, \qquad q_i(t, x_i) = \frac{m}{2}\int c_i c^2 f(t, x_i, \xi_i)\,d\xi \tag{3.1}$$
$$M_{ijk} = \int c_i c_j c_k f\,d\xi \quad \text{и т. д.} \quad (c_i = \xi_i - u_i)$$

Here u_i stands for the components of the vector of the macroscopic velocity, P_{ij} for the components of the tensor of stresses, q_i for the components of the flow of energy, etc.

Let us approximate the function of the distribution of some analytical dependence

$$f(t, x_i, \xi_i) = F(\xi_i, A_1, \ldots, A_\tau) \tag{3.2}$$

where A_α $(\alpha = 1, \ldots, \tau)$ are some functions of t and x_i. The form of the function F and the number of parameters A_α are determined by the character of the concrete problem and the required precision of the approximation, which should correspond to the precision of the whole computation (i. e., to the precision of the original data and boundary conditions, the selected step, etc.).

The function F can be chosen different in the different parts of the flow and should take into account the discontinuous character in accordance with ξ of the behavior of the function of distribution at the boundaries.

By substituting (3.2) in (3.1) one can express ν moments through ν coefficients of A_α and vice versa.

Considering that molecules with ξ velocities greater than ξ_{max} are very few and can be disregarded, we will select Δt in such a way that the integral J will change little during the time Δt and over the distance $\xi_{max} \Delta t$. In Boltzmann's equation the velocity ξ comes in as a parameter. If we fix some number of values ξ_γ ($\gamma = 1, \ldots, m$) and for each ξ_γ write Boltzmann's equation then we will get a system from m joint ordinary differential equations for m functions of $f(t, x_i, \xi_\gamma)$. The left sides of these equations contain only the derivatives along the direction ξ_γ from the functions $f(t, x_i, \xi_\gamma)$ and the right sides depend on all m functions.

The selected m directions can be considered as characteristic and the solution can be worked out in the same way as this is done for hyperbolic differential equations. In the solution of hyperbolic equations the characteristic directions are determined by the original equations. In the case under consideration the selection ξ_γ, and consequently also the selection of the characteristic directions, is at our disposal. Therefore they may be chosen so that in the computation of the moments in some node of the mesh x_i all m points $x_i - \xi_\gamma \Delta t$ also will be nodes of the mesh[1]. With such a selection of ξ_γ there are not required interpolations of the data obtained on the $(n-1)$-th step.

On the $(n-1)$-th step in each of the nodes of the mesh let all ν moments from the function f_{n-1} be known. By multiplying (2.2) respectively

[1] The choice of Δt depends on the number of selected equations m.

by $1, \xi, \ldots$, etc. we get ν moments from f_n at the point x_i at the moment of time t_n.

For calculating the integral from the function $f(t_{n-1}, x_i - \xi_i \Delta t, \xi_i)$, the respective values of this function are computed by (3.2) with the aid of values known in the nodes. The integrals

$$\int J_{n-1} d\xi \equiv \int \xi_i J_{n-1} d\xi = (c_1^2 + c_2^2 + c_3^2) J_{n-1} d\xi \equiv 0 \quad (d\xi = d\xi_1 d\xi_2 d\xi_3)$$

since they express, respectively, the conservation of mass, impulse, and energy in the collision of molecules. There is also no need for computing at what point there are the higher moments from J_{n-1}. With the given approximation and law of interaction of molecules the squaring in accordance with ξ and η can be done once, so that these integrals will be known functions from the moments. Therefore the computation of the integrals

$$\int c_i c_j J_{n-1} d\xi \quad \text{and} \quad \int c_i c_j c_k J_{n-1} d\xi$$

converges to some number of algebraic operations. Speaking generally, the computation of the moments from the integral of collisions is simpler than the computation of the integral itself, since in integration in accordance with ξ the integral becomes symmetrical relative to the velocities η and ζ.

In the report [9] it is shown, for example, that for Maxwell molecules with a random function of distribution represented by an infinite series in accordance with Hermite's polynomials, the moments from J have a specially simple form

$$\int c_i c_j J d\xi = A_1 p_{ij} \rho, \quad \int c_i c^2 J d\xi = A_2 q_i \rho \quad (p_{ij} = P_{ij} - \delta_{ij} p)$$

where A_1 and A_2 are the magnitudes depending on the kind of molecules. In this same work there are presented expressions which give a good approximation also with other laws of interaction of molecules. In any case for each law of interaction and selected approximation (3.2) it is necessary only once to carry out the respective squaring, so that in the computation of the flow the moments from the integral of the collisions enter as algebraic functions of/

the moments from the function of distribution and not the function itself.

Sec. 4. The above-described non-stationary approach has the advantage that it enables one to make the calculation by the direct method, i. e., to compute directly the values of the unknown functions for the n-th step in accordance with the values for these functions at the (n—1)-th step. But this approach has the shortcoming that the step Δt should be less than the two characteristic times T_1 and T_2. Therefore with the diminishing of the time of relaxation there is necessary a constantly greater number of steps. In a number of cases it may prove to be to the point to change the procedure somewhat passing to the solution of the stationary problem.

Let us replace (2.2) by the equation

$$f(x_i, \xi_j) = f(x_i - \xi_j \Delta t, \xi_j) + J(x_i, \xi_j)\,\Delta t \qquad (4.1)$$

where Δt is selected in such a way that the integral J changes little over the distance $\xi_{max}\Delta t$. By selecting as above m values of ξ_j, so that in the computation of f in the node of the mesh x_i all m points of $x_i - \xi_j \Delta t$ also prove to be nodes of the mesh, and multiplying (4.1) by the respective combinations of velocities, besides integrating in accordance with ξ, we get the system $N_1 v$ of joint algebraic equations for determining v moments in each of the N_1 nodes of the mesh. The problem is reduced to the solution of the system of nonlinear equations for macroscopic values. The problem becomes more complicated at $T_2 \to 0$ since the integral J has singularity at $T_2 = 0$.

In the usual method the function of distribution also is charged by some approximation function depending on some number of moments. By multiplying Boltzmann's equation by the corresponding combinations of velocities one gets the necessary number of differential equations for the moments.

Meanwhile the the type and the number of equation depend on the selected approximations and moments. Therefore for each concrete case it was necessary to develop one's methods of solution of the occurring complex systems of dif-

ferential equations. Here, just the same as above, there is possible a stationary and a nonstationary approach to the solution of the problem. However, the number of the characteristics, and consequently also the character of the boundary problems for this system, is determined by the choice of approximations. From the complexity of the equations it is difficult to follow the physics of the phenomena.

With the integral-moment approach the method of solution of any problems is identical. At each step of the computation by the integral-moment method there is traced a physical picture of phenomena.

The author is grateful to A. A. Dorodnitsyn and L. I. Sedov for useful discussion.

Entered Dec. 20, 1963.

Literature Cited

1. Jaffe, G., On the method of the kinetic gas theory, Ann. Phys. 1930, 6, 195.

2. Grad, H., Principles of the kinetic theory of gases, Handbuch Phys. (physics manual), 1958, Vol. XII.

3. Enskog, D., On the basis equations in the kinetic theory of liquid and gases, Arch. of Math. Astron. Phys. A, 1928, Ser. 21, No. 1.

4. Kogan, M. N., On the equations of the motion of a rarefied gas, PMM, 1958, Vo. 22, Iss. 4.

5. Heinemann, M., Theory of drag in highly rarefied gases, Comm. Appl. Math., 194, Vol. 1, No. 3 (Russ. Trans.: Heinemann, M., On the theory of frontal resistance in highly rarefied gases, Coll. of Trans. "Mekhanika" Foreign Lit., 1951, Iss. 2)

6. Willis, D. R., Theoretical solutions to some nearly free molecular problems, rarefied gas dynamics, Proc. of the First International Symposium 1958.

7. Perepukhov, V. A., On the resistance of a flat plate in a flow of highly rarefied gas, Zh. Vychislit. matem. e matem. fiz. (Journ. of numerical Math. and Math. Phys.) 1961, Vol. 1, No. 4.

8. Kogan, M. N., On hypersonic flows of rarefied gas, PMM, 1962 Vo. 224, Iss. 3.

9. Grad, H., On the kinetic theory of rarefield gases., Commns Pure and Appl. Math., 1949, Vol. 2, No. 4

NONEQUILIBRIUM DISTRIBUTION OF ENERGY BY OSCILLATORY DEGREES OF FREEDOM OF MOLECULES DURING DISTURBANCE OF MAXWELLIAN DISTRIBUTION

A. I. Osipov and Ye. V. Stupochenko

(Moscow)

There is examined the distribution of oscillatory energy in gas, perturbed by sources of "fast" particles. For a model of the harmonic oscillators constituting a small admixture in a light monatomic gas perturbed by sources of the same particles, whose initial kinetic energy is less than $h\nu$, this distribution is characterized by a temperature θ. For θ differing from temperature of a light gas there is obtained an explicit expression in terms of parameters of the sources.

A disturbance of Maxwellian distribution is accompanied, generally speaking, by the disturbance of equilibrium distribution of energy in all degrees of freedom. For a number of processes perturbations of distribution functions concentrated in region of far energies are of interest. In reference to Maxwellian distribution this means that perturbations are concentrated in the tail of Maxwellian function, far off from region of thermal energies. The nonequilibrium distributions of such a type will be reflected in the different degrees of freedom of molecules. The exchange of energy between translational and rotational degrees of freedom occurs with participation of molecules in region of average thermal speeds. Inasmuch as in this region Maxwellian distribution markedly is not disturbed, then the distribution of energy in the rotational degrees of freedom will be close to equilibrium. Another assumption posed will be with vibrational and electron degrees of freedom. The transition of energy from translational to vibrational and electron degrees of freedom at not too high temperatures occurs with participation of molecules lying in tail of Maxwellian distribution. A marked disturbance of Maxwellian

distribution in this region will result in the disturbance of equilibrium distribution of energy in the vibrational and electron degrees of freedom.

The purpose of this work is determination of distribution function of energy on the basis of the vibrational degree of freedom in the presence of a quasi-stationary, but not equilibrium distribution on basis of translational degree of freedom. Problems of such a type are of interest in the chemistry of "hot" atoms, and also in the study of reactions in which fast particles appear.

Let us consider for simplicity the following case. In monatomic gas with small admixture of diatomic molecules there acts a source, creating the same monatomic particles with a kinetic energy E_0, satisfying the inequality $(-E_0/kT) \ll 1$. We shall assume that mass m of a monatomic particle is small in comparison to mass M of the molecule and, consequently, exchange in kinetic energy during collisions of these particles is hampered. Then, independently of the relative concentration, the distribution of kinetic energy of molecules will be practically Maxwellian. Distribution function of a light component (with a not-too-low concentration) practically will coincide with distribution for a single-component system perturbed by the source of particles. This distribution is determined in [1, 2] and has the form:

$$\begin{aligned} f_-(x) &= [\rho + J(x)(x - {}^3/_2)]\, f^0(x) + N\tau_0\delta(x - x^0) \quad (x \leqslant x^0) \\ f_+(x) &= [\rho + J(x^0)(x - {}^3/_2)]\, f^0(x) + N\tau_0\delta(x - x^0) \quad (x \geqslant x^0) \end{aligned} \tag{1}$$

In these equalities

$$J(x) = \frac{N}{\sqrt{\pi}} \sqrt{\frac{m}{2\pi kT}} \frac{(x^0 - {}^3/_2)}{d^3\rho} \int_0^{x - x^0} \frac{d^3 dt}{(t^0 - 2t)^3}$$

$$(x = mv^2/2kT,\ x^0 = E_0/kT)$$

Here $f^0(x)$ is the Maxwellian distribution normalized for a unit; τ_0 is the time of free path of particle with an energy E_0 in monatomic gas; N is the number of particles with an energy E_0, developing in

system per unit of time in unit of volume; d is the diameter of particles (model of solid spheres). The value ρ is determined from condition of normalization $f_{\mp}(x)$; practically it is possible to assume

$$\int_0^{\infty} f_{\mp}(x)\,dx = \rho \qquad (\rho = \rho_0 + N\eta)$$

The constant η is determined in such a manner that denominator in integrand at $t = \eta$ is of the order of unity. With such a selection of η, the function $f_{\mp}(x)$ is found to be insensitive to η and coefficient at $f^{o}(x)$ on the right hand side of (1) is determined with an accuracy up to magnitudes of order $\rho \exp(-x^{o}) \ll \rho$. In expression (1) the number of generating particles N is assumed small in comparison to the total number of collisions per unit of volume in a unit of time. However, method does not postulate the smallness of perturbation in region of far energies but (1) describes also the finite perturbations in the tail of distribution. The distribution of energy by vibrational degrees of freedom of diatomic molecules will be found as follows. The system of equations describing the distribution of molecules by oscillatory levels has the form [4]

$$\frac{dx_n}{dt} = Z\left(P_{n+1,n}x_{n+1} - P_{n,n+1}x_n + P_{n-1,n}x_{n-1} - P_{n,n-1}x_n\right) \qquad (n = 0, 1, 2, \ldots) \qquad (2)$$

where Z is the number of collisions of the molecule per second; $x_n(t)$ is the concentration of molecules in n-th oscillatory level; P_{mn} is the probability of transition of molecule from level m to level n, relative to one collision.

Stationary solution of the system (2) (considering constancy of concentration of molecules) satisfies equation

$$\frac{x_{n+1}}{x_n} = \frac{P_{n,n+1}}{P_{n+1,n}} \qquad (3)$$

Under equilibrium conditions,(3) is satisfied by Boltzmann distribution and $P_{n+1,n}$ and $P_{n,n+1}$ are associated by the relationship

$$P_{n+1,n} \exp(-\varepsilon_{n+1}) = P_{n,n+1} \exp(-\varepsilon_n) \qquad (\varepsilon_n = E_n^\circ / kT) \tag{4}$$

being the expression of principle of detailed equilibrium.

Under conditions of a quasi-stationary but not equilibrium distribution (1), relationship (4) is not realized. For a determination of the distribution function x_n under these conditions it is necessary to calculate P_{mn}.

We proceed from the general expression [4]

$$ZP_{mn} = \int_0^\infty v p_{mn}(v) \sigma f(v)\, dv \qquad \left(\sigma = \frac{\pi d_{12}^2}{4}\right) \tag{5}$$

Here d_{12} is the diameter of collision of monatomic particle with molecule; p_{mn} is the probability of transition $m \to n$ during the collision with a relative speed v; $f(v)\,dv$ is the distribution by speeds, of the relative motion of molecules and monatomic particles. In view of smallness of the ratio m/M instead of f(v) there may be substituted the distribution (1). In calculating the probability of deactivation in the integrand the region of average thermal speeds plays a basic role. In this region distribution (1) practically does not differ from the Maxwellian.

Therefore, for $P_{n+1,n}$ it is possible to use an expression which is obtained under equilibrium conditions

$$P_{n+1,n} = P^\circ_{n+1,n} \tag{6}$$

The probability $P^\circ_{n+1,n}$ is obtained from formula (5) with substitution of the Maxwellian distribution instead of f(v).

In calculating $P_{n,n+1}$ we shall assume that

$$E_0 < \Delta E \equiv E_1^\circ - E_0^\circ$$

Inasmuch as the chief contribution to $P_{n,n+1}$ is introduced by the fairly narrow energy band $mv^2/2$ of an order ΔE (in accordance with theory of adiabatic collisions [3]

$$P_{n,n+1} \sim \exp(-\Delta E\tau/\hbar)$$

where $\tau \sim 1/v$ is the duration of the collision) then in (5) instead of $f(v)\,dv$ it is possible to substitute $f_+(x)\,dx$, not changing the limits of integration and dropping the δ-form component. In such a case

$$P_{n,n+1} = \frac{\rho + J(x^*)(x^\circ - x^*)}{\rho} 2\left(\frac{m}{2kT}\right)^3 \int_0^\infty v^3 P_{n,n+1}(v) \exp\left(\frac{-mv^2}{2kT}\right) dv \equiv$$
$$\equiv (1+a) P_{n,n+1}^\circ, \qquad a = \frac{J(x^*)(x^\circ - x^*)}{\rho} \qquad (7)$$

Here $P_{n,n+1}^\circ$ is the value of probability $P_{n,n+1}$ under conditions of equilibrium; x^* is the x value, at which integrand in (7) attains a maximum. Integral included in (7) usually is calculated by method of steepest descents [3]. In such case x^* is the point of steepest descent. Taking into account (6) and (7) equation (3) acquires the form

$$\frac{z_{n+1}}{z_n} = (1+a)\frac{P_{n,n+1}^\circ}{P_{n+1,n}^\circ}$$

The equilibrium values P_{mn}° are associated by relationship (4), therefore,

$$\frac{z_{n+1}}{z_n} = (1+a)\exp(\varepsilon_n - \varepsilon_{n+1}) \qquad (8)$$

Distribution (8) implicitly depends on time through ρ and T and is valid for any (not too small) values of time. Actually, it satisfies the condition (4) with an accuracy up to terms of an order

of $N/Z\rho P_{10}$, which are considered small.

The smallness of this parameter means that the characteristic time associated with change of density in number of particles and temperature of monatomic gas as a result of action of source, is much greater than the time of an oscillatory relaxation determined by exchange of energy between the translational and vibrational degrees of freedom.

Under these conditions it is possible to speak of the existence at each given moment of time of a quasi-stationary distribution which is determined by value ρ and T at the same moment of time.

For an evaluation of distribution (8) we shall use the model of a harmonic oscillator. In this case

$$\frac{z_{n+1}}{z_n} = (1+a)\exp\frac{-h\nu}{kT} \qquad (9)$$

Distribution (9) can be presented as a Boltzmann distribution corresponding to a temperature determined by relationship

$$\frac{1}{\theta} = \frac{1}{T}\left[1 - \frac{kT}{h\nu}\ln(1+a)\right] \qquad (10)$$

At $a \ll 1$, which corresponds to sources of small intensity,

$$\frac{1}{\theta} = \frac{1}{T}\left(1 - a\frac{kT}{h\nu}\right)$$

For fairly intense sources (in the realizing of the obligatory condition $N/Z\rho P_{10} \ll 1$) it may be found that $a \gg 1$.

In such a case

$$\frac{1}{\theta} = \frac{1}{T}\left[1 - \frac{kT}{h\nu}\ln a\right]$$

and temperature of the vibrational degrees of freedom θ may greatly exceed the temperature T.

It is important to note that this result – the finite deviation of distribution of oscillatory energy from the equilibrium – is associated with the relatively insignificant perturbation of the Maxwellian distribution (insignificant in the sense that the finite perturbation occupies only a small portion of all particles of monatomic gas belonging to the region of far energies).

Submitted
14 March 1963

Literature

1. Ye. V. Stupochenko. On the distribution of kinetic energy in systems with sources of particles. DAN SSSR, 1949, V. 67, No. 4, p. 635.

2. Ye. V. Stupochenko. On distribution of kinetic energy in a "single-component" system with sources of particles. News of Moscow Univ. 1953, No. 8, p. 57.

3. A. I. Osipov and Ye. V. Stupochenko. Nonequilibrium distributions of energy in the vibrational degree of freedom in gasses. Successes of physical sciences. 1963, V. 79, No. 1, p. 81.

4. S. Chapman and T. G. Cowling. Mathematical theory of nonuniform gases. Foreign Literature Press, 1960.

ON THE MEASUREMENT OF PRESSURE IN A SPIN TRANSVERSE WAVE

V. V. Mitrofanov, V. A. Subbotin and M. Ye. Topchiyan

(Novosibirsk)

As is known [1] the detonation of gas mixtures in tubes near the ends occurs in a spin mechanism. The structure of spin wave has been ascertained in works [2-6]. In the front there will be formed transverse wave, rotating in a circle along walls of the tube. Calculations show [6] that in a transverse wave the maximum pressure is 170 to 180 times greater than the initial pressure of the mixture, i.e., 10 times higher than at the Chapman-Jouguet point for the detonational wave as a whole.

In work [7] there were presented the results of measurements of the pressure field in a spin wave by small-size piezotransducers, which gave a good agreement between the measured and the calculated magnitudes. However, owing to the lack of calibration of transducers for the absolute values of pressures and of the excessive shrinkage of oscillograms along the time axis these measurements could not be considered adequately reliable. Later the experiments were repeated more thoroughly, and the obtained results are discussed in this report.

Spin detonation was carried out in smooth walled brass tube with a diameter of 27 mm and length 140 cm with a plastic end section (20 cm) screwed on. A mixture of $2CO + O_2 + 3\% H_2$ with an initial pressure of 0.1 atm was initiated by a batch of azide of lead of about 0.1 g. The direction of rotation of spin was set by the coil of wire spiral placed inside tube close to the place of initiation.

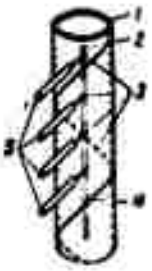

Fig. 1. Location of transducers in detonational tube: 1 – Plexiglas tube; 2 – slot in opaque flap; 3 – marker; 4 – direction of motion of transverse wave; 5 – transducers.

Measurements were made in the end section simultaneously by four pressure piezotransducers. Their location in the tube is shown in Fig. 1.

The transducers had the following design. In cylindrical brass tube with an outer diameter of 6 and an internal of 4 mm there was placed along the axis a zinc rod with a diameter of 1 or 2 mm with a Wood's alloy soldered polarized plate of barium titanate of the same diameter and thickness 0.8 mm on the end. The space between them was filled with beeswax. The rod was connected with central core of a coaxial cable and the body of transducer (brass tube) – with braiding of cable and by means of copper wire with a diameter of 0.07 mm immersed in wax with an external silvered surface, receiving piezoplate (the solder also was made of Wood's alloy). In the described experiments here, two transducers had a diameter of the sensitive element 1 mm, two others – 2 mm. These transducers were used previously in work [8] and are of nearly same design as in work [7].

Electrical signals from transducers were fed through cathode followers into two-gun oscillograph OK-17M. The input of time constant amounted to about $7 \cdot 10^{-4}$ sec. The time of scanning was about 60 microseconds.

In order to improve the quality of oscillograms it was necessary to attain as completely as possible the removal of parasitic oscillations generating both inside the transducer itself, and also those being transmitted from wall of the detonational tube. Natural oscillations of transducers of the described design in a careful preparation can be made small. The transmission of oscillations from walls of tube is greatly diminished when onto the body of transducer there was

slipped on a rubber tube with thickness of wall 1 mm and only after that transducer was inserted into the apparatus. Surface of sensing element of transducer coincided with internal surface of detonational tube, all deviations of internal surface from cylindrical at the place of output of transducer were puttied from within by wax, so that transducer did not introduce extraneous perturbations in the flow of the gas behind the front of detonation. In order to remove the elastic wave on walls from explosion of azide of lead at a distance of 20 cm from place of initiation the brass tube had a rubber connection.

The transducers were calibrated in the on-position of a shock wave in air obtained by an explosion of azide of lead, where there was fixed both a normal wave and also the reflected wave from a solid barrier, set at a distance of about 5 mm from transducer. A typical calibrated oscillogram is shown in Fig. 2. The speed of the incident wave was measured at a distance of 70 mm directly ahead of transducer being calibrated. The pressure differential in incident and reflected waves was calculated by known formulas at $\gamma = 1.4$. Speed of incident wave did not exceed 815 m/sec which corresponded to an excess pressure of 5.4 atm in incident wave and 25 atm in the reflected

Fig. 2. Pressure oscillogram in a normal and reflected shock wave in the air (calibration).

For establishment of trajectories of motion of transducers relative to the spin wave in the experiments there was made also a photoregistration, through longitudinal slot, of picture of self-glow onto the moving film. Speed of film coincided in magnitude and direction with speed of image of the transverse wave at moment of interception of slot (method of full compensation used in works [2-8]).

The relative location of slot and transducers is shown in Fig. 1. Intersections of slot by imaginary spiral lines passing along internal surface of detonational tube through sensing elements of transducers and along parallel lines of the motion of the "head" of spin, were indicated by opaque marks. Since, in the system of coordinates moving along any such spiral with the speed of the "head," the structure of flow is stationary, then on phototracings the dark lines indicated by the marks are trajectories of transducers relative to the detonational wave.

One of phototracings is shown in Fig. 3. There is evident the alternating of distinct and indistinct half-periods where the distinct correspond to the passage of a transverse wave wide of the slot along near wall of tube; the blurred - along the opposite. Each period coincides with the development into a plane of the cylindrical surface of tube, on which there is plotted the instantaneous position of luminescent fronts [2-5].

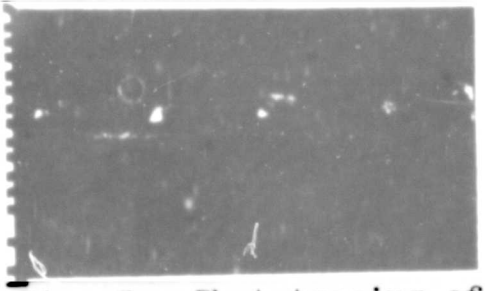

Fig. 3. Phototracing of a spin wave. Dark lines are trajectoies of transducers in the system of coordinates associated with the transverse wave.

The scheme of the fronts near the wall forming the spin wave is sketched in Fig. 4a. Transverse wave in separated rectangle is illustrated to the right on a larger scale. There are plotted the trajectories of the transducers which passed through the most interesting regions of the flow. Corresponding oscillograms are presented in

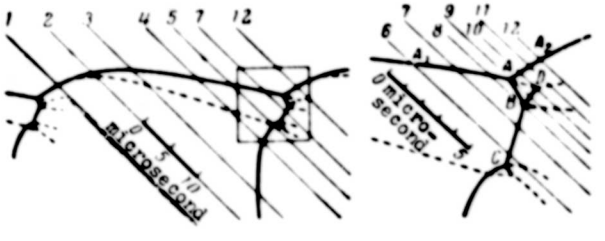

Fig. 4a. Diagram of shocks near wall with trajectories of pressure transducers (they correspond to oscillograms in Fig. 4b). The solid heavy lines are shock and detonation shocks, the dotted are contact breaks.

Fig. 4b. Here there have been selected oscillograms obtained by one transducer which gave best quality of recording and was most thoroughly calibrated (diameter of sensing element is 1 mm). The calibration curve of this transducer was presented in work [8]. After the termination of all experiments the calibration was repeated, where the points lay on the same curve with a dispersion in pressure of not more than 7%.

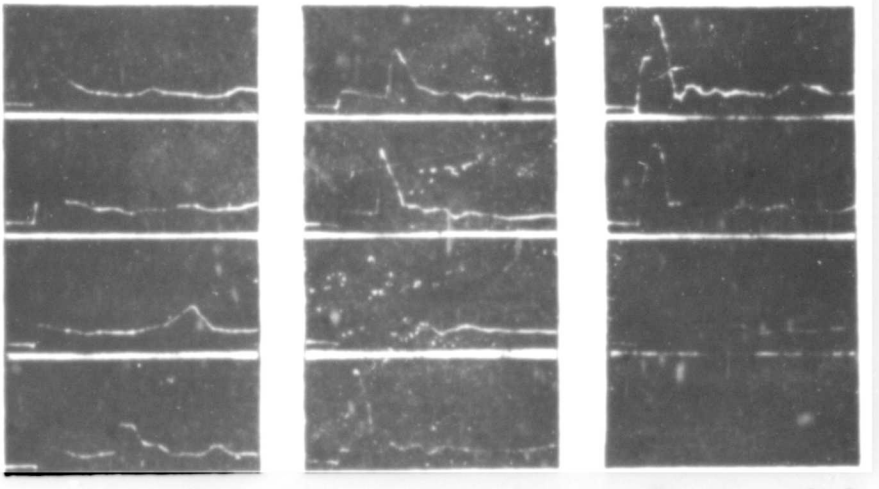

Fig. 4b. Pressure of oscillograms. One division along the vertical corresponds to 25 p_0, along the horizontal to 5 microseconds.

Oscillograms 6, 7 and 8 correspond to passage of transducer through transverse front. Near point B there is registered a pressure of 160 p_0 in the transverse front. In a motion in the direction from point B to C the pressure after the transverse front gradually drops to approximately to 110 p_0.

For a corroboration of the scheme of shocks proposed in work [6], especially important is oscillogram 9. Here transducer passed through region after the shock AB (Fig. 4a) with pressure of 62 p_0 and it fixed shock BD with pressure of about 165 p_0. The existence of front BD is evident from a theoretical construction of the diagram of flow, but by other means (Toepler, photographs of

self-luminosity) it could not be ascertained. Continuous rise of pressure from 45 up to 62 p_0 on this oscillogram is caused by the fact that transducer passed directly through the triple point A and on part of its area for a certain time the pressure ahead of shock AB (about 19 p_0) exerted its influence. Between front AA_2 and the contact break AD the flow is subsonic, therefore, transducers passing higher than point D record a smooth variation of the pressure.

We present for comparison a contrast of the measured magnitudes of pressure p/p_0 after the shocks with those calculated in the vicinity of the triple points A and B:

shock	A_1A	AA_2	AB	BD	BC	
$\frac{p}{p_0}$ =	19.2	54.5	54.5	170	170	calculation
	19 ± 1	52 ± 5	60 ± 5	160 ± 10	155 ± 10	experiment

The calculation was made for a mixture of $2CO + O_2$ at $p_0 = 0.1$ atm and $T_0 = 293^{\circ}K$. Influence of hydrogen in view of its small concentration in the working mixture was not taken into consideration. The composition of the gas after BC and AA_2 was assumed to be in chemical equilibrium (there were considered the reactions $2CO + O_2 \rightleftarrows CO_2$ and $O_2 \rightleftarrows 2O$), after remaining shocks — nonreacting.

Initial data for the calculation of triple configurations were the speed of undisturbed flow in the system of coordinates associated with the transverse wave, $u_0 = 2370$ m/sec (D = 1700 m/sec) and the angle between its direction and front A_1A $\varphi_0 = 34.5^{\circ}$, determined experimentally [6].

After the indicated shocks and also everwhere along the leading edge $AA_n \ldots A_1A$ the calculated pressures within an accuracy of 10% agree with the measured pressures.

We note that after the transverse front BC the transducers did

not reveal the layer of the shock-compressed gas preceding the zone of reaction in which the pressure must be by calculation 195 p_0. The highest measured pressure is even somewhat lower than calculated on the assumption of an instantaneous reaction.

All of the presented oscillograms in experiments described here were repeated many times, therefore, diagram of flow in spin wave proposed in works [2-6] may be considered finally corroborated.

The authors are grateful to B. V. Voytsekhovskiy for his attention given to the work.

Submitted
1 February 1963

Literature

1. Kh. A. Rakipova, Ya. K. Troshin, and K. I. Shchëlkin. Spin at the limits of a detonation. Jour. Tech. Physics, 1947, V. 17, No. 12.

2. B. V. Voytsekhovskiy. On spin detonation. DAN SSSR, 1957, V. 114, No. 4.

3. B. V. Voytsekhovskiy. Investigations of structure of front of a spin detonation. Trans. MFTI, V. 1, 1958.

4. B. V. Voytsekhovskiy and B. Ye. Lotov. Optical investigations of front of a spin detonational wave. News of the Academy of Sciences of USSR, 1958, No. 4.

5. B. V. Voytsekhovskiy. Spin and stationary detonation. Scientific council on the economic use of an explosion. Novosibirsk, 1960, No. 10.

6. B. V. Voytsekhovskiy, V. V. Mitrofanov and M.Ye. Topchiyan. On the structure of the flow in a spin detonational wave. PMTF, 1962, No. 3.

7. M. Ye. Topchiyan. Experimental investigations of spin detonation by pressures transducers. PMTF, 1962, No. 4.

8. V. V. Mitrofanov. Structure of detonational wave in a two-dimensional channel. PMTF, 1962, No. 4.

LAMINAR FLAME IN A TURBULENT FLOW

A. M. Klimov

(Novosibirsk)

There are obtained equations describing a laminar flame in nonuniform hydrodynamic field in the case, if the curvature of front of flame can be ignored (effect of large-scale turbulence). There are explained basic properties of such flame. A possible mechanism of attenuating of flame is obtained and the mechanism of turbulent combustion is discussed.

1. The non-uniformity of hydrodynamic field is of paramount importance for mechanism of turbulent combustion; we shall consider turbulence as a random field of gradients of speeds. We shall designate by l the dimension of region in which gradients of the speeds during certain time (time of existence of this region) slightly depend on position of point within region, although they may in an arbitrary way depend on time. This dimension is identical to the scale of turbulence. We shall introduce also characteristic dimension δ of the "temperature" region, determining it as the distance in direction of temperature gradient (or concentration), in which the temperature (concentration) essentially changes. In our case this will be thickness of laminar flame in a homogeneous mixture. The character of phenomenon, obviously, greatly depends on the relationship between

l and δ. If $l \gg \delta$ (large-scale turbulence) the front of flame is slightly distorted ($r \gg \delta$, where r is radius of curvature of front of flame), but the area of its surface continuously varies: flame is elongated or, conversely, is contracted. Below there is investigated namely this case ($l \gg \delta$).

We shall consider field of speeds of region l without combustion, which we shall call the external hydrodynamic field. The simplest example is field of pure shear (Fig. 1a) when a correlation between components of the speed is lacking. Another example is "flow at the critical point" (Fig. 1b), generating if, for example, in regions A and B there developed a rarefaction. A correlation between the components of speed here manifests itself in a pure form. Field of speeds of the arbitrary region l is the superposition of these two extreme cases. For example, in a two-dimensional case, taking into account the continuity equation, the field of speeds has the form

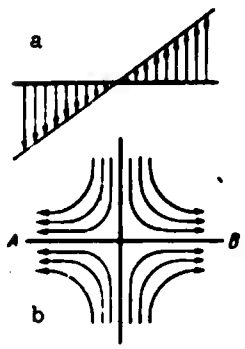

Fig. 1a, b.

$$u^* = k(t)x + k_1(t)y, \qquad v^* = -k(t)y + k_2(t)x$$

It is evident that onto the "flow at critical point" $u = kx$, $v = -ky$ there are superimposed the arbitrary shifts $u = k_1 y$, $v = k_2 x$. The three-dimensional case in principle does not differ from the two-dimensional.

Assumptions essential for obtaining the equations will be the ordinary assumptions of theory of slow combustion: 1) constancy of pressure (the equation of motion is not considered), 2) in equation of energy there is considered only the thermal energy of the gas.

Furthermore, we shall consider only primary processes of

transfer and shall assume that rate of heat release is determined by the concentration of a single component of the gas mixture and the temperature, and the Lewis number equal to 1. Then, as is known, the equation of diffusion can be eliminated.

In conventional designations in a two-dimensional case we shall have

$$\rho C_p\left(\frac{\partial T}{\partial t}+u\frac{\partial T}{\partial x}+v\frac{\partial T}{\partial y}\right)=\frac{\partial}{\partial x}\left(\lambda\frac{\partial T}{\partial x}\right)+\frac{\partial}{\partial y}\left(\lambda\frac{\partial T}{\partial y}\right)+F(T)$$
$$\frac{\partial\rho}{\partial t}+\frac{\partial(\rho u)}{\partial x}+\frac{\partial(\rho v)}{\partial y}=0\quad\left(\frac{\rho}{\lambda}=\frac{\rho(T)}{\lambda(T)}\right) \tag{1.1}$$

Furthermore, there is given external field u^0, v^0. Suppose the external field is a pure shear. Without loss of generality it is possible to assume $u^0 = a(t)y$, $v = 0$; orientation of initial distribution of temperature (being one-dimensional) relative to external field is given by angle ψ, where $\varphi\varphi$ is the front of the flame (Fig. 2).

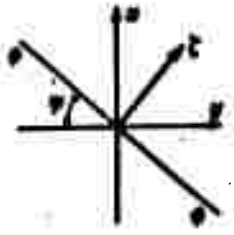

Fig. 2.

The true hydrodynamic field will differ from external, because during the combustion owing to the thermal expansion of gases, there appears a motion, normal to front of flame. On the whole the phenomenon is such: the front of flame is turned by the external field in plane xy with a change in the area of its surface; simultaneously it moves relative to the gas, creating a supplemental field of speeds as the result of the thermal expansion.

The solution of equations (1.1) we shall seek in the form

$$T=T(t,\xi),\quad u=ay+V(t,\xi)\left[1+\left(\operatorname{tg}\psi-\int_0^t a\,dt\right)^2\right]^{-1/2}$$
$$v=V(t,\xi)\left[\operatorname{tg}\psi-\int_0^t a\,dt\right]\left[1+\left(\operatorname{tg}\psi-\int_0^t a\,dt\right)^2\right]^{-1/2}$$

where

$$\xi=\left[x+y\left(\operatorname{tg}\psi-\int_0^t a\,dt\right)\right]\left[1+\left(\operatorname{tg}\psi-\int_0^t a\,dt\right)^2\right]^{-1/2}$$

For the determination of $T(t, \zeta)$ and $V(t,\zeta)$ we shall obtain the equations

$$\rho C_p\left[\frac{\partial T}{\partial t}+\varphi(t)\zeta\frac{\partial T}{\partial \zeta}+V\frac{\partial T}{\partial \zeta}\right]=\frac{\partial}{\partial \zeta}\left(\lambda\frac{\partial T}{\partial \zeta}\right)+F(T)$$
$$\frac{\partial \rho}{\partial t}+\varphi(t)\zeta\frac{\partial \rho}{\partial \zeta}+\frac{\partial(\rho V)}{\partial \zeta}=0 \qquad (1.2)$$

Here
$$\varphi(t)=\alpha\left[\operatorname{ctg}\psi-\int_0^t \alpha\,dt\right]\left[1+\left(\operatorname{ctg}\psi-\int_0^t \alpha\,dt\right)^2\right]^{-1}$$

Coordinate ζ always is normal to the surface of the flame.

The speed V is associated with the expansion of gas. If products of combustion and fuel mixture occupy a half-space, it is natural to assume V = 0 for a fresh mixture. The initial and boundary conditions for equations (1.2) in this case will be

$$T=T^0(\zeta) \quad \text{at } t=0, \qquad V\to 0 \quad \text{at } \zeta\to-\infty.$$

If at the initial moment of time the products of combustion occupy band of finite width with a symmetric distribution of temperature, the simplest initial and boundary conditions will be

$$T=T^0(\zeta) \quad \text{at } t=0, \qquad \frac{\partial T}{\partial \zeta}=V=0 \quad \text{at } \zeta=0$$

Let us assume that now $u^0 = -k(t)x$, $v^0 = k(t)y$. The solution of equations (1.1) we shall seek in the form

$$T=T(t,\zeta)$$
$$u=-kx+V(t,\zeta)\operatorname{ctg}\psi\exp\left(2\int_0^t k\,dt\right)\left[1+\operatorname{ctg}^2\psi\exp\left(4\int_0^t k\,dt\right)\right]^{-1/2}$$
$$v=ky+V(t,\zeta)\left[1+\operatorname{ctg}^2\psi\exp\left(4\int_0^t k\,dt\right)\right]^{-1/2}$$

where
$$\zeta=\left[y+x\operatorname{ctg}\psi\exp\left(2\int_0^t k\,dt\right)\right]\left[1+\operatorname{ctg}^2\psi\exp\left(4\int_0^t k\,dt\right)\right]^{-1/2}$$

For determining $T(t, \zeta)$ and $V(t, \zeta)$ we obtain (1.2) where

$$\varphi(t) = k\left[1 - \operatorname{ctg}^2\psi \exp\left(4\int_0^t k\,dt\right)\right]\left[1 + \operatorname{ctg}^2\psi \exp\left(4\int_0^t k\,dt\right)\right]^{-1}$$

In the general case we also obtain equations (1.2). The characteristics of each case are included in function $\varphi(t)$.

It is readily verified that $\varphi(t)$ is the relative rate of change of surface area of flame taken with opposite sign.

Equations (1.2) can be obtained also by assuming that flame remains two-dimensional and the function $\varphi(t)$ is given. Let us assume that ξ, η, ζ is a system of coordinates oriented so that the ζ-axis always is normal to surface of the flame, and let us assume that v_ξ, v_η, v_ζ are the respective speeds.

Since surface of flame is flat,

$$T = T(t, \zeta), \qquad v_\zeta = v_\zeta(t, \zeta)$$

Consequently,

$$\rho C_p\left(\frac{\partial T}{\partial t} + v_\zeta \frac{\partial T}{\partial \zeta}\right) = \frac{\partial}{\partial \zeta}\left(\lambda \frac{\partial T}{\partial \zeta}\right) + F(T)$$
$$\frac{\partial \rho}{\partial t} + \rho\left(\frac{\partial v_\xi}{\partial \xi} + \frac{\partial v_\eta}{\partial \eta} + \frac{\partial v_\zeta}{\partial \zeta}\right) + v_\zeta \frac{\partial \rho}{\partial \zeta} = 0 \qquad (1.3)$$

Let us consider small element of surface $d\xi\, d\eta$ in the arbitrary plane ζ = const. The relative rate in change of its area

$$-\varphi(t) = \frac{1}{d\xi\, d\eta}\frac{d(d\xi\, d\eta)}{dt} = \frac{\partial v_\xi}{\partial \xi} + \frac{\partial v_\eta}{\partial \eta} \qquad (1.4)$$

Presenting v_ζ in the form $v_\zeta(t, \zeta) = \varphi(t)\zeta + V(t, \zeta)$ and taking into consideration (1.4) we shall obtain from (1.3) the equations (1.2).

We shall introduce the dimensionless magnitudes

$$\tau = t u_0 / \delta_0, \quad \beta = \zeta / \delta_0, \quad w = V / u_0, \quad \Phi = (T - T_0)/(T_1 - T_0)$$
$$\rho' = \rho / \rho_0, \quad \lambda' = \lambda / \lambda_0, \quad f = F / F_0, \quad \varepsilon = \varphi \delta_0 / u_0 \quad (\delta_0 = \lambda_0 / \rho_0 u_0 C_p)$$
$$\rho_0 = \rho(T_0), \quad \lambda_0 = \lambda(T_0), \quad F_0 = \rho_0 u_0 C_p (T_1 - T_0)/\delta_0$$

Here u_0 is speed of propagation of a normal flame; δ_0 is distance, at which in a normal flame Φ varies approximately by e times (exactly

by e times in Michelson's solution); T_0, T_1 are the initial and final (adiabatic) temperatures of the gas; F_0 is average rate of heat release in normal flame.

The parameter ε is the ratio of characteristic time of normal combustion $t_0 = \delta_0/u_0$ to the characteristic time of action $t_1 = 1/\varphi$ for a flame of external hydrodynamic field; t_1 is the time during which at φ = const the surface area of flame varies by e times or, what amounts to the same time, the time during which the distance between surfaces of a constant temperature would vary be e times in the absence of a chemical reaction and thermal conduction.

In the adopted designations the system (1.2) has the form

$$\rho\left[\frac{\partial\theta}{\partial\tau}+\varepsilon(\tau)\beta\frac{\partial\theta}{\partial\beta}+\omega\frac{\partial\theta}{\partial\beta}\right]=\frac{\partial}{\partial\beta}\left(\lambda\frac{\partial\theta}{\partial\beta}\right)+f(\theta)\qquad\frac{\partial p}{\partial\tau}+\varepsilon(\tau)\beta\frac{\partial p}{\partial\beta}+\frac{\partial(\rho\omega)}{\partial\beta}0 \qquad (1.5)$$

Here and henceforth the primes at ρ and λ are omitted.

The new terms, in comparison to equations of the one-dimensional flame, in (1.5) are of an order $\varepsilon(\tau)$. We shall make numerical evaluations. Suppose, for example, the speed of turbulent pulsations $v' \sim 10$ m/sec with the scale of turbulence $l \sim 1$ cm; then $t_1 \sim 10^{-3}$ sec. For most fuel-air mixtures close to the stoichiometrical, $t_0 \sim 10^{-3}$ sec also rapidly increases to 10^{-2} sec with the impoverishment or enrichment of mixture approximately by 1.5 times. Correspondingly, we shall obtain $\varepsilon \sim 1$ to 10, depending on the composition of mixture.

The parameter ε is in close conformity with parameter $\gamma = v'\delta_0/u_0 l$, proposed [1] for an evaluation of the relative role of "surface" and "volume" combustion. Difference between them is in the fact that in γ the magnitude v'/l is an averaged gradient of the speed, and the magnitude φ in ε is instantaneous and local. Therefore, ε may be a magnitude both positive, and also negative. From (1.4) it is evident that gradients of different components of speed may introduce a

different contribution to the change of surface area of flame – the flame may be elongated or be contracted in all directions, but may also be contracted in one direction and be elongated in the other.

We shall write out equation (1.5) in system of coordinates associated with front of flame, i.e., in system of coordinates whose origin is associated with a certain temperature ϑ_0. The coordinate β_0 of point with temperature ϑ_0 is determined by equation

$$\frac{d\beta_0}{d\tau} = [s(\tau)\beta_0 + \omega] - [m(\tau) + \omega] = s(\tau) - m(\tau)$$

Consequently,

$$\beta_0(\tau) = \exp\int_0^\tau s(\tau)\,d\tau\left[\beta_{00} - \int_0^\tau m(\tau)\exp\left(-\int_0^\tau s(\tau)\,d\tau\right)\right] \qquad (\beta_{00} = \beta_0(0))$$

In the variables $\alpha = \beta - \beta_0$, τ the system (1.5) will acquire the form

$$\rho\left[\frac{\partial\Phi}{\partial\tau} + (m + s\alpha + \omega)\frac{\partial\Phi}{\partial\alpha}\right] = \frac{\partial}{\partial\alpha}\left(\lambda\frac{\partial\Phi}{\partial\alpha}\right) + f(\Phi)$$
$$\frac{\partial\rho}{\partial\tau} + (m + s\alpha)\frac{\partial\rho}{\partial\alpha} + \frac{\partial(\rho\omega)}{\partial\alpha} = 0 \qquad (1.6)$$

Function $m(\tau)$ is determined in the solution of concrete problem. Initial value $m(\tau)$ must be given.

Equations (1.6) may also be obtained from equations (1.5), assuming that the latter are obtained from (1.3), where ξ, η, ζ is the system of coordinates associated with front of flame. It is necessary only to present ω in the form

$$\omega(\beta, \tau) = m(\tau) + \omega_1(\beta, \tau), \qquad m(\tau) = \omega(-\infty, \tau)$$

2. Previous to constructing the solution of the problem, we shall give a qualitative description of considered picture of phenomenon.

In a uniform hydrodynamic field ($\varepsilon = 0$) the solution of system (1.6) under certain assumptions relative to function of heat release

$f(\$)$ and with corresponding initial and boundary conditions tends to a solution not depending on the time, and describing distribution of temperature in normal flame. Here $m(\tau) \to 1$. The stationary form of normal flame is result of the equilibrium of opposite "forces": the smoothing action of thermal conduction is balanced by opposite effect of the chemical reaction.

At $\varepsilon \neq 0$ there appears a new factor: the convection heat transfer $\varepsilon\alpha\ \partial\$/\partial\alpha$, which either smooths ($\varepsilon > 0$) or increases ($\varepsilon < 0$) the curvature of the temperature distribution.

If $\varepsilon \to \text{const} < 0$, the solution of the system (1.6) must tend to a certain, steeper stationary distribution of temperature than a normal flame.

The situation is different at $\varepsilon > 0$. In the adopted model of gas medium, thermal perturbations are propogated with an infinite speed. Practically this speed also is very great (speed of sound). Therefore, the thermal influence of hot region instantaneously penetrates a great distance into the cold region. At the same time, at a fairly large distance from the origin of coordinates in the direction of cold gas (i.e., with a fairly large negative α) the convection heat flux acquires the same direction as heat flux caused by the thermal conduction. In a slow combustion such a heat transfer to the cold region is in no way compensated; conditions at a great distance from the front of flame all the time vary and the entire process becomes nonstationary.

For the quantity q of heat being liberated per unit of surface of flame per unit of time (proportional to the amount of burning matter) we have, assuming that $\partial\$/\partial\alpha \to 0$ at $\alpha \to \pm\infty$, the relationship

$$q = \int_{-\infty}^{\infty} j\,d\alpha = \int_{-\infty}^{\infty} \rho \frac{\partial\theta}{\partial\alpha} + \int_{-\infty}^{\infty} \rho(m + \varepsilon\alpha + \omega)\frac{\partial\theta}{\partial\alpha}\,d\alpha$$

In a normal flame $q = \rho(m + \omega) = \text{const}$. In the remaining cases ($\varepsilon \neq 0$ or $\varepsilon = 0$, but phenomenon is nonstationary) q is not associated explicitly with $\rho(m + \omega)$ and, in general, is variable.

In intervals of time when external field disappears, the flame is one-dimensional, but nonstationary.

The structure of such flame, has much in common with structure of flame at $\varepsilon \neq 0$; therefore, we shall consider it in greater detail.

In a one-dimensional nonstationary flame $m + \omega$, being speed of temperature $\$_0$ relative to the gas (m – relative to a fresh mixture, $m + \omega$ – relative to particles of gas with other temperatures), may acquire any values, in particular negative values. If $m + \omega < 0$, the gas flows towards a given plane α-const not from the direction of fresh mixture, but from direction of the combustion products. The flux of molecules (the same as flux of heat) is composed of fluxes of convection and diffusion. In a normal flame the convection and diffusion fluxes of the fuel are added. In a nonstationary flame they may be subtracted. Isolating conditionally the zone of reaction, it is possible to encounter a situation when the gas flows to this zone from the direction of the products of combustion, and the fuel is transmitted toward convection flux by diffusion. Let us assume that, for example, initial function for equation (1.5) will be

$$\$(\beta,0) = 0 \text{ at } \beta<0, \qquad \$(\beta,0) = 1 \text{ at } \beta>0 \tag{2.1}$$

Before there is established a normal flame, in which any temperature moves toward the fresh mixture, during a certain time points with a temperature close to $\$ = 1$ will move toward the combustion products. Consequently, at least in part of zone of reaction the convection flux of fuel (in the system of coordinates α)

will be directed against the diffusion. Establishment of normal flame in this case occurs by means of levelling effect of thermal conduction and di fusion.

If function , 0), conversely, slopes very gently in comparison to case of a normal flame, the chief factor of establishment of normal flame will be the local increase in temperature owing to chemical reaction. Here the speed, relative to gas, of points with temperatures close to $\$ = 1$ during the first moments of time will be significantly greater than this speed in normal flame having the same direction.

From equations (1.6) it is evident that in nonuniform hydrodynamic field the concept of speed of propagation of front of flame, strictly speaking, has no sense. At any $\varepsilon \neq 0$ the speed of the gas relative to a fixed temperature $\$_0$ varies in the range $(-\infty, +\infty)$, depending on temperature of particles of gas. Certainly, at small $|\varepsilon|$ this concept may have an approximate meaning. Hydrodynamic field in system of coordinates of flame is similar to the above-mentioned "flow at critical point" with plane of symmetry parallel to front of flame. At small $|\varepsilon|$ this plane is located far from region with large temperature gradients (region of the main portion of change of temperature from zero to unity); the field of mass speed in the latter is close to the uniform and flame differs little from the one-dimensional. At fairly large $|\varepsilon|$ the plane of symmetry shifts to region with large gradients of temperature and the concept of speed of propagation of front of flame does not have even an approximate meaning.

5. Integration of the first equation (1.6) over τ gives

$$\$(a, \tau) = \$(a, 0) - \int_0^\tau (m + \omega a + w)\frac{\partial \$}{\partial a}\,d\tau + \int_0^\tau \frac{\partial}{\partial a}\left(\lambda \frac{\partial \$}{\partial a}\right)d\tau + \int_0^\tau J\,d\tau$$

If at the initial moment flame was normal, for small τ at ε = const we shall obtain

$$\Phi(\alpha, \tau) = \Phi(\alpha, 0) - \varepsilon\tau \frac{\partial \Phi(\alpha, 0)}{\partial \alpha} + O(\tau^2)$$

In normal flame $\partial\Phi/\partial\alpha \geq 0$; consequently, the distribution of temperature begins to be smoothed at values $\varepsilon > 0$ and to become steeper at $\varepsilon < 0$.

We shall investigate behavior of flame at larger $|\varepsilon|$. In this case the distribution of temperature everywhere, with the exception of narrow layer of thickness $h \sim 1/\sqrt{|\varepsilon|}$ in the vicinity of point $\alpha = 0$, is described by the equation

$$\frac{1}{\varepsilon}\frac{\partial \Phi}{\partial \tau} + \varepsilon \frac{\partial \Phi}{\partial \alpha} = 0 \qquad (3.1)$$

which is obtained from (1.6) by means of discarding the small terms.

This equation possesses a system of characteristics $\mu = \alpha \exp(\varepsilon\tau)$, along which Φ = const.

Let us assume that $\varepsilon < 0$. Then from (3.1) it is evident that during the time $\tau \sim 1/|\varepsilon|$ almost all the change in temperature is concentrated in the layer h. At $|\varepsilon| \to \infty$ we have $h \to 0$, and the profile of temperature tends to be discontinuous.*

At $\varepsilon > 0$ (3.1) gives "a spreading" of the flame with the same characteristic time $\tau \sim 1/\varepsilon$; the distance between points with any two temperatures increases proportionally to $\exp(\varepsilon\tau)$; correspondingly, everywhere the temperature gradient decreases.

---

*If we take into consideration the thermal conduction, for distribution of temperature we shall obtain

$$\Phi = \frac{1}{2} + \frac{1}{2}\operatorname{erf}\left(\sqrt{\frac{\varepsilon}{2}}\alpha\right) \qquad (-\infty < \alpha < +\infty)$$

changing at $\varepsilon \to -\infty$ to (2.1), if in (2.1) by β there is implied α.

In order to obtain solution at finite $|\varepsilon|$, we shall use function $f(\$)$, corresponding to the infinitely narrow zone of reaction:

$$f(\theta) > 0, \quad f(1) = 0, \quad f(\theta) = 0 \text{ at } \theta < 1, \quad \int_0^1 f(\theta)\,d\theta = \int_0^1 f_0\,d\theta \tag{3.2}$$

where f_0 is true function of the heat release. Let us assume that

$$f(\theta) > 0 \text{ at } 0 < \theta_0 < \theta < 1, \; f(\theta) = 0 \text{ at } \theta < \theta_0, \; f(\theta_0) = f(1) = 0$$

Then, if $\$_0 \to 1$ and $f(\$)$ tends to function (3.2), there is valid, as also in case of a normal flame [2], the relationship

$$\lim_{\$_0 \to 1}\left[\frac{\partial\theta}{\partial\alpha}\right]_{\alpha=-0} = \left[\frac{2}{\lambda(1)}\int_0^1 f\,d\theta\right]^{1/2} \tag{3.3}$$

We shall prove it. From equations (1.6) we have

$$-\frac{\rho^2}{d\varphi/d\theta}\frac{\partial\omega}{\partial\alpha} = \frac{\partial}{\partial\alpha}\left(\lambda\frac{\partial\theta}{\partial\alpha}\right) + f(\theta)$$

Hence

$$-\left[\frac{\rho^2}{d\varphi/d\theta}\right]_{\theta_1}\int_{\theta_1}^{1}\frac{\partial\omega}{\partial\theta}\,d\theta = \int_{\theta_1}^{1}\frac{d\lambda}{d\theta}\left(\frac{\partial\theta}{\partial\alpha}\right)^2 d\theta + \int_{\theta_1}^{1}\lambda\frac{\partial\theta}{\partial\alpha}\,d\left(\frac{\partial\theta}{\partial\alpha}\right) + \int_{\theta_1}^{1} f(\theta)\,d\theta =$$

$$= \left(\frac{d\lambda}{d\theta}\right)_{\theta_1}\left[\theta_0\left(\frac{\partial\theta}{\partial\alpha}\right)^2_{\alpha=-0} - \theta_1\left(\frac{\partial\theta}{\partial\alpha}\right)^2_{\alpha=-0}\right] - \lambda(\theta_1)\frac{1}{2}\left(\frac{\partial\theta}{\partial\alpha}\right)^2_{\alpha=-0} + \int_{\theta_1}^{1} f\,d\theta \tag{3.4}$$

where $\$_0 \le \$_1, \$_2, \$_3, \$_4 \le 1$. In obtaining (3.4) there was used an integration by parts and condition $\partial\$/\partial\alpha = 0$ at $\$ = 1$ was used.

The function ω (speed of gas associated with the heat expansion) must have the limited derivative $\partial\omega/\partial\alpha$.

Having attained in (3.4) the limiting transition at $\$_0 \to 1$, we shall obtain (3.3). We note that in this case

$$q = \text{const} = \lambda(1)\left[\frac{\partial\theta}{\partial\alpha}\right]_{\alpha=-0}$$

Thus, using function (3.2), we shall have $\$ = 1$ at $\alpha \ge 0$, $\partial\$/\partial\alpha = \text{const}$ at $\alpha = -0$. In region $[-\infty, 0]$ function $\$$ is described by the equations (1.6) with $f = 0$.

We shall seek stationary solution of these equations at

$\varepsilon = -c = \text{const} < 0$. For obtaining a qualitative picture we shall limit ourselves to the approximation $\rho = \lambda = 1$. Assuming that $\partial\$/\partial\alpha = 1$ at $\alpha = 0$, we find

$$\$ = \int_{-\infty}^{\alpha} e^{-\alpha^2/2m\alpha}\, d\alpha \qquad (-\infty < \alpha \leq 0)$$

The magnitude m is determined from condition

$$\int_{-\infty}^{0} e^{-\alpha^2/2m\alpha}\, d\alpha = 1$$

In particular

$$m = 1 \text{ at } c = 0, \quad m = 0 \text{ at } c = \pi/2$$
$$m \sim -\sqrt{2c \ln \sqrt{c}} \text{ at } c \to \infty$$

Solutions for different c are given in Fig. 3.

At $c > \pi/2$ we have $m < 0$, i.e., gas flows to the zone of reaction (point $\alpha = 0$) from the direction of combustion products. The curve $\$(\alpha)$ at the point $\alpha = -0$ has a positive slope at $m > 0$ and negative at $m < 0$. In sector of convexity of this curve the speed of gas $m - c\alpha$ is negative and diffusion flux of fuel is directed opposite to the convection flux.

The sequence of the $\$(\alpha)$ curves with a change of c from ∞ to 0 qualitatively is identical to the sequence of curves in the establishment of normal flame from a discontinuous profile of temperature (2.1).

At $\varepsilon > 0$ the stationary solution of the equations (1.6), satisfying the conditions $\$(-\infty) = 0$, $\$(+\infty) = 1$, does not exist. The physical reasons for this were clarified in Section 2.

However, at $\varepsilon \ll 1$ there can be obtained an approximate stationary solution introducing a fictitious heat sink at $\$ = 0$. If the strength of the heat sink is small in comparison to the strength of heat source it may be assumed that distribution of temperature will evolve slowly and during certain time will differ little from the solution

with a sink.

Using (3.2), at $\rho = \lambda = 1$ in a stationary case we shall obtain

$$\frac{\partial \Phi}{\partial \alpha} = e^{m\alpha + \alpha^2/2} \qquad (3.5)$$

The heat sink q_0 will be minimum, if it is found at point $\alpha_0 = -m/\varepsilon$ ($q_0 = \exp(-m^2/2\varepsilon)$). The boundary conditions for (3.5)

$$\Phi = 1 \text{ at } \alpha = 0, \qquad \Phi = 0 \text{ at } \alpha = -m/\varepsilon$$

Consequently,

$$\Phi = \int_{-m/\varepsilon}^{\alpha} e^{m\alpha' + \alpha'^2/2}\, d\alpha' \qquad (-m/\varepsilon < \alpha < 0)$$

The condition for determining m will be

$$\int_{-m/\varepsilon}^{0} e^{m\alpha' + \alpha'^2/2}\, d\alpha' = 1 \qquad (3.6)$$

In the solution of (3.6) with respect to m there appears an ambiguity, readily, however, removeable by condition $m = 1$ at $\varepsilon = 0$.

We present results of calculations m and α_0 for certain values of ε

$\varepsilon =$	0	0.087	0.18	0.26	0.40	0.516	0.57	0.58
$m =$	1.0	1.10	1.20	1.26	1.26	1.22	1.07	1.0
$-\alpha_0 =$	∞	11.3	6.67	4.85	3.16	2.36	1.88	1.72

Curves $\Phi(\alpha)$ are presented in Fig. 3. Close to reality there will be solutions obviously only up to $\varepsilon \approx 0.2$ when the magnitude of the sink still is small ($q_0 = \exp(-2)$ at $\varepsilon = 0.18$). At $\varepsilon > 0.3$ influence of the sink is so great that m begins to decrease. The solution does not exist at $\varepsilon > 0.58$ (at $\varepsilon = 0.58$ we have $q_0 \approx 1/e$). Thus, at $\varepsilon \sim 1$ the phenomenon becomes essentially nonstationary.

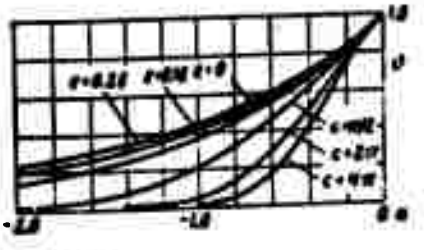

Fig. 3.

4. The use of function (3.2) does not make it possible to find a change in q. For the solution of this problem it is necessary to use a zone of reaction of finite width. Nevertheless, the ascertained general properties of the phenomenon make it possible to make qualitative conclusions without an accurate solution of the problem. Actually

$$q = \int_{-\infty}^{+\infty} j\,dx = \int_0^1 j \frac{\partial x}{\partial \theta}\,d\theta$$

At $\varepsilon < 0$ in region of the main portion of temperature change (and consequently also in the main part of zone of reaction) $\partial\alpha/\partial\$$ decreases in comparison to a normal flame; at $\varepsilon > 0$ — it increases. In other words the zone of reaction contracts or expands; correspondingly, q decreases or increases.

It is obvious that influence of ε on q will be greater, the wider is the zone of reaction in the normal flame.

If we consider the quantity of heat Q being released per unit of initial surface of flame, then it is possible to point out that with time, Q begins to increase at $\varepsilon < 0$ and to decrease at $\varepsilon > 0$, if at initial moment the flame was normal. At $\varepsilon < 0$ in a stationary case $Q \sim q \exp(c\tau)$. In a turbulent flow the elongation of the flame ($\varepsilon < 0$) statistically predominates over the contraction ($\varepsilon > 0$). This directly follows from form of the functions $\varphi(t)$, but can be considered also as an experimental fact. The result is an increase of burning velocity in the presence of turbulence.

In flame with a chain mechanism of the chemical reaction a change in the thickness of the flame will exert an influence on the diffusion of active centers and, apparently, q will change more gradually than in a thermal mechanism of a chemical reaction.

There is possible also change of mechanism of reaction: a decrease in thickness of flame will shift mechanism towards a chain reaction; an increase — to a thermal.

5. If $f(\$) = 0$ at $\$ \leq \$_0 > 0$, $f(\$) \neq 0$ at $\$_0 \leq \$ \leq 1$, then at fairly large c there does not exist a stationary solution of equations (1.5), satisfying boundary conditions different from zero

$$\theta \to 0 \quad \text{at } \beta \to \pm\infty, \qquad \frac{\partial \theta}{\partial \beta} - \omega = 0 \quad \text{at } \beta = 0$$

That is, with a fairly intense and prolonged extension, finite volumes of the combustions products, surrounded by a fresh mixture, may disappear. Process of such attenuation of flame is very simple. Let us assume that at initial moment of time the combustion products occupy in the plane ζ a band of finite width $d \gg \delta_0$. At fairly large c the narrowing of band under the action of external hydrodynamic field can not be compensated by the combustion process and the band width starts to decrease. If here there is attained $d \sim \delta_0$, the influence of cold regions is closed and there occurs a lowering of the temperature accompanied by the cessation of burning.

6. The investigation conducted above makes it possible to draw certain conclusions about mechanism of turbulent combustion (in the case of large-scale turbulence).

The parameter $\gamma = v'\delta_0/u_0 l$ plays an important role. The order of magnitude of γ, obviously, coincides with the most probable value of absolute magnitude of the parameter $\varepsilon = \varphi\delta_0/u_0$.

At $\gamma \ll 1$ the combustion occurs in laminar fronts. Perceptible deviations of flame from normal and phenomena associated with damping of flame (resorption of finite volumes of combustion products, flame bursts, ejection of combustion products into the fuel mixture) are of low probability.

At $\gamma \sim 1$ the structure of laminar flames, as a rule, deviates from normal: the concept of speed of propagation of front of flame loses sence, profile of temperature and amount (specific) of burning substances are variable. Probability of attenuation of flame increases; but, assuming that for the possibility of the attenuation of the flame $|\varepsilon|$ must be fairly large ($c > \pi/2$ in the idealized scheme of Section 3) and a certain time which increases as $|\varepsilon|$ decreases is necessary, it must be recognized that this probability is still small. Thus, at $\gamma \sim 1$ combustion occurs chiefly under "frontal" conditions; contribution of "bulk" burning associated with attenuation of flame is small.

At $\gamma >> 1$ the structure of laminar flames strongly deviates from normal and the probability of attenuation of flame becomes significant. Combustion occurs both in laminar fronts, which constantly burst out and die down, leaving a "warm" region, and also by means of volumetric reactions, proceeding in "warm" regions and constantly accompanied by self-ignition with formation of laminar flame.

The author is grateful to S. A. Khristianovich and K. I. Shchelkin for their discussions of the work, remarks and opinions.

Submitted
12 January 1963

Literature

1. L. Kovasznay. A comment on turbulent combustion. Jet Propulsion, 1956, V. 26, No. 6, p. 485.

2. Ya. B. Zel'dovich. On the theory of propagation of flame. Journal of Physical Chemistry, 1948, V. 22, No. 1.

PROPAGATION OF ZONE OF CHEMICAL REACTION IN PURE ACETYLENE AND MIXTURES WITH OTHER GASES

B. A. Ivanov and S. M. Kogarko

(Moscow)

Results are presented for an experimental research on limiting diameters of flame propagation in pure acetylene in the interval of pressures 0.65-4.00 a.a* at a temperature of 18°C. There are discussed the possible causes of discrepancy between the obtained dependency and available source data. Results of analogous experiments in closed tubes of large volume are discussed.

A theoretical calculation of the decomposition flame temperature of acetylene at a pressure of 1 a.a, which by taking into account the dissociation of hydrogen and carbon was found to be equal 2980° ± 50°K. We examine the possible conditions of the decomposition magnitude of energy and types of initiation of acetylene. There is discussed concept "cascade explosion," which, in the opinion of authors, is unsuitable.

The possibility of spontaneous propagation of a decomposition flame in pure acetylene is associated with the fact that during decomposition of a molecule of acetylene into elements there is released a large quantity of heat 54.29 kcal/mole. This magnitude is obtained from consideration of following scheme of the decomposition:

$$C_2H_2 \rightarrow 2H + 2C_{gas} + 389\,140 \text{ cal}$$
$$\tfrac{1}{2}H_2 \rightarrow H - 51\,632 \text{ cal}$$
$$C_{solid} \rightarrow C_{gas} - 169\,585 \text{ cal}$$

*a.a = atmospheres (absolute) [Tr. Ed. Note]

Finally we obtain:

$$C_2H_2 \rightarrow H_2 + 2C_{solid} - 54.29 \text{ kcal.}$$

The experimentally determined heat of dissociation of acetylene is equal to 54.2-58.0 kcal/mole.

Depending upon initial parameters of acetylene, and also on the dimensions and shape of vessel in which it is found, there are possible different types of decomposition: flash, slow combustion (deflagration), detonation and ignition during reflection of shock wave from a barrier.

While the first three types of decomposition have been studied [1, 2] sufficiently in detail, the latter conditions of decomposition, at which there are developed pressures hundreds of times exceeding the initial, have been studied very little. We shall dwell in greater detail on this question.

Ignition during reflection of shock wave at the end. In certain cases in the propagation of a flame of pure acetylene, just as for two-component mixtures of fuel with oxygen or air, there are recorded on the ends of pipelines pressures significantly exceeding values for given mixtures in case of their stationary detonation. In works [3, 4] there is shown experimentally and theoretically that this is connected with so-called conditions of rapid nonstationary burning whose mechanism consists in the following. Before a continuously accelerating flame there will be formed a shock wave of such amplitude which is insufficient for ignition of the gas during the period of its compression in the passing wave. During reflection of this shock wave from obstacle in the nonreacting gas with a supplemental shock the temperature approximately doubles and significantly the density increases. The gas in which reaction could not penetrate to a sufficient depth during its compression in the passing shock wave

ignites under conditions of reflection of the same wave from the obstacle. At the same time there is not excluded possibility of appearance of detonation in the still nonreacting shock-compressed gas at the end of pipe.

In work [3] it is shown that in acetylene the mode of nonstationary fast burning develops under conditions where there becomes already impossible a stationary detonation. Thus, for example, in pipe with diameter 100 mm and length of 20 m the limiting initial pressure at which there still is realized a transition of burning into detonation is 2.45 a.a. At a lower initial pressure always there is realized the conditions of slow burning with small increase of pressure for face of pipe. In experiments with an initial pressure close to 2.4 a.a sometimes there are realized conditions of rapid nonstationary burning with extraordinarily high pressures at end of pipe. From obtained photoregistrations (Fig. 1) it is clear that the flame in last section of pipe continuously is accelerated and attains a speed of 800 m/sec (detonation 1920 m/sec). In Fig. 1 in products of reaction distinctly one may see two traces of shock waves: the wave propagating ahead of zone of reaction and the wave developing from explosion of nonreacting mixture at end of pipe. In experiments with such a mode of burning there was registered an increase of pressure at the end exceeding the initial by 656 times.

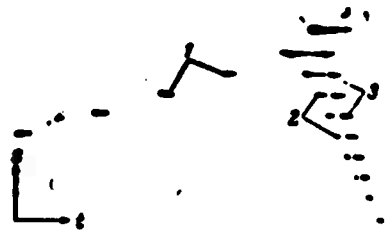

Fig. 1. Photoregistration of conditions of nonstationary rapid burning of acetylene: 1) trace of flame, 2) trace of shock wave, spreading before front of flame, 3) trace of shock wave appearing as a result of ignition at the end.

In literature [2] for explanation of similar extraordinarily high pressures there is advanced hypothesis of "cascade explosion."

It is assumed that part of initial gas is turned into products in a mode of deflagration and there occurs smooth rise in pressure in the entire system; then suddenly in remaining compressed gas a detonation develops. Losses of heat to the walls of pipe will be ignored. Under the assumptions made by calculation it is shown that the larger the portion of gas converted into products of reaction is, the greater will be the pressure at the end of the pipe, i.e., simply there is taken into account the pressure of reflection of detonational wave for all increasing initial densities of the nonreacting gas. With such an explanation it is impossible to agree for the following reason. Mechanism of transition of burning into detonations is connected with continuous acceleration of motion of front of flame and formation ahead of a shock wave in the still nonreacting gas. Ahead of shock wave being formed, the pressure, density and temperature of gas maintain an initial value. Furthermore, by hypothesis [2] for one and the same initial pressure of acetylene there may be observed different pressure of the detonation depending upon place of transition of burning into a detonation. However, experiments show [3] that independently of the fact where burning passes into a detonation – at beginning or end of pipe - the pressure during reflection of detonational wave from end remains practically constant. A sudden transition from a slowly spreading flame to a detonation without formation of shock wave is impossible. Therefore, the assumption that under these conditions the mode of a deflagrational burning passes into a detonation is in contradiction with all known experimental and theoretical assumptions in the theory of burning.

Decomposition temperature. The temperature of decomposition flame of acetylene was not determined experimentally. However, there exist certain approximate evaluations of this magnitude on basis of

pressure of explosion. In connection with the fact that experimental data on measurement of pressure of explosion differ by 20% and in the calculation of temperature of burning there are not taken into consideration the reactions of dissociation of hydrogen and carbon, authors made theoretical calculation of decomposition temperature of acetylene. With the use of data on dependence of heat capacity of amorphous carbon on temperature [5] with extrapolations of them in region of high temperatures by numerical integration there was obtained enthalpy of carbon at different temperatures. Taking value of vapor pressure of carbon and heat of sublimation from work [6] on the assumption that the vapor consists only of molecules C_2 and vapor pressure is equal total vapor pressure of molecules C_1, C_2, C_3, and using coefficients of dissociation and enthalpy values for hydrogen from [7], by the usual method [8] there was calculated decomposition temperature of acetylene at a constant pressure of 1 a.a. There was assumed the following equilibrium reaction:

$$C_2H_2 \rightarrow aC_{2\,solid} + bC_{2\,gas} + cH_2 + dH$$

where a, b, c and d were calculated. The decomposition temperature determined in such a way was found to be equal to 2980 ± 50°K. In view of great uncertainty of magnitude of vapor pressure of carbon there was made one more evaluation. Maxima of vapor pressure from work [5] were used. In this case temperature is equal to 2920 ± 50°K.

Limiting pressure of propagation of flame in pure acetylene. Limiting pressure of propagation of flame determined in works [1, 2, 9] is equal to 1.35 to 1.4 a.a. It was assumed that at pressures lower than this value, in acetylene it is a spontaneous propagation of flame is impossible, i.e., under these conditions acetylene was considered nonexplosive. Authors of indicated works note the very great sensitivity of acetylene to magnitude of source of ignition

and possibility of lowering of limiting pressure with an increase of energy of initiation. This fact is viewed, however, as the disturbance of initial conditions and is presented without an appropriate analysis.

From source material it is known that energy necessary for ignition of pure acetylene at limiting pressure of 1.4 a.a is very great (8 joule) and significantly exceeds the magnitude of energy of ignition of even limiting fuel-air mixtures whose heat of explosion is essentially lower than the heat of dissociation of acetylene. Furthermore, limiting diameters of pipes, in which there is possible the propagation of decomposition flame of acetylene at different pressures, also are very large. Thus, at a pressure of 1.4 a.a the limiting diameter is equal to 60-70 mm, at 2.2 a.a - 25 mm. Limiting diameters of pipes for limiting fuel-air mixtures with such pressures do not exceed 1 mm. From these data it may be concluded that width of zone of the chemical reaction in acetylene is significantly greater than all known magnitudes of zones of reaction for explosive gas mixtures. Consequently, for initiation of decomposition of pure acetylene it is necessary to apply sources of ignition significantly more powerful than are applied usually for ignition of gas mixtures.

Proceeding from the discussion above there were set up experiments in determining the limiting pressure of propagation of flame [10]. The experiments were made in a steel pipe with an internal diameter 160 mm, length 1500 mm, i.e., volume of 30 liter. In the pipe there were four windows, each 250 mm long. The registration of propagation of decomposition flame of acetylene was produced on photographic film secured on a revolving drum of the photoregister. Initiation was carried out at one end of pipe either by the heating

and fusing of Nichrome and molybdenum wire, or by means of discharge of condenser through spark gap, or by burning in the acetylene a certain quantity of explosive mixture in thin rubber shell. The experimentally determined limiting pressure of propagation of flame did not depend on type of initiation. In Fig. 2 there is presented the obtained dependence of energy of ignition (capacitance discharge) on the initial pressure of acetylene in the experiment. As can be seen from graph, with an initial pressure of 1.6 a.a the energy of ignition is small and amounts to 1 joule. In the limit – 0.65 a.a - the value of spark energy is equal to 1200 joules. With the use of comparatively strong sources of igintion (5-8 joules) the pressure is found to be equal to 1.35-1.4 a.a. Thus, the previously determined value, repeatedly cited in the literature, of the limiting pressure of propagation of flame corresponds to sources of initiation at 5-8 joules which had been applied but does not correspond to the absolute limit on basis of pressure. On basis of these experimental data of dependence of energy of ignition on the initial pressure it is possible approximately to estimate width of zone of reaction in acetylene. At a pressure 580 mm Hg it was found to be equal to approximately 16 mm, i.e., significantly greater than in usual explosive gas mixtures. We note here also the following. The ignition of acetylene by means of heating of metallic wires is a more complex process in comparison with ignition by condensed spark. Initiation by heating is essentially a temporary process. Special experiments of ignition by slow and rapid heating of wires showed that besides it is necessary to take

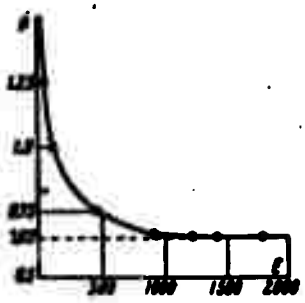

Fig. 2. Dependence of energy necessary for ignition of spark $E = 1/2\ cu^2$ (joule) on initial pressure of acetylene p_0 (a.a).

into consideration both the time of their own heating, and also volume which they can simultaneously heat.

The application for ignition of sources of such great energy, as is required in case of acetylene naturally requires knowledge and a calculation of their influence on initial parameters of the gas. If it is considered that, during ignition by condensed spark, of the thermal efficiency of the spark at place of discharge is equal to 15%, then application of source of ignition with a power of 1200 joules in a bomb with capacity of 30 liter at 0.7 a.a yields a total increase in pressure by 10 mm Hg or 2% of the initial. There were made control experiments in the ignition of pure acetylene, when influence of source can be completely ignored.

1. With an initial pressure of 1.05 a.a in 380-mm pipe 20 m long (volume 2.5 m^3) there was conducted the initiation of acetylene with a capacitance discharge (E = 500 joule). The flame passed through the entire pipe with average speed of 30 m/sec.

2. With an initial pressure of 0.65 a.a in 150-mm steel pipe 6 m long there was obtained the decomposition of acetylene. Energy of ignition was 1200 joules. Average speed of propagation of flame was 10 m/sec.

3. With initial pressures of 0.4, 0.5, 0.55 a.a in a 400 mm – bomb 1000 mm long (volume of 125 liters) there could not be obtained flames of the decomposition of acetylene during application of an ignition source with energy of 1800 joules.

Thus, the limiting pressure of propagation of flame in pure acetylene is equal to 0.65 ± 0.05 a.a. This value of the pressure must be taken into consideration for creating safe conditions of work with acetylene, its storage, and transportation.

Critical diameters of propagation of flame. We demonstrated

that in pipe of critical diameter during ignition at the open end the flame spreads for distances 2 to 3 diameters of pipe, while during ignition at closed end – 30 to 50 diameters and only then dies out. In both cases in process of experiment pressure was not increased. For pure acetylene there were determined critical diameters at pressures between 0.65 and 4.00 a.a. Experiments were made in an installation whose diagram is shown in Fig. 3. The receiver with nitrogen had a capacity >120 liters, the experimental containers – not more than 7 liters. Under these conditions, maximum increase of pressure in system at the end of burning was not more than 0.10 a.a.

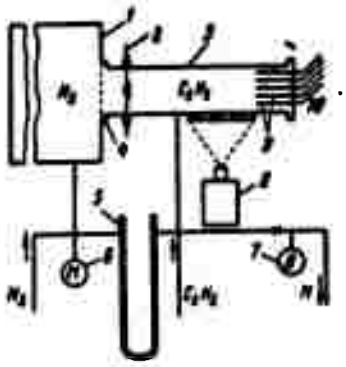

Fig. 3. Diagram of installation: 1) receiver, 2) ignition electrodes, 3) experimental container, 4) separating film, 5) differential manometer, 6) manometer, 7) vacuum gage, 8) photoregister, 9) ionization transducers, 10) to oscillograph, 11) to pump.

Receiver with nitrogen and container with acetylene were seperated by a thin polymer film which was melted out before experiment, creating an open end. Pressure in vessels was levelled by means of a differential manometer. Igniting was produced for "open" end of pipe by discharge of capacitor or incandescence of wire. In Fig. 4 there are presented the obtained experimental data, and also data from works [1,2]. In Fig. 4 there are plotted also the results of our experiments during ignition at the closed end in the experimental

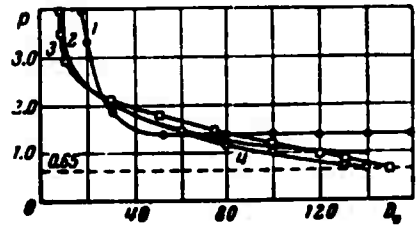

Fig. 4. Critical diameters D_x (mm) of the propagation of flame depending on initial pressure (a.a) of acetylene: 1) data of work [1], 2) data of work [2], results of present work, 3) ignition at open end, 4) in closed pipes.

pipe end closed from both sides (there were used pipes 6 m in length and 60, 80, 100, 130, 140 mm in diameter). It is evident that value of critical diameters fairly well agree with data in work [2], but are not correct because during experiment the pressure was increased, and initial state of propagation was assured, as already has been discussed, by the ignition at the closed end. The deviation of values of magnitude of critical diameter during increased pressures (higher than 2.2 a.a), obviously, is explained by purely experimental difficulties in view of very strong dependence of the limiting pressure on the diameter of pipe.

Upper concentration limits of the flame propagation in mixtures of acetylene and oxygen, air, and nitrogen at a pressure of one atmosphere. In connection with the fact that in pure acetylene there is possible the propagation of flame up to pressure of 0.65 a.a, of great scientific and practical interest is the question on the reality of existence of an upper concentration limit of propagation of flame in a mixture of acetylene with oxygen and air. On the basis of source material [11], concentration of acetylene in oxygen at upper limit at a pressure of 1 a.a corresponds to 87-93%, and in air – 56-75%.

Our experiments showed [12] that upper concentration limits of propagation of flame for mixture of acetylene with oxygen and air at the atmospheric pressure do not exist. In Fig. 5 there is presented the dependence of energy of ignition of spark on the addition of oxygen, air, and nitrogen to acetylene at P = 1 a.a. From the graphs it is evident that addition of oxygen continuously lowers energy necessary for ignition. With 8% oxygen the mixture readily is ignited by an induction discharge from a Ruhmkorff coil (E ≈ ≈ 1 joule). In the mixture of acetylene with air with the air content

up to 23.5% the energy necessary for ignition of spark is greater than for pure acetylene. With 33% air the mixture is ignited from a Ruhmkorff coil. The dilution of acetylene with nitrogen results in a continuous increase of ignition energy and with 20% nitrogen the mixture can not be ignited with a spark energy at 1200 joules. The unique change in energy of the igniting spark from contents of air in the mixture is explained by the fact that on initial sector of reaction curve of nitrogen in air as diluent it prevails over oxygen, facilitating the ignition. With contents in mixture of air up to 10%, experimental variation of curve agrees well with the calculated obtained from two other graphs.

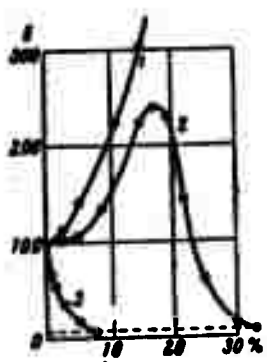

Fig. 5. Dependence of energy E necessary for ignition on composition of mixture:
1) $C_2H_2 + N_2$
2) C_2H_2 + air
3) $C_2H_2 + O_2$

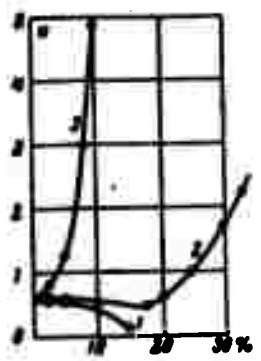

Fig. 6. Dependence of average speed U(m/sec) of propagation of flame on the composition, in %:
1) $C_2H_2 + N_2$
2) C_2H_2 + air
3) $C_2H_2 + O_2$

In experiments in determining the magnitude of ignition energy simultaneously there was made a photoregistration of propagation of flame. In Fig. 6 there are given, in the form, of graphs the dependences of mean values of apparent velocity of propagation of flame in the

sector 600 mm from source of ignition on the percentage of addition agent. From graphs shown in Figures 5 and 6 there can be made the important practical conclusion about the fact that small additions of oxygen to acetylene make this mixture more dangerous than pure acetylene, whereas addition of air (up to 23.5%) makes this mixture less dangerous in comparison to pure acetylene. From graph in Fig. 5 there readily is discerned the following. The previously determined values of upper concentration limits of acetylene with oxygen and air correspond to the energy of initiation usually applied for ignition of acetylene and its mixtures (fusing and calcination of wires).

Concentration limits of propagation of flame in a mixture of acetylene with air depending on initial pressure. The authors conducted experiments in determining the concentration limits of propagation of flame in mixture of acetylene with air depending on initial pressure [13]. To work with one fixed source of ignition which assures the ignition of the most difficult ignitable mixture at the limiting pressure in entire interval of pressures and concentrations in case of mixture acetylene-air is found to be impossible. This is connected with the fact that energy of mixture, beginning from certain values of the composition and pressure in those containers, which might be used under laboratory conditions is found to be comparable with magnitude of the ignition energy. Therefore, the determination of concentration limits was made on basis of following scheme. For a fixed composition of the mixture there was determined dependence of ignition energy on the initial pressure in the experiment. Such dependence has a plateau, on basis of which there readily is determined the limiting pressure of ignition for mixture of a given composition, and by the point of transition of curve on plateau there is determined limiting maximum ignition energy which usually is

called saturating ignition energy. By the obtained limiting values of the pressure in such experiments it is possible to construct concentration limits of propagation of flame dependent on the pressure.

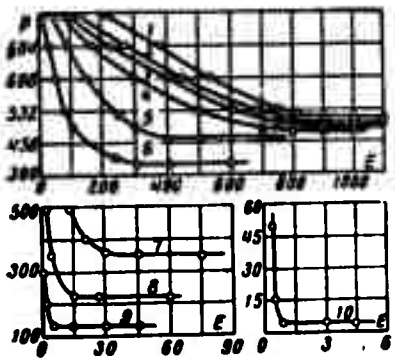

Fig. 7. Dependence of spark energy necessary for ignition on initial pressure of mixture (mm Hg):
1) 85% C_2H_2 + 15% air;
2) 90% C_2H_2 + 10% air;
3) pure acetylene;
4) 75% C_2H_2 + 25% air;
5) 70% C_2H_2 + 30% air;
6) 65% C_2H_2 + 35% air;
7) 60% C_2H_2 + 4% air;
8) 50% C_2H_2 + 50% air;
9) 45% C_2H_2 + 55% air;
10) 30% H_2H_2 + 70% air to 5% C_2H_2 + 95% air.

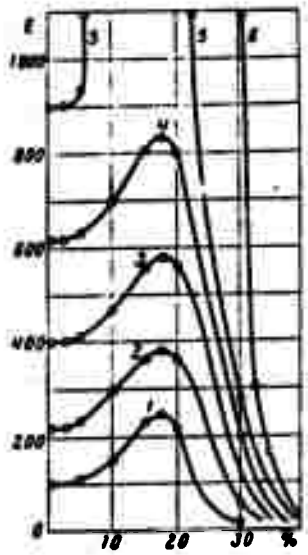

Fig. 8. Dependence of ignition energy on composition of mixture acetylene – air for different initial pressures, (in abs.atm):
1) 1.0 a.a, 2) 0.9 a.a. 3) 0.8 a.a, 4) 0.7 a.a, 5) 0.65 a.a, 6) 0.58 a.a.

In Fig. 7 are given the indicated dependences. In Fig. 8 there is shown dependence of ignition energy on composition of mixture at different initial pressures. The curves are analogous to the already described curve 2 in Fig. 2. The maximum ignition energy is observed

when amount of air in mixture is about17.5% for all the investigated pressures. A mixture with contents of air up to 5% and with contents of air about 23% has an ignition energy equal to ignition energy of pure aceylene at the same pressure. From the graphs it is evident that both the limiting pressure of propagation of flame and also ignition energy necessary at this pressure, beginning from 23% air, decrease with an increase in content of air in the mixture.

From data in Figures 7 and 8 there readily is constructed the dependence of limiting initial pressure of the flame of propagation on composition of the mixture (Fig. 9). Region lying above the curve is called region of ignition or region in which the propagation of flame is possible. The region, lying below the curve is called region of incombustible compositions of the mixture.

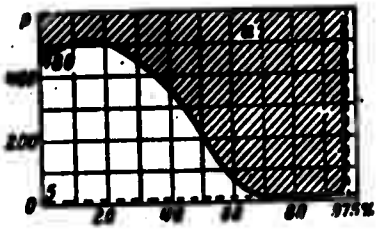

Fig. 9. Limiting pressure (mm Hg): propagation of flame depending on composition of mixture acetylene-air; a is the region of ignition.

From the graph given in Fig. 9 it follows that with strong dilution of acetylene with air, character of dependence of limiting pressure on composition of mixture is very similar to analogous dependences for other fuel mixtures. Here also exists a lower concentration limit of propagation of flame quantitatively coinciding with values given in the literature [11]. However, for mixture of acetylene with air there is absent an upper concentration limit which is connected with possibility of a flame propagation in pure acetylene. Therefore, left branch of the shown curve, not having an asymptote, is not inherent to the usual mixtures of hydrocarbons with air or oxygen.

Submitted
29 October 1962

Literature

1. W. Reppe. Chemie und Techik der Acetylen-Druck-Reaktionen, 2, Verlag Chemie, Weinheim, 1952.

2. H. B. Sargent. How to design a hazard-free system to handle acetylenes. Chem. Engineering, 1957, Vol. 2, No. 64, p. 250.

3. S. M. Kogarko and A. A. Borodulin et al. Investigation of propagation of zone of chemical reaction in acetylene in pipes of large diameter. Chem. Industry, 1962, No. 7, p. 30-35.

4. S. M. Kogarko. Investigation of pressure at end of pipe during nonstationary rapid burning. Journal of Tech. Physics, 1958, V. XXVIII, p. 2041.

5. M. P. Slavinskiy. Physico-chemical properties of elements. Metallurgy Publishing House, 1952.

6. A. N. Nesmeyanov. Vapor pressure of chemical elements. Publishing House of Academy of Sciences of USSR, Moscow, 1961.

7. M. V. Vukalovich. Thermodynamic properties of gases. Mashgiz, 1953.

8. B. L'yuis and G. El'be. Combustion, flame, and explosions in gases. Foreign Literature Press, 1948.

9. G. Schmidt and K. Haberl. Sicherheitsmassnahmen beim Zerfall von Acetylen bei niedrigem Druck. Techn. Überwachung, 1955, No. 12.

10. S. M. Kogarko and B. A. Ivanov. On the limiting pressure of spontaneous propagation of zone of reaction in acetylene. Reports of Academy of Sciences of USSR, 1961, V. 140, No. 1.

11. H. F. Coward and G. W. Jones. Limits of flammability of gases and vapors. Bureau of Mines. Bulletin 503, 1952.

12. B. A. Ivanov and S. M. Kogarko. On the upper concentration limit of propagation of flame in mixture of acetylene with oxygen and air. Reports of Academy of Sciences of USSR, 1962, V. 142, No. 3, p. 637.

13. S. M. Kogarko, B. A. Ivanov and A. Ye. Grunin. Concentration limits of propagation of flame in a mixture of acetylene with air. Reports of Academy of Sciences of USSR, 1962, V. 145, No. 6, p. 1308.

EXPERIMENTAL DETERMINATION OF COEFFICIENT OF THERMAL CONDUCTION OF HEAT-INSULATING MATERIALS BY METHOD OF SELF-SIMULATING CONDITIONS

G. I. Vasil'yev, Yu. A. Dem'yanov, V. I. Kurnakov, A. V. Malakhov, Kh. A. Rakhmatulin and A. N. Runynskiy

(Moscow)

Existing methods of experimental determination of thermal coefficients of materials in most cases are based on results ensuing from an analysis of particular solutions of the linear heat-conduction equation (methods of regular conditions, unlimited standard, instantaneous source and others) [1-3]. These methods have a number of defects: complexity of the equipment and experiment, especially for the case of high temperatures where its realization is very formidable, the possibility of obtaining from a single experiment only one value of coefficient of thermal conduction (at the temperature of heated model) and, what is most important, they proceed from the condition of independence of thermo-physical coefficients on the temperature. Of the methods assuming the variability of thermo-physical coefficients, well known is O. A. Krayev's method for determining the thermometric conductivity, which is based on approximate solution of a nonlinear heat-conductivity equation for unlimited cylinder [4-5]. In present article there is considered method of determining the coefficient of thermal conductivity based on use of an accurate nonlinear heat-conductivity equation [6], which makes it possible to use comparatively simple means of experimenting. There are presented experimental data on the thermal conductivity of foam grog with an initial specific gravity of $\gamma_0 = 820$ kg/m^3 in the temperature range of 50 to 750°C.

With the use of liquids having a high coefficient of heat transfer during condensation (for example, water), by water proposed method it is possible to determine coefficients of

thermal conduction of not only heat-insulator but also of materials having a relatively high thermal conduction (close to thermal conduction of metals).

1. Essence of method being considered consists in the following. The tested model is selected in such form that during the time of measurements in its central part the process of propagation of heat occurs just as in a semi-infinite rod (one-dimensional case), i.e., transverse dimensions and height must be much greater than thickness of heating up of model during the period of experiment. For example, for a model there can be taken a fairly thick rectangular plate. During experiment temperature of heated surface of model is maintained constant.

From theory of thermal conduction (see, for example, [7]) on the basis of an analysis of dimensionality it follows that in considered case the process of propagation of temperature in model being tested will occur according to the law (self-simulating solution)

$$T = T(\xi), \qquad \xi = \frac{x}{\sqrt{t}}$$

Here x is the distance of point of body from the surface being heated, t is the time.

By virtue of mentioned fact, the equation of propagation of heat which is, in a general case, a nonlinear partial differential equation of the second order, for given experiment reduces to the ordinary equation

$$c_p \gamma \frac{dT}{d\xi} = -\frac{1}{2}\frac{d}{d\xi}\left(\lambda \frac{dT}{d\xi}\right) \qquad (1.1)$$

Here λ is the coefficient of thermal conductivity subject to determination and is function of the temperature; c_p and γ are the heat capacity and specific gravity which are considered as known* functions of T.

---

*This circumstance imposes certain limitations on applicability of the method.

Thus, it is sufficient to determine character of change of temperature at one point of model in order to know the entire field of the temperatures $T = T(\xi)$.

Integrating equation (1.1) from ξ to ∞ and assuming that $\partial T/\partial \xi \to 0$ at $\xi \to \infty$, we obtain

$$\lambda(\xi) \quad \frac{1}{2\left(dT/d\xi\right)} \int_{\xi}^{\infty} c_1 \gamma \frac{dT}{d\xi} \xi d\xi \qquad (1.2)$$

From formula (1.2) on the basis of the experimentally determined field there is determined $\lambda(\xi)$ and, consequently, $\lambda = \lambda(T)$.

The use of self-simulating heating-up makes it possible to find $\lambda(T)$ by a single differentiation of experimentally found dependence $T(t)_{x=const}$. In the opposite case of an arbitrary dependence of surface temperature on time, the determination of $\lambda(T)$ would be associated with experimental finding of the dependence $T(x)_{t=const}$ and with its differentiation with respect to x, which results in large errors, inasmuch as this dependence may be found only be discrete values of x.

The determination of the $T(\xi)$ profile on the basis of interpreting the readings of several additional thermocouples mounted in different sections makes it possible to judge about errors introduced by errors of measuring apparatus and deviations of temperature of the surface being heated from the constant. It is necessary to note that maintenance of constancy of surface temperature of model being tested is associated with certain technical difficulties, especially at high temperatures.

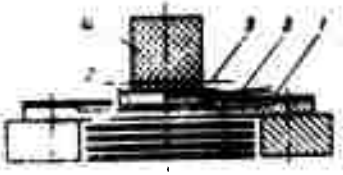

Fig. 1.

2. Experimental realization of method was carried out by means of an installation whose diagram is presented in Fig. 1.

The main parts of installation are the

flat graphite heater 1, by the regulation of whose power the constancy of the temperature of buffer metallic plate 2 controlled by thermocouple 3 is maintained (by means of radiation). The buffer plate is insulated from elements of the installation under a voltage potential.

The adjustment of power being consumed by the heater was carried out by means of a step-down transformer to whose primary winding there is connected an autotransformer. The model 4 being tested consisted of two parallelepipeds ground against each other with a total base of 100 × 100 mm each, between which there was placed a measuring thermocouple 5 with junction at center of base.

In order to decrease the influence of inconstancy of temperature of surface of model during initial period of experiment (~5 to 10 sec), and also for lowering the relative error of determining the coordinate of thermocouple (thickness of thermocouple was 0.5 mm) the latter was placed at a relatively great distance from heated surface (~10 mm). The total height of model amounted to ~120 mm; this assured the condition of semilimitedness required for application of the method.

The experiment begins with the establishment of a steady-state mode of buffer plate (1000 ± 20°C) together with auxiliary model secured on its surface. Then the auxiliary model was replaced by model being tested and simultaneously there were connected the measuring instruments. The recording of the thermocouple readings (Chromel-Alumel thermoucouples) were made in the electronic potentiometers EPP-09.

As follows from formula (1.2), the determination of $\lambda(T)$ in region of low temperatures (50 to 200°C) at high values of temperature of heater may be insufficiently accurate owing to relatively large error in determining $dT/d\xi$ in the indicated interval of temperatures. For the purpose of increasing the accuracy in determining

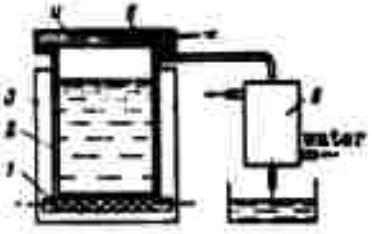

Fig. 2.

$\lambda(T)$ in range of temperatures of 50 to 200°C by the method of self-simulating conditions there was used installation (Fig. 2), assuring a high accuracy of maintaining a constant surface temperature owing to the condensation of vapors of spindle oil. Preliminarily from the oils there were evaporated low-boiling fractions.

The oil was flushed into the heat-insulated boiler 2, 3, on bottom of which there was mounted a electrical heater 1.

During the investigation of the thermal conductivity of porous materials the condensation is realized on the thin metallic flange 4 (analog of buffer plate) having a low thermal resistance with the thermocouple 5 caulked on the surface. During the investigation of the thermal conductivity of nonpourous materials the condensation is made directly on the surface of the model. The condensation of excess oil vapors is realized in the condenser 6.

3. In Figures 3 and 4 there are presented the functions $T = T(\xi)$, obtained in experiments with temperatures of heated surface of model ~1000 and ~200°C. Dependences of true heat capacity c_p and specific gravity γ on temperatures are obtained by means of calculation on basis of known chemical composition and coefficient of linear expansion of material.

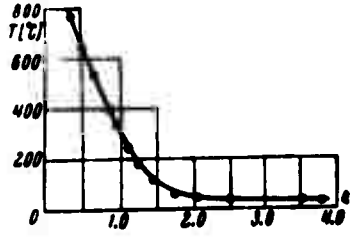

Fig. 3.

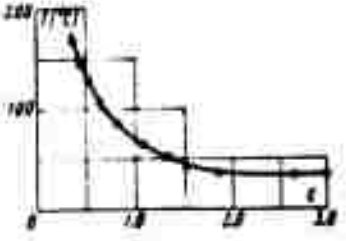
Fig. 4.

We present results of chemical analysis of investigated foam grog:

Component	SiO_2	Al_2O_3	Fe_2O_3	MnO	FeO
Contents %	62.60	32.00	4.00	0.06	100

Dependences $c_p = c_p(T)$ for components of investigated material are derived from work [8], the dependence of coefficient of linear expansion $\alpha = \alpha(T)$ was obtained by the authors experimentally. Graph of change of $c_p\gamma$ with temperature is presented in Fig. 5.

The dependence $\lambda = \lambda(T)$, obtained as a result of the processing of the experimental data, is presented in Fig. 6, where 1, 2 and 3 correspond to different experiments; the light points refer to method of self-simulating conditions, the black – to Krayev's method.

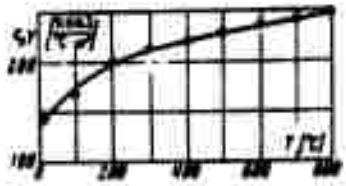

Fig. 5.

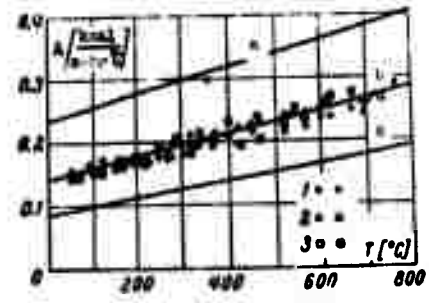

Fig. 6.

Curves a and b in Fig. 6 are constructed on the basis of equations

$$\lambda = 0.24 + 0.0002T, \quad \lambda = 0.09 + 0.000125T \text{ [kcal/m·hr°C]} \quad (3.1)$$

for specific gravity of foam grog $\gamma = 950$ kg/m^3 and $\gamma = 600$ kg/m^3, respectively [8].

The dependence b obtained by method of self-simulating conditions for foam grog with $\gamma = 820$ kg/m^3 may be approximated by the equation

$$\lambda = 0.14 + 0.000175T \text{ [kcal/m·hr°C]} \quad (3.2)$$

The dispersion of the experimental points relative to averaging curve does not exceed ±7%.

The λ values at room temperature obtained from equations (3.1) and (3.2) agree well with dependence $\lambda = \lambda(\gamma)$ for analogous materials [8].

The experimental data presented in Fig. 6 for foam grog with a specific gravity $\gamma = 820$ kg/m^3, obtained by the authors according to method of O. A. Krayev (black points), agree well with results of experiments conducted according to method of self-simulating conditions.

Submitted
12 June 1962

Literature

1. G. M. Kondrat'yev. Normal thermal conditions. State Technical Press, 1954.

2. A. V. Lykov. Theory of thermal conduction. State Technical Press, 1952.

3. A. F. Chudnovskiy. Heat exchange in dispersion media. State Technical Press, 1954.

4. O. A. Krayev. Method of determining the dependence of the thermometric conductivity on the temperature for one experiment. Heat-Power Engineering, 1956, No. 4.

5. O. A. Krayev. Determination of thermometric conductivity of heat insulating materials. Heat-Power Engineering, 1958, No. 4.

6. Yu. A. Dem'yanov, Kh. A. Rakhmatulin and A. N. Rumynskiy. Method of determining coefficients of thermal conduction of solid bodies, based on use of self-simulating conditions. Bulletin of Inventions, 1960, No. 8.

7. L. Boltzmann. Ann. Physik., 1894, Vol. 53, p. 959.

8. Thermophysical properties of substances. Reference Book edited by N. B. Vargaftik. Moscow-Leningrad, State-Power Engineering Publishing House, 1956.

THEORY OF THE DEPOSITION OF A VISCOUS LIQUID ONTO A FIBER OR WIRE BEING WITHDRAWN FROM THE LIQUID

B. V. Deryagin

(Moscow)

In the depositing of liquid onto a cylinder of radius r being drawn from it at a constant speed U there sets in a steady state characterized by the fact that velocities of the liquid particles at any point of space become constant and independent of time.

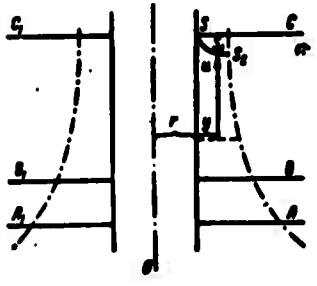

Fig. 1.

We designate Q_s as flow rate of liquid through any normal to its axis and stationary plane AA_1, BB_1, CC_1 in space (Fig. 1). Obviously,

$$Q_s = 2\pi \int_0^h (r + y)\, u\, dy \qquad (u = u(y)) \tag{1}$$

where y is the distance from subfilm, and u is the speed in direction of axis of cylinder in a stationary system of coordinates, h is the thickness of film. From conditions of stationarity there is evident the relationship

$$Q_s = \text{const} \tag{2}$$

From (1) and (2) it is readily concluded that, if there is known the amount of liquid "being occupied" by a unit of perimeter of cylinder during a unit of time and equal to Q, then it is possible to calculate definitive thickness of liquid deposit h_∞ by the formula

$$h_\infty = \frac{Q}{U} \qquad (h_\infty < r) \tag{3}$$

so that h_∞ does not depend either on temperature and viscosity of liquid or on other conditions at a height different from level of liquid, as long as these conditions will not be found incompatible with the given value Q.

The definitive thickness h_∞ is understood to be the thickness obtained after loss of fluidity by film as the result of consolidation.

In any sector of film prior to its consolidating the particles of liquid farther away from surface of cylinder will lag behind its motion under action of gravity. Thus, u is a diminishing function of y. This function satifies Navier-Stokes equations which for case of axial symmetry, and ignoring the inertia terms, give

$$\frac{\partial^2 u}{\partial y^2} + \frac{1}{r+y}\frac{\partial u}{\partial y} = -\frac{\rho g}{\eta} \tag{4}$$

where η is the viscosity, ρ is the density of liquid, g is the acceleration of gravity.

In integrating equation (4) there must be taken into account the following boundary conditions:

$$u = U \quad \text{at } y = 0, \qquad \frac{\partial u}{\partial y} = 0 \quad \text{at } y = h \tag{5}$$

of which the first expresses absence of slipping between liquid and filament, and the second is evident from the fact that on free surface of film of liquid there is applied only the air pressure normal to it, and normal stresses are absent.

It is readily seen that for cases when $h/r \ll 1$ the second term in formula (4) cannot exert a marked influence on the result of the integration; being limited to the case of films, this term will be ignored.

Here the integration (4) under boundary conditions (5) gives

$$u = \frac{\rho g}{2\eta}(h - y)^2 - \frac{\rho g}{2\eta}h^2 + U \tag{6}$$

and, according to (1),

$$Q = Uh - \frac{1}{3}\frac{\rho g}{\eta}h^3 \tag{7}$$

If gravity did not act (g = 0), then in entire thickness of liquid film there would be

$$u = U = \text{const}, \qquad Q = Uh \tag{8}$$

The parabolic profile SS_1S_2 of the speeds in cross section of liquid film, according to (6), is shown in Fig. 2.

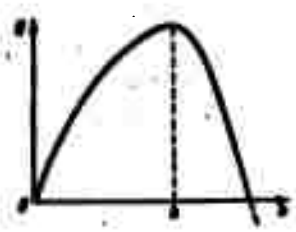

Fig. 2.

It is readily seen from equation (7) that with an increase of h from zero, Q at first also increases from zero and attains a maximum equal to

$$Q_m = \frac{2}{3}Uh_m = \frac{2}{3}U^{3/2}\left(\frac{\eta}{\rho g}\right)^{1/2} \quad \text{at} \quad h_m = \left(\frac{\eta U}{\rho g}\right)^{1/2} \tag{9}$$

and then diminishes, becoming negative (Fig. 2) at values $h > \sqrt{3}h_m$.

Comparing (9) with formula (3), we find that the maximum possible thickness of deposit h_∞ is equal to

$$h_\infty = \frac{2}{3}h_m = \frac{2}{3}\sqrt{\frac{\eta U}{\rho g}} \tag{10}$$

As was pointed out theoretically [1, 2, 3] and verified

experimentally [4], in those cases when it is possible to ignore the effect of capillary pressure of meniscus near the "water line" (this pressure according to the first Laplacian law depends on surface tension and curvature of the meniscus), actually there is realized namely this, the maximum possible thickness of the deposit. However, during the depositing of liquid films it is impossible to ignore the capillary forces.

We shall endeavor to examine concurrently those capillary and hydrodynamic phenomena taking place in zone of meniscus and near the water line which determine "capture" of liquid and thereby thickness of the deposit h_∞.

In order to be freed from circumstances incapable of rendering an essential influence on result, but capable of complicating treatment of the posed problem, we shall formulate it in following manner. Suppose that from a liquid as a whole at rest there is extracted at constant speed U an infinite cylinder (Fig. 3) of a circular section SS with the vertical axis OO. Maintaining the same interpretation of the designations η, ρ and g as previously, we shall designate σ as the surface tension of the liquid.

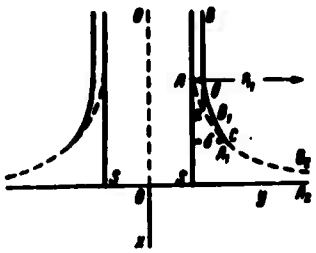

Fig. 3.

In a stationary position of cylinder being moistened by liquid the meniscus of the liquid has the shape AA_1A_2 shown in Fig. 3 by the dashed line. Motion of surface being withdrawn from the liquid must cause, in addition to formation of its moistening and the film being dragged upwards, a change in the shape of the meniscus; here it is obvious that deformation of meniscus, with increasing distance from surface of cylinder, must decrease as it tends to zero. The magnitude of this

distortion in the shape of the meniscus must depend on speed of withdrawal of cylinder from liquid, decreasing simultaneously with it. Therefore, at fairly small U, the zone in which the meniscus is minutely deformed must reach up to a distance δ from the wall, small in comparison to radius of curvature of meniscus near the "water line" R_1.

It can be assumed fairly obvious that, inasmuch as deformation of meniscus owing to drag of liquid films by the surface of cylinder decreases with distance from the latter, the slope of tangent at individual points of deformed meniscus (the solid curve BB_1B_2 in Fig. 3) to surface will be less than at points of a nondeformed meniscus located at the same distance from wall (points a and b in Fig. 3).

On the other hand, these slope angles, as is evident from simple geometric considerations are small for points of a nondeformed meniscus which are located at distances from wall less than δ.

It is evident from this that these slopes are also small for analogous points of deformed meniscus (located in Fig. 3 above point C). Thus, at small U the deformed surface of liquid may be obtained by cross-linking (connecting) the surface limiting the film with a thickness slightly varying along the wall, and the nondeformed surface which, consequently, satisfies equations of capillary statics of liquids.

Under this assumption there is deduced, as we now shall see, the genuine key to mathematical solution of the problem, which no longer will present other difficulties except the purely calculating difficulties.

We shall place the axes of the rectangular system of coordinates so that the x axis will be located along axis of cylinder in direction downwards, and the y axis will be directed towards the liquid film. If

h is the thickness of the liquid film in the sector of wall with abscissa x, then the relationship

$$h = h(x)$$

will determine the shape of surface of liquid and, simultaneously, the profile of the enclosed film. Condition of slope of this profile above the point of cross-linking C can be written in the form

$$\frac{dh}{dx} \ll 1 \text{ at } h < \delta \tag{11}$$

We shall consider hydrodynamic equations for a gentle sector of the liquid film with thickness from $h = h_0$, for $x = -\infty$, up to $h = \delta$. For such a sector, as previously, it may be assumed that in first approximation, velocities of the liquid particles are parallel to the surface of the wall. Conditions (5) will remain in force as previously. However, equation (4) must be modified, since now we must consider the inconstancy of hydrodynamic pressure in the film.

Actually, inasmuch as surface of the film is no longer cylindrical, pressure p under surface, according to first Laplacian law of capillarity is associated with external pressure p_0 by the relationship

$$p = p_0 - \frac{\sigma}{R_1} - \frac{\sigma}{R_2} \tag{12}$$

where R_1 is the radius of curvature of meridional section of surface of liquid film at point near which there is sought p; R_2 is the radius of curvature of normal section of surface perpendicular to meridional section. Under the conditions

$$\frac{h}{r} \ll 1, \quad \frac{dh}{dx} \ll 1, \quad R_2 \approx r = \text{const} \tag{13}$$

the curvature of normal section of this surface perpendicular to the

vertical section is almost constant.

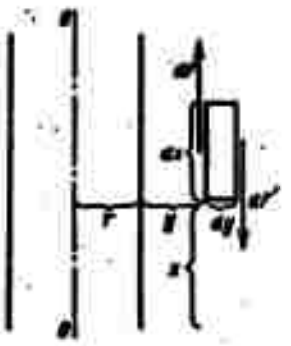

Fig. 4.

By virtue of condition (11) it is possible to assume approximately

$$\frac{1}{R_1} \approx \frac{\partial^2 y}{\partial x^2}$$

and then, instead of (12), taking into consideration (13) we obtain

$$p = p_0 - \sigma \frac{\partial^2 y}{\partial x^2} - \frac{\sigma}{r} \qquad (14)$$

Thus, now $dp/dx \neq 0$. Ignoring the forces of inertia and projecting the remaining forces onto the x- and y-axes we obtain

$$\frac{\partial p}{\partial x} - \rho g = \eta \frac{\partial^2 u}{\partial y^2} + \frac{\eta}{(r+y)} \frac{\partial u}{\partial y} \cdot \frac{\partial y}{\partial x} - \eta \frac{\partial^2 u}{\partial x \partial y} \qquad (15)$$

Due to slope of film of liquid

$$\frac{\partial u}{\partial x} < \frac{\partial u}{\partial y} \cdot \frac{\partial y}{\partial x} < \frac{\partial u}{\partial y}$$

Therefore, from (15) it is evident that

$$\frac{\partial p}{\partial y} < \frac{\partial p}{\partial x} \qquad (16)$$

and in the approximation being considered the pressure p may be considered constant across the film. From (16) it follows that in (15) it is possible for any y to take $\partial p/\partial x$ values corresponding to p values which are directly under the actual surface of flim. Therefore, differentiating (14), it is possible instead of (15) to write

$$\frac{\partial^2 u}{\partial y^2} + \frac{1}{(r+y)} \frac{\partial u}{\partial y} = -\frac{\rho g}{\eta} - \frac{\sigma}{\eta} \frac{\partial^3 y}{\partial x^3} \qquad (17)$$

The expression obtained for $\partial^2 u/\partial y^2$ differs from that, which is in equation (4) (besides the opposite sign, owing to change in direction of x-axis to the reverse) by the presence of second

term on the right-hand side. Integrating equation (4) (ignoring, in addition, second term on left-hand side) and satisfying conditions (5), we obtained equations (6) and (7). Since the integration was based only on independence of right-hand side (4) on y, and (17) possesses the same property, then integrating (17) we shall obtain (after the signs are changed and the second term on left-hand side of (17) has been discarded):

$$u = -\left[\frac{\sigma}{2\eta}\frac{d^3h}{dx^3} + \frac{\rho g}{2\eta}\right](h-y)^2 + \left[\frac{\sigma}{2\eta}\frac{d^3h}{dx^3} + \frac{\rho g}{2\eta}\right]h^2 - U \tag{18}$$

$$Q = -\int u\,dy = Uh - \frac{1}{3}\left[\frac{\sigma}{\eta}\frac{d^3h}{dx^3} + \frac{\rho g}{\eta}\right]h^3 \tag{19}$$

Transforming (19), we obtain the equation

$$\sigma\frac{d^3h}{dx^3} + \rho g = 3\eta\left(\frac{U}{h^2} - \frac{Q}{h^3}\right) \tag{20}$$

The thickness of emulsion layer in its upper part tends asymptotically (at $x \to -\infty$) to a constant value, which we shall designate as h_0; here, obviously, simultaneously all the deriatives h in x tend to zero. Substituting the corresponding magnitudes in (21), we shall find

$$Q = Uh_0 - \frac{\rho g}{3\eta}h_0^3 \tag{21}$$

Introducing instead of h the dimensionless magnitude

$$H = h/h_0 \tag{22}$$

and taking into consideration (21), we transform (20) to the form

$$\frac{d^3H}{dx^3} + \frac{\rho g}{\sigma}\frac{1}{h_0} = \frac{3\eta}{h_0^3\sigma}\left[\frac{U}{H^2} - \frac{U - (\rho g/3\eta)h_0^2}{H^3}\right] \tag{23}$$

Introducing the dimensionless variable X, and also dimensionless parameter β by the formulas

$$X = \left(\frac{3\eta U}{\sigma}\right)^{1/3}\frac{x}{h_0}, \qquad \beta = \frac{\rho g}{3\eta U}h_0^3 \tag{24}$$

equation (23) can be reduced to

$$\frac{d^3H}{dX^3} + \beta = \left[\frac{1}{H^3} - \frac{(1-\beta)}{H^4}\right] \qquad (25)$$

Equation (25) is valid according to assumption made (11), in the region

$$H < \theta \cdot \quad \left(\theta = \frac{\delta}{\delta_0} > 1\right) \qquad (26)$$

i.e., within limit at any arbitrary large values of H. In integrating (25) there must be sought the solution satisfying conditions

$$H \to 1 \text{ at } X \to -\infty, \quad H \to \infty \text{ at } X \to +\infty \qquad (27)$$

ensuing from the setting-up of the problem.

At first glance it seems that inasmuch as (25) is of third order and, consequently, its integral should contain three arbitrary constants, condition (27) still is not determined explicitly by the sought profile of liquid film. However, it is readily seen that one of three arbitrary constants must be included in integral of equation (25) in such a way that its variation only displaces, as integer, the surface of film, expressed on certain scale by equation $H = H(X)$ parallel to X-axis; not changing its shape, and, consequently, results in an identical shape of liquid film in the zone of thickness being considered.

This circumstance is evident from the fact that in equation (25) there does not enter the independent variable X itself; therefore, if $H = H(X)$ is one solution of this equation, then $H = H(X + C)$, where C is an arbitrary constant, expresses a number of other solutions.

The integration of equation (25) is not reduced to quadratics; however, there is readily found the behavior of its solution for that region where H already is close to unity. Actually, designating $H - 1$ in terms of Y and ignoring the higest powers of Y, we shall

obtain for its determination the linear differential equation

$$\frac{d^3Y}{dX^3} = (1 - 3\beta)Y.$$

Its general solution has the form

$$Y = C_1e^{\alpha_1 X} + C_2e^{\alpha_2 X} + C_3e^{\alpha_3 X}$$

where C_1, C_2, C_3 are arbitrary constants and α_1, α_2, α_3 are three values of cube root of $(1 - 3\beta)$. Of these three roots, two will be complex values with a negative real part. Therefore, for observance of condition (27) it is necessary that $C_2 = C_3 = 0$ and, consequently,

$$H = 1 + C \exp\left[(1 - 3\beta)^{1/3} X\right] = 1 + \exp\left[(1 - 3\beta)^{1/3} (X - C_0')\right]$$

where $(1 - 3\beta)^{1/3}$ is the usual (real) value of cube root of $(1 - 3\beta)$. The limiting formula for H also ascertains that the variation of the remaining arbitrary constant C influences only the location of surface of the liquid film relative to the origin of coordinates, but not on its shape.

As was shown earlier, for the solution of posed problem of determining h_0 it is necessary to cross-link, at point where $H = \varepsilon$ and $h = \delta$, the solution of equation (23) or its equivalent (25) with the solution of equations of capillary statics. For this purpose we shall multiply term by term both sides of equation (25) by $(d^2H/dX^2)dX$ and shall integrate from $X = -\infty$ to zone of cross-linking, corresponding to the value $X = X_0$. As a result, we shall obtain

$$\frac{1}{2}\left[\frac{d^2H}{dX^2}\right]^2 + \beta\frac{dH}{dX} = \int_{-\infty}^{X_0}\left[\frac{1}{H^2} - \frac{(1-\beta)}{H^3}\right]\frac{d^2H}{dX^2}dX \qquad (28)$$

But from (25) it follows that as $X \to \infty$, when $H \gg 1$ and right-hand side (25) can be ignored, the asymptotic expression for H has the form

$$H = \frac{\beta}{6}X^3, \quad \frac{dH}{dX} \approx \frac{\beta}{2}X^2 \approx \left(\frac{6H}{\beta}\right)^{2/3}\frac{\beta}{2} = \frac{\beta^{1/3}}{2}(6H)^{2/3}.$$

It follows from this that

$$\int_{X_0}^{\infty}\left[\frac{1}{H^2}-\frac{(1-\beta)}{H^3}\right]\frac{d^2H}{dX^2}dX<\int_{X_0}^{\infty}\frac{\beta^{1/2}}{3}\frac{6\,dH}{d^{1/2}H^{1/2}}<\frac{3^{1/2}\beta^{1/2}}{2^{1/2}H^{1/2}}$$

Therefore, the integral in (28) as $X_0 \to \infty$ converges and at $H = \varepsilon >> 1$ the left-hand side of (28) is close to its limiting value, which is

$$\lim_{H\to\infty}\left[\frac{1}{2}\left(\frac{dH}{dX}\right)^2+\beta\frac{dH}{dX}\right]_{H=\infty}=B(\beta) \tag{29}$$

Here $B(\beta)$ is a certain magnitude depending only on β. Consequently, instead of (28) we have the right to write approximately

$$\left[\frac{1}{2}\left(\frac{dH}{dX}\right)^2+\beta\frac{dH}{dX}\right]\approx B(\beta) \tag{30}$$

We now consider surface of liquid extending to the right of point of cross-linking C, corresponding to the values $H >> \varepsilon$, which surface by assumption satisfies equations of capillary statics, i.e., first law of Laplacian capillarity. This law for the case under consideration is expressed by equation (12). But according to fundamental law of hydrostatics

$$p=p_0-\rho gz \tag{31}$$

Here z is the height above the level where hydrostatic pressure is equal to the atmospheric. In the case when on surface of liquid there is flat horizontal section, from its level, obviously, one should read off z. Combining (12) and (31) we shall obtain

$$\frac{\sigma}{R_1}+\frac{\sigma}{R_2}=\rho gz \tag{32}$$

But it is known that

$$\frac{1}{R_1}=\frac{d\alpha}{ds}=\frac{d\alpha}{dz}\frac{dz}{ds}=\sin\alpha\frac{dz}{ds}=-\frac{d\cos\alpha}{ds} \tag{33}$$

where α is the angle of inclination to horizon of tangent to meridian

section of our surface and ds is the element of arc of this curve, corresponding to the increment $d\alpha$ of angle α. It is obvious that near point of cross-linking C, where $\alpha \approx \frac{1}{2}\pi$, it is possible to assume that $d(1/R_2) \approx 0$. Assuming this and expressing dz in terms of $d(1/R_1)$ with the aid of (32) and substituting in (33), we shall obtain at α close to $\frac{1}{2}\pi$

$$-d\cos\alpha = \frac{e}{kT}\frac{1}{R_1}d\frac{1}{R_1} - \frac{e}{2kT}d\frac{1}{R_1^2}$$

Hence, integrating, we have

$$C - \cos\alpha = \frac{e}{2kT}\frac{1}{R_1^2} \qquad (34)$$

We shall designate R_1 at $\alpha = \frac{1}{2}\pi$ in terms of R. Then the constant of integration

$$C = \frac{e}{2kT}\frac{1}{R^2}$$

consequently, instead of (34) we shall obtain

$$\cos\alpha = \frac{e}{2kT}\left(\frac{1}{R^2} - \frac{1}{R_1^2}\right) \qquad (35)$$

At point C, where $h = \delta$ (Fig. 3), $\alpha = \frac{1}{2}\pi - \Delta\alpha$, where $\Delta\alpha$ is, by hypothesis, a small slope angle of surface of emulsion to the base.

Expanding cos α in a series in powers of $\Delta\alpha$, discarding term with powers of $\Delta\alpha$ higher than the first, and, finally, replacing $\Delta\alpha$ by dh/dx, and 1/R by d^2h/dx^2 we shall obtain

$$\frac{e}{2kT}\left(\frac{d^2h}{dx^2}\right)^2 + \frac{dh}{dx} = \frac{e}{2kT}\frac{1}{R^2} \qquad (36)$$

Changing, with aid of (22) and (24), from variables h, x to variables H, X, we transform (36) to the equation

$$\frac{1}{2}\left(\frac{d^2H}{dX^2}\right)^2 + \beta\frac{dH}{dX} = \frac{e}{2kT}\frac{1}{R^2}\beta\left(\frac{e}{3\pi U}\right)^{1/3} \qquad (37)$$

Comparing (37) with (30), we determine the condition of the

cross-linking

$$\frac{\sigma}{2\pi\eta}\frac{1}{R^2}\left(\frac{\sigma}{3\eta U}\right)^{1/3}\beta = B(\beta) \tag{38}$$

or

$$\frac{\beta}{B(\beta)} - \frac{2\pi\sigma}{\eta}\left(\frac{3\eta U}{\sigma}\right)^{1/3} = 0 \tag{39}$$

Having a graph of the function $B(\beta)$, it is possible from (38), by knowing the wetting conditions U, η and σ, to find β and, consequently, according to (24), also the thickness being sought.

In order to find from (29) magnitudes B for different (but small) values of parameter β it is necessary by means of integrating equation (25) to determine dH/dX and d^2H/dX^2 for large values of H. Since equation (25) is not reduced to quadratics, then there was undertaken the numerical integration of it by means of electrical integrator of Gutenmacher system. This part of work was carried out by Yu. G. Tolstov at our request. In such a way there are found values of function $B(\beta)$ for different values of (β). In particular, there was found principal value

$$B(0) = B_0 = 0.204\ldots \tag{40}$$

This value for B(0) makes it possible to find limiting expression for small h_0, corresponding, obviously, to limitedly small U and, consequently, for extremely small values of the dimensionless parameter

$$\gamma = \frac{\eta U}{\sigma} \tag{41}$$

From (41) it is evident that to small values γ there correspond small values of the parameter β. Therefore, from (24), (38) and (40) we shall obtain

$$h_0 = mR\left(\frac{\eta U}{\sigma}\right)^{2/3}, \qquad m = 2^{1/3}\cdot 3^{2/3}\cdot B_0^{2/3} = 1.32\ldots \tag{42}$$

For the determination of thickness of deposit h_∞ there should be

used formulas (42), (3) and (21). The calculations give

$$h_\infty = h_0\left(1-\frac{\rho g h_0^2}{3\sigma}\right) = 1.32\ldots R\left(\frac{\psi}{\theta}\right)\left(1-\frac{\rho g h_0^2}{3\sigma}\right) \qquad (43)$$

It should be noted that under the condition of smallness of γ the second term in bracket is small in comparison to first, as a consequence of which $h_\infty \approx h_0$.

The calculated determination of radius of meridional section in the water line of cylinder or, what is equivalent, of the height of the latter above level of liquid into which it was lowered, in general is an unsolved problem of the theory of capillarity. The solution is entirely elementary in the case when $r \gg \sqrt{\sigma/\rho g}$, but this corresponds to the two-dimensional problems for the deposition of a liquid onto a flat surface analyzed previously [1-5]. For the opposite limiting case $r \ll \sqrt{\sigma/\rho g}$ the value R was found (also by method of cross-linking) by us previously [6]. As a first approximation

$$R \approx r$$

Substituting this value R in (42) or (43), we shall obtain the calculation formula for the thickness of liquid film being derived during the withdrawal of a thin thread from the liquid; this is of great practical importance (for example, in glass fiber, textile, electrical, synthetic fiber industries and others).

From the derivation of formulas (42), (43) it follows that condition of their validity may be presented in one of two equivalent forms

$$\frac{h_0}{r} \ll 1, \quad \text{or} \quad \frac{\psi}{\theta} \ll 1 \qquad (44)$$

The question, however, remains open as to what limit it is

possible to use equations (42), (43) with the specific requirements for an admissible error. The experimental instructions of this are given in [4].

Institute of Physical Chemistry of
Academy of Sciences of USSR

Submitted
15 May 1962

Literature

1. B. V. Deryagin. On the thickness of liquid film remaining on walls of vessels after their emptying, and theory of deposition of photographic emulsion in the wetting of motion picture film. Reports of Academy of Sciences of USSR, 1943, V. 39, p. 11.

2. B. V. Deryagin. About thickness of a liquid film remaining on walls of vessels after their emptying, for the case, when the influence of surface tension can be ignored. Journal of Experimental and Theoretical Physics, 1945, V. 15, p. 503.

3. B. V. Deryagin. On the thickness of a liquid film adhering to the walls of a vessel after emptying. Acta phys. chim., 1945, V. 20, p. 349.

4. B. V. Deryagin and A. S. Titiyevskaya. Experimental study of thickness of liquid film adhering on solid walls behind a retreating meniscus. Reports of Academy of Sciences of USSR, 1945, V. 50, p. 307.

5. B. V. Deryagin and S. M. Levi. Physical chemistry of deposition of films on nonstationary subfilm. Academy of Sciences of USSR. Publishing House, 1959.

6. B. V. Deryagin. Theory of distortions of a flat liquid sufrace by small objects and its application for measurement of contact wetting angles of thin filaments and fibers. Reports of Academy of Sciences of USSR, 1946, V. 51, p. 519.

TURBULENT PULSATIONS IN A LIQUID JET, AND ITS ATOMIZATION

G. P. Skrebkov

(Novosibirsk)

An attempt at approximate analysis of process of atomization during subsonic outflow through ordinary nozzles into a quiescent gaseous medium proceeding from simplified scheme according to which the jet is assumed to be consisting of totality of separate liquid moles subject to pulsation is undertaken. It is assumed that atomization sets in when the speed of a mole in transverse direction (taking into account the effect of aerodynamic forces) is found to be sufficient for overcoming the forces of viscosity and surface tension. Calculation of viscous and aerodynamic forces is made with much schematization of real picture with use of experimental coefficients.

The results necessary for present work were the investigations of G. Melig [1] and Halbronn [2]. Melig explained atomization by presence of transverse speeds in the jet. Halbronn showed that owing to transverse speeds in the jet. speeds in an open rapid flow there may occur an ejection of the water particles and, as a result of this, an aeration of the flow.

At the A. A. Skochinskiy Institute of Mining the author set up experiments for the study of influence of transverse pulsational speeds on atomization. In these experiments with cylindrical nozzles with a length of 100 to 200 diameters there were measured the cone angle of the atomization, exhaust velocity, and loss of pressure head along length of nozzle with different degrees of roughness of its walls.

On the basis of the losses of the pressure head there was calculated the coefficient of hydraulic friction λ.

For determining the transverse pulsational speed there

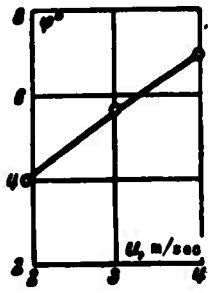

Fig. 1. Influence of transverse pulsational speed on cone angle of atomization of a water jet: D = 7 mm, v = = 45 m/sec.

were used results of Ye. M. Minskiy [3], according to which the averaged transverse pulsational speed u can be expressed in the form

$$u = \beta v \sqrt{\frac{l}{D}},$$

Here v is the escape velocity of jet, $\beta = 1.2$ near wall, according to Ye. M. Minskiy.

Results of one series of experiments presented in Fig. 1 show that angle φ of the cone of atomization strongly depends on transverse pulsational speed u.

We shall assume now a flow in nozzle consisting of individual liquid particles of various magnitude (moles), which are in state of turbulent mixing.

We shall take for characteristic dimension of a liquid mole l the diameter of a sphere* equivalent in volume; let us assume that $l = \alpha D$, where D is the diameter of the nozzle, α is a certain coefficient

Pulsational speed of stream

$$u = Tv$$

Here v is the average speed of jet; T is a coefficient, the so-called degree of turbulence. Let us assume that ρ^0 is the density of the liquid; initial kinetic energy of liquid mole is equal to

$$E_0 = \frac{1}{12}\pi\rho^0 l^3 u^2 = \frac{1}{12}\pi T^2 \alpha^3 \rho^0 D^3 v^2$$

*According to the opinion of Ye. M. Minskiy [3] who made a photograph for the purpose of evaluating the geometric dimensions of traveling masses, the dimension of the liquid mole is approximately identical lengthwise and transverse to the flow.

During the escape beyond the limits of free surface of the jet this kinetic energy will be partially expended in surmounting the forces of surface tension and viscosity. Work of forces of surface tension, as is well known, is equal to product of coefficient of the surface tension σ and the increment of area of free surface

$$A_1 = \sigma\pi l^2 = \sigma\pi a^2 D^2$$

For an evaluation of work of forces of viscosity it is necessary to know magnitude of the tangential stress on surface of liquid mole during its escape from the jet (Fig. 2). As is known, viscous stresses are equal to

$$\tau = -\mu\, du/dn$$

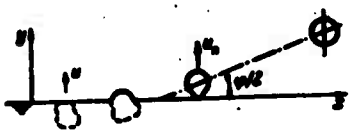

Fig. 2. Successive positions of liquid mole during its escape from a jet.

Let us assume that at the surface the speed of the mole is equal to u, and at moment of separation from the jet – u_*. Then the average speed of mole on the path l is equal to $1/2(u + u_*)$.

Assuming that free distance between neighboring moles is proportional to the diameter of the mole, we shall obtain an approximate evaluation

$$\frac{du}{dn} \sim \frac{\frac{1}{2}(u+u_*)}{l} \sim \frac{u+u_*}{l} = \frac{Tv+u_*}{l}$$

Force of viscosity for an arbitrary state of a liquid mole will be

$$F = k\mu\frac{Tv+u_*}{l}s \quad \left(s = \sigma\pi l^2,\ k = k\left(\frac{y}{l}\right),\ \sigma = \sigma\left(\frac{y}{l}\right)\right)$$

where s is the area of that part of surface of mole which is located in the jet, expressed in terms of the area of entire surface of mole; a and k are coefficients which take into consideration the distribution of speeds around a liquid mole and which depend on position of mole with respect to free surface of stream. Then work of forces of viscosity will be expressed in the form

$$A_1 = \int_0^l F\,dy = \pi\mu l\,(Tv + u)\int_0^l k\left(\frac{y}{l}\right)a\left(\frac{y}{l}\right)dy = \pi a^2\mu D^2\,(Tv + u^0)\,K$$

where K is the mean value of integrand.

As soon as part of liquid mole will escape beyond the limits of free surface of jet it will be subject to the action of aerodynamic forces. These forces will deform the mole and "extend" it from the jet.

The force "extending" the mole from the jet may be determined by the known formula

$$P = c\omega\rho' v^2 \qquad \left(\omega = bx^2,\ c = c\left(\frac{y}{l}\right),\ b = b\left(\frac{y}{l}\right)\right)$$

where c is an aerodynamic coefficient, ρ' — density of gas, ω — area of cross section of that part of mole which goes out beyond the contour of free surface (expressed in terms of area of cross section in the final position of mole, b is a coefficient).

Then work of the aerodynamic forces will be equal to

$$A_2 = \pi x^2\rho' v^2\int_0^l c\left(\frac{y}{l}\right)b\left(\frac{y}{l}\right)dy = \pi x^2 D^2\rho' v^2 C$$

where C is the mean value of integrand. The work of viscosity forces of the gas, and also work of gravity, are not considered since they are assumed to be negligibly small. Kinetic energy of drop (mole) at moment of its separation from the jet will be equal to

$$E_0 = E_0 - A_1 - A_2 + A_0$$

By this energy there readily is determined transverse speed of drop u_* which makes it possible to calculate cone angle of jet of atomization in terms of the ratio of transverse speed to the axial: $\tan(1/2)\varphi = u_*/v$.

Using the determined expressions, we shall obtain

$$\operatorname{tg}\frac{\varphi}{2} = \left[T^2 + 12C\rho + \left(\frac{6K}{aR}\right)^2 - \frac{12}{a\rho'} - \frac{12KT}{aR}\right]^{1/2} - \frac{6K}{aR}$$

Here W is the Weber number, R is the Reynolds number, ρ is a number characterizing relative density of the gaseous medium

$$W = \frac{\rho^{o} D v^{2}}{\sigma}, \quad R = \frac{Dv}{\nu^{o}}, \quad \rho = \frac{p'}{\rho^{o}} \quad (\nu^{o} - \text{viscosity of liquid})$$

It is obvious that with a small initial kinetic energy of the mole and the weak action of aerodynamic forces the mole cannot escape from the jet. From the condition $\varphi = 0$ (or $E_{*} = 0$) we shall obtain then the critical Weber number at which atomization begins:

$$W_{*} = \frac{12}{aT^{2} + 12aC\rho - 12KT/R}$$

In this way there can be obtained also formula for speed of jet v_{*} at which the atomization begins:

$$v_{*} = \frac{6\nu TK}{AD} + \left[\left(\frac{6\nu TK}{AD}\right)^{2} + \frac{12\sigma}{AD\rho^{o}}\right]^{1/2} \quad (A = aT^{2} + 12aC\rho)$$

Magnitudes of coefficients C and K were determined by us on the basis of experiments of A. S. Lyshevskiy [4]. For determining C there was used a number of experiments in which the influence of density of stream on the cone angle of atomization was investigated. The magnitude C was calculated from the equation

$$\operatorname{tg}^{2}\frac{\varphi_{2}}{2} - \operatorname{tg}^{2}\frac{\varphi_{1}}{2} = 12C(\rho_{2} - \rho_{1})$$

Averaged value of coefficient C at ρ = 0.0012-0.022 was found to be equal to C = 0.10-0.11.

For the determination of K there were used two series of experiments made by A. S. Lyshevskiy, in which there was studied dependence of cone angle of atomization on the exhaust velocity; one series of experiments has been published [4], the other was used through the courtesy of the author. Mean value was found to be equal to K = 4.

The coefficient α, characterizing relative dimension of the calculated mole,* is assumed, in first approximation, equal to $\alpha = 0.07$. Such value of α was obtained by Ye.M. Minskiy [3] for uniform flow without pressure head on the basis of calculations of transverse scale of turbulence (transverse scale of turbulence according to Ye.M. Minskiy amounts to about 0.14 of the depth of flow) and is transposed by us to a pressure flow owing to absence of similar measurements in a pressure flow. A similar transposition is, in our opinion, fully admissible in the stage of qualitative analysis of phenomenon of atomization. Furthermore, error in selecting α is compensated partially by the fact that K is determined from experiment with an already selected α.

Magnitude of degree of turbulence T depends on many conditions: the shape and design of the nozzle, roughness of walls, escape velocity, etc. In a general case, the magnitude T can be determined experimentally.

According to available data [5] the degree of turbulence in relatively short pipes can attain $T = 0.10$. This means that with an escape velocity of 100-200 m/sec the transverse pulsational speed will attain 10-20 m/sec. It is fully obvious that with such high transverse velocities the liquid will be intensely atomized laterally.

In Figures 3-6 there are presented the results of the calculation on bases of the obtained formulas at the above-indicated values of coefficients C, K and α. The magnitude T was selected from the condition of best approximation of calculation for the experiment.

---

*In short nozzles where turbulent boundary layer can not be developed over entire thickness of the flow, probably, a more correct dimension of the mole is associated not with diameter of the nozzle but with thickness of boundary layer at the end of the nozzle.

Results of the calculation presented in Figures 3-6 show that obtained formulas truly reflect influence of individual factors on process of atomization; this indicates their correct structure.

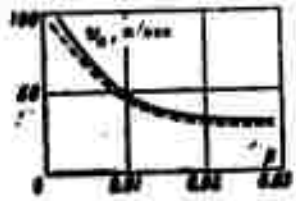

Fig. 3. Speeds at beginning of atomization v_* for diesel fuel depending upon relative density ρ of a gaseous medium at values D = 0.5 mm, $\nu^0 = 0.05$ cm^2/sec and $\sigma = 0.03$ g/cm; continuous curve — on the basis of the empirical Lyshevskiy's formula [9]; dashed — on basis of obtained formula at T = 0.072.

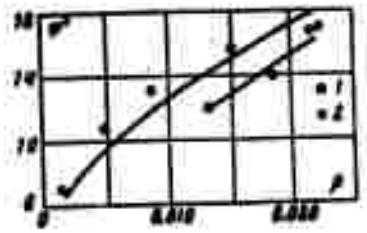

Fig. 4. Change of cone angle of atomization depending upon relative density of gas medium: 1) Kukharev's experiments [7] at values v = 100 m/sec, D = = 0.7 mm, $\nu^0 = 0.052$ cm^2/sec and $\sigma = 0.028$ g/cm; 2) experiments by Zass [8] at values v = 165 m/sec, D = = 0.57 mm, $\nu^0 = 0.06$ cm^2/sec and $\sigma = 0.035$ g/cm; curve — according to formula obtained at T = 0.072.

Experimental data have been taken from [4-8]. In view of the lack of experimental data in the USSR on the speed of the beginning of atomization for comparison with results of the calculations there is used Lyshevskiy's [9] empirical formula.

The calculations made, have shown that magnitude of the cone angle of atomization in the general case is determined by many factors. However, under certain conditions the cone angle is determined at most by only one or two factors. Thus, in an atomization into the atmosphere the cone angle depends primarily on the degree of turbulence and speed of jet; during an atomization into a gas medium whose density

is 10 to 20 times greater than air density, the cone angle of atomization is determined mainly by the aerodynamic forces.

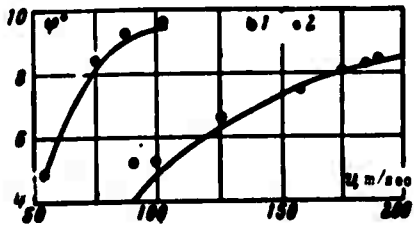

Fig. 5. Variation of cone angle of atomization depending upon speed of jet: 1) Pobyarzhin's experiments [6] at D = 0.38 mm, ν^0 = 0.014 cm^2/sec, σ = 0.021 g/cm, ρ = = 0.0014 and T = 0.107; 2) Lyshevskiy's experiments [4] at D = 0.54 mm, ν^0 = 0.05 cm^2/sec, ρ = 0.0014, T = = 0.095 and σ = 0.035 g/cm; curve — on basis of the obtained formula.

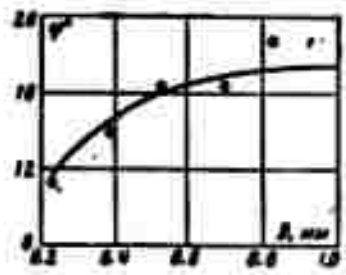

Fig. 6. Dependence of cone angle of atomization on the diameter of nozzle D at values v = 160 m/sec, ν^0 = = 0.05 cm^2/sec, σ = = 0.035 g/cm and ρ = = 0.0156; Lyshevskiy's experimental points are [4] for nozzles with a length of about 4 D; the curve — according to the obtained formula at T = 0.095.

The equality of kinetic energy of a mole to the work of its escape from the jet makes it possible also to analyze influence of individual factors, and in particular parameters of turbulence of flow in nozzle, on dimensions of the drops obtained as a result of atomization of jet on escaping from the nozzle.

The evaluations of diameter of the mole obtained by Ye. M. Minskiy, mentioned above, pertain to those moles which are subject to maximum pulsations. Together with the huge moles in turbulence flow there are moles of smaller dimensions. Condition $E_* = 0$ determines dimension of that limiting small mole which still is in a state to be separated from the jet under action of transverse pulsations at a given escape velocity of the jet, exceeding v_*, while

$$\alpha_{min} = \frac{12}{W(T^2 + 12C\rho)} + \frac{12KT}{K(T^2 + 12C\rho)}$$

It is natural that fineness of the atomization will be the greater, the smaller is α_{min}. From formula it is evident that the fineness of the atomization must increase with an increase of degree of turbulence of the flow, decrease of viscosity, increase of escape velocity, etc; this completely corresponds to results of numerous experiments [6, 9, 10]. The fineness of atomization will depend also on what dimension of the moles predominates.

Submitted
23 April 1962

Literature

1. G. Melig. Physical bases of the formation of fuel-jets in diesel engines. Collection of translated articles edited by S. N. Vasil'yev "Internal-combustion engines," Vol. 1, ONTI NKTP SSSR, 1936.

2. Halbronn. Étude de la mise en régime des écoulements sur les ouvrages está forte pente. La Houille Blanche, 1952, Vol. 7, No. 1, 3, 5.

3. Ye. M. Minskiy. Turbulence of channel flow. Hydrometeorological Publishing House, 1952.

4. A. S. Lyshevskiy. Experimental research of development of jet of atomized liquid and generalization of experimental data on cone angle of a jet. Transactions Novocherkasski Polytechnical Inst., 1960, Vol. 107.

5. Ye. P. Dyban, S. K. Rudkin, M. V. Starodomskiy, N. T. Shvets and E. Ya. Epik. Investigation of radial component of the pulsation of speeds during turbulent flow of air in relatively short pipes with a varying level of initial perturbations. Engineering Physics Journal, 1961, No. 11.

6. P. I. Pobyarzhin. Investigation of influence of internal eddy formation in a burner on the quality of atomization and jet of an atomized fuel. Transactions. MVTU, Mashgiz, 1958, No. 78.

7. M. N. Kukharev. Investigation of atomization of fuel with respect to high speed diesel engines. Transactions. Sci. Inst. of automobiles and engines, M., 1959, No. 87.

8. F. Zass. Compressorless diesel engines. GNTI, Moscow, 1931.

9. A. S. Lyshevskiy. Principles of fractionating liquids by mechanical pressure atomizors. Publishing House of Novocherkassk Polytech. Inst., 1961.

10. T. S. Mel'kumov. Theory of high speed motor with self-ignition. Oborongiz, 1953.

SCALAR EFFECT AND INFLUENCE OF DURABILITY IN A DIRECTED EXPLOSION

V. M. Kuznetsov and Ye. N. Sher

(Novosibirsk)

The theoretical bases of directed explosion are presented in work [1]. Results of experiments conducted in soft ground [2] showed the fundamental correctness of the proposed scheme and made it possible to modify law of location of the explosive substance (BB) on surface of the ejected ground mass. Below there are discussed results of further investigations and experiments in this direction.*

Experiments showed that question on the similarity in a directed explosion most closely is associated with question about magnitude of tamping. In a general case the index of simulation depending upon degree of tamping may vary from 3.5 to 7.

Furthermore, in a directed explosion in rocky ground it is necessary to take into account the durability properties of the medium, whose calculation introduces essential corrections in the scheme of an ideal incompressible fluid. Direction of ejection depends on sequence of initiating the charges of the BB. A delayed detonating in a number of cases may result in an essential decrease of consumption of the BB.

1. Scalar effect. Suppose that ejected ground mass is limited by an arbitrary surface with characteristic linear dimension l. Let

*The investigations were made in the summer of 1962 at the Institute of Hydrodynamics of the Siberian Division, Academy of Sciences of USSR jointly with the "Soyuzvzryvprom" Trust in rocky ground.

us assume that, further, this linear dimension increases by k times with conservation of the geometric similarity of the regions. Then with an increase of total momentum I, being communicated by the BB by k^3 times, the speed of ejected ground mass will not vary. Inasmuch as distance of flight of ground is proportional to v^2, then for obtaining a geometrically similar ejection the speed v must be increased by $k^{1/2}$ times. Thus, for obtaining geometrically similar craters and piles of broken ground with an increase of scale of experiment by k times momentum being communicated by BB to ground, during directed explosion must be increased by $k^{3.5}$ times. This conclusion follows, of course, also from general considerations of dimensionality, inasmuch as the determining parameters in this case are: momentum J, linear dimension l, density of medium ρ and acceleration due to gravity g. From these parameters there is constituted only one dimensionless combination, which is the formula of modeling in a directed explosion

$$\frac{J}{\rho^{0.5} g^{0.5} l^{3.5}} = \text{const} \qquad (1.1)$$

As is evident from work [2] the dependence of specific momentum on the weight of the BB per unit of area under different conditions of work of charge may vary. If the blasted volume of ground is in the air or is surrounded by a very compressible medium, then momentum pulse is proportional to energy (weight) of the BB. In this case the simulation formula of the directed explosion coincides with known formula for major explosions for an ejection [3]. If, however, ground is ejected from nondisturbed ground, then, assuming that mass of ground, set into motion during the time of action of load, exceeds many times the mass of products of detonation, we obtain

$$J = \sqrt{2mE} \qquad (1.2)$$

where E is the energy of the BB, m is the mass of ground set in motion.

If in this expression m is the total ejected mass of ground, then $m \sim l^3$ and from (1.1) and (1.2) we obtain another well known formula for powerful explosions for an ejection [4]

$$\frac{E}{\rho g l^4} = \text{const} \qquad (1.3)$$

which also is evident from general considerations of dimensionality theory in the case, when the determining parameter instead of the pulse is the energy.

However, practically the magnitude m in expression (1.2) is not equal to total ejected mass of ground, but is determined by the time of action of load, i.e., it depends on the tamping of the bores. The case $m \sim l^3$ is in this sense limiting and takes place then, when the outflow of gases i.e., products of detonation through outlet of the bores is absent.

However, in practice it always takes place and may play an essential role, especially during explosions in rocky ground. If, for example the tamping remains constant with an increase of the scale, as was observed in experiments described below, then it is natural to assume that the mass m, set in motion is proportional to the thickness of layer of BB, or, approximately, $m \sim l$. In this case from (1.1) and (1.2) it follows that degree of simulation is equal to 6. We can also imagine the case when the value of m in general does not change with a change in scale of the explosion. This, obviously, will take place during explosions in very hard rocks with a tamping constant in magnitude. Thus, in general we may write the formula of simulation for a directed explosion in the form

$$\frac{E_0}{\rho g l^4} = \text{const}$$

where μ is a magnitude depending on properties of ground and on magnitude of tamping, the index of simulation n varies within the limits

$$3.5 < n < 7$$

Experimental explosions were produced in limestone of 6th category of durability on basis of scheme in Fig. 1 at a depth along a normal equal to 2.1, 4.2 and 5.7 m. Specific consumption of BB in first experiment amount to 3 kg/m^3. The change in total amount of BB during transition to larger scales is shown in Fig. 2, where two straight lines limit region of change of simulation index. The results of these explosions are shown in Fig. 3 in the form of schematic profiles of craters and piles of broken up ground.

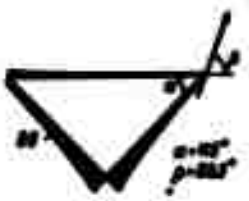

Fig. 1.

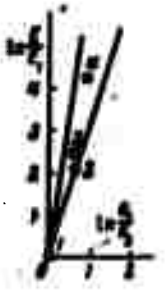

Fig. 2.

Fig. 3.

Comparing results of experiments, we see that despite large values of simulation index, adopted in the calculation, the craters and piles of broken ground happened to be dissimilar: with an increase in scale of explosion the relative quantity of ground, ejected from the crater, decreases. Since in the transition from a depth of 2.1 m to a depth 5.7 m the magnitude n was assumed equal to 4.8, from this it is evident that in this case index of simulation is included within the limits

Such large values of index of simulation result in a sharp over-consumption of BB in a directed explosion in comparison to the usual explosions for an ejection. It is necessary, however, to remember that in soft ground the role of tamping is less essential so that n varies within a narrower interval between 3.5 and 4. During explosions in rocky ground the role of tamping is very important, this must be remembered in practice in general, especially in a directed explosion. With the realization of a fairly reliable tamping the consumption of BB may be greatly lowered.

2. Influence of durability properties of the medium in a directed explosion. Theoretical scheme of directed explosion [1] is based on simulation of an ideal incompressible fluid. Considering ground as an ideal incompressible fluid, we take into account only the inertial forces developing during explosion and disregarding its durability properties. Such approach makes it possible to grasp basic features of the phenomenon, assuming that the influence of other factors, in particular durability, can be considered as the correction for the basic model.

Experimental explosions in clay ground [2] corroborated the correctness of this approach. At the same time there was ascertained a number of details which were not contained in the framework of a model of an ideal imcompressible fluid and were lacking in its explanation of the involvement of durability characteristics of the ground. Thus, in experiments 25 and 26 of work [2] with an identical scale and law of the spacing the consumption of the BB is second case was two times greater.

According to general theory discussed in the first section it

would have been possible to expect that distance of thrust in second case will be double that of the first. Actually it was found that distance of ejection increased more than three times. Qualitatively this result can be explained as follows. According to the theory for realization of a directed ejection it is necessary that the entire mass of ground is covered with a solid layer of BB. In practice the BB is placed in bore holes, located over the relief of ground mass to be ejected at a certain distance from each other, so that between the bore holes the ground remains undisturbed.

For the detachment of the blasted mass of ground from the non-disturbed ground there must be accomplished a certain amount of work proportional to surface of ejected volume of ground. It is obvious that in the above-mentioned example magnitude of this work remains constant inasmuch as scale of explosions does not change. Thus, in second case in communicating the kinetic energy to the ground a relatively large part of all the energy of the BB was expended.

We shall present one more example. In the same ground there was drilled a number of holes at an angle of 45° at whose bottom there were located concentrated charges of BB. As a result of undermining a large part of ground was ejected in the direction of slope of the holes – the minor disturbance of continuity of nondisturbed ground from the direction of the holes essentially influenced the direction of the ejection.

Still more significantly there is shown the influence of durability properties of medium during explosions in rocky grounds. In the course of experiments there was revealed one interesting circumstance. It was found that direction of ejection depends on place of initiation of charges. The fact is that in practice charges of BB placed in the holes are conveniently connected to each other by a detonating cord

and the undermining is made from one place. The scheme of the initiation which is used in experiments in rocky ground is shown in Fig. 4, where 1 and 2 – are bore holes of charges 1 and 2, the figure 3 indicates groove of charge 3, and 4 – the point of ignition; the point of ignition was placed both on the side of charge 1, and also on the side of charge 2. In both cases ejection of ground occurs towards that direction, whence the ignition begins the initiation. The speed of detonation is a magnitude of an order of several thousand meters per second, and speed of ground in the cited experiments amounted to only several tens of meters per second.

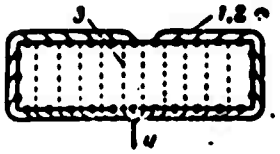

Fig. 4.

Thus, during the time, during which detonation spreads to all charges of the BB, the volume of ground being ejected will not change essentially its shape. Consequently, cause of observed effect must be sought in another.

We shall note here that an analogous phenomenon during an explosion in soft ground was ascertained by S. A. Davydov [5]. In our experiments linear dimensions of ejected mass of ground were such that the ratio of length of trench to its width was equal to four. If we assume the speed of detonation in detonating cord is equal to 7 to 8 km/sec and speed of shock wave in ground 3 to 4 km/sec, then during the period of delay, during which detonation will spread from first charge to the latter one, shock wave can traverse the entire ejected volume of ground.

On the other hand, it is known that in the initial stage gases i.e., products of detonation expand according to the law $pV^3 = \text{const}$. It is evident from this that a major part of work is performed by the products of detonation just in initial stage of the expansion. Thus,

with an increase in radius of hole by 20% potential energy of gases amounts to only 47% of the initial, and the remaining is transmitted to the ground. Since at initial moment the rate of the expansion is great, then during the time of delay the charges, initiated at the beginning, may be almost completely "depleted," i.e., they can transmit their own energy to the ground. This energy is expended in the destruction of the ground and in creation of a field of speeds in it. Thus, the influence of nonsimultaneity of the undermining develops in two relationships – energy and kinematic. From the point of view of energy, the charge, being undermined at the beginning, produces large part of the destruction of ejected mass of ground and its detachment from the nondisturbed ground, but owing to this the speeds acquired by the ground, happen to be smaller in magnitude than in the scheme of an ideal incompressible liquid. Charge, which is undermined later on transmits its own energy to the ground already destroyed and detached from the nondisturbed ground and, consequently, determines the direction of ejection. Kinematic influence of the nonsimultaneity of the undermining appears in creation of new threshold surfaces and change of boundary conditions on the surface of ejected volume of ground. This question can be examined within the framework of an ideal imcompressible fluid. In the experiments of the authors ejected volume of ground had in cross section the shape of a triangle, but ejection was made at an angle of 63.5°. The distribution of potential at boundary of region for the given case is shown in Fig. 5, where the arrow indicates the direction of explosion.

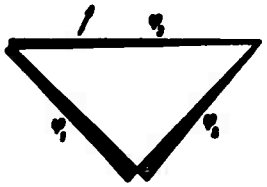

Fig. 5.

We shall consider two cases. In the first there are undermined charges 1 and 3 (this corresponds to undermining from direction of

charge 1), and then charge 2, where as a result of explosion of charges 1 and 3 there will be formed a free surface at the place of charge 3 and a line of flow at the place of charge 1. In the second case at first there are undermined charges 2 and 3, and then – charge 1, where at the place of charges 2 and 3 there will be formed, respectively, a line of flow and a free surface. The subsequently generating fields of speeds and total fields of speeds are shown in Figures 6 and 7. Direction of ejection during a simultaneous undermining of charges is shown in these figures by arrows, the solid lines are equipotentials, and the dashed lines are lines of flow. Pictures of the flows are obtained in integrator EGDA-9-60. The nonsimultaneity of undermining from kinematic point of view results in an increase of angle of ejection so that main mass of ground acquires speeds directed almost vertically upwards. Owing to thoroughly discussed energy consideration above the charge, being undermined later, communicates to the ground relatively higher speeds than during a simultaneous undermining. Thus, in first case ground may be ejected in a direction opposite to that which takes place during a simultaneous undermining. In second case (during an undermining from the direction of charge 2) ejection should occur in the required direction. These conclusions were corroborated by experiments.

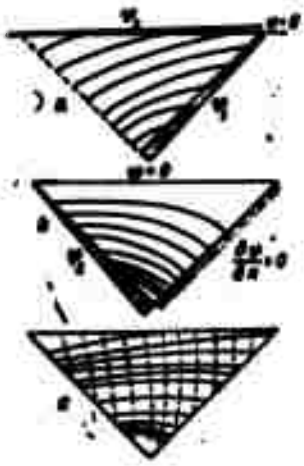

Fig. 6.

Fig. 7.

3. Application of delayed detonating in a directed ejection. In practice in certain cases it is more profitable to apply delayed detonating

in a directed ejection since this results in a decrease in consumption of BB per unit of volume of ground.

Leaving open question about the delay times, it is possible theoretically to consider two extreme cases: a) from charges, located in the ground, initially undermined charge excavates volume of nondisturbed ground and creates in its place a free surface (this case will obviously, take place during longer delay times); b) initially undermined charge does not excavate the ground from the nondisturbed ground and does not create a new surface. Taking into consideration the durability of ground outside ejected volume owing to pressure head on the part of nondisturbed mass, we may assume in second case that in place of initially detonated charge there will be formed a line of flow. This case has been considered above.

Let us assume that region as previously is a triangle (Fig. 5). We shall introduce following designations: φ_i is the potential, corresponding to forward motion of ejected mass of ground in a given direction; Φ_i is the pulse, created by the i-th charge of BB; Φ_{ik} is the pulse obtained at place of i-th charge during explosion of the single k-th charge. The magnituges i and k pass the values 1, 2, 3. In order that as a result of undermining of all charges the ground obtains a forward motion, it is necessary to fulfill the following relationships:

$$\begin{aligned} \Phi_1 + \Phi_{12} + \Phi_{13} &= \varphi_1 \\ \Phi_2 + \Phi_{21} + \Phi_{23} &= \varphi_2 \\ \Phi_3 + \Phi_{31} + \Phi_{32} &= \varphi_3 \end{aligned} \tag{3.1}$$

Charge 3 is found on free surface, therefore,

$$\Phi_{31} = \Phi_{32} = 0 \tag{3.2}$$

and, consequently, $\Phi_3 = \varphi_3$, i.e., the magnitude of charge 3 remains the same as during a simultaneous undermining. In the case a), furthermore, charges 1 or 2 create free surfaces depending upon which of them explodes first. If sequence of detonating is 2-1-3, then

$$\Phi_{21} = \Phi_{23} = 0, \ \Phi_2 \cdot \varphi_2$$

Thus, in this order of the detonating charge 2 also does not change its own magnitude in comparison to case of simultaneous detonating, and charge 1 should have the magnitude $\Phi_1 = \varphi_1 - (\Phi_{12} + \Phi_{13})$, i.e., weight of charge 1 should be less than during simultaneous undermining. By this method it is possible to make a calculation for any sequence of undermining charges. In particular, the most profitable from the point of view of expense of the BB is the following order of undermining: 3-2-1. In case b) both charges being located in the ground, alter the magnitude in comparison to the case of simultaneous undermining. The method of calculation remains the same. The problem, however, is complicated by the fact that on the newly forming surfaces the boundary conditions a priori are unknown. Nevertheless, also in this case a nonsimultaneous detonating may result in a decrease of consumption of BB. Below as an illustration there is presented the problem, analyzed by Ye. N. Sher.

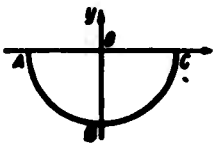

Fig. 8.

Let us assume that from a half-space filled with an ideal incompressible fluid there must be tossed upwards* an infinite cylinder, whose section is one-half of a unit circle (Fig. 8)

$$z = e^{\theta} \qquad (-\pi < \theta < 0) \tag{3.3}$$

*Incomplete phrase in original Russian not indicated in errata sheet has been deleted [Tr. Ed. note]

The complex potential of such a flow is z/i. This flow we assume to obtain as sum of two flows with the potentials w_1 and w_2.

First flow is result of application of impulse load on arc BC. The second is on arc AB. The region of the flow in first case is the lower half-plane with cut-out arc BC, in second — lower half-plane with cut-out arc AB. In both cases on actual axis $\varphi = 0$. There is required to determine function φ_1 and φ_2 on the arcs BC and AB, in such a way that in semicircle (3.3) there was fulfilled the condition

$$w_1(z) + w_2(z) = \frac{z}{i} \tag{3.4}$$

Owing to symmetry of problem we have

$$w_2(z) = \overline{w_1(-z)} \tag{3.5}$$

where $\overline{w}(z)$ is the function conjugate with w(z). Contition (3.4) will acquire the form

$$w_1(z) + \overline{w_1(-z)} = \frac{z}{i} \tag{3.6}$$

We note that with any impulsive load distributed along the arc circumference with center of the real axis, the remaining part of circumference is a line of flow, if potential at boundary of half-plane is equal to 0. This corroboration becomes evident, if we make a linear-fractional transformation translating one point of intersection of circumference and actual axis 0, and other infinity. It is readily verified that circumference at the same time develops into the axis of symmetry of a new half-plane. Using this property, it is possible to assume that $\psi_1 = 0$ on the arc AB. We shall write out condition (3.6) for point $\xi = e^{i\theta}$, lying on the arc BC; we have

$$\varphi_1(\xi) + i\psi_1(\xi) + \varphi_1(-\bar{\xi}) - i\psi_1(-\bar{\xi}) = y - ix \tag{3.7}$$

Hence

$$\psi_1(\xi) + \psi_1(-\bar{\xi}) = y, \quad \psi_1(\xi) - \psi_1(-\bar{\xi}) = -x \tag{3.8}$$

But $\psi_1(-\bar{\xi}) = 0$, since the point $-\bar{\xi}$ lies on the arc AB. We shall show that function w(z), satisfying the boundary conditions

$$\psi = 0 \text{ at } y = 0, \quad \psi = 0 \text{ on } AB, \quad \psi = -x \text{ on } BC \tag{3.9}$$

is unique. We shall introduce into the analysis the function

$$Y(z) = w_1(z) + \overline{w_1(-\bar{z})} - \frac{z}{l} \quad (Y(0) = 0)$$

For this function we have

$$\operatorname{Re} Y = 0 \text{ at } y = 0, \quad \operatorname{Im} Y = 0 \text{ on } AB, \quad \operatorname{Im} Y = C \text{ on } BC$$

Such mixed problem has, [6], the unique solution Y = 0.

The solution of problem with boundary conditions (3.9) is found with the aid of Poisson integral for circle [6] and has following form:

$$\psi = \frac{\sin\theta}{2} + \frac{\cos\theta}{2\pi} \ln \frac{1+\sin\theta}{1-\sin\theta} \tag{3.10}$$

In case of simultaneous detonation the potential assuring a forward motion of unit semicircle vertically upwards has the form

$$\psi = \sin\theta \tag{3.11}$$

In Fig. 9 the solid line shows the distribution of potential during a nonsimultaneous detonating, and dotted line during a simultaneous.

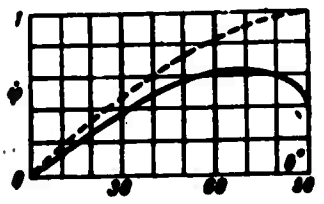

Fig. 9.

Areas limited by corresponding curves characterize in themselves the total momentum being communicated by ejected volume of ground to one of charges of the BB. If we designate J' as the momentum communicated during

simultaneous undermining, and J" – during a nonsimultaneous, then from Fig. 9 we have I'/I" = 1.3. If we assume then that momentum is associated with weight of the BB by the relationship (1.2), then E'/E" = 1.69 and, economy in consumption of the BB will amount in case of delayed detonating to almost 70%.

In the experimental works, Ye. Gorbachev and Ye. Klyukvin of the PEU Soyuzvzryvprom (All-Union Explosive Industry) participated.

Submitted
16 January 1963

Literature

1. M. A. Lavrent'yev, V. M. Kuznetsov and Ye. N. Sher. On a directed ejection of ground by means of an explosive substance. PMTF, 1960, No. 4.

2. V. M. Kuznetsov and Ye. N. Sher. Experimental nvestigation of a directed explosion in ground. PMTF, 1962, No. 3.

3. G. I. Pokrovskiy. Basic premises for calculating major changes of explosives for an injection. Collection of articles, "Blastings," 1956, Issue 3.

4. L. I. Sedov. Methods of theory of similarity and dimensionality in mechanics. 4th Ed., 1957.

5. S. A. Davydov. Explosive method of driving in ditches with a directed ejection. Collection of articles "Blasting work," 1939, Issue 37.

6. M. A. Lavrent'yev and B.V. Shabat. Methods in theories of functions of a complex variable. 1958.

SIMILARITY OF COMPRESSION WAVES DURING EXPLOSIONS IN GROUNDS

B. G. Rulev

(Moscow)

1. Questions of similarity of the motion of ground during explosions underlie all practical calculations, both of the ejection of ground, and also of seismic oscillations. They are expressed in formulas of the calculation of weight of charges, intended for ejection of grounds and calculation of seismoexplosion-free zones [1-3]. The latter requires a knowledge of relationships between weight of charge, the depth of its laying, distances from source and parameters of oscillations being excited in ground during the explosions.

This will entail the necessity of studying such questions, as nature and property of seismic waves during explosions and their forming near the source. Numerous experiments (measurement of ejection of ground, determination of field of speeds and others) have established that here there is observed the so-called, "geometric similarity" of elements in the motion of the medium. The term is not quite appropriate, because here there are modelled the kinematic and dynamic parameters.

Such a modeling satisfies Cauchy's dimensionless number $\rho u^2/E =$ = const, obtained during a reaction in a system of elastic forces, when the deformation occurs within limits of initial linear sector of the pressure-compressibility curve. Moreover, in similar systems parameters of motion of the media are associated by relationships [4, 5]: $r_2 = \alpha r_1$ – the linear dimensions, $t_2 = \alpha t_1$ is the time, $u_2 = u_1$ is the speed, $\sigma_2 = \sigma_1$ is the stress (pressure), $\rho_2 = \rho_1$ is the density, $\vartheta_2 = \alpha^3 \vartheta_1$ is the energy etc. Here α is the linear scale.

Investigations confirming the geometric similarity of the ground's of motion during explosions, in an overwhelming majority were made in deformations going out beyond the limits of elasticity, when in medium there occur irreversible processes. Such a similarity of compression waves may occur in media whose model contains only parameters having the dimensionality of pressure and density. In such a model the stresses are independent of the speed of deformation [6]. In this case the scalar relationships between parameters of compression wave remain the same, as during the similarity of elastic systems. This is the consequence of the fact that the dependence "pressure-density" (characteristic of state of medium) is independent of the scale of the explosion.

It may be assumed that under certain conditions, on the processes occuring in grounds during an explosion, there can be exerted essential influence by another force – the force of gravity. Here the parameters of the waves must satisfy the Froude number of similarity u^2/gl = const and must be found in the following relationships: $r_2 = \alpha r_1$ – the linear dimensions, $t_2 = \alpha^{1/2} t_1$ – the time, $u_2 = \alpha^{1/2} u_1$ – speed, $\vartheta_2 = \alpha^4 \vartheta_1$ – the energy etc.

The method applied here for the proof of similarity of the course of processes assumes that medium is subject to the action of

only one force. Owing to the impossibility of simulating properties of the medium the similarity will be determined by condition of identity of only one dimensionless number and consequently there will be determined the conditions and limits of primary influence of any one type of the forces.

In a comparison of parameters of the medium's motion as the basis there is taken not the linear dimension, but the weight of the charge C. Assuming that energy of the ground's motion is proportional to the energy of the explosion, and consequently also to weight of charge, and comparing parameters of all explosions with parameters of an explosion of specific magnitude of charge (C = 1 kg), we find:

with a geometric modeling

$$\frac{C_2}{C_1} = \frac{r_2^3}{r_1^3} = e^3 \quad \text{or} \quad e = C^{1/3}$$

with a modeling on basis of Froude

$$\frac{C_2}{C_1} = \frac{r_2^3}{r_1^3} \quad \text{or} \quad e = C^{1/3}$$

2. The measurements of parameters of seismic waves of being excited by explosion were made at a number of sites different in geological structure. In present work there are considered explosions in fairly monotypic grounds.

Sites K2, K3, K4 (schematic structure of which is shown in Fig. 1) are located in Southern Kazakhstan (vicinity of station Arys)

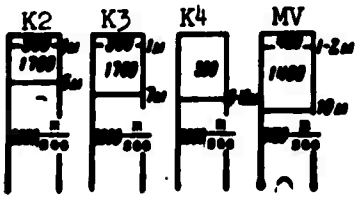

Fig. 1.

are a thick layer of blue clays with speeds of propagation of longitudinal waves of an order of 2000 m/sec and a density ρ = = 2 g/cm^3. On top the blue clays are covered with a thin layer of brownish green clays (V_p = 1700 m/sec) and loess-like loam (V_p = 500 m/sec). The loess-like loam as the result of the great

difference in its own properties (large porosity and small speed of longitudinal waves) at site K4 where its depth is fairly great, introduced certain distortions in parameters of seismic waves.

Characteristic peculiarity of the MV site located in Stavropolskiy Kray, is presence of water-bearing layer with a depth up to 10 m. This layer also was cause of certain deviations from general principles.

Measurements of seismic waves were made in longitudinal profiles with variable (increasing with distance) spacing between the instruments. The length of the profiles during different-scalar explosions varied corresponding approximately to the geometric similarity. Instruments were placed at a depth of 0.5 m in pits opened on basis of dimensions of sensing devices and then compactly tamped. At great distances where accelerations were insignificant, seismographs were placed (at half-meter depth) into the tamped ground.

Measurement of seismic oscillations was made with seismographs VBP [7] with parameters: sensitivity S_b = 1 mv·sec·cm^{-1}; internal resistance R_s = 50 ohm; period of pendulum T_1 = 1.6 sec, given length of pendulum l_o = 65 cm, damping of pendulum equal to 0.7 of critical and VEGIK seismographs [8] with parameters: S_b = 200 mv·sec·cm^{-1}, R_s = 50 ohm, T_1 = 1.1 sec, l_0 = 9.5 cm, damping of pendulum equal to 0.7 of the critical. The registration was made on POB-12 oscillographs with galvanometers GB-III, whose parameters are: natural frequency of 5 cycles per second, internal resistance of 130 ohm, critical resistance of 5000 ohm, sensitivity 25000 mm/ma. The channel on the whole gives a recording of displacements with constant increase in range of frequencies from 2 to 100 cycles per second. This equipment assures registration of oscillations with amplitudes from 3 μ to 300 mm.

3. Characteristic recording of oscillations of ground during

one of explosions is shown in Fig. 2. (Explosion in clay, C = 10^3 kg, h = 5 m.) In the recording it is possible to distinguish three basic waves, propogating from place of explosion. The normal longitudinal wave (phase P) is observed at first entry to vertical component. Near focus of explosion, where in this wave the subsequent phase of rarefaction is small in comparison with the initial phase of compression, it is called a compression wave. At these distances compression wave carries a maximum of energy. At greater distances the surface waves become maximum in intensity. One of them – wave R (in Fig. 2 there are marked its phases R_1, R_2, R_3..., in the vertical component) is a surface wave of Rayleigh type. The motion of the particle during passage of this wave is elliptic, counterclockwise with approximately equal ratios between vertical and horizontal components. Second wave N is observed at first entries (phase N_0, N_1, N_2,... in the horizontal component). The motion of particle during its passage is elliptic (clockwise) and more intense in the horizontal component.

In vicinity of station Arys, in addition to the above-mentioned there was made series of one-ton explosions in the twenty-five meter layer of loess-like loam. The recording of oscillations during one of these explosions is shown in Fig. 3 (C = 10^3 kg, h = 5 m). From a comparison of seismograms during explosions in clay and loess it is evident that in loess-like loams there are observed only long-period surface waves R and N, and compression wave owing to great porosity and compressibility of loess is almost wholly absorbed near the focus. A qualitative analysis of seismograms and comparison of recordings in the compact porous grounds shows that body waves are not the cause of formation of surface waves. Surface waves are formed directly in the epicenter (their first phases are traced to crater of explosion) owing to the relatively gradual expansion of medium under

reaction of gaseous products of explosion whereas compression wave will be formed from the suddenly applied pressure on surface of chamber.

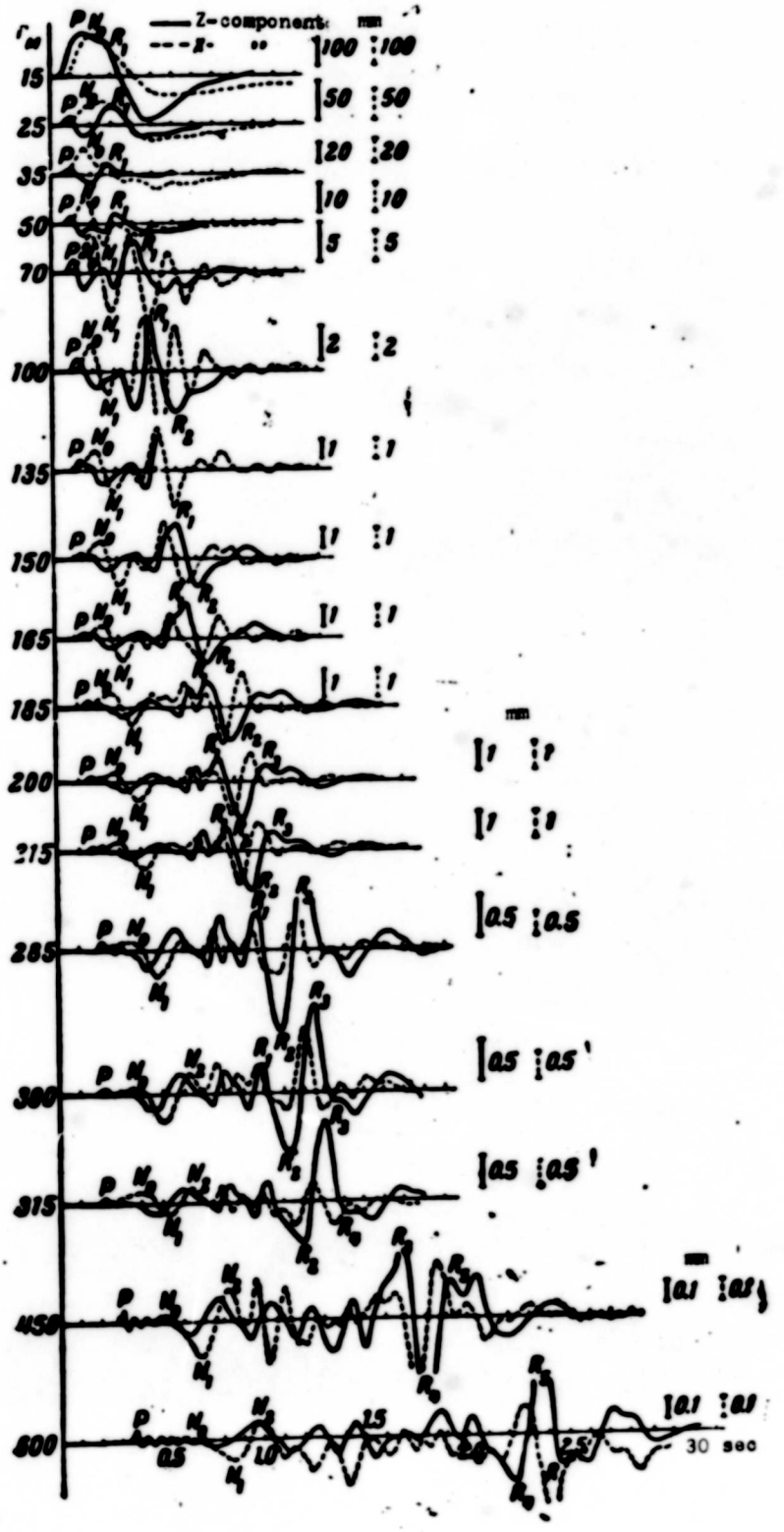

Fig. 2.

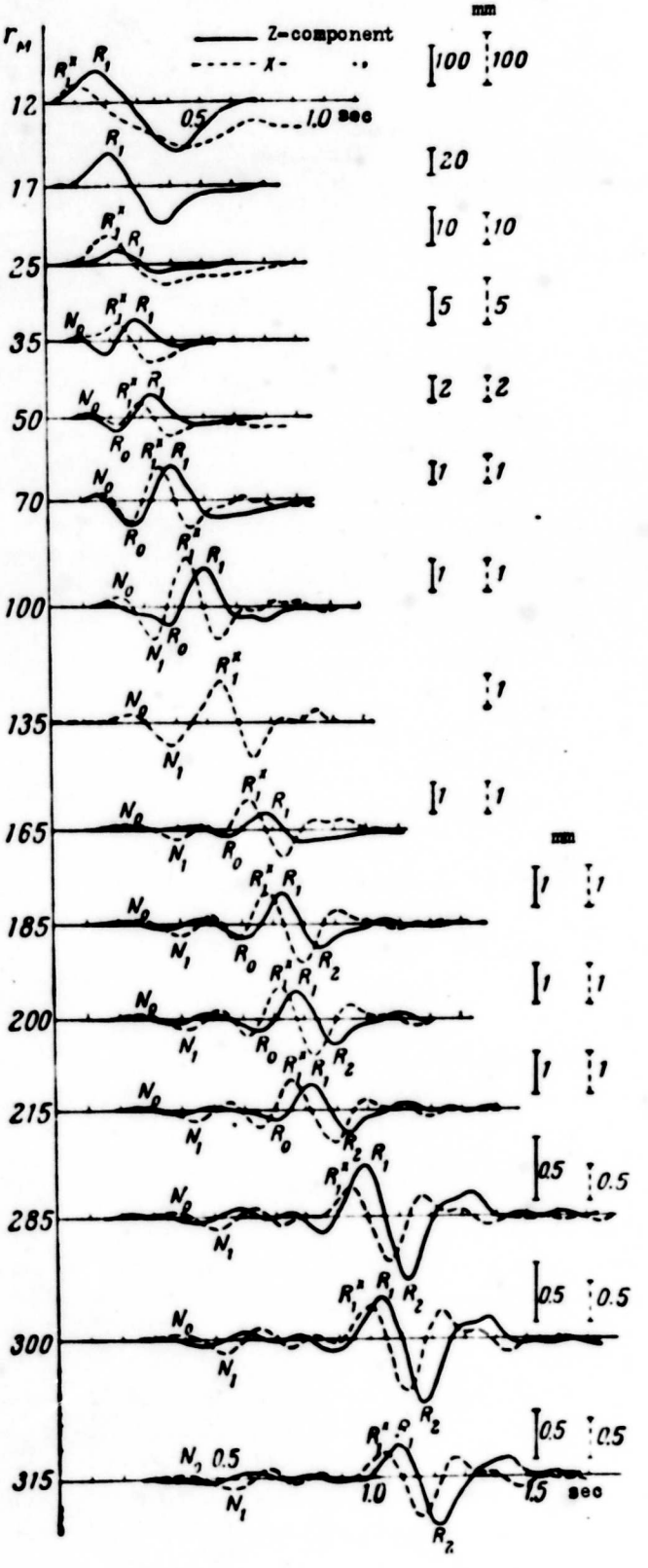
Z-component
X-
mm
100
100
12
0.5
1.0 sec
17
20
25
10
10
35
5
5
50
2
2
70
1
1
100
1
1
135
1
165
1
1
185
1
1
200
1
1
215
0.5
0.5
285
0.5
0.5
300
0.5
0.5
315
1.0
1.5 sec

Fig. 3.

It is possible to indicate analogous processes occurring during explosions in water, when there will be formed shock wave and motion of water owing to expansion of gas bubble [9].

This, obviously, is associated with such properties of explosives, as high-explosive action and brisance. The brisance is associated with head portion of pulse proportional to maximum pressure and furthermore depends on properties of medium, on which the explosion acts i.e., it is associated with the energy being transferred at the front of wave. On these parameters also compression wave chiefly depends. The high-explosive effect of explosion is associated with the complete pulse, moreover in motion there are involed masses of ground, located at a comparatively significant distance from the charge.

With closely located outer surface there occurs ejection of the rocks or uplift of ground (dome) with deeper laying of the charge. This process also is a source of the formation of surface waves.

Such a distinction in formation of these waves will make it possible separately to approach its study, by considering reaction of the same medium to a different character of excitation. Further quantitative analysis of experimental data pertains only to compression wave (phase P, Fig. 3).

4. On seismograms it is evident that compression wave (normal longitudinal wave) emerges almost normally to surface, since first entry in horizontal component pertains to the longer period wave N. It is possible to assume that one of causes of normal emergence of beam is presence of a velocity gradient by depth in layer of blue clays, since it is difficult to assume that several meters of upper layer of lowered speed could exert such a strong influence on direction of propagation of front of a wave 100 to 400 m in length. For

parameters of compression waves these have been adopted: maximum amplitude of displacements a (mm); time of increment of displacement to maximum τ_2 (msec); maximum velocity of particles u (cm/sec), determined by maximum slope angle of tangent on the recorded curve of displacements. Dependence of maximum velocities of particles u on the given distance $r^o = rC^{-1/3}\ \mu g^{-1/3}$ is presented in Fig. 4; in Fig. 5 – the dependence of maximum displacements a on the distance r; in Fig. 6 – the time of increment of displacements to a maximum – τ_2 where a is with the modeling on basis of Froude number, b – with geometric modeling. For a and u the relationships between the indicated parameters are approximated by the exponential functions of form

$$a = Kr^n$$

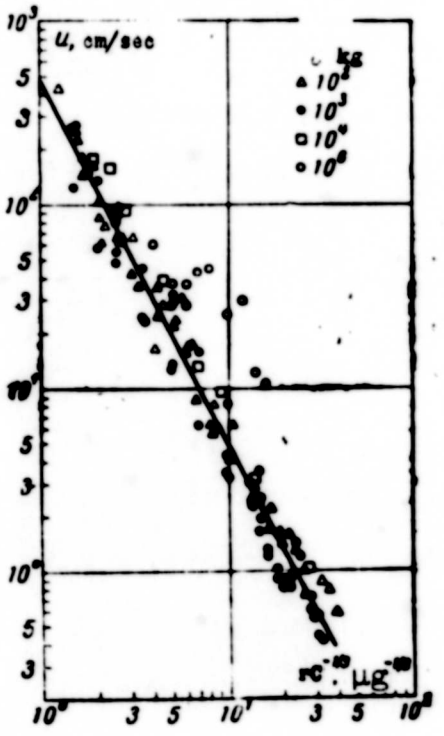

Fig. 4.

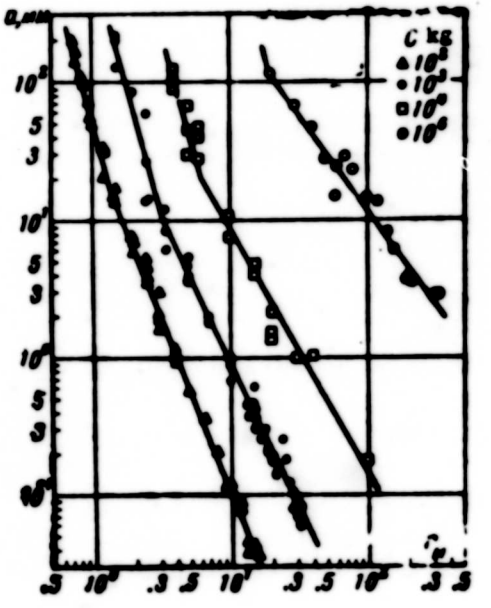

Fig. 5.

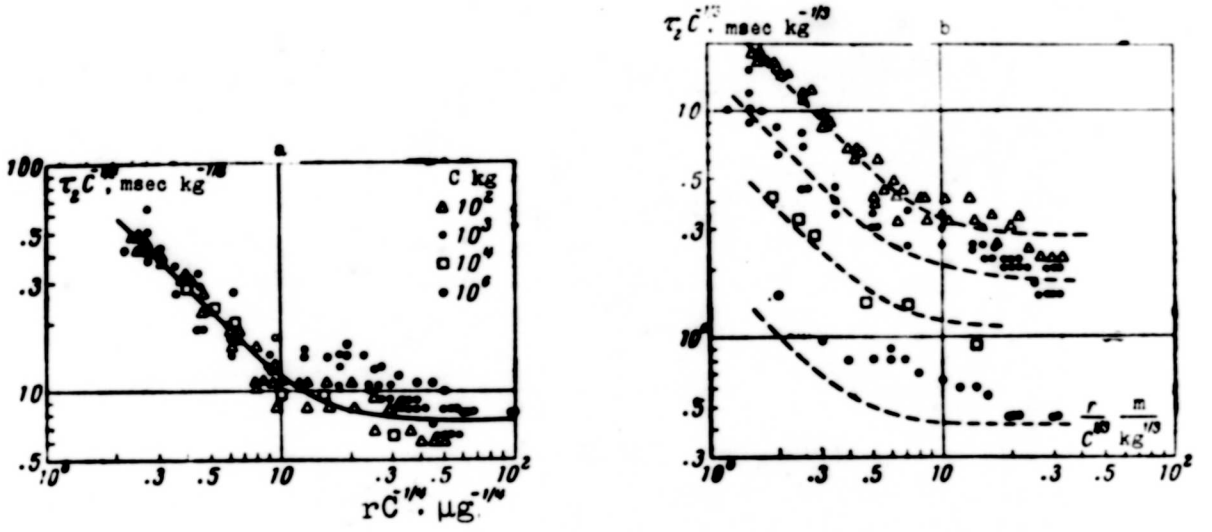

Fig. 6.

Coefficients K and n and their mean square errors ε_n and ε_k were determined by method of least squares

$$n = \frac{m\Sigma \lg r_i \lg a_i - (\Sigma \lg r_i)(\Sigma \lg a_i)}{m\Sigma \lg^2 r_i - (\Sigma \lg r_i)^2}, \qquad \lg K = \frac{1}{m}(\Sigma \lg a_i - n\Sigma \lg r_i)$$

$$\varepsilon_n = \left(\frac{\Sigma \varepsilon_i^2}{m-2}\right)^{1/2}\left(\frac{m}{m\Sigma \lg^2 r_i - (\Sigma \lg r_i)^2}\right)^{1/2}, \qquad \lg \varepsilon_k = \left(\frac{\Sigma \varepsilon_i^2}{m(m-1)}\right)^{1/2}$$

$$(\varepsilon_i = \lg K + n \lg r_i - \lg a_i)$$

Here m is the number of observations, the integration is made from i = 1 to i = m.

For a comparison of coefficients K and the elimination of the error ε_k of an inaccuracy determined by the error ε_n, magnitudes of K and ε_k were determined with an averaged index n on basis of all explosions.

The maximum mass speeds satisfying geometric law of modeling (Fig. 4), over entire measured range of distances are described by the relationship of the form

$$v = K\left(\frac{C^{1/3}}{r}\right)^n$$

Values of coefficients n and K (the latter is determined with an averaged n = 1.9) are given in Table 1.

Table 1

Site	No. of explosion	Weight of charge C, kg	μ^{h° -%	μ^{r° -%	m	n	$\pm\varepsilon_n$	K	ε_K %
M2	1	10^3	0.45	1.5—31.5	15	1.83	0.03	280	+3.0 −2.8
	2	10^3	0.80	1.5—31.5	15	1.88	0.07	300	+6.0 −5.7
	4	10^3	0.70	1.5—28.5	9	1.84	0.07	510	+6.8 −6.3
	5	10^3	1.5	1.5—31.5	15	1.80	0.05	800	+4.5 −4.3
K3	6	105	0.72	1.53—17.0	12	1.89	0.05	500	+4.2 −4.0
	7	80	0.74	1.88—39.2	14	1.79	0.06	480	+7.0 −6.5
	8	120	0.51	1.58—26.4	11	1.85	0.08	390	+7.4 −7.1
	9	120	0.39	1.34—19.7	12	1.97	0.10	400	+8.8 −8.0
	10	10^3	0.44	2.0—15.0	7	1.88	0.10	540	+7.0 −6.5
	11	10^4	0.42	1.88—13.9	7	2.00	0.09	800	+5.8 −5.5
MV	13	10^4	0.42	1.85—48.4	6	1.82	0.15	880	+13.0 −11.6
	14	10^4	0.42	1.85—8.3	5	1.69	0.40	980	+24.0 −19.4

Coefficient K constitutes relative characteristic of energy of explosion being transmitted by body seismic waves. For a concentrated charge of one and the same explosive with a constant density of charge this energy depends on the depth of laying of charge and on physico-mechanical properties of medium, in which there is made an explosion. The experiments made in clay grounds were inadequate for determing the degree of influence of these factors on intensity of the compression wave. However, a comparison with analogous data, obtained during explosions in rock, makes it possible to make in this respect certain conclusions. In Fig. 7 there is given the dependency of coefficient K on a given depth of laying of charge $h^\circ = h_c C^{-1/3}$. Maximum velocities of particles during a number of experiments in clays coincide with values of velocities during explosions in a rock.

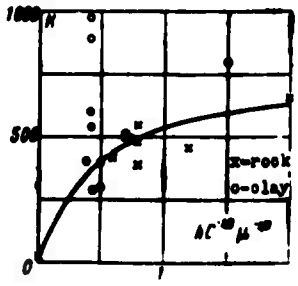

Fig. 7.

These were found to be explosions made in "dry" clays with the content of water by volume equal approximately to 40%. All experiments, made in clays with high humidity, gave excessively high values of the particle volocities. During explosions in loess-like loam containing approximately 15% water by volume and about 30% air, a compression wave practically is not recorded. Consequently, an increase in contents of water increases intensity of Compression wave and an increase in contents of air acts in the opposite direction. Such limited information about ground and in sufficient number of experiments make it possible to make only qualitative conclusions about influence of ground conditions.

Processes determining the amount of energy being transmitted to a wave of compression, occur in the zone directly adjacent to charge, since outside the zone in measured interval of distances between 20 to 600 radii of the charge the dispersion of energy (at the stage of load of medium) is identical for all explosions in clay and rock (for velocities of particles $n = 1.9 \pm 0.1$).

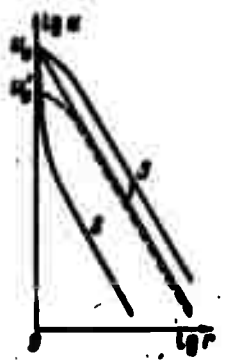

Fig. 8.

If curve of velocity of particles – distance with deeper sinking of the charge, i.e., with a maximum release of energy is extended to wall of chamber of charge, then velocities of the particles at boundary of cavity u_0 will correspond to the initial pressure of the gases, according to the relationship $\sigma = \rho V u$ (curve 1, Fig. 8).

In shallow explosions this curve in the sector from 20 to 600 radii of the charge lies parallel but at a lower level (Fig. 7). But in approaching the charges the velocities must coincide on wall of cavity with value u_0 (curve 2, Fig. 8). Consequently, at closer distances during shallow explosions the velocities of particles (and pressure) must decrease more intensely.

This is associated obviously, with a degree of counteraction of surrounding medium of the expanding products of the explosion. During shallow explosions the gases encounter less resistance in the direction of outer surface, the cavity expanded more significantly and by the moment of the detachment of compression wave the pressures will be smaller than during underground explosions.

Apparently, analogously also the resistivity of various types of grounds exerts an influence. Thus, an insignificant increase in the porosity, little reflecting on the magnitude of density, and consequently also on u_0, owing to high compressibility greatly decreases the velocities of particles at great distances. An increase in humidity, i.e., a filling in of the pores, decreases the compressibility and level of velocity distance curves rises. In this case at near distances the damping of velocity of particles with distance must be less than at remote distances (curve 3, Fig. 8).

This may explain the coincidence of values of velocities of particles during explosions in rock and clay at remote distances. With one and the same pressure on walls of the cavity the value u_0 in rock will be smaller, but near the charge owing to smaller compressibility velocities of particles attenuate more slowly and at measured distances of 20 to 600 radii of the charge they may coincide (dashed curve of Fig. 8).

5. A further analysis of parameters of a compression wave pertains to main mass of experiments made under faily uniform ground conditions with insignificant variations of depth of laying of charge ($h = 0.4 - 0.75\ C^{1/3}$). For them the dependence of maximum velocities of particles on charge and distance (Fig. 4) it is possible to represent by expression

$$\sigma = \sigma_0 \left(\frac{r_0}{r}\right)^{\alpha}$$

Maximum displacements in the same experiments depending on distance for different magnitudes of charge are shown in Fig. 5. In the graph fairly distinctly there can be seen the change in degree of damping of displacements with distance. Amplitudes of displacements very sharply drop near epicenter of explosion, following the same law for all charges, and at a certain distance ($r = R_n$) begin to attenuate to a smaller degree varying on magnitude of the charge.

The initial sector during the conducted observations, having obtained the conditional designation "near zone", is interesting in the fact that at its beginning near the crater there were noted (visually) dislocations of the ground. This made it possible to assume that within limits of entire section there must be irreversible permanent dislocations. At the same time there must be exceeded the ultimate strength and the cohesion between ground particles must be destroyed. A comparison between the recordings of the particle velocities and displacements in this sector (Fig. 9) shows that

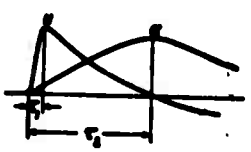

Fig. 9.

velocity of the particles (and consequently, also the pressure) increases up to maximum value during the time τ_1, equal to several milliseconds.

During this period there occurs a loading of medium and there is expended energy being transmitted by compression wave. During the same time the displacements attain very insignificant magnitudes in comparison to the maximum at moment of time τ_2, whose absolute value is more than 50 msec (Fig. 6). Consequently, over entire stage of the increment of displacements, when there occurs an unloading of the strain state of the medium, the particles of ground move freely one with the other

owing to the kinetic energy obtained at moment of time τ_1 and which will be equal to the potential energy of lifting the ground to a height a at moment of time τ_2. Thus, there must be observed the relationship

$$a = \frac{u^2}{2g} \quad \text{or} \quad a = 1000 \frac{C^{1.00}}{r^{2.0}} \text{ м/м}$$

The latter result is obtained by substitution of values of acceleration due to gravity g and velocity of particles u.

The straight lines in Fig. 5 in the near zone, have been drawn according to the obtained formula, and results of the analysis given in Table 2, show that this dependence fairly accurately reflects obtained results on the basis of the measurement of the displacements. In this talbe: $K^* = 10^3 C^{1.27}$ are values from the formula, K_1 are magnitudes obtained from observations at $n_1 = 3.8$.

Table 2

C	m	n_a	δ_n	K_1	δ_K	K^*	$K_n C^{-n_a}$
10^3	11	−3.67	±0.26	$3.58.10^3$	$+0.22.10^3$ $-0.20.10^3$	$3.46.10^3$	2.8
10^3	8	−4.14	±0.88	$5.43.10^3$	$+1.25.10^3$ $-1.00.10^3$	$6.45.10^3$	3.2
10^3	9	−3.72	±0.66	$1.55.10^3$	$+0.16.10^3$ $-0.14.10^3$	$1.20.10^3$	2.8

Consequently, in the second stage of the process, beginning from the moment of time τ_1, medium is subject to the effect of gravity and parameters of motion must satisfy the Froude number i.e.,

$$\frac{a}{C^{n_a}} = K\left(\frac{C^{n_a}}{r}\right)^{2.0} \quad \text{or} \quad a = K\frac{C^{1.00}}{r^{2.0}}$$

We shall note that dependence on magnitude of charge in a geometric modeling must be

$$\frac{a}{C^{n_a}} = K\left(\frac{C^{n_a}}{r}\right)^{2.0} \quad \text{or} \quad a = K\frac{C^{1.00}}{r^{2.0}}$$

The observed results show that displacements and equally also the times τ_2 (Fig. 6) are close to the Froude number, but do not satisfy it completely. This is caused by the fact that in the given process the initial conditions (speed u) are modelled according to another law. The fact that parameters of the motion in second stage are close to the Froude number is explained by small difference in the structure of formula of the particle velocities:

in a geometric modeling

$$\cdot u = K\left(\frac{C^{1/3}}{r}\right)^{1.9} \quad \text{or} \quad u = K\frac{C^{0.633}}{r^{1.9}}$$

in modeling according to Froude number

$$\frac{u}{C^{1/3}} = K\left(\frac{C^{1/3}}{r}\right)^{1.9} \quad \text{or} \quad \cdot u = K\frac{C^{0.633}}{r^{1.9}}$$

In the second sector ("remote" zone), beginning from distance R_n, equal to approximately 60 radii of charge, the displacements are approximated by dependence of the type $a = K_2 r^{n_2}$. Coefficients K_2 and n_2 are presented in Table 3.

Table 3

C	m	a	Δa	$-a_0$	K_2	ΔK_2, %
10^3	20	−2.57	±0.04	−2.60	$1.44 \cdot 10^4$	+3.0 −2.8
10^3	37	−2.17	±0.05	−2.20	$1.98 \cdot 10^4$	+3.5 −3.3
10^4	11	−1.87	±0.16	−1.85	$4.31 \cdot 10^4$	+9.3 −8.6
10^4	17	−1.87	±0.07	−1.85	$3.61 \cdot 10^4$	+5.8 −5.3

For the remote zone there is observed change of degree of damping of displacements with distance of depending on the charge (Fig. 10). This is characteristic for viscoelastic media where absorption of energy depends on frequency of oscillations, becoming larger with its increase. Consequently, during explosions in clay with the passage of compressional wave (normal longitudinal wave) in remote

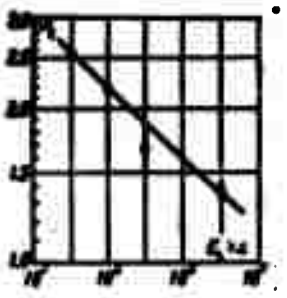

Fig. 10.

zone the medium is subject to action of two forces – elastic and viscous friction which are commensurable in magnitude. Under such conditions the wave parameters must satisfy two criteria, and a similarity determinated by simple scalar factors will not exist.

In conclusion author thanks D. A. Kharin for his advice and criticisms.

Submitted
23 March 1962

Literature

1. G. I. Pokrovskiy and I. S. Fedorov. The action of an impact and explosion in deformable media. Promstroyizdat, 1957.

2. M. A. Sadovskiy. The simplest method of determining the seismic danger of large-scale explosions. Academy of Sciences of the USSR, 1956.

3. F. A. Kirillov. Seismic effect of an explosion. Transactions of the Seismological Institute of the Academy of Sciences of the USSR, 1947, No. 121.

4. A. P. Zegzhda. Theory of similarity and the method of designing of hydrotechnical models. Gosstroyizdat, 1938.

5. L. I. Sedov. Methods of similarity and dimensionality in mechanics. Gostekhteoretizdat, 1957.

6. S. S. Grigoryan. On fundamental hypothesis of dynamics of grounds. PMM, 1960, Vol. 24, Issue 6.

7. B. G. Rulev and D. A. Kharin. Seismographs for recording major displacements. Transactions of the Institute of Physics of Earth, Academy of Sciences of the USSR, 1961, No. 16 (183).

8. D. P. Kirnos, B. G. Rulev and D. A. Kharin. The VEGIK seismograph for work in engineering seismology and the recording of near earthquakes. Transactions of Institute of Physics of Earth, Academy of Sciences of the USSR, 1961, No. 16 (183).

9. R. Koul. Underwater explosions. Foreign Literature Press, 1950.

WAVES IN THE SURFACE REGION OF A GROUND HALF-SPACE DURING A CONTACT EXPLOSION

V. D. Alekseyenko

(Moscow)

In measuring the field of stresses excited by contact explosion on surface of soft ground it is ascertained that the wave in the ground near the free surface has two maxima.

In Fig. 1 there is presented an experimental oscillogram with the recording of four normal stresses at a point remote from center of explosion at a distance R = 40 r^{o}, in direction of beam, emanating from center of explosion at an angle of 12° to the free surface (r^{o} – radius of charge). Beams 1, 2, 3, 4 correspond to recording of stresses in time σ_{θ}, σ_{n}, σ_{z}, σ_{r} (Fig. 2). Scale of time was fixed by marker to time with frequency of oscillations 500 cps. In order to establish nature of these two maxima of the stress, we shall consider phenomena occurring during contact explosion.

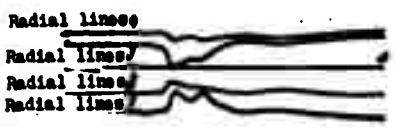

Fig. 1.

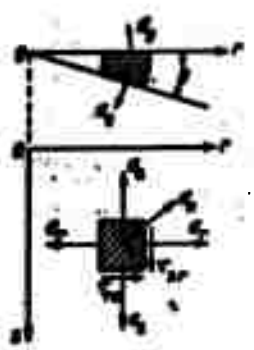

Fig. 2.

After detonation of charge of an explosive substance BB part of energy is radiated into

the air, generating in it an air shock wave propogating along free surface. The other part of energy of explosion is radiated directly in ground half-space exciting a wave in it. The air shock wave also generates waves propogating from free surface into the depth of the half-space.

In accordance with this a contact explosion schematically we shall present as action of concentrated pulse at center of explosion and air shock wave propogating along free surface with a speed D_f variable in time.

We shall consider at first picture of developing waves here in the half-space for the case when it is filled with a uniform elastic medium. The wave picture developing in this case, is shown in Fig. 3. Air shock wave generates in elastic half-space two fronts inclined to the free surface – the longitudinal DG and the transverse DE. The concentrated pulse excites in this same half-space three waves: the one longitudinal AGO_2 and the two transverse CBO_1 and AB.

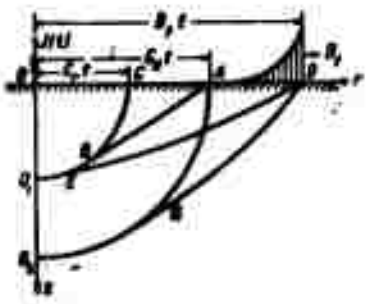

Fig. 3.

Waves generated by air shock wave owing to damping of speed of propagation of its front D_f and constancy of speed of propagation of waves in elastic half-space are distorted, as is shown in Fig. 3. However, if speed of propagation in half-space is inconstant and attenuates with distance from center of explosion, then the distortion of the fronts DG and DE may be opposite to that shown in Fig. 3 which is characteristic as the experiments showed for soft grounds. The concentrated pulse generates longitudinal (AGO_2) and transverse (CBO_1) wave of spherical form, and also transverse head wave (AB), whose slope depends on relationship of speeds

of longitudinal and transverse waves (in process of propagation there are formed surface waves which here are not considered).

Considering wave picture shown in Fig. 3, we note that near the free surface there are propagated five wave fronts of which two are longitudinal and three are transverse. Soft ground as is known, is the solid medium. Consequently, in conducting the experiments in ground all these waves, in general must be fixed. However, as the conducted experiments showed in the surface region there are observed only two fronts (Fig. 1).

There arises the question just what fronts are fixed in the experiments. For obtaining the answer to this question we set up special experiments. As a result it was established that fixed fronts are fronts of the longitudinal waves. The first front is excited by air shock wave, inasmuch as $D_f > D_{gr}$ (this front corresponds to DG in Fig. 3), second front propagates from center of explosion (front AGO_2, Fig. 3). The fact that front, corresponding second maximum of the stress, is not transverse, is confirmed by the following.

First, as is evident from the oscillogram (Fig. 1), all four components of tensor of stresses including σ_θ tolerate a discontinuity. In the case, if the front being considered were transverse, the stress σ_θ on this must not tolerate a discontinuity, inasmuch as on the front of a transverse wave only the tangential stress, tangent to its surface, tolerates a discontinuity.

All remaining components of the stresses (σ_n, σ_z, σ_r) must have tolerated a discontinuity, inasmuch as the indicated tangential stress is a linear combination of σ_n, σ_z, σ_r.

Secondly, if second front were transverse, then difference between the times of arrival at the same point of two maxima of stresses in approaching to the free surface would decrease and on the

free surface would vanish. However, experimental data contradict this, in approaching the free surface this difference increases.

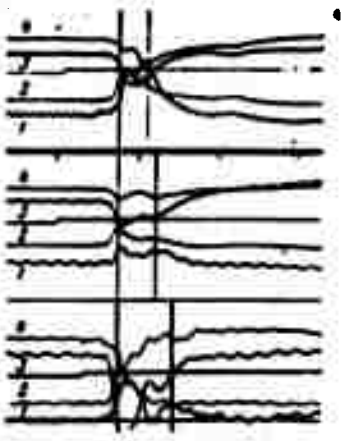

Fig. 4.

In Fig. 4 there are presented experimental oscillograms with recordings of stresses in a sandy ground unsaturated with water ground (of natural composition) at points remote from center of explosion at a distance R = 40 r^{o} and located on radial lines emerging from center of explosion at angles to free surface of (downward) 18, 12 and 6^{o} respectively. Scale of time on all oscillograms is the same. Essentially these data are adequate in order to clarify nature of the two maxima of the stress on the experimental oscillograms.

For a direct check of the corroboration expressed above on nature of two maxima in the wave of stresses, in addition to the described experiments, there were conducted special experiments in sandy loam ground of natural composition unsaturated with water with the cutting off of waves, proceeding through the ground either from center of explosion, or away from free surface from air shock wave. In Fig. 5 there is presented a diagram of experiment with cutting off of wave, proceeding through ground from the center of the explosion. At the points of measurement 1 and 2 symmetrically located with respect to center of explosion 0 there were placed single-component strain-gauge sensing devices so that their sensing surfaces were oriented in the meridional plane z0r. In front of point 1 there was excavated the trench A, 2 meters long and 1.10 m deep,

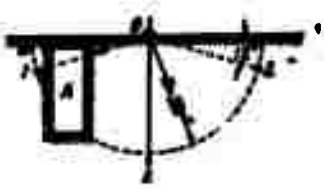

Fig. 5.

which from above was covered by wooden shield mn and was covered by ground flush with free surface in order to exclude an inflow of the air shock wave.

In Fig. 6 there is given the oscillogram corresponding to this experiment. The radial 1 pertains to point of measurement 1, radial line 2 — to point 2. From oscillogram it is evident that at point 1 there is fixed only one maximum of stress (first) generated by the air shock wave, at point 2 there are recorded two maxima of the stresses. In both radial lines the first maxima of stresses coincide in time.

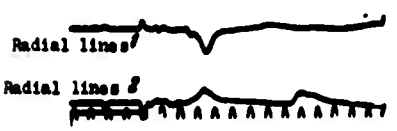

Fig. 6.

In Fig. 7 there is presented a diagram of experiment with interception of the air shock wave. Thus, as also in the preceding experiment, there were two symmetric points of measurement 1 and 2. On free surface above point 1 there was placed a box B (dimension 0.8 × 0.8 × 0.4 m), which was heaped around by ground. Furthermore, in this box there was placed a large wooden box MN of dimension 2.5 × 2.5 × 0.25 m., which also was heaped with ground from above and from sides, in order to exclude the inflow of an air shock wave.

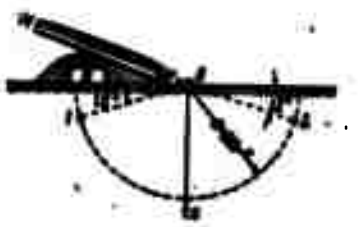
Fig. 7.

In Fig. 8 there is presented the oscillogram belonging to this experiment from which it is evident that on the radial 1, corresponding to point 1, there is only one maximum of stress coinciding in time with the second maximum of stress on radial line 2, pertaining to point 2. Consequently, second

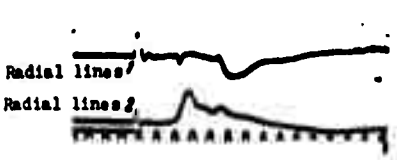

Fig. 8.

maximum of the stress is generated by the wave, propagating through the ground from center of explosion. The entire discussion makes it possible to make the conclusion that recorded maxima on oscillograms of the stresses are generated by the two fronts of longitudinal waves.

The experiments showed that in case, when half-space consists of soft ground unsaturated with water the difference in speeds of propagation of front of air shock wave and front of waves in ground is fairly large, especially at small distances from center of explosion ($R \leq 40r^0$). As a result of this the slope angle of the fronts of the longitudinal and moreover of the transverse waves generated by air shock wave with respect to free surface is small.

Therefore, intensity of transverse wave DE is small and it is not recorded by the sensing devices. As to the fronts AB and CBO_1, then their intensity, obviously is small by virtue of the fact that in considered range of distances the motion of ground is accompanied by significant plastic deformations, so that speed of transverse wave CBO_1 is found to be small in comparison to speed of longitudinal wave AGO_2. Owing to this the slope of front AB to free surface is found to be small which makes the intensity of this wave insignificant and therefore, it is not recorded by the sensing devices.

The considerations expressed relative to fronts of transverse waves in plastically deformed media are preliminary in nature and require special study.

In conclusion author considers his duty to express gratitude to S. S. Grigoryan and Z. V. Narozhnaya for their assistance in completing this work.

Submitted
26 December 1962

ON THE CONDITION OF TOTAL PLASTICITY FOR AN AXIALLY SYMMETRIC STATE

D. D. Ivlev and T. N. Martynova

(Voronezh)

In examining problems of plastic flow of ideally-plastic bodies a major simplification in the solution is attained owing to the use of piecewise-linear approximations of conditions of fluidity (the Tresca condition of maximum given stress and others). Hencky [1] showed that if state of strain corresponds to a rib of prism interpreting in space of the principal stresses the Tresca condition of plasticity (condition of total plasticity), then problem of determination of the stresses is statically determinate. The solutions of a number of problems under the condition of total plasticity are given in works of A. Yu. Ishlinskiy [2], R. Shield [3] and others.

Below there are considered relationships of the axially symmetric problem of rigid plastic imcompressible bodies, when the stress and strain states correspond to rib of arbitrary piecewise-linear surface of fluidity interpreting the condition of plasticity in space of the principal stresses. It is shown that also in this case problem of determination of stresses is statically determinate.

1. Let us examine the space of the principal stresses σ_1, σ_2

and σ_3. Equations of rib of surface of fluidity in this space have the form

$$a_1\sigma_1 + b_1\sigma_2 + c_1\sigma_3 = h_1, \qquad a_2\sigma_1 + b_2\sigma_2 + c_2\sigma_3 = h_2 \qquad (a, b, c, h = \text{const}) \tag{1.1}$$

Let us assume that condition of plasticity does not depend on first invariant of tensor of stresses, then for coefficients of equations (1.1) we have the conditions

$$a_1 + b_1 + c_1 = 0, \qquad a_2 + b_2 + c_2 = 0 \tag{1.2}$$

From equations (1.1) under condition (1.2) we shall obtain

$$\sigma_1 - \sigma_2 = 2k_3, \qquad \sigma_2 - \sigma_3 = 2k_1, \qquad \sigma_3 - \sigma_1 = 2k_2 \tag{1.3}$$

Here

$$k_3 = \frac{1}{2m}(b_1c_2 - b_2c_1), \qquad k_1 = \frac{1}{2m}(b_1b_2 - b_2b_1)$$
$$k_2 = \frac{1}{2m}(b_2c_1 - b_1c_2), \qquad m = a_1c_2 - a_2c_1, \qquad k_1 + k_2 + k_3 = 0$$

We note that magnitude m is not equal to zero, otherwise the planes (1.1) will be parallel to each other.

Condition of plasticity (1.1) finally may be written out in the form

$$\sigma_1 - \sigma_2 = 2k_3, \qquad \sigma_2 = p + k_2 - k_3, \qquad p = \frac{1}{2}(\sigma_1 + \sigma_3) \tag{1.4}$$

Let us consider axially symmetric state of the body under the condition of plasticity (1.4) in the cylindrical coordinates ρ, θ, z.

By virtue of assumed symmetry of the state of strain the stress σ_θ will be the principal subsequently we shall assume $\sigma_\theta = \sigma_3$. Between the components of the stress σ_ρ, σ_z, $\tau_{\rho z}$ and the principal stresses σ_1, σ_2 there take place the relationships

$$\sigma_\rho = \sigma_1\cos^2\varphi + \sigma_2\sin^2\varphi, \qquad \sigma_z = \sigma_1\sin^2\varphi + \sigma_2\cos^2\varphi$$
$$\tau_{\rho z} = -(\sigma_1 - \sigma_2)\sin\varphi\cos\varphi, \qquad \sigma_\theta = \sigma_3 \tag{1.5}$$

where φ is the angle between first cardinal direction and axis ρ.

Using expressions (1.4) and (1.5), we shall have

$$\begin{aligned} \sigma_\rho &= p + k_0 \cos 2\eta, & \sigma_z &= p - k_0 \cos 2\eta \\ \tau_{\rho z} &= -k_0 \sin 2\eta, & \sigma_\theta &= p + k_0 - k_0 \end{aligned} \tag{1.6}$$

From (1.6) the condition of plasticity (1.4) may be written out in the form

$$(\sigma - \sigma_\theta)^2 + 4\tau_{\rho z}^2 = 4k_0^2, \qquad \sigma_\theta = \frac{1}{2}(\sigma_\rho + \sigma_z) + k_0 - k_0 \tag{1.7}$$

Substituting relationship (1.6) into equations of equilibrium, we shall obtain system of two differential equations of hyperbolic type relative to functions p and ψ

$$\begin{aligned} \frac{\partial p}{\partial \rho} - 2k_0 \sin 2\eta \frac{\partial \eta}{\partial \rho} - 2k_0 \cos 2\eta \frac{\partial \eta}{\partial z} &= \frac{k_0 - k_0 - k_0 \cos 2\eta}{\rho} \\ \frac{\partial p}{\partial z} - 2k_0 \cos 2\eta \frac{\partial \eta}{\partial \rho} + 2k_0 \sin 2\eta \frac{\partial \eta}{\partial z} &= \frac{k_0 \sin 2\eta}{\rho} \end{aligned} \tag{1.8}$$

Equations of characteristics of system (1.8) have the form

$$\frac{dz}{d\rho} = -\operatorname{tg}\left(\eta \mp \frac{\pi}{4}\right) \tag{1.9}$$

where upper sign here and below corresponds to the first family of characteristics, lower – to the second. From equations (1.9) it is evident that characteristics are mutually orthogonal to each other. Along characteristics (1.9) there take place the relationships

$$dp \mp 2k_0 d\eta = \frac{(k_0 - k_0) d\rho \mp k_0 dz}{\rho} \tag{1.10}$$

Taking the condition of plasticity for the plastic potential, we shall write out the relationships of associated law of flow in the form

$$\varepsilon_\rho + \varepsilon_z + \varepsilon_\theta = 0, \qquad \frac{\sigma_\rho - \sigma_z}{\tau_{\rho z}} = \frac{\varepsilon_\rho - \varepsilon_z}{\gamma_{\rho z}} \tag{1.11}$$

Substituting in equations (1.11) values of rates of deformation in terms of rates of the displacement and using (1.6), we shall have

$$\frac{\partial u}{\partial \rho} + \frac{\partial w}{\partial z} + \frac{u}{\rho} = 0, \quad \left(\frac{\partial u}{\partial \rho} - \frac{\partial w}{\partial z}\right)\sin 2\varphi + \left(\frac{\partial u}{\partial z} + \frac{\partial w}{\partial \rho}\right)\cos 2\varphi = 0 \tag{1.12}$$

where u, w are the rates of displacement along the ρ and z axes respectively.

Equations (1.12) relative to the two unknown functions u and w belong to the hyperbolic type and have characteristics coinciding with characteristics of field of stresses (1.9). Along the characteristics there take place the relationships

$$du \pm dw\,\mathrm{tg}\left(\varphi \pm \frac{\pi}{4}\right) \pm \frac{u}{\rho}\,d\rho = 0 \tag{1.13}$$

We now consider condition of Tresca's plasticity (the hexagon ABCDEF in Fig. 1). Rib A is intersection of the edges

$$\sigma_1 - \sigma_3 = 2k, \qquad \sigma_2 - \sigma_3 = 2k$$

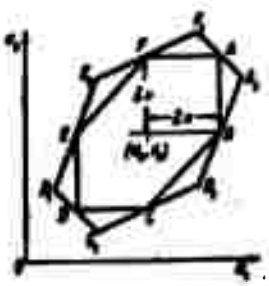

Fig. 1.

In this case $k_a = 2k$, $k_b = -2k$, $k_c = 0$ and relationships (1.10) may be integrated [3]

$$p + 4k \ln \rho = \text{const}$$

For ribs B, C, E, F from (1.10) there ensue well known relationships under the condition of total plasticity [1-3]

$$dp \mp 2k\,d\varphi = \frac{2k(d\rho \mp dz)}{\rho}$$

In case of a condition of maximum given stress (hexagon $A_1B_1C_1D_1E_1F_1$ in Fig. 1) rib A_1 is formed by intersection of the edges

$$\sigma_1 - \tfrac{1}{3}\sigma_2 - \tfrac{1}{3}\sigma_3 = 2k, \quad -\sigma_1 + \tfrac{1}{3}\sigma_2 + \tfrac{1}{3}\sigma_3 = 2k$$

In this case $k_a = k_c = 4/3k$, $k_b = -8/3k$ and relationships (1.10) take the form

$$dp \pm \frac{4}{3} k\, d\varphi = -\frac{4}{3} k \frac{2\rho \pm dz}{\rho}$$

Analogous expressions take place for ribs C_1, D_1 and F_1.

Rib B_1 is formed by the intersection of the edges

$$\sigma - \frac{1}{2}\sigma - \frac{1}{2}\sigma = 2k, \qquad -\sigma + \frac{1}{2}\sigma + \frac{1}{2}\sigma = 2k$$

In this case $k_a = k_b = -4/3k$, $k_c = 8/3k$ and relationships (1.10) take the form

$$dp \mp \frac{8}{3} k\, d\varphi = \mp \frac{8}{3} k \frac{dz}{\rho}$$

Analogous expressions take place for rib E_1. The solutions found depend essentially on selection of rib.

These results can be extended to ideally plastic media whose fluidity conditions depend on the first invariant of tensor of stresses.

Conditions of Tresca plasticity and maximum given stress limit all possible conditions of fluidity [4, 5].

Thus, the solution of axially symmetric problems under the condition of total plasticity (condition of conformity of stress and strain states to ribs of piecewise-linear conditions of fluidity) can make it possible to find the upper and lower limits of the solutions.

Submitted
21 January 1963

Literature

1. G. Hencky. On certain static determinate cases of equilibrium in plastic bodies. Collection of articles "Theory of Plasticity," Moscow, Foreign Lit. Publishing House, 1948.

2. A. Yu. Ishlinskiy. Axially symmetric problem of plasticity and the Brinell test. PMM, 1944, Vol. VIII, Issue 3.

3. R. Shield. On the plastic flow of metals under conditions of axial symmetry. Collection of translations. "Mechanics," Foreign

Lit. Publishing House, 1957, No. 11.

4. D. D. Ivlev. On formulating the theory of ideal plasticity. PMM, 1958, Vol. XXII, Issue 6.

5. R. M. Kheyzornsveyt. Range of change of conditions of fluidity for stable ideal-plastic bodies. Collection of translations. "Mechanics," Foreign Lit. Press, 1961, No. 5.

CONDITION OF DEFORMATION OF A RIGID PLASTIC BODY IN ONE PLANE DURING SEPARATION OF CHIP

V. I. Sadchikov

(Tomsk)

Let us assume that a semi-solid plastic body moves uniformly with a speed v_0 and interacts with absolutely hard stationary wedge (figure). In certain protion of the stationary space filled with moving particles of this body stressed up to the yield point there will occur a continuous plastic flow as a result of which from body there will be separated a chip and will be displaced along fore of wedge with a constant speed v_1. The condition under which the deformation will be localized in one plane must be found.

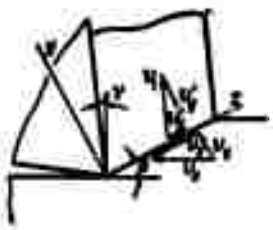

Figure

Such problem is one of technological problems on an established plastic flow; it is of practical value for studying the deformation of metal during cutting. During the last 10 to 15 years problem of cutting has been solved, for example, D. Drucker [1], Lee and Shaffer [2], Hill [3] and others. Survey of the most popular investigations and new variants of solution of these problems are given in works [4, 5]. In a larger portions of

these works it was assumed that body being deformed in one plane is ideally hard-plastic, in other works it was endowed with properties of viscosity and hardening. In all works the solutions were made on the basis of equations of equilibrium, i.e., in components of acceleration of the element of medium, passing through the zone of deformation not only the local part, but also the translational part is assumed equal to zero. Such an approach to this problem did not provide the possibility of finding the condition at which deformation there may be localized in one plane, since this condition is determined by state of hardening and inertial stress.

In order to locate this condition, we shall substitute in system of equations of quasi-static two-dimensional flow of a hard-plastic body [6] the equations of equilibrium with equations of motion and the yield point on the condition of plasticity of Von Mises we shall assume a variable magnitude. Then system of equations will take the form

$$\left.\begin{aligned}
&\frac{\partial \sigma_x}{\partial x}+\frac{\partial \tau_{xy}}{\partial y}=\rho\left(\frac{\partial v_x}{\partial x}v_x+\frac{\partial v_x}{\partial y}v_y\right)\\
&\frac{\partial \sigma_y}{\partial y}+\frac{\partial \tau_{xy}}{\partial x}=\rho\left(\frac{\partial v_y}{\partial x}v_x+\frac{\partial v_y}{\partial y}v_y\right)
\end{aligned}\right\}\ \text{(equation of motion)}$$

$$\frac{\partial v_x/\partial x}{\sigma_x-\sigma}=\frac{\partial v_y/\partial y}{\sigma_y-\sigma}=\frac{\partial v_y/\partial x+\partial v_x/\partial y}{2\tau_{xy}}\ \text{(law of flow)}\qquad (1)$$

$$\frac{\partial v_x}{\partial x}+\frac{\partial v_y}{\partial y}=0\ \text{(condition of incompressibility)}$$

$$(\sigma_x-\sigma_y)^2+4\tau_{xy}^2=4I^2\ \text{(condition of plasticity)}$$

Here σ_x, σ_y and τ_{xy} are components of the stress, σ is the mean normal stress, I is the yield point, v_x and v_y are components of the speed and ρ is the density of medium.

Assuming that deformation during separation of shaving is realized in one plane, we shall find conditions for speeds and stresses on the lower and upper sides of this plane.

As follows from figure, in system of Cartesian coordinates x, y, indicated in this figure, tangents and normal components of speeds are determined by the relationships: on the lower side of plane of deformation

$$v_x = -v_0 \cos\beta, \qquad v_y = v_0 \sin\beta \tag{2}$$

on its upper side

$$v_x' = v_1 \sin(\beta - \gamma), \qquad v_y' = v_1 \cos(\beta - \gamma) \tag{3}$$

where β is the angle between plane of deformation and horizontal, γ is the angle between front edges of cutter and the vertical. Plane of deformation in field of speeds is plane of discontinuity along which normal component of speed must be continuous, therefore, $v_y = v_y'$ and

$$v_0 \sin\beta = v_1 \cos(\beta - \gamma) \tag{4}$$

The tangential component of speed across the plane of deformation tolerates a discontinuity, equal to

$$v_x' - v_x = v_1 \sin(\beta - \gamma) + v_0 \cos\beta = v_0 \frac{\cos\gamma}{\cos(\beta - \gamma)} \tag{5}$$

Thus, component of the speed v_y maintains a constant value, equal, for example, $v_0 \sin\beta$ everywhere in field of speeds, and component of speed v_x varies only during transition through plane of deformation. For zone of deformation

$$\frac{\partial v_x}{\partial x} = \frac{\partial v_y}{\partial x} = \frac{\partial v_y}{\partial y} = 0 \tag{6}$$

and $\partial v_x / \partial y$ does not exist.

By virtue of (6) the condition of incompressibility of the system (1) is identically satisfied; law of flow, second equation of

motion and condition of plasticity establish that

$$\sigma_x = \sigma_y = \sigma = f(x) \tag{7}$$

and what

$$|\tau_{xy}| = k \tag{8}$$

and does not depend on coordinate x.

Thus, mean normal stress varies only along plane of deformation and the tangential stress across this plane.

Plane of discontinuity in field of speeds may be assumed as the threshold case of a thin layer enclosed between parallel planes and giving continuous transition from field of speeds of body being deformed to field of chip speeds. For such layer of conditions from (2) to (6) conserves the force and the derivative of v_x in y exists. In addition the first equation of the motion in system (1) takes form

$$\frac{\partial \tau_{xy}}{\partial y} - \rho \frac{\partial v_x}{\partial y} v_y = -\frac{\partial \sigma}{\partial x} \tag{9}$$

This equality is possible only in the case if also its left-hand and right-hand sides represent the same constant k

$$\frac{\partial \tau_{xy}}{\partial y} - \rho \frac{\partial v_x}{\partial y} v_y = k, \quad -\frac{\partial \sigma}{\partial x} = k \tag{10}$$

We shall designate width of thin layer by the letter h and shall integrate first equation of (10) fron initial deformed state on the lower boundary of this layer, where $y = y_0$, $\tau_{xy} = \tau_0$ and $v_x = -v_0 \cos \beta$, up to final deformed state on upper boundary, where $y = y_0 + h$, $\tau_{xy} = \tau_1$ and $v_x = v_1 \sin (\beta - \gamma)$. Then we shall have

$$k = \tau_1 - \tau_0 - \rho v_0^2 \frac{\sin \beta \cos \gamma}{\cos (\beta - \gamma)} \tag{11}$$

At $h \to 0$ each of variables entering into this equality, will tend toward a corresponding magnitude during a deformation in one

plane, and condition (11), written out in the same designations, will acquire the form

$$\tau_1 - \tau_0 = \rho v_0^2 \frac{\sin\beta\cos\gamma}{\cos(\beta-\gamma)} \qquad (12)$$

where τ_1 and τ_0 are the tangential stresses acting respectively on the upper and lower sides of plane of deformation. Right-hand side of obtained equality represents the inertial stress.

Since $|\tau_1| > |\tau_0|$ and for the possible β and γ the right-hand side of equality (12) is a positive value, then $\tau_1 > 0$ and $\tau_0 > 0$. Then by virtue of (8) tangential stresses τ_0 and τ_1 are equal respectively to the yield points of initial and final deformed states, i.e., $\tau_0 = I_0$ and $\tau_1 = I_1$. Furthermore, the relationship

$$\varepsilon_{xy} = \frac{\gamma_2' - \gamma_2}{\gamma_2} = \frac{\cos\gamma}{\sin\beta\cos(\beta-\gamma)}$$

is the component of shear and determines degree of deformation of material. Here to condition (12) there may be imparted the form

$$I_1 = I_0 + \rho v_0^2 \varepsilon_{xy} \sin^2\beta \qquad (13)$$

Relationships (12) and (13) are different forms of the necessary deformation condition of chip-formation of a hard-plastic body in one plane. They show that with such form of deformation the hardening of the medium is equal to the inertial stress and express the relationship between geometric characteristics of problem, the speed v_0, measure of deformation and the hardening of the medium.

From relationship (11) it follows that in hard-plastic medium with arbitrary degree of hardening the deformation of the chip-formation in one plane is impossible because in this case $h \neq 0$. Relationship (13) shows that such deformation is impossible also in

an ideally hard-plastic medium because at $I_1 = I_0$ the magnitude $\rho v_0^2 \varepsilon_{xy} \sin^2 \beta = 0$. Consequently, all the solutions [1-5] of the cutting problem on the deformation in one plane both of an ideally hard-plastic body and also of a hard-plastic body with an arbitrary degree of hardening was found to be based on inconsistent premises.

In the solution of problems on an established plastic flow with a discontinuity of field of speeds usually there are used equations of equilibrium. An example of the solution of a cutting problem showed that such a use of these equations is not justified because a consideration of the inertial force radically changed the concept of this problem.

Submitted
5 November 1962

Literature

1. D. C. Drucker. An analysis of the mechanics of metal cutting. Journal of Applied Physics, 1949, Vol. 20, No. 11.

2. E. Lee and B. Shaffer. Application of theory of plasticity to problems of machining of metals, IL, Mechanics, 1952, No. 5.

3. R. Hill. The Mechanics of Machining: A New Approach. Journal of the Mechanics and Physics of Solids, 1954, Vol. 3, No. 1.

4. M. Shaw, N. Cook and I. Finnie. The shear – angle relationship in metal cutting. Transactions of the ASME, 1953, Vol. 75, No. 2.

5. Kobayasi and Thompson. Analysis of process of cutting of metals. Transactions of the American Society of Engineers-Mechanics. Designing and Machine Building, 1962, No. 1.

6. R. Hill. Mathematical theory of plasticity. Moscow, State Publishing House, 1956.

ADAPTABILITY OF THICK-WALLED PIPES DURING NONUNIFORM HEATING

D. A. Gokhfel'd and P. I. Yermakov

(Chelyabinsk)

Problem on the strength of thick-walled pipe with the repeated effects of the internal pressure and the temperature field is important for power-machinery engineering and certain other fields of technology [1]. Below there is considered the solution of this problem on the basis of theory of adaptability. As is known, this theory makes it possible by proceeding from assumption about ideal plasticity to determine the conditions at which repeated loads will not result in a sign-alternating or increasing plastic flow. With a limited number of cycles, characteristic for thermocyclic load, absence of repeated plastic flow can with a certain approximation be assumed as condition of strength. Creep and relaxation in present work are not taken into consideration. It is assumed that the length of period of a pipe under conditions of high temperature is relatively small.

1. Fundamental equations. We shall analyze the stresses in a long hollow cylinder with bottoms. Henceforth it will be convenient to use dimensionless magnitudes; in particular, in the mentioned

below expressions of stresses pertain to the value of yield point at a certain initial temperature.

Stresses from the internal pressure in pipe are equal [2]

$$\sigma_r = p\left(1-\frac{1}{\rho}\right), \quad \sigma_\theta = p\left(1+\frac{1}{\rho}\right), \quad \sigma_z = p \quad \left(p=\frac{p_a}{\sigma_0}\frac{k^2}{1-k^2},\ \rho=\frac{r^2}{ab},\ k=\frac{a^2}{b^2}\right) \tag{1.1}$$

Here p is the load parameter; p_a is the internal pressure; a, b, r are the internal, external and current radii respectively.

We shall assume that the pipe is under the effect on an axially symmetric thermal field, invariable over its length. Admitting a quasi-stationary mode of heating and cooling, we shall assume that the temperature is distributed according to the logarithmic law

$$t = t_b + t_1\frac{\ln\rho}{\ln k} \qquad (t_1 = t_a - t_b) \tag{1.2}$$

The subscripts denote values of the temperature on corresponding radii, t_1 is the temperature differential.

The generating thermal stresses are determined by expressions [2], which can be reduced to the following form (q is the parameter of the thermal field):

$$\sigma_r = -q\left(1-\frac{1}{\rho}+\delta\ln\rho\right), \qquad \sigma_\theta = -q\left[1+\frac{1}{\rho}+\delta(2+\ln\rho)\right]$$
$$\sigma_z = -2q\left[1+\delta(1+\ln\rho)\right] \quad \left(q=t_1^0\frac{k}{1-k},\ t_1^0=\frac{\alpha E t_1}{2\sigma_0(1-\nu)},\ \delta=\frac{1-k}{k\ln k}\right) \tag{1.3}$$

The state of spontaneous stress in a solid body is function of an infinite number of parameters. In the solution of problem being posed we shall consider as is usually assumed only one of the parameters differing from zero and its corresponding state of spontaneous stress similar to the distribution of thermal stresses (1.3). Such an assumption proceeds to the "reserve of strength" since here there is obtained a lower evaluation of adapting values of load and temperature [3].

Thus, total stresses in the tube are determined by the expressions

$$\begin{aligned} \sigma_r &= p\left(1-\frac{1}{\rho}\right)+(m-q)\left(1-\frac{1}{\rho}+\delta\ln\rho\right) \\ \sigma_\theta &= p\left(1+\frac{1}{\rho}\right)+(m-q)\left[1+\frac{1}{\rho}+\delta(2+\ln\rho)\right] \\ \sigma_z &= p+2(m-q)[1+\delta(1+\ln\rho)] \end{aligned} \qquad (1.4)$$

We shall assume that yield point remains constant at $t \leq t_b$, and at higher temperature decreases according to the linear law

$$\sigma_{st} = \sigma_s[1-\alpha(t-t_b)] = \sigma_s(1-\lambda q\delta\ln\rho), \quad \lambda = \frac{2(1-\nu)\alpha\sigma_s}{\alpha E} \qquad (1.5)$$

Tnen the Huber-Mises plasticity condition (for dimensionless stresses) will have the form

$$(\sigma_r-\sigma_\theta)^2+(\sigma_\theta-\sigma_z)^2+(\sigma_z-\sigma_r)^2 = 2(1-\lambda q\delta\ln\rho)^2 \qquad (1.6)$$

2. Region of possible states. If expression for the stresses (1.4) are substituted in condition of plasticity (1.6), we shall obtain equation of the family of boundary surfaces limiting regions of the variation of the parameters p, q, m, within which deformation on corresponding radii of the tube will be elastic

$$a_{11}q^2+a_{22}m^2+a_{33}p^2+2a_{12}qm+2a_{23}mp+2a_{13}qp+2a_{14}q+a_{44}=0 \qquad (2.1)$$

Coefficients of equation (2.1) are functions of current radius

$$\begin{aligned} a_{11} &= a_{22}-a_{12}^2, \quad a_{12} = -a_{22} = -\frac{3}{\rho}\left(\frac{1}{\rho}+\delta\right), \quad a_{14} = \lambda\delta\ln\rho \\ a_{23} &= -a_{13} = [1+\delta(1+\ln\rho)]^2+3\left(\frac{1}{\rho}+\delta\right)^2, \quad a_{33} = \frac{3}{\rho^2}, \quad a_{34} = -1 \end{aligned}$$

Equation (2.1) determines family of elliptic cones having the bisector of quadrant in the plane p = 0 as a common axis. Coordinates of summits of cones are equal to

$$q_0 = m_0 = \frac{1}{a_{44}} = \frac{1}{\lambda\delta\ln\rho} \qquad (2.2)$$

For points of tube located on external radius ($\rho = 1$), as is evident from (2.2), the top recedes to infinity, and from (2.1) we obtain the equation of the cylinder

$$4(1+\delta)^2(q-m)^2-8(1+\delta)(q-m)p+3p^2-1=0 \qquad (2.3)$$

Region of possible (elastic) states [4] for a tube is shown in Fig. 1. It is limited by surfaces of cone constructed for the value $\rho = k$, and cylinder (2.3). Surfaces of the family (2.1), corresponding to other values of current radius are located outside the indicated region.

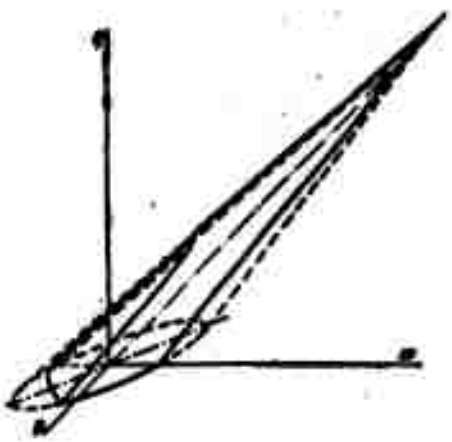

Fig. 1. Region of possible (elastic) states.

Form of boundary surfaces is determined by condition of plasticity, and also by adopted tolerances relative to the state of spontaneous stress and the law of change of yield point according to the temperature [5]. An analogous solution is fairly simple and may be obtained on the basis of Saint Venant's condition of plasticity. In this case instead of elliptic cones we shall have hexahedral pyramids, and instead of a cylinder – a prism.

Considering section of region of possible states by the planes $p = \text{const}$, we shall obtain following expressions determing the maxima of parameter of thermal field at which adaptability is possible:

during relatively small pressures

$$q^* = \frac{(1+\lambda\delta)\sqrt{4k^2-3p^2}-\lambda k(1-k)}{2(1+\lambda\delta)^2-0.5\lambda^2(1-k)^2} \qquad (2.4)$$

during higher pressures

$$q^* = \frac{2p-\sqrt{4-3p^2}}{4(1+\delta)} - \frac{2p-\sqrt{4k^2-3p^2}}{4(1+\lambda\delta)} \qquad (2.5)$$

Hence there can be obtained dependence between temperature of adaptability (the maximum value of temperature potential t_1, at which the adaptability will take place) and internal pressure in tube invariable during the cycle. Corresponding curves are given in Fig. 2, where temperature of adaptability is defined as a function of the ratio of the internal pressure to its limiting value (construction is made for the ratio $a/b = 0.8$ and $\lambda = 0.17$). Curve 1 determines maxima of temperature differential in tube, at which repeated heatings and cooling will not result in a sign-alternating plastic flow;

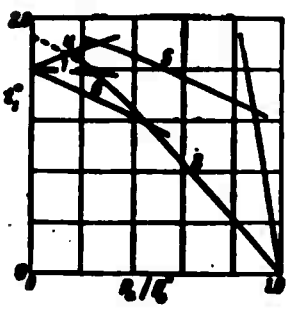

Fig. 2. Diagram of adaptability.

curve 2 – the potential at which these influences will not cause an increment of plastic flow with each cycle.

In the literature [6] there was marked analogy of diagram of adaptability (Fig. 2) with "finite ratio" between loads in theory of the limiting state (according to A. A. Il'yushin). It is not difficult to note also that curves 1 and 2 are analogous to the well known Haigh diagram, determining the dependence between constant and variable components of the limiting cycles of the stresses.

Sections of the region of possible states with planes $q = \text{const}$ provide the possibility of determining limiting pressure for the tube and its dependence on temperature differential (curve 3 in Fig. 2). A comparison of curves 1 and 2 with curve 3 illustrates influence of the variability of thermal field on the strength of tube.

As one should have expected the limiting pressure, determined with the aid of diagram of possible states is found to be somewhat smaller than its exact value [2]

$$p_0^* = \frac{2}{\sqrt{3}} q^{lim}. \qquad (2.6)$$

This difference is the result of assumption taken on distribution of initial stresses and corresponds to the well-known extreme principle [3]. It happened to be small and, naturally, decreasing with an increase in ratio between internal and external radii of tube (Fig. 3). It is possible the obtained lower evaluation for temperature of adaptability which also is small (and smaller as the ratio a/b becomes larger) differs from its actual value.

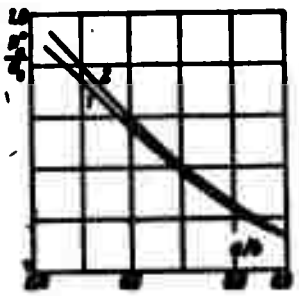

Fig. 3. Curves of limiting pressures: 1) approximately, with respect to region of possible states; 2) precisely according to formula (2.6).

The region of elastic states makes it possible also to investigate cycles, in which not only temperature, but also the pressure is a variable. If we take the proportional dependence between parameters of load and thermal field, for their adapting values we shall obtain the formulas

$$q_0^* = \frac{(2\lambda + 3\rho)(1 + \lambda\delta) - \lambda\lambda(1 - \lambda)}{4(1 + \lambda\delta)^2 - \lambda^2(1 - \lambda)^2} + \frac{\sqrt{(2\lambda + 3\rho)(1 + \lambda\delta) - \lambda\lambda(1 - \lambda)]^2 - 3\rho(\lambda + \rho)[4(1 + \lambda\delta)^2 - \lambda^2(1 - \lambda)^2]}}{4(1 + \lambda\delta)^2 - \lambda^2(1 - \lambda)^2} \qquad (2.7)$$

$$q_0^* = \frac{3\rho - \sqrt{4 - 3\rho^2}}{4(1 + \delta)} + \frac{\lambda}{2(1 + \lambda\delta)} \qquad (2.8)$$

In the diagram of adaptability (Fig. 2) these expressions correspond to curves 4 and 5. We note that during relatively large pressures under given conditions the adapting load coincides with the threshold.

Finally, for the cycle, corresponding to general formulation of problem of theory of adaptability, when pressure and temperature may be changed according to an arbitrary program, taking into consideration

section of region of possible states with the planes m = const and eliminating this parameter from the equations, we shall obtain

$$q_1^0 = \frac{2k_1 - \beta p + (1-\beta)\sqrt{4k^2 - 3p^2}}{2\beta[1 + \lambda\theta_0 + \lambda(1-\beta)]} \qquad (2.9)$$

This expression corresponds to curve 6 in Fig. 2. Formula for q_2^0 coincides with (2.5).

In the same figure with dashed lines there is shown position of curves for the cycle with arbitrary program without calculating the influence of temperature on the yield point ($\lambda = 0$). A comparison shows that influence of temperature on yield point in given problem reduces to a certain decrease of the adaptability region. Here only the position of line 6 changes, determining condition of sign-alternating deformation on the internal configuration of tube section.

Submitted
25 December 1962

Literature

1. A. A. Il'yushin and P. M. Ogibalov. Elasto-plastic flows of hollow cylinders. Publishing House of Moscow University, 1960.

2. S. D. Ponomarev, et al. Designs for strength in machine building, II, Mashgiz, 1958.

3. V. Koyter. New general theorem of the adaptability of elasto-plastic designs. Collection: "Mechanics" Foreign Literature Press, 1957, No. 3.

4. A. R. Rzhanitsyn. The design of structures with plastic properties of the materials taken into account. State Construction Publishing House, 1954.

5. D. A. Gokhfel'd. On adaptability under conditions of repeated thermal influences. Academy of Sciences of Ukrainian SSR, Collection Thermal stresses in turbomachine elements, 1961, Issue 1.

6. V. I. Rozenblyum. On the theory of adaptability of elasto-plastic bodies. News Academy of Sci. of USSR, OTN, 1958, No. 6.

ON THE STABILITY OF AXIALLY COMPRESSED CYLINDRICAL SHELL IN PLASTIC FLOWS

G. V. Ivanov

(Novosibirsk)

There is examined the axially symmetric form of loss of stability of axially compressed cylindrical shell. The critical stresses are determined by criterion [1] with the limitation that in the transition from the fundamental state to the adjoining there are not tolerated perturbations causing an unloading. The material is assumed incompressible and its hardening – linear. The critical stresses, determined according to the theory of plastic flow is somewhat less but very close to critical also according to criterion [1], and by Shanley's dimensionless number [2] stresses determined according to the theory of small elasto-plastic flows, i.e., in this problem, as previously there are considered problems on stability of plates [1, 3], with the use by criterion [1] there does not appear known paradox, encountered with the use of Shanley's dimensionless number.

There is pointed out the error of the solution in Lee's work [4] according to the theory of plastic flow of problem on nonaxially symmetric form of the buckling of axially compressed cylindrical shell taking into account initial "irregularity" of shape of shell

and in connection with this on nonsubstantiation of the conclusion in work [4] that in this problem calculation of initial "irregularities" does not make it possible to avoid the paradox.

1. It is assumed that during deformation of shell in the basic state there takes place an uniaxial compression

$$\varepsilon_x = -\varepsilon_0, \quad \varepsilon_0 = \frac{P}{2\pi Rh} > 0, \quad \varepsilon_y = \varepsilon_z = \gamma_{xy} = \gamma_{xz} = \gamma_{yz} = 0 \tag{1.1}$$

Here P – the axial force compressing the shell, R – radius, h – thickness of shell, axis of coordinates x is directed along generatrix axis of coordinates y, z – respectively along tangent to middle surface and along inner normal to it so that they form an orthogonal system of coordinates.

Stresses corresponding to force P, deformations, displacements, during deviations from basic state are characterized by differences between these stresses, deformations, displacements and stresses corresponding to the same magnitude of force P, deformations, displacements in the basic state. These differences are called secondary stresses, secondary deformations and secondary displacements.

They are analyzed only as conveniently small axially symmetric deviations from the basic state. In this case

$$\varepsilon_x = -\varepsilon_0 + \varepsilon_x'', \quad \varepsilon_y = \varepsilon_y'', \quad \varepsilon_z = \gamma_{xy} = \gamma_{xz} = \gamma_{yz} = 0 \tag{1.2}$$

$$\varepsilon_x'' = e_1 - \varkappa z, \quad \varepsilon_y'' = e_2 = -\frac{w}{R}, \quad \varkappa = \frac{d^2w}{dx^2} \tag{1.3}$$

In (1.2), (1.3) the slanting cross as indicated secondary stresses, secondary deformations, w – secondary displacements along the axis z, e_1, e_2 – secondary deformations of middle surface. All these magnitudes with as small as desired deviations from the basic state are as small as desired. This is taken for determining deviations as small as desired.

If during deviations from basic state the shell is in equilibrium

only under action of axial force P then from determining the secondary stresses and equations of equilibrium it follows that

$$N_x^* = \int \sigma_x^* dz = \text{const} = 0 \qquad (1.4)$$

(integration is made from -h/2 to +h/2), the stress N_y^x and bending moment M^x

$$N_y^* = \int \sigma_y^* dz, \qquad M^* = \int \sigma_x^* z dz \qquad (1.5)$$

are associated by the equation

$$\frac{d^2}{dx^2} M^* - \omega k \frac{d^2 w}{dx^2} + \frac{1}{R} N_y^* = 0 \qquad (1.6)$$

The neighboring equilibrium state is called the equilibrium different from the basic state of shell during action of only the force P. In Shanley's statement of the problem [2] (in any case there is possible such an interpretation) and in the statement in [1] there is admitted the possibility of a transition from basic state to neighboring equilibrium state under action of perturbations of type of surface forces during change of external compressing force from value $P - \alpha$, $\alpha \geq 0$, to the value P. In Shanley's statement of the problem α is zero, or a magnitude as small as desired; in statement [1] a magnitude α any of the interval [0, P]. Below in the solution in statement [1] there are considered only such transitions from basic state to the neighboring equilibrium state, in which nowhere in the shell does unloading occur. Under this condition the association between secondary stresses and secondary deformations is described by equations of theory of plasticity, corresponding only to process of active loading which essentially simplifies the investigation.

2. From (1.1) and equations of the theory of plastic flow with

hardening [2] it follows that in the basic state

$$d\varepsilon_x^{\circ} = -\frac{1}{E'}\,d\sigma_0, \qquad d\varepsilon_y^{\circ} = d\varepsilon_z^{\circ} = -\frac{1}{2}\left(-K + \frac{1}{E'}\right)d\sigma_0, \qquad K = \frac{1-2\nu}{E} \tag{2.1}$$

Here E' is the tangent modulus of diagram of uniaxial compression corresponding to the stresses σ_0, ν is Poisson's ratio, E is Young's modulus.

Substituting (1.2) in equations of theory of plastic flow with hardening [2], by maintaining in them magnitudes as small as desired of only first order and subtracting equation (2.1), we find equation of association between secondary stresses and secondary deformations

$$\begin{aligned} d\varepsilon_x'' &= \frac{1}{E'}\left(d\sigma_x'' - \nu\, d\sigma_y''\right) + \frac{3}{2}\,d\left[F(T_0)\,T_0\left(\sigma_x'' - \frac{1}{2}\,\sigma_y''\right)\right] \\ d\varepsilon_y'' &= \frac{1}{E'}\left(d\sigma_y'' - \nu\, d\sigma_x''\right) - \frac{1}{2}\,d\left[F(T_0)\,T_0\left(\sigma_x'' - \frac{1}{2}\,\sigma_y''\right)\right] + \frac{1}{2}\,F(T_0)\,dT_0\,\sigma_y'' \end{aligned} \tag{2.2}$$

where

$$F(T_0) = \frac{3}{4T_0}\left(\frac{1}{E'} - \frac{1}{E}\right), \qquad T_0 = \frac{\sigma_0}{\sqrt{3}}, \qquad E' \neq E$$

Equations (2.2) are differential. Therefore, the association between the secondary stresses and secondary deformations in neighboring equilibrium state at a magnitude P of the axial force (to which there corresponds a certain value T_0, namely, $T_0 = P/2\pi$ Rh $\sqrt{3}$) essentially depends on magnitude of interval [P - α, P] (correspondingly, the intervals $[T_0 - \alpha_1, T_0]$, $T_0 - \alpha_1 = (P - \alpha)/2\pi$ Rh $\sqrt{3}$) and the path of transition in this interval from the basic state to the neighboring equilibrium state. In connection with this the critical stresses in Shanley's statement and in statement [1] are different. Below the magnitude of axial force P is characterized by magnitude T_0 – corresponding to this force P with an intensity of tangential stresses in the basic state.

In Shanley's statement of the problem there is admitted the possibility of a transition from basic state to neighboring equilibrium state under action of perturbations of type of surface forces only

with infinitesimally small change (including zero) of the axial force, i.e., in the interval $[T_0 - \alpha_1, T_0]$, where α_1 is zero, or magnitude as small as desired. In this case the integral is

$$\int_{T_0-\alpha_1}^{T_0} \beta(T)\varepsilon_y^{\circ}\,dT,$$

a magnitude of the second order as small as desired. Taking this into consideration and the condition that secondary stresses and secondary deformations are equal to zero (shell is found in the basic state) with an intensity $T_0 - \alpha_1$, from equations (2.2) we find that secondary stresses and secondary deformations in neighboring equilibrium state corresponding to an intensity T_0, are associated by the equations

$$\varepsilon_x^{\circ} = \frac{1}{E}(\sigma_x^{\circ} - \nu\sigma_y^{\circ}) + \frac{3}{2}\beta(T_0)T_0\left(\varepsilon_x^{\circ} - \frac{1}{2}\varepsilon_y^{\circ}\right)$$
$$\varepsilon_y^{\circ} = \frac{1}{E}(\sigma_y^{\circ} - \nu\sigma_x^{\circ}) - \frac{3}{2}\beta(T_0)T_0\left(\varepsilon_x^{\circ} - \frac{1}{2}\varepsilon_y^{\circ}\right)$$

i.e., by equations, usually used in the solution in Shanley's statement of the problem.

In statement [1] there is admitted the possibility of transition from basic state to neighboring equilibrium state under action of perturbations of type of surface forces with any change of the axial force, i.e., in the interval $[T_0 - \alpha_1, T_0]$, where α_1 – any of the interval $[0, T_0]$. If we were limited to the case of incompressible material ($\nu = 1/2$), then the equations (2.2) take the form

$$d\varepsilon_x^{\circ} = d\left[\frac{1}{E}\left(\sigma_x^{\circ} - \frac{1}{2}\sigma_y^{\circ}\right)\right]$$
$$2G(d\varepsilon_x^{\circ} + 2d\varepsilon_y^{\circ}) = d\sigma_y^{\circ} + 3\beta(T_0)\,dT\,\sigma_y^{\circ} \qquad \left(G = \frac{1}{3}E\right) \tag{2.3}$$

and are easily integrated also in final interval $[T_0 - \alpha_1, T_0]$. By means of (1.3)-(1.5) we change (2.3) to the magnitudes M^x, $N_y{}^x$, $\varkappa_1$, e_2. Integrating the obtained equations in the interval $[\tau_s, T_0]$, τ_s is the yield point during shear, we find that in case of linear

hardening ($E'(\xi) = \text{const}$, $\xi \in [\tau_s, T_0]$)

$$N^{x} = -\left(D^{x} + \frac{1}{12}B^{x}h^{2}\right)\varkappa_{x}, \quad D^{x} = \frac{Eh^{3}}{12\sigma_{x}(T_{0})\varphi(T_{0})}\left[\varkappa_{x}(\tau_{s}) + \int_{\tau_{s}}^{T_{0}}\varphi(\tau)\frac{d\varkappa_{x}}{d\tau}d\tau\right]$$

$$N_{0}^{x} = B^{x}\varepsilon_{0}, \quad B^{x} = \frac{4Eh}{(1+\lambda_{0})\sigma_{x}(T_{0})f(T_{0})}\left[\varepsilon_{x}(\tau_{s}) + \int_{\tau_{s}}^{T_{0}}f(\tau)\frac{d\varepsilon_{x}}{d\tau}d\tau\right] \tag{2.4}$$

$$\varphi(T_{0}) = \exp\left(2G\int_{\tau_{s}}^{T_{0}}F(T_{0})\,d\tau_{0}\right) - \left(\frac{\sigma_{s}}{\sigma_{0}}\right)^{\frac{2G}{\gamma}} \quad \left(\gamma = \frac{E'}{E},\ \sigma_{s} = \sqrt{3}\,\tau_{s}\right)$$

$$f(T_{0}) = \exp\left[2\left(\frac{1}{E'} + \frac{3}{E}\right)^{-1}\int_{\tau_{s}}^{T_{0}}F(T_{0})\,d\tau_{0}\right] - \left(\frac{\sigma_{s}}{\sigma_{0}}\right)^{\frac{2(1-\nu)}{1+\nu}}$$

It is not difficult to prove by the same method by which there is proved analogous corroboration in work [1] that functionals D^{x}, B^{x} in a class of piecewise continuous functions with piecewise continuous derivatives

$$\varkappa_{x}(\xi), \quad \varepsilon_{x}(\xi), \quad \xi \in [\tau_{s}, T_{0}]$$

satisfying at $\xi \in [\tau_s, T_0]$, any of the inequalities

$$\begin{array}{llll} \varkappa_{x}(T_{0}) > 0, & \varkappa_{x}(T_{0}) > \varkappa_{x}(\xi), & \varkappa_{x}(T_{0}) < 0, & \varkappa_{x}(T_{0}) < \varkappa_{x}(\xi) \\ \varepsilon_{x}(T_{0}) > 0, & \varepsilon_{x}(T_{0}) > \varepsilon_{x}(\xi), & \varepsilon_{x}(T_{0}) < 0, & \varepsilon_{x}(T_{0}) < \varepsilon_{x}(\xi) \end{array} \tag{2.5}$$

attain a minimum at

$$\varkappa_{x}(\xi) = \text{const}, \quad \varepsilon_{x}(\xi) = \text{const}, \quad \xi \in [\tau_{s}, T_{0}]$$

i.e., there takes place the inequalities

$$D^{x} \geq \frac{Eh^{3}}{12\sigma_{x}(T_{0})} = D^{x*}(T_{0}), \qquad B^{x} \geq \frac{4Eh}{(1+\lambda_{0})f(T_{0})} = B^{x*}(T_{0}) \tag{2.6}$$

Multiplying equation (1.6) by w, and integrating by parts, we find

$$\omega^{2} = -\left[\int_{0}^{L}\left(\frac{dw}{dx}\right)^{2}dx\right]^{-1}\int_{0}^{L}\left(N^{x}\frac{d^{2}w}{dx^{2}} + N_{0}^{x}\frac{w}{R}\right)dx \tag{2.7}$$

where L is the length of shell. We substitute (2.4) in (2.7)

$$\omega^{2} = -\left[\int_{0}^{L}\left(\frac{dw}{dx}\right)^{2}dx\right]^{-1}\int_{0}^{L}\left[\left(D^{x} + \frac{1}{12}E'h^{2}\right)\left(\frac{d^{2}w}{dx^{2}}\right)^{2} + B^{x}\left(\frac{w}{R}\right)^{2}\right]dx$$

For the critical stress, we shall designate it in terms of σ_k, we assume

$$\sigma_k h = \min\left[\int_0^L \left(\frac{dw}{dx}\right)^2 dx\right]^{-1} \int_0^L \left[\left(D^{**} + \frac{1}{12} E' h^3\right)\left(\frac{d^2w}{dx^2}\right)^2 + B^{**}\left(\frac{w}{R}\right)^2\right] dx$$

minimum is sought for in class of functions w, satisfying corresponding boundary conditions and inequalities (2.5).

By virtue of inequalities (2.6) the problem reduces to seeking the minimum of the functional

$$\left[\int_0^L \left(\frac{dw}{dx}\right)^2 dx\right]^{-1} \int_0^L \left[\left(D^{**} + \frac{1}{12} E' h^3\right)\left(\frac{d^2w}{dx^2}\right)^2 + B^{**}\left(\frac{w}{R}\right)^2\right] dx$$

in the class of functions w, satisfying corresponding boundary conditions, or which is equivalent to seeking the least value σ_0, at which equation

$$\left(D^{**} + \frac{1}{12} E' h^3\right)\frac{d^4w}{dx^4} + \sigma_k h \frac{d^2w}{dx^2} + \frac{1}{R} B^{**} w = 0$$

has nonzero solution under corresponding boundary conditions.

Assuming that $w = A \sin(\pi x/l)$, where l is the length of a semiwave in direction of generatrix, we find

$$\sigma_k h = \min\left[\left(D^{**} + \frac{1}{12} E' h^3\right)\frac{\pi^2}{l^2} + \frac{1}{R} B^{**} \frac{1}{\pi^2/l^2}\right] \qquad (2.8)$$

Here min designates the minimum of expression in bracket as a function of l under the condition that $l \leq L$ and $\sigma_k \geq \sigma_s$, σ_s is the yield point during compression. From (2.8) it is evident:

1) if $\frac{2}{3}\sqrt{E'E}\,\frac{h}{R} \geq \sigma_s$, then

$$\sigma_0 = \frac{2}{3}\sqrt{E'E}\,\frac{h}{R}\left(\frac{\varepsilon[1+2\varphi(T_0)]}{(1+3\varepsilon)\varphi(T_0)/(T_0)}\right)^{1/2} \quad \left(T_0 = \frac{\sigma_0}{\sqrt{3}}\right) \qquad (2.9)$$

Here l is determined by the formula

$$l = \pi\left(\frac{1}{12\varphi(T_0)\varepsilon}(1+3\varepsilon)(1+2\varphi(T_0))/(T_0)R^2h^2\right)^{1/4} \qquad (2.10)$$

2) if, however, $\frac{2}{3}\sqrt{E'E}\,\frac{h}{R} < \sigma_s$, then

$$\sigma_k = \sigma_s$$

Here l is determined by equation

$$\sigma_s h = \left[D^{(n)}(\tau_s) + \frac{1}{12} E' h^2\right] \frac{\pi^2}{l^2} + \frac{1}{R^2} B^{(n)}(\tau_s) \frac{1}{\pi^2 / l^2}$$

i.e., by equation

$$\sigma_s = \frac{1}{36} E (1 + 3\delta) h^2 \frac{\pi^2}{l^2} + \frac{4E'}{(1 + 3\delta) R^2} \frac{1}{\pi^2 / l^2} \qquad (2.11)$$

In the case, when l of (2.10) or (2.11) is larger than L – the length of shell, σ_k is found from equation

$$\sigma_s h = \left[D^{(n)}(T_s) + \frac{1}{12} E' h^2\right] \frac{\pi^2}{L^2} + \frac{1}{R^2} B^{(n)}(T_s) \frac{1}{\pi^2 / L^2} \qquad (2.12)$$

In the absence of hardening (in area of fluidity) condition of stability of shell in the sense of maintaining its cylindrical shape can be obtained from (2.11), (2.12) by the threshold limit during $E' \to 0$. Namely, the shell maintains a cylindrical shape, if

$$\sigma_s < \frac{1}{36} E \left(\frac{\pi h}{L}\right)^2 \qquad (2.13)$$

If inequality (2.13) is not fulfilled, the cylindrical shape is unstable and bulges are formed while l is determined by equality $\sigma_s = \frac{1}{36} E (\pi h / l)^2$.

Let us note that condition (2.13) is the same, as in case of cylindrical shape of buckling of plate in area of fluidity.

3. According to the theory of small elasto-plastic flows the association between secondary stresses and secondary deformations are the same independently of the interval [P - α, P] and the path of transition in this interval from the basic state to neighboring equilibrium state under the condition that unloading in process of transition does not develope. Therefore, also and in Shanley's statement of the problem and in statement [1] the critical stresses

according to the theory of small elasto-plastic flows are the same. These critical stresses in case of an axially compressed fairly thick cylindrical shell satisfactorily will agree with experimental data [4, 5].

During a linear hardening and condition of incompressibility of material the critical stress according to the theory of small elasto-plastic flows σ_*, the critical stress in Shanley's statement of the problem according to the theory of a plastic flow σ^* and also the lengths of half-waves corresponding to it – the l values are determined by equations [6-8]

$$\sigma_* = \frac{2}{3}\sqrt{E'E_c(\sigma_*)}\,\frac{h}{R}, \qquad \sigma^* = \frac{2}{3}\sqrt{E'E}\,\frac{h}{R} \tag{3.1}$$

$$l = \pi\left(\frac{1+3E'/E_c(\sigma_*)}{12\sqrt{E'/E_c(\sigma_*)}}Rh\right)^{1/4}, \qquad l = \pi\left(\frac{1+3\eta}{12\sqrt{\eta}}Rh\right)^{1/4} \tag{3.2}$$

where $E_c(\sigma_*)$ is the secant modulus of diagram of uniaxial compression corresponding to the stress σ_*. As before, if $\frac{2}{3}\sqrt{E'E}\,\frac{h}{R} < \sigma_s$, then $\sigma_* = \sigma^* = \sigma_s$, and l is found from equation (2.11). If l of (3.2) or (2.11) is larger than L, then σ_* and σ^* are determined by equations

$$\sigma_* = \frac{1}{36}\left(1+3\frac{E'}{E_c(\sigma_*)}\right)E_c(\sigma_*)h^2\frac{\pi^2}{L^2} + \frac{4E'}{\left[1+3E'/E_c(\sigma_*)\right]R^2}\frac{1}{\pi^2/L^2}$$

$$\sigma^* = \frac{1}{36}(1+3\eta)\frac{Eh^2\pi^2}{L^2} + \frac{4E'}{(1+3\eta)R^2}\frac{1}{\pi^2/L^2}$$

In the absence of hardening (in area of fluidity) condition of maintaining the cylindrical shape of shell according to the theory of small elasto-plastic flows will be

$$\sigma_* < \frac{1}{36}E_*\left(\frac{\pi h}{L}\right)^2$$

and according to the theory of plastic flow – condition (2.13). In comparing the critical stresses σ_k, σ_*, σ^*, it is convenient to present equations (2.9), (3.1) in the form

$$\frac{\sigma_2}{\sigma_1}=\left(\frac{\sigma_2}{\sigma_1}\right)^{\frac{n+m}{2(n+m)}}\left\{\left(3+\frac{1}{g}\right)\left[3g+\left(\frac{\sigma_2}{\sigma_1}\right)^{\frac{n+1}{g}}\right]^{-1}\right\}^{\frac{1}{n+1}}$$
$$\frac{\sigma_2}{\sigma_1}=\frac{1}{g}\left[\frac{\sigma_2}{\sigma_1}\left(\frac{\sigma_2}{\sigma_1}-1+g\right)\right]. \quad \frac{\sigma_2}{\sigma_1}=\frac{1}{\sqrt{g}}\frac{\sigma^*}{\sigma_1} \tag{3.3}$$

Here σ_* is the critical stress during elastic deformations, $\sigma_* = \frac{2}{3}Eh/R$. Comparison of conditions (3.3) for case $g = 1/4$ is presented in the figure. Curves 1, 2 correspond to the first two of these conditions (3.3) straight line 3, to the last condition. From the figure it is evident that critical stress in the sense of criterion [1] according to the theory of plastic flow is somewhat less, but very close to critical stresses according to the theory of small elasto-plastic flows (in the figure curves 1 and 2 respectively), i.e., during use of criterion [1] there does not arise the paradox which is encountered with use of Shanley's dimensionless number [2].

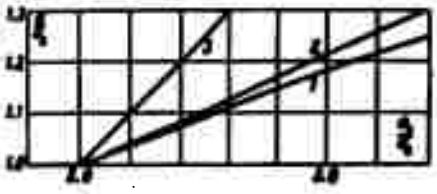

Fig. 1.

4. Statement [1] is nothing more than a scheme of the actual phenomenon, having the purpose of reflecting, more completely than in the scheme adopted in Shanley's statement of the problem, the influence of initial "irregularity" of the shape of plates and shells on their deformation. Therefore, absence of paradox in the solution in statement [1] makes it possible to trust that in a solution taking into account directly initial "irregularity" of shape of plates and shells the paradox does not arise not only in problem on torsion buckling of plate which Ye. Onat and D. Draker [9], demonstrated, but also in other problems on the stability of plates and shells.

The solutions of problems according to the theory of plastic flow

taking into account initial "irregularities" of the shape are very difficult. The difficulty consists in necessity of using complete (nonlinearized) equations of the theory of plastic flow (see equations (2), (3) in work [9]), generally speaking, we integrate them in the interval corresponding to interval of change of load from value when there develop plastic flows up to the critical value. Linearization of equations of the theory of plastic flow (use of equations of the type of equations (2.2)), obviously, is inadmissible, since, for example, in the problem on torsion buckling of plate it results in a certain "straightening" of the curve load – angle of torsion owing to which there is lost the maximum of this curve which determines the critical load.

In work [4] there was undertaken an attempt to solve by taking into account initial "irregularities" of shape of shell the problem on nonaxially symmetric form of the buckling of an axially compressed cylindrical shell. During the solution according to the theory of plastic flow the dependence between moments, curvatures and torsion, and also between stresses and strains of middle surface was determined not by integrating equations of theory of plastic flow in the interval corresponding to interval of change of load from value when plastic flows developed up to a critical value, but was set up the same as during the solution in Shanley's statement of problem which, of course is inadmissible. Namely, therefore, the obtained solution in [4] according to the theory of plastic flow was found to be close to the solution according to the theory of plastic flow of this problem in Shanley's statement of the problem. Thus, conclusion in work [4] that a consideration of initial "irregularity" does not make it possible to avoid paradox in problem about nonaxially symmetric form of buckling of an axially compressed cylindrical shell is based on

an erroneous solution.

Submitted
9 February 1963

Literature

1. G. V. Ivanov. On stability of equilibrium during nonelastic deformations. PMTF, 1961, No. 1.

2. L. M. Kachanov. Fundamentals of theory of plasticity. State Technical Press, 1956.

3. G. V. Ivanov. On stability of equilibrium of plates according to the theory of plastic flow. PMTF, 1963, No. 2.

4. L. H. Lee. Inelastic buckling of initially imperfect cylindrical shells subject to axial compression. Journal of the Aerospace Sciences, 1962, Vol. 29, No. 1.

5. A. N. Bozhinskiy and A. S. Vol'mir. An experimental investigation of stability of cylindrical shells beyond the limits of elasticity. DAN SSSR, 1962, Vol. 142, No. 2.

6. G. Gerard. Plastic stability theory of thin shells. Journal of the Aeronaut. Sciences, 1957, Vol. 24, No. 4.

7. E. I. Grigolyuk. On taking into account compressibility when determining lower critical loads (in connection with Gerard's article). News of Academy of Sciences of the USSR, Division of Technical Sciences, 1958, No. 5.

8. E. I. Grigolyuk. Purely plastic bucking of thin shells. PMM, 1957, Issue 6.

9. Ye. Onat and D. Draker. Inelastic buckling and the theory of flow. Collection of Translations "Mechanics," 1955, No. 3.

ON DETERMINING THE DIAGRAM OF COMPRESSION OF LOW-CARBON STEEL IN THE REGION OF ELASTO-PLASTIC DEFORMATIONS

Yu. S. Stepanov

(Moscow)

There is considered a simplified scheme for the design of the diagram of compression of solid bodies above their dynamic elastic limit as examplified by low-carbon steels. The design was checked directly by measurement of the kinematic parameters in a passing compressional wave.

Designations

v – speed of impact,
w – speed of free surface,
σ – stress,
ε – deformation,
x – axis of impact,
u – mass speed,
a – wave speed,
L_0 – initial length of hammer,
l_0 – initial length of plate,
d – initial diameter of hammer and plate,
S – initial area of cross section of hammer and plate,
K – modulus of manifold compression,
μ – shear modulus,
ρ – density of medium,
T – temperature,
p – pressure,
V – volume,
c_v – heat capacity at constant volume,
E – kinetic energy,
U – strain energy,
m – mass,
α,β,γ – coefficients in the equation (1.7) ($\gamma = 1.4$ in equation (2.1) and $\beta = 8.4$ in equation (3.1)).
A – coefficient in equation (3.1).

§ 1. Let us consider flat coaxial collision of cylindrical hammer and plate of one and the same diameter d from identical material, where the plate prior to impact is at rest, and $L_0 > d \gg l_0$, where L_0 and l_0 are the initial lengths of the hammer and plate.

We shall assume that build-up of stresses and deformations after collision can be replaced by a single wave with constant parameters behind the front, and common zone of load in the hammer and plate can by presented consisting of a zone of elastic and a zone of elasto-plastic flows separated from unloaded part of medium and from each other by intense fracture surfaces. We shall disregard lateral unloading and transverse deformations, assuming the load as uniaxial (the x-axis is the axis of impact).

We now consider system hammer – plate at moment of time, when fore front of elastic compressional wave in plate emerged on its rear surface. Taking into consideration the assumptions made, we shall obtain the distribution of stresses σ and mass speeds u in the direction of impact x in the hammer and plate illustrated in Fig. 1. The subscript 0 subsequently we shall relate to parameters in unloaded zone, 1 – to parameters in zone of elastic compression, 2 – of plastic compression.

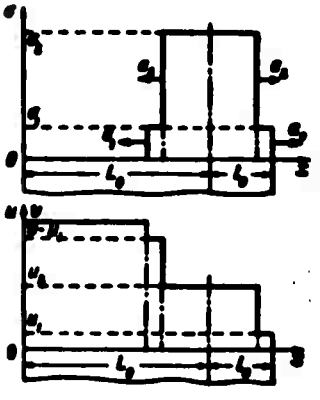

Fig. 1.

We shall designate limit of dynamic elasticity as σ_1, modulus of manifold compression K, shear modulus μ and initial density of the medium ρ_0. Then we shall obtain speed of fore front of elastic wave a_1, the density ρ_1, deformation ε_1 and mass speed u_1 behind the front from the relationships

$$c_0=\left(K+\frac{4}{3}\mu\right)a_0, \quad \rho_1=\frac{\rho_0 c_0}{c_0-u_1}, \quad u_1=c_0\varepsilon_0, \quad c_1=\left(\frac{K+4/3\mu}{\rho_0}\right)^{1/2} \tag{1.1}$$

In elastic zone all these parameters do not change their values. On surface of fracture between elastic and plastic zones there are fulfilled conditions of conservation of mass and momentum

$$\rho_1(c_0-u_1)=\rho_0(c_1-u_1) \tag{1.2}$$
$$\sigma_1+\rho_1(c_0-u_1)^2=\sigma_0+\rho_0(c_1-u_1)^2 \tag{1.3}$$

Equation (1.2), ignoring terms of the order ε^2, may be written out as

$$u_0-u_1=a_0(c_0-c_1) \tag{1.4}$$

From (1.2) and (1.3) there is evident the relationship

$$\sigma_0=\sigma_1+\rho_0(c_0-u_1)(u_0-u_1) \tag{1.5}$$

Equation of energy balance for the moment of time in Fig. 1 will be written out as

$$E=E'+E''+U'+U'' \tag{1.6}$$

were E is the kinetic energy of hammer prior to impact, E' is the kinetic energy of a part of hammer, not encompassed by the perturbation, E" is the kinetic energy of remaining part of hammer and plate, encompassed by perturbation, U' is the energy of elastic deformations in entire zone of load of hammer and plate, U" is the energy of irreversible deformations in plastic zone of load of hammer and plate.

According to the assumptions made the volume of the hammer and plate encompassed by lateral unloading is negligible in comparison to the volume of zones being considered of uniaxial state of stress. Since material of medium is identical, the zones of elastic and plastic load in the hammer and plate have an identical length. If area of their cross section is S, then the volume encompassed by the elastic

load, is equal to $Sl_0\ (1 - a_2/a_1)$, by the plastic load $- Sl_0 a_2/a_1$. Assuming the masses of the hammer and plate equal to m_1 and m_2, the speed of hammer equal to v, we shall write value E, E', E", U' and U"

$$E = \frac{m_1 v^2}{2}, \quad E' = \frac{(m_1 - m_2) v^2}{2}$$

$$E'' = 2Sl_0 \frac{\sigma_2}{a_1} \rho_2 \frac{u_2^2}{2} + \rho_2 Sl_0 \left(1 - \frac{a_2}{a_1}\right)\left[\frac{u_2^2}{2} + \frac{(v - u_2)^2}{2}\right]$$

$$U' = 2Sl_0 \sigma_2$$

$$U'' = 2Sl_0 \frac{\sigma_2}{a_1} (a_2 - a_1)(a_2 - a_1)$$

Substituting the described terms in equation (1.6), expressing σ_2 from (1.5), ρ_2 from (1.2), ε_2 from (1.4) and solving the obtained expression with respect to a_2, we shall obtain the quadratic equation

$$\alpha a_2^2 + \beta a_2 + \gamma = 0 \qquad (1.7)$$

where

$$\alpha = 2\rho_2 \rho_1 - \rho_1 [u_2^2 + (v - u_2)^2] + 4\rho_1 (a_2 - a_1)^2$$

$$\beta = [u_2^2 + (v - u_2)^2](\rho_2 a_1 + \rho_1 a_2) - 2a_2 \rho_2 a_1 + 4a_2 a_1 - 4\rho_1 (a_2 - a_1)^2 (a_2 + a_1) - \rho_2 v^2 a_1$$

$$\gamma = 4\rho_1 (a_2 - a_1)^2 a_2 a_1 + \rho_2 v^2 a_2 a_1 - \rho_1 [u_2^2 + (v - u_2)^2] a_2 a_1 - 4a_2 a_2 a_1$$

We shall set up an experiment in which there are measured speed of impact v of hammer over plate and mass speed corresponding to it in plastic zone u_2. Then, assuming as known from the relationships (1.1) written above the parameters in elastic zone, there can be found from equation (1.7) the corresponding speeds of front of plastic flows a_2, and according to them, σ_2, ε_2 and the temperature T.

§ 2. As means of loading a specimen of low-carbon steels there served cylindrical hammer with the same diameter and of the same material accelerated by compressed air in the barrel of pneumatic gun of 23.4 mm gauge. In Fig. 2 there is given a diagram experimental installation and

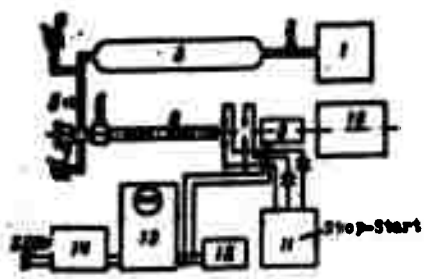

Fig. 2.

recording equipment.

Compressor 1 pumped the air into the high-pressure cylinder 3 up to pressures ~100 atm and above. The pressure indicator was a manometer 4 for 160 atm. Prior to experiment the hammer was placed in the barrel and was pressed in lock 6 by special clamp pellets, setting in recesses, made for this purpose in the hammer. When according to manometer 4 in the cylinder 3 there was found to be sufficient pressure for imparting to hammer the required speed, the compressor was turned off and there was closed the high-pressure valve 2. In conducting the experiment there was opened valve 5 and air was passed through to the active volume of barrel of gun behind the hammer. According to standard manometer 7 for 50 atm calibrated on basis of speed of hammer of constant weight which were used in the experiments, there was determined air pressure in the active volume with a high degree of accuracy. When it attained the required magnitude, lock 6 was opened and the hammer emerged from channel of barrel 8, before which there was placed measuring unit 9 and a bullet receiver 10. During each experiment its speed was measured on scalar 11, giving a reading of the time with an accuracy of 10 microseconds. The measuring unit was connected with recording equipment (generator of standard signals 12, oscillograph 13, block of power supply 14). The speed of the hammer according to pressure in channel of barrel p_0 can also be calculated by formulating the equation of energy balance. Then

$$v = \left[\frac{2}{m_1 + m\beta}\left(\frac{p_0 V_0}{\gamma - 1}\left[\frac{1}{V_0^{\gamma-1}} - \frac{1}{(V + V_0)^{\gamma-1}}\right] - p_a V\right)\right]^{1/2} \qquad (2.1)$$

where m_1 is the mass of hammer (in performed experiments it is equal to 350 g), m is the mass of air behind the hammer, p_0 is the pressure

determined by standard manometer 7, V_0 is the active volume behind the hammer, V is the volume behind hammer directly in channel of the barrel, $\gamma = 1.4$ for air, p_a is the atmospheric pressure.

In Fig. 3 there is shown the reinforcement of load d specimen 6 placed in ebonite ring 7. To the barrel of pneumatic gun 1 by means of clamp screws 2 there was joined the muzzle cap 3, having the recesses 4, removing formation of air compression ahead of the moving hammer. Before the specimen there were placed electrocontacts 5 for starting the oscillograph, and behind the specimen electrocontacts 9 connected through electrical circuit (Fig. 5) with recording equipment. They were clamped in ebonite bushing 11 and cap 10, which by clamp screws 8 was rigidily bound with the muzzle cap 3.

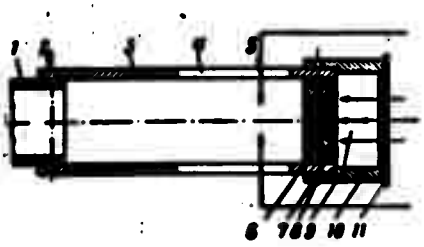

Fig. 3.

In Fig. 4 there is given the dependence calculated by formula (2.1) (thin line) and experimental (thick line) dependence of speed of hammer on the pressure p_0. Experimental curve lies somewhat below the calculated owing to the fact that during calculation there were not considered the lossess in kinetic energy of the hammer to friction in the channel of barrel.

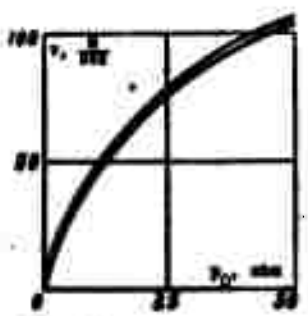

Fig. 4.

Mass speed behind the front of plastic wave u_2 was determined on basis of measured speed of free surface of plate, which moved after the emergence of plastic wave onto the free surface. Here measured speed was assumed to be double the mass speed. As it was shown in work [1],

this is true for pressures incommensurably exceeding that attained in the conducted experiments. It is necessary nevertheless to note that linear character of unloading results in an approximate fulfillment of law of doubling the mass speeds with an accuracy up to ratio a_2/a_1. Actually, during propagation of wave of unloading with constant speed $a_* \approx a_1$ within loaded plate on the basis of law of conservation of mass in a system of coordinates moving with constant speed u_2, we have

$$\rho_* a_* = (a_* + u_*)\rho_0$$

where ρ_*, u_* are the density and mass speed after reflected wave of unloading.

Since

$$\varepsilon_1 = 1 - \frac{\rho_0}{\rho_1}, \qquad \varepsilon_* = 1 - \frac{\rho_0}{\rho_*}$$

then

$$u_* = a_1\left(\frac{\rho_*}{\rho_0} - 1\right) = a_1\left(\frac{1-\varepsilon_2}{1-\varepsilon_*} - 1\right) = a_1\frac{\varepsilon_* - \varepsilon_2}{1-\varepsilon_*} \approx a_1(\varepsilon_* - \varepsilon_2) \text{ (for small } \varepsilon_2)$$

From linear character of unloading it is evident

$$\frac{\varepsilon_*}{\varepsilon_* - \varepsilon_2} = \frac{\varepsilon_1}{\varepsilon_1} \quad \text{or} \quad u_* = u_1\frac{\varepsilon_*}{\varepsilon_1}$$

Using σ_2 in the form of (1.5), ρ_1 and u_1 in the form of (1.1) and taking into account that $\sigma_1 = \rho_0 a_1^2 \varepsilon_1$, we shall obtain

$$u_* = \varepsilon_* a_1 + \frac{\rho_1}{\rho_0}\left(u_1\frac{\varepsilon_*}{\varepsilon_1} - u_1\varepsilon_1 - \varepsilon_* a_1 + \varepsilon_* a_1 \varepsilon_1\right)$$

Since previously there was ignored the quadratic terms in ε, then

$$\frac{\rho_1}{\rho_0} = \frac{1}{1-\varepsilon_1} \approx 1 + \varepsilon_1$$

and speed of the free surface

$$w = u_1 + u_* = u_1\left(1 + \frac{\varepsilon_*}{\varepsilon_1}\right) + u_1\left(1 - \frac{\varepsilon_*}{\varepsilon_1}\right) \qquad (2.2)$$

If a_2 does not strongly differ from a_1 then

$$w \approx 2u_2$$

It must be mentioned that, substituting u_2 from (2.2) in (1.7), there may be obtained a stricter solution for a_2 in terms of w, v and the known magnitudes.

However, owing to insufficient accuracy in experimental determination of w, this was found to be inexpedient.

The error introduced in calculating u_2 from equality $w = 2u_2$ in the computed values of a_2, determinate from equation (1.7), was corrected during a direct experimental measurement of a_2, corresponding to the given speeds of the free surface.

Speeds of free surface were measured by means of electrocontacts [1, 2]. As electrocontacts there were used thin wires, not rendering resistances to motion of plate and fastened tightly parallel to each other with constant base of measurement between upper and lower contacts determinate with an accuracy up to 0.01 mm. For their assembly there was used a specially created instrument – template for this purpose.

In experiments conducted the distance between upper electrocontacts and free surface of plate was equal to approximately one millimeter and therefore, the measured speed corresponded to moment of time after emergence of plastic wavt onto the free surface [3].

While carrying out of experiments there was assured a flat collision of the hammer and plate which was the condition necessary for simultaneous emergence of all parts of front of plastic wave onto free surface of the plate. In order that the wave of unloading reflected from rear end of hammer after impact could not reach the free surface and distort its speed, the hammer was made fairly long ($L_0 \gtrsim 10\ l_0$) and the base of measurement was selected sufficiently

small (1-1.5 mm). In the experiments performed loaded specimen had a length much smaller than its diameter and the diameter of the hammer. Owing to this during the period of emergence of wave of load onto rear surface of plate the lateral unloading could be propagated for an insignificantly small distance within specimen and transverse deformations therefore, it could not be taken into consideration. This is a validly made assumption at the beginning on an uniaxial load. During the period of measurement the distortions from lateral unloading could not reach the central zone of plate of small area (radius 1-2 mm), whose motion was recorded by a measuring unit placed in front of it.

The electrical circuit used in the measuring unit is shown in Fig. 5. Signals from electrocontacts 1, 2 were delivered to oscillograph with a driven sweep 5. Signal for "starting" of oscillograph was delivered a little before moment of collision of hammer and plate. The generator of standard signals 6 modulated the scanning by time marks of constant frequency variable depending on period of time measured on the oscillograph. In experiments there were used the oscillograph OK-17M, generator of standard signals GSS-6, 3 resistors (49 kilohm) and battery 4 (BAS-G-60-U-1.3). In order to eliminate external interferences, for the lead of the signal contacts at entries of oscillograph and starting contacts for "starting" of oscillograph there were used shielded wires. The entire pneumatic gun for this purpose was grounded.

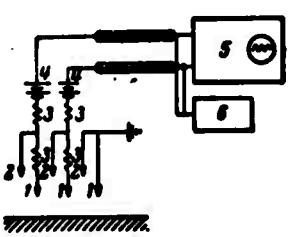

Fig. 5.

As is evident from the description of the experiment, moment of measurement of the free-surface speed did not correspond to moment of time shown in Fig. 1 for which there was formulated equation (1.6).

At moment of measurement the plastic wave already had emerged onto free surface of plate, and the reflected elastic wave began to interact with the plastic. However, considering that length l_0 is small the width of elastic zone can be ignored (furthermore, also u_2 is significantly larger than u_1), and as a result of the small base of measurement and small distance from the fore contacts up to free surface of plate it may be assumed that plastic wave up to moment of measurement did not succeed in changing its parameters owing to dissipation of energy in the middle of the plate.

Velocities of the plastic wave a_2 corresponding to the measured velocities v and w were also measured in analogous experiments by electric-contact method [1-3]. Results of experiments showed satisfactory agreement of experimental values with the calculated. A typical oscillogram obtained during measurement of w and a_2, is shown in Fig. 6.

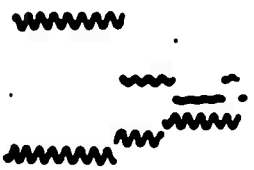

Fig. 6.

§3. Results of experiments are presented in Figures 4 and 7. In a comparison of experimentally measured speeds of hammer (solid line) and free surface of loaded plate (dotted line) it is evident that during low pressures speed of free surface is somewhat higher (see Fig. 7). This difference is explained by insignificant deceleration of hammer on thin wires, from which signal is delivered to scaler owing to their flexures during low impact velocities v. At the the same time speed of free surface never exceeds calculated speed of the hammer.

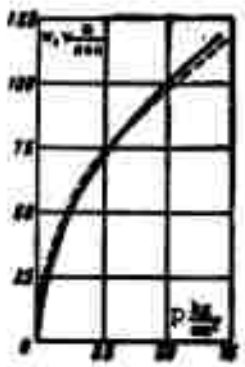

Fig. 7.

Using experimental data for each pair of values for v and u_2, by equation (1.7) there were found speeds of plastic flows a_2, and

by equations (1.4), (1.2), (1.5) there were determined corresponding deformations ε_2 densities ρ_2 and stresses σ_2. In Fig. 8 there is given the dependence of averaged values of the experimental and calculated magnitudes a_2 on the mass speed u_2. It is compared with Broberg's dependence [5] – 1 and Al'tshuler's [1] – 2. The dashed line designates the interpolation. According to relationships (1.1), at u_1, = 14.3 m/sec speed a_1 is constant and is equal to 5.99 km/sec. Then wave speed sharply drops. In region, where there may be formed shock waves (i.e., where speed of each subsequent plastic wave is higher than in the preceding), a_2 linearly increases with the increment of u_2 [1, 2]. This corresponds, as is evident from Fig. 9, to the values $\varepsilon_2 > 10^{-2}$. The obtained results are presented in Fig. 9 and in the table. In Fig. 9 there are adopted the following designations: 1 – the obtained data, 2 – Broberg's [5] calculated data, dashed line – the possible extrapolation of obtained data, dash-dot

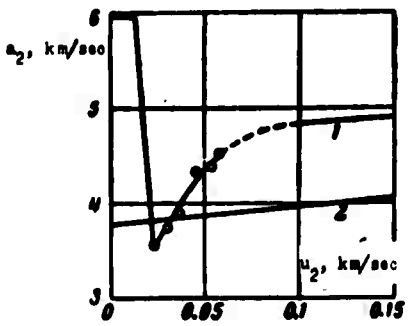

Fig. 8.

Table

No.	v_{cal} m/sec	v_{exp} m/sec	w_{exp} m/sec	u_0 m/sec	a_0 km/sec	σ_0 kg/cm^2	ε_0	ρ_0 g/cm^3	ΔT °C
1	89.0	49.0	49.8	24.9	3.56	9870	0.00526	7.894	1.2
2	82.0	80.8	82.2	31.1	3.73	11640	0.00666	7.906	2.2
3	77.3	72.7	74.4	37.2	3.90	13780	0.00845	7.916	3.1
4	82.0	82.0	81.2	45.6	4.34	17400	0.00980	7.927	4.6
5	112.7	110.0	108.8	53.4	4.38	20150	0.01133	7.941	6.3
6	122.0	122.0	114.0	57.0	4.46	21780	0.01193	7.948	7.1

Note 1: Parameters in elastic zone of loads calculated from relationships (1.1): ρ_1 = = 7.87 g/cm^3, a_1 = 5.99 km/sec, $\varepsilon_1 = 2.38 \times 10^{-3}$, u_1 = 14.3 m/sec (ρ_0 = 7.85 g/cm^3, $\sigma_1 = 6.7 \cdot 10^3$ bar).

Note 2: In calculating a_2 from formula (1.7) there were taken the experimental values v. In the table there are placed averaged values of experimental and calculated magnitudes of a_2.

line – the linear approximation of obtained data.

The experimentally measured density of the applied low-carbon steels was found to be equal to 7.85 g/cm^3. According to experimental data of Minshall and Campbell for dynamic load of low-carbon steels there was adopted the value of dynamic elastic limit $\sigma_1 = 6.7 \cdot 10^9$ bar [3, 4]. The same closely agrees with experimental data of Nadeyeva ($\sigma_1 = 6.44 \cdot 10^9$ bar) obtained at the Moscow State University. Values K and μ were adopted from Broberg equal to $17.1 \cdot 10^8$ and $8.36 \cdot 10^8$ g/cm^2 respectively [5].

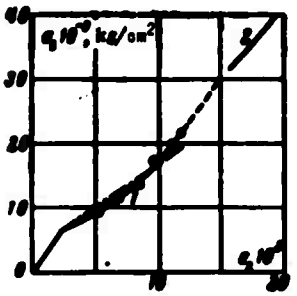

Fig. 9.

In Fig. 9 there is given a comparison of obtained data with stress – strain diagram for steel constructed by Broberg on the basis of equation of state by Pack, Evans and James [5]

$$p = A\left(\frac{\rho}{\rho_0}\right)^{\frac{1}{\beta}}\left\{\exp\beta\left[1-\left(\frac{\rho_0}{\rho}\right)^{\frac{1}{\beta}}\right]-1\right\} \qquad (3.1)$$

where $A = 6.11 \cdot 10^8$ g/cm^2, $\beta = 8.4$ for steel.

From Fig. 9 it is evident that the plotted points (each of which is a result of several experiments) with sufficient accuracy up to $\varepsilon_2 > 10^{-2}$ can be approximated by the straight line

$$\sigma_2 = 0.35 \cdot 10^9 + 140 \cdot 10^9 \varepsilon_2 \qquad (3.2)$$

where σ_2 is expressed in kg/cm^2.

The temperatures calculated by equation (1.6) where it is possible to distinguish the thermal and elastic terms in the energy [1], are small and therefore, they can be ignored. Increase of temperature was calculated by the formula

$$\Delta T = \frac{\sigma_2 \varepsilon_2}{\rho C_v} \qquad (3.3)$$

where value C_v was assumed equal to 0.11 cal/kg·deg. From Fig. 9 it is evident that during deformations $\varepsilon_2 > 14.9 \cdot 10^{-3}$ there operates the dependence which Broberg calculated and which also obeys the equation of state (3.1). It is evident also that at $\varepsilon_2 > 10^{-2}$ dependence $\sigma_2 (\varepsilon_2)$ becomes nonlinear which obviously corresponds to the beginning of formation of shock waves in the steel.

Thus, in summarizing what has been discussed, there can be made the conclusion that in region of elasto-plastic flows within limits $2.38 \cdot 10^{-3} \leq \varepsilon_2 \leq 11.93 \cdot 10^{-3}$ low-carbon steel satisfactorily obeys dependence (3.2), which is valid, however, only under assumptions made at the beginning and therefore, must be considered approximate.

Author expresses his sincere gratitude to E. I. Andriankin for his helpful remarks.

Submitted
30 July 1962

Literature

1. L. V. Al'tshuler, K. K. Krupnikov, B. N. Ledenev, V. I. Zhuchikhin and M. I. Brazhnik. Dynamic compressibility and equation of state for iron under high pressures. ZhETF, 1958, Vol. 34, No. 4, p. 874.

2. Yu. S. Stepanov. Contemporary methods of determining the equation of state of solids. Moscow State University Press, 1961.

3. Stanley Minshall. Properties of elastic and plastic waves determined by pin contactors and crystals. Journal of Applied Physics, 1955, Vol. 26, No. 4, p. 463.

4. J. D. Campbell and J. Duby. The yield behavior of mild steel in dynamic compression. Proc. of the Royal Soc., Ser. A, 1956, Vol. 236, No. 1204, p. 24.

5. K. B. Broberg. Shock waves in elastic and elasto-plastic medium. Gosgortekhizdat, 1959.

ON THE METHOD OF INVESTIGATING THE SCALAR EFFECT OF CAVITATION EROSION

I. I. Varga, B. A. Chernyavskiy and K. K. Shal'nev

(Budapest, Moscow)

In selecting materials for hydraulic machines and hydraulic designs operating under conditions of cavitation, usually there are not considered those conditions of operation of these materials, which are imposed by various forms, types and stages of cavitation. As a result the materials, used in practice, do not correspond in their own mechanical and physical properties to those destructive forces which are peculiar to the above mentioned different forms of cavitation. Attempts have been made to anticipate possible zones of erosion and intensity of destructive action by means of test of turbine models. However, here there were not considered the factors of scaling the erosion and cavitation. Below there is described an experiment of conducting experiments with erosion during cavitation of a circular cylinder taking into account basic parameters of a hydromechanical modeling: scale numbers for dimensions of models, cavitation, and speeds of the flow.

1. On setting up the investigations. a. Characteristic of the intensity of erosion. For test of materials for resistivity to

cavitational erosion there are used the following methods [1].

Methods of transient cavitation, in which tested material is subjected influence of cavitation forming in flow in wake of steep-streamlined bodies or on walls of aperatures and nipples.

Methods of wave cavitation including magnetostrictive vibration and irradiation of sonic and ultrasonic wave.

Method of rotation in which specimen of tested material revolves together with disk, on which it is braced flush with its surface, and is subjected to influence of cavitation, forming in the wake of flanges or cavities specially made on surface of disk.

The jet shock method in which revolving specimen is subject to collision with a free jet; in this case it is assumed that mechanism of destruction under influence of collision of jet and specimen is identical to mechanism of destruction under influence of caviation. This assumption appears now controversial, therefore, it was expedient to use for our work a method with direct influence of cavitation.

In the selection of a "cavitational" method it must be remembered that cases of cavitational erosion encountered in practice are explained by the effect chiefly (if we mention only one type of cavitation) – burbling forming in zone of vortices of steeply streamlined surfaces [2]. It is evident from this that the closest to the natural condition is method of transient cavitation. The destruction of material by erosion requires an expenditure of certain amount of energy; therefore, of the methods of transient cavitation one must be selected, which would make it possible most simply to associate intensity of erosion with cavitational resistance of body – with the energy of flow expended in surmounting of the resistance of body during a cavitational flow-around. As a first approximation to natural conditions there was a selected case of

cavitation of model of round profile — a round cylinder being flowed around by two-dimensional flow in the working chamber of water tunnel (Fig. 1). This model in distinction from all other models with a different profile in maximim detail was investigated depending upon parameters of flow and cavitation [3].

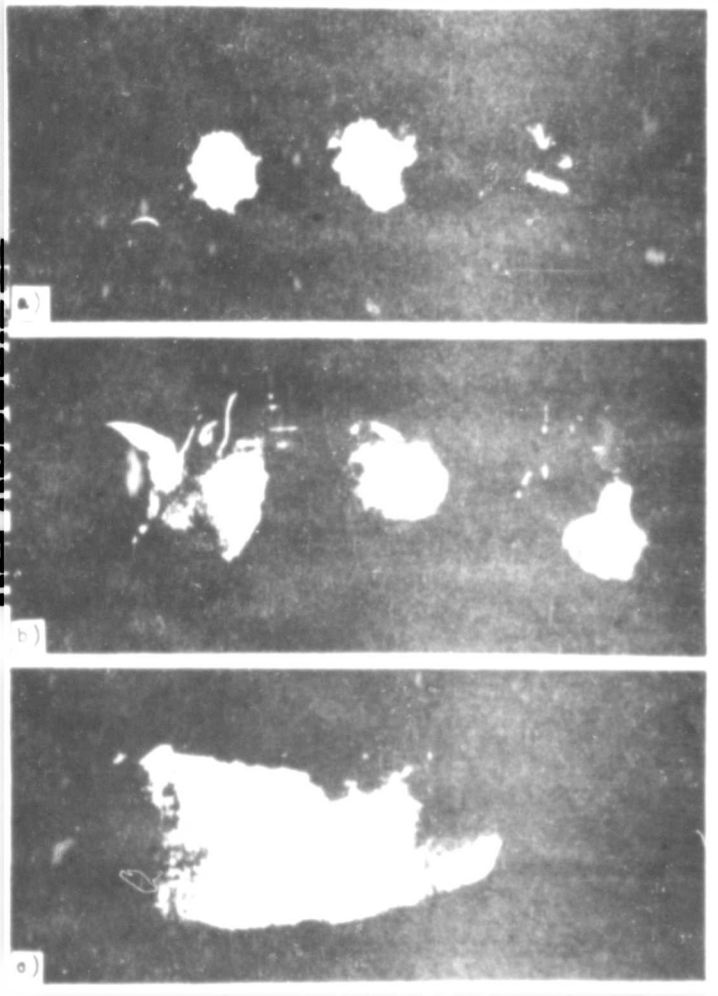

Fig. 1. Photographs of zone of cavitation in wake of round cylinder d = 48 mm on basis of experiments in cavitational pipe at Budapest University: a) stroboscopic photograph during doubled Strouhal frequency of light pulses; $\varkappa = 1.79$, $R = 6.6 \times 10^5$; b) during flash in $5 \cdot 10^{-5}$ sec, $\varkappa = 2.18$, $R = 6.35 \times \times 10^5$, c) the same $\varkappa = 1.47$, $R = 6.6 \times 10^5$.

However, existing parameters for evaluating the intensity of erosion are not associated with hydromechanical parameters of the flow [4]. Intensity of erosion was evaluated by the following magnitudes:

a) depth and area of location of the erosion [5, 6] pits;

b) loss as in weight of specimen after any period of test [7, 8];

c) loss of volume per unit of area of unit of time [1];

d) the same weight [9];

e) number of erosion pits, forming per unit of area per unit of time [10];

f) loss of volume of specimen, as related to characteristic dimension of body [11];

g) loss of intensity of radiation of isotopes applied together with paint on surface of body [12], destroyed by cavitation;

h) duration of test of specimen to certain stage or degree of destruction visually determined [13].

Of the enumerated parameters a large part of them is determined by weighing of specimens before and after the experiment. The method of isotopes was applied in field tests of turbines of radial-axial type. Rata [14] used change of ohmic resistance of specimen during erosion, but in final result associated it with a loss of volume. Gowinda Rao [15] offered dimensionless parameter of cavitational erosion in the form of a ratio of mechanical energy of destruction of certain volume of a solid body lost to erosion, to the energy of cavitational bubbles being destroyed during decrease of cavitation.

In the given case in calculating the energy of destroyed bubbles with use of Rayleigh's theory there is allowed considerable conventionality. According to theory of Rayleigh the bubble must be surrounded by a continuous fluid, whereas, in experiments of Gowinda Rao which served as basis for deriving the parameter, the zone of cavitation consisted of totality of bubbles. Furthermore, there is not taken into account the influence of surface tension of fluid on destruction of bubbles. In mechanical relationship Gowinda Rao's erosion parameter presents its own type of coefficient of the harmful effect of cavitation and depends on duration of the effect of cavitation on the specimen and also on stage of development of cavitation.

b. Energy parameter. Such parameter of erosion [4] is called volume of erosion related to unit of certain portion of cavitational resistance of model. Reciprocal of energy parameter gives a measure

of the strength of the material during destruction of its cavitational erosion in units of work required for destruction of unit of volume of material. In distinction from all previously proposed parameters the new parameter does not depend for given stage of cavitation and material either on speed of flow or on dimensions of model or on the Reynolds R and Weber W dimensionless numbers.

Reciprocal of parameter gives the true resistance of material of cavitational erosion in distinction from other parameters, by means of which there is determined only the relative resistance of erosion, i.e., in the comparison of one material with another.

In accordance with results of investigations of work of destruction of metals made by Gillemot and Sinay [16], according to whom the work of destruction does not depend on type of destructive mechanical forces of compression or extension energy parameter makes it possible to establish interrelationship between works of destruction from forces of cavitation and from mechanical forces. For metals not subject to chemical corrosion during cavitation, work of destruction of metal from cavitation, in all probability should be identical to work of destruction by mechanical forces. If, however, in destruction of metal during cavitation there act also corrosion forces, then, the work of destruction determined by means of energy parameter must add to previous new characteristic of physico-mechanical properties of metals – the resistance to cavitation.

According to the determination given previously [4], energy parameter is expressed by formula

$$\Delta V_0 = \frac{\Delta V 10^6}{36 \Delta C_z \lambda \rho_m v_m^3} \text{ м}^3 \text{кг}^{-1} \quad \left(\Delta V = \frac{\Delta G}{\gamma_0 \tau} \text{ мм}^3 \text{ час}^{-1}, \; \rho_m = \frac{v_m^2}{2g} \right) \qquad (1.1)$$
$$\Delta C_z = C_{zm} - C_z + |\Delta C_z'|$$

Here ΔV is the volume of erosion, ΔG is the loss of weight of

specimen to erosion during the time of τ hours, γ_s is the specific gravity of material of specimen, d is the diameter of cylinder, h is the height of cylinder, v_∞ is the speed of flow taking into account influence of boundaries, γ is the weight of unit volume of fluid, C_x is the resistance of cylinder in absence of cavitation, C_{xc} is the resistance of cylinder during cavitation, $\Delta C_x'$ is a certain portion of cavitational resistance obtained by the extrapolation of dependence $C_{xc} - C_x = f(W^{-1})$ up to value of Weber number $W^{-1} = 0$. The Weber number $W = \sigma/(\rho v_\infty^2 d)$, where σ is the surface tension, ρ is the density of liquid.

c. Scale effect. By means of energy parameter there is presented the possibility of determining the scale effect – to determine loss of volume of material in the field by experiments with a model. If stages of cavitation geometrically are similar and the fluids in model and in field are identical, then, after formulating for model and the field of the expressions on basis of (1.1) and equating them, we shall obtain

$$\Delta V_0 = \Delta V_m L^\alpha V^\beta \tag{1.2}$$

where L is the scale number for linear dimensions of model and cavitation and V is the scale number for speeds of the flow. Formula (1.2) gives those conditions whose observance is necessary in conducting experiments with erosion in models. At the same time, according to (1.1) the exponents are $\alpha = 3$ and $\beta = 5$, this is confirmed in certain experiments also of other authors. According to investigations by Knapp [10], with models of axially symmetric bodies and with a turbine in the field [17], in which intensity of erosion was evaluated by number of pits, the exponent $\beta = 4$ to 6. Kerr and Rosenberg [12] on basis of experiments in the field with application

of methods isotopes assume that the most probable value is $\beta = 5$. In experiments by Rata [14] within a narrow range of speeds the exponent $\beta = 4$ to 8. In experiments by Gowinda Rao [15] with cylinders $\beta = 5.3$ to 8 with rectangular blocks $\beta = 4$ to 8.

Influence of dimensions of model is characterized by the table, compiled on basis of our experiments. In it there are given magnitudes of volume of erosion for three variants of dimensions of round-cylinder model and relationships of volumes during four variants of speeds of flow. Hence one can determine experimental value of α. Average magnitudes of relationships of volumes are close to the theoretical $\alpha = 3$.

Table

v_0 m/sec^{-1}	ΔV_0 mm^{3}hr^{-1}	ΔV_m mm^{3}hr^{-1}	ΔV_m mm^{3}hr^{-1}	$\frac{\Delta V_m}{\Delta V_0}$	$\frac{\Delta V_m}{\Delta V_m}$	$\frac{\Delta V_m}{\Delta V_0}$
14	0.18	1.74	—	—	—	9.7
17	0.76	4.80	48.2	63.5	10.7	6.0
20	1.78	15.42	101	57	6.6	8.5
23	2.86	19.3	—	—	—	7.4
		Average:		60.3	8.8	7.9
		on the basis of formula (1.2):		64	8	8

Other investigations of influence of dimensions are not known. Knapp [16] negates the influence of dimensions on intensity of erosion.

The diversity of results attests first of all to how thoroughly there must be thought out the devices in the experiments, and also determination of magnitudes characterizing the intensity of the erosion.

2. Experimental devices. a. Water tunnels. Experiments with cavitational erosion were conducted in cavitational water tunnels GT-2 and GT-3 at Institute of Mechanics of Academy of Sciences of USSR jointly with Budapest University and Hungarian Academy of Sciences [19]. All enumerated tunnels have closed circulation of the water,

agitated by a centrifugal pump. Adjustment of speed is produced by electric motor drive and the pressure is regulated independently of speed. In the tunnel at Budapest University the maximum speed of flow in an active chamber of 200 × 200 mm^2 may be attained equal to 10 m/sec^{-1}. In the tunnels at the Institute of Mechanics, the speed in diverse models of active chambers may vary from 0 to 25 m/sec^{-1}. Here there have been described certain positions of the GTZ tunnel (Fig. 2), having a maximum value during experiments with erosion.

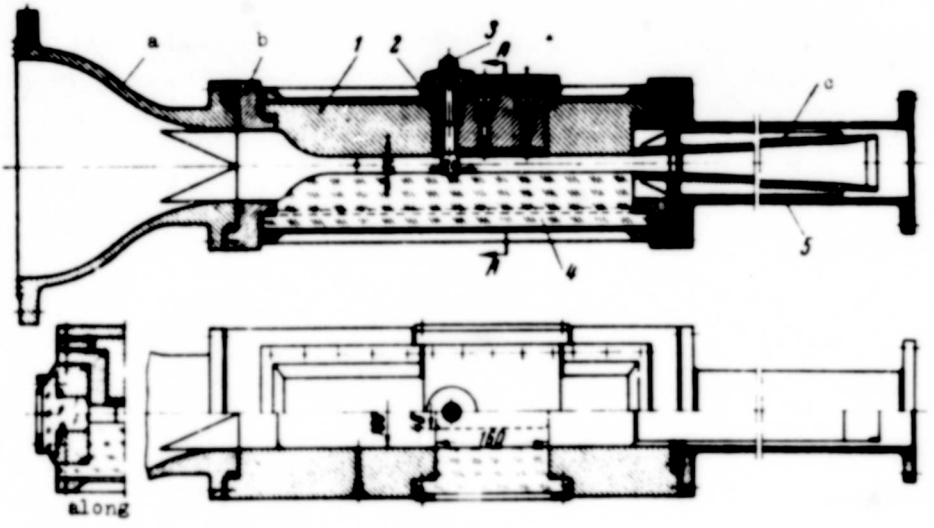

Fig. 2. Experimental device GTZ IMEKh: a) nozzle, b) active chamber, c) diffuser, 1) metallic header, 2) assembly insert with specimen, 3) model of round profile – cylinder, 4) plexiglas window, 5) tube.

b. Nozzle of tunnel. The nozzle is located between pressurized reservoir and active chamber. On the tunnel nozzle there are imposed major requirements, since it determines structure of the flow in the active chamber. The nozzle must generate a flow at exit, uniform over entire section, and reduce to a minimum longitudinal and transverse pulsations in flow proceeding to active chamber. This is attained by proper adjustment of the flow. The adjustment of flow or the ratio of areas of entry and outflow is made equal to 7.5 for nozzles according to [20]. Longitudinal profile of nozzles

consists of two curves. On the first entry sector the curve serves as a smooth interlinking of it with curve of outlet sector of nozzle. The profile of outlet sector of nozzle was outlined on the basis of Witoszinski's curve [21].

For preventing the formation of vortex zones in the interlinking between the first and second sectors of nozzle the length of nozzle is increased to $l = 3d_0$ owing to the length of the first sector. Simultaneously the nozzle, being calibrated is used as indicator of the discharge or rate of flow in the active chamber.

c. Active chamber. In three installations of water tunnels in experiments with erosion there were used the active chambers with four cross-section variants:

a) in tunnels of Institute of Mechanics with a section 6 × 12, 12 × 50 and 24 × 100 mm^2, b) in tunnel at Budapest University 48 × × 200 mm^2.

We shall give a constructive description of one variant of active chamber 24 × 100 mm^2. Body of chamber is cut out of a circular Duralumin rung 300 mm in diameter. It consists of four ribs connected one to another by flanges. Ribs form quadrilateral frame with slots, into which the headers with flanges are inserted. The frame and headers are sealed by rubber cords. Headers depending upon purpose of experiment can be made either of metal, or of transparent plexiglas. For the purpose of economy of time in the assembling of the specimen and economy of material going into manufacture of plexiglas headers, in both headers there are made assembly inserts. One of inserts the metallic serves for reinforcing the specimens and the circular profile model, the other, the plexiglas, is used for observations. In the drawing (Fig. 2) one of headers entirely transparent is shown.

The specimen is made of the composite: of the sublayer and the

specimen itself. Sublayer has a recess under the bolts by which it is clamped to assembly insert. The specimen made of rolled lead is soldered to sublayer by Wood's alloy, after which it is worked out thoroughly. The model – a cylinder, made of rolled bronze, is braced to assembly insert together with specimen. The other free end of cylinder is set into socket in opposite plexiglas insert.

d. Diffuser. The shape of the diffuser determines cavitational quality of the water tunnel, since to a greater degree than other items of tunnel is subject to cavitation. Cavitation of diffuser will entail sharp increase in resistance of tunnel and drop of productivity of pump. Proceeding from the above mentioned considerations the expansion angle of diffuser was made 7° which is somewhat smaller than that recommended for wind tunnels. For the sake of simplicity of manufacture the diffuser is made a composite: of external body – straight duct of round section – and inserts, of the diffuser proper with rectangular section, variable in its length.

3. Determination of basic magnitudes. a. Determining the speed in the measuring alignment. Usually there is determined average speed of flow ahead of model by the flow rate determined by any measuring attachment: spray nozzle, measuring flange or Venturi-type fuel gauge. For rapid preliminary calculations it is possible to use speed on axis of flow determinate by means of preliminary calibration by cylindrical cap with the piezo-aperture on cylindrical surface.

We shall designate as p_1 – the pressure at entry to nozzle, p_2 – the pressure at outlet of nozzle, p_3 – the pressure at entry to active chamber, p_4 – the pressure on wall of chamber at place of passage of axis of cylinder in its absence, p_c – the pressure at the fore singular point of cylinder located at the middle of its height

(height of chamber). The experiments determine

either $p_0 - p_4 = f(p_1 - p_3)$ or $p_0 - p_4 = f(p_1 - p_3)$

$p_0 - p_4 - (p_0 - p_3) = q = f(p_1 - p_3)$ $\quad (q = \rho v^2/2)$

and then, using graphic constructions [22]

$$\varphi = f(p_1 - p_3), \qquad \varphi = \sqrt{2q}$$

Influence of boundaries of tunnel is considered by means of equation of the flow rate. Then the speed of flow-around will be equal to $v_\infty = vb/(b - d)$, where b is the width of active chamber. In the analysis of results of experiments we shall use following magnitudes of speeds: v is the average speed ahead of model, v_∞ is the average speed taking into account influence of constraint of flow by model, v_0 is the speed along axis of flow, $v_{\infty 0}$ is speed along axis of flow taking into account the constraint. The termination of speed is a very responsible problem, because volume of erosion depends on the speed to the power $\beta \approx 5$.

b. Determination of pressure in measuring alignment. The pressure in the measuring alignment p_4 is not determined directly. During experiments there is determined the pressure p_3 at point 3, located in front of model. Then, using dependence $p_3 - p_4 = f(p_1 - p_3)$, determined preliminarily in absence of cylinder, we determine $p_4 = p_3 - [p_3 - p_4]$, taking into consideration therby drop in pressure head for resistance of sector of active chamber from point 3 to point 4.

c. Determination of coefficient of cavitation $\varkappa$. The determination of coefficient of cavitation $\varkappa$ is required in determining ΔC_x. Its value may be determined either by taking into account influence of boundaries or without taking it into account.

Therefore, in the general form

$$\varkappa = \frac{p_\infty - p_v}{\gamma q_n}$$

where p_∞ is equated to p_4, q_n is the pressure head of speed determined according to method under adoption (see 3a). The magnitude p_v is the pressure of the water vapors and γ is the weight of a unit volume of water.

d. Length of zone of cavitation. The length of zone of cavitation is determined assuming from axis of cylinder to tip of the visually evaluated stable part of zone of cavitation l_c, and is given in the conventional units $\lambda = l_c/d$, where d is the diameter of the cylinder.

e. Determination of ΔC_x. For the determination of ΔC_x we use the well known dependences $C_x(R, \varkappa)$ and $\lambda(\varkappa)$, presented in work [3, 4] (Fig. 3). The data cited in it should be supplemented both for larger Reynolds numbers, and also smaller ones, in order to obtain reliable data on magnitudes of C_x, satisfying requirements of practice. The simplest and at the same time most accurate method of determing C_x is the method according to distribution of pressure, on an average, along the height of the model's cross section. In other methods of determination C_x, for example, by weights, there must be considered the influence of slots – structural clearances between model and walls of the chamber. The presence of clearances results in the distortion of flow-around model in comparison to these which exist

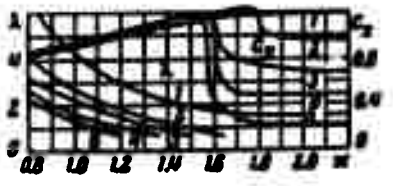

Fig. 3. Averaged curves of experimental magnitudes C_x, C_{xc} and λ depending upon $\varkappa$ and the Reynolds number R: 1) at R = $= 4 \cdot 10^4$ to $8 \cdot 10^4$, d = = 5-10 mm, 2) $11 \cdot 10^4$ to $16 \cdot 10^4$, 20 mm; 3) $18 \cdot 10^4$ to $23 \cdot 10^4$, 30 mm; 4) $25 \cdot 10^4$ to $30 \cdot 10^4$, 40 mm; 5) $30 \cdot 10^4$ to $43 \cdot 10^4$, 50 mm.

in experiments with erosion.

By means of dependences $C_x(R, \varkappa)$ and $\lambda(\varkappa)$ there is found dependence of C_x, C_{xc} and ΔC_x on the Weber number W (Fig. 4). According to (1.1), the magnitude ΔC_x will be somewhat larger than excess of cavitational resistance over resistance in the absence of cavitation, and, furthermore, $\Delta C_{xc} - \Delta C_x = f(W)$ is determined by extrapolation up to value $W = 0$. Therefore, for each experimental setup it is desirable to determine the indicated dependence independently.

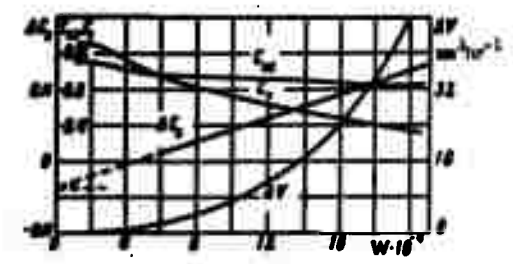

Fig. 4. Averaged experimental magnitudes C_x, C_{xc}, ΔC_{xc} and ΔV – depending on the Weber number W^{-1}.

f. Determination of ΔV. The volume of erosion is determined by loss of weight of specimen ΔG and by duration of experiment τ

$$\Delta V = \frac{\Delta G}{\gamma_s \tau} \text{ mm}^3\text{hr}^{-1}$$

where γ_s is the specific gravity of material of specimen. For avoidance of large errors it is desirable preliminarily to construct dependence $\Delta V = f(W)$, averaged on basis of some experimental data ΔV in the combined graph $\Delta C_x = f(W)$ (Fig. 4).

g. Determination of ΔG. The loss of weight of specimen to erosion is determined by weighing it before and after experiment with proper accuracy, depending on magnitude of ΔG. The admissible accuracy of weighing commensurate with accuracy of determining other magnitudes may be adequate within the limits ±1%.

h. Determination of τ. In accordance with analysis of factors of influence on accuracy of obtaining of results of experiments (see 4) duration of each experiment on erosion has been designated depending

on purposes of experiment. If experiments were performed depending only on speed of flow with a constant experimental device d = const, λ = const, then the duration of each experiment was set up with such calculation, that the ΔG values were equal. If experiments were made depending on dimensions of model, then duration of experiments was set up with such calculation, that $\Delta G_n/\Delta G_m \approx L^3$.

i. Temperature of water. Temperature of water is determined by a thermometer placed in socket of large flange of nozzle. Socket was filled with machine oil.

j. Other magnitudes. Barometric pressure was determined by a mercurial barometer. All remaining magnitudes, which were required for calculating formulas (1.1) and (1.2), once: a) weight of unit of volume of water γ; b) specific gravity of material of specimens γ_s; c) pressure of water vapors p_v; d) surface tension of water σ; e) kinematic viscosity of water ν – were determined from the tables of physical constants.

4. Factors of influence on accuracy of results. To such, one should include conditions of experiments which are ignored.

a. Influence of composition of air. According to data of experiments by Nowotny [23], with cavitational erosion obtainable by method of vibration on magnetostrictive instrument in water of varying origin, composition of air can render a significant influence on intensity of erosion. Thus, the loss to erosion in distilled water is 80% greater than in a water line. The loss decreases by 30% in tap water during its transmission through air. From what has been said it is evident that the experiments with erosion must be made with constant content of air in the water. For this purpose in the design of tunnels there is provided the insulation of free horizon of water in pressure tank from direct contact with air, there was

maintained a constancy of added fresh quantity of water during disassembling of specimens.

b. Influence of temperature. Investigations of influence of temperature of water on intensity of erosion were conducted usually at a constant pressure as a result of which to influence of temperature there was combined in addition the influence of the stage of cavitation or its structure. Our investigations [2] under conditions of transient cavitation with lead specimens during observance of constancy of stage or dimensions of zone of cavitation and speed of flow showed that within limits of variation of temperature between 10 and 26°C the decrease in intensity of erosion may vary from 0 to 7% (Fig. 5). Inasmuch as increase of temperature of water in our experiments varied within limits of 1 to 8°C, then its influence on intensity of erosion was not taken into consideration.

Fig. 5. Averaged experimental dependence of volume of erosion ΔV and area of erosion f on temperature of water T C°.

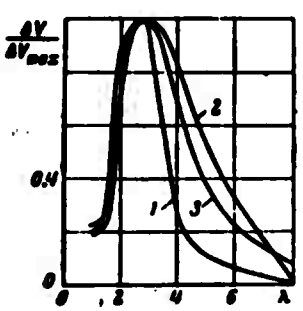

Fig. 6. Averaged experimental dependence of volume of erosion ΔV on length of zone of cavitation λ: 1) with a speed of v_0 = = 14 m/sec^{-1}, 2) with v_0 = 17 m/sec^{-1}, 3) with v_0 = 20 m/sec^{-1}.

c. Influence of stage of development of cavitation. According to our investigations [2], there is a stage of development of cavitation of round cylinder $\lambda_{max} = 3$, at which intensity of erosion is at a maximum (Fig. 6). During a deviation of λ_{max} to $\lambda = 2$ intensity of erosion diminishes by 25% and with a deviation to $\lambda = 4 - \geq 16\%$. It was assumed that the possible maximum error in determining ΔG is equal to $\delta_G = \pm 5\%$.

d. Influence of relative dimensions of the model. Under conditions of our experiments influence of relative dimensions of model l/d where l is the length of cylinder is identical to influence of height of section of active chamber a/d. According to our investigations [1], there is an optimum length of model l/d = = 1, at which intensity of erosion is maximal (Fig. 7). The intensity of erosion sharply decreases with an increase of l/d; with increase l/d by 10% intensity of erosion decreases also by 10%, and with increase l/d by 30% decreases 3 to 4 times. Inasmuch as in our experiments the variations of l/d due to inaccurate observance of given dimensions did not exceed ±1%, then this inaccuracy in assembling the model might result in an error of determining ΔV within limits of ±1%.

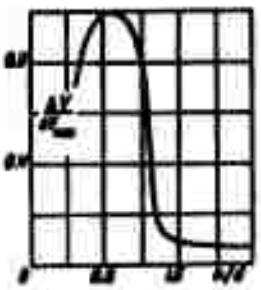

Fig. 7. Averaged experimental dependence of volume of erosion ΔV on the relative dimensions of model l/d or a/d.

e. Influence of duration of experiment. Dependence $\Delta V(\tau)$ for metals is determined, on the one hand, by the plastic properties of material under test and on the other – character of the forces, causing the erosion. During the initial period of destruction there is noted for plastic metals the so-called incubation period during which there occurs deformation of surface layers (cold hardening) without the loss of weight (Fig. 8). For a lead specimen with the setting in of brittel fracture the loss to erosion $\Delta G/\tau$ increases with passage of time linearly to certain

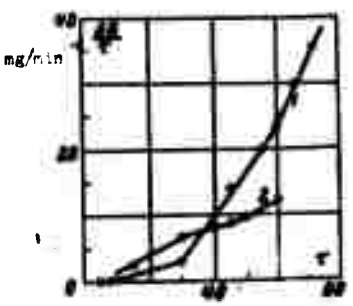

Fig. 8. Experimental dependence of volume of erosion ΔV on duration of test of specimen τ for two specimens, tested in active chambers 25 × × 100 mm^2, 6 × 25 mm^2.

magnitude characterized by the formation of explicitly expressed foci of erosion – pits of round form. In all probability, with formation of these pits mechanical reaction of the cavitation is intensified by cumulative effect of streams with the decrease of cavitation. In order to obtain comparable results of experiments there should be selected such a duration of experiments at which the fracture would be determined chiefly by forces of cavitation.

f. Effect of treating surface of specimen. Such an effect was revealed in comparing ΔV_0 of the specimens whose surface was cleaned with linens with different coarseness of abrasive [4]. For comparability of obtained results it is necessary exactly to hold technological rules of preparing the specimens must be precisely adhered to.

g. Influence of number of experiments. As was noted above, the exponent of scale number of speeds is evaluated by various authors within the limits $\beta = 4$ to 8. Using detailed data of Gowinda Rao's experiments, presented in tables of his article [18], there was made a graphic treatment of materials on cylinders and on blocks. It was ascertained that both for a cylinder, and also for blocks the exponent β in formula (1.2) may be taken $\beta = 5$, if we ignore the extreme magnitudes of ΔV at low speeds. Certain experiments were set up with three variants of speed which evidently is inadequate because the dependence $\Delta V(v)$ is determined graphically. In experiments by Rata wide variations $\beta = 4$ to 8 may also be explained by random errors, since the speeds were close, $v \approx 30$ to 40 m/sec^{-1}.

h. Possible maximum error in determining ΔV_0 and ΔV_n. According to rules of an approximate calculation of the errors [24], there may be compiled following expressions for the possible maximum error in determining ΔV_0:

$$\delta_0 = \delta_G + \delta_\gamma + \delta_{G_s} + \delta_h + \delta_t + 3\delta_v + \delta_\varepsilon + \delta_\gamma$$

and for ΔV_n

$$\delta_n = \delta_m + 2\delta_L + 3\delta_V = \delta_m + 3.2\delta_l + 5.2\delta_v$$

In given formulas δ designates the maximum possible errors of magnitudes being determined and indicated by subscripts. When determining δ_G one should proceed not so much from the accuracy of weighing the samples, as from the basic fact of the constancy of λ, l/d, and the other factors mentioned above were observed as constants. On the basis of considerations it is possible to calculate

$$\delta_0 = 0.05 + 0.01 + 0.05 + 0.005 + 0.005 + 3\cdot 0.02 + 0 + 0 = 0.18 \approx \pm 18\%$$

and

$$\delta_n = 0.06 + 3\cdot 2\cdot 0.005 + 5\cdot 2\cdot 0.02 = 0.29 \approx \pm 30\%$$

Such comparatively large magnitudes of possible errors explains the scattering of experimental magnitudes of ΔV_0 in the graph $\Delta V_0(W)$ [4]. The error may be especially large in determining the intensity of erosion in the field in experiments with models.

5. Conclusions. In investigations of the scale effect of cavitational erosion special attention must be given to: a) to the accuracy of determining speed of flow of cavitational resistance, loss to erosion – erosion spaces; b) to observance of identity of stages of cavitation and relative dimensions of the models; c) to the proper designation of duration of experiments. In order to avoid a large magnitude of error it is necessary to setup the experiments within a wide range of speeds and for a large number of their variants.

Submitted
25 February 1963

Literature

1. K. K. Shal'nev. Hydromechanical aspects of cavitational erosion. News. Academy of Sciences of the USSR. Division of Technical Sciences, 1958, No. 1.

2. K. K. Shal'nev. Conditions for the intensity of cavitational erosion. News. Academy of Sciences of the USSR. Division of Technical Sciences, 1956, No. 1.

3. V. A. Konstantinov. Influence of Reynolds number on a detached flow. News. Academy of Sciences of the USSR. Division of Technical Sciences, 1946, No. 10.

4. K. K. Shal'nev. Energy parameter and scale effect of cavitational erosion. News. Academy of Science of the USSR. Division of Technical Sciences, 1961, No. 5.

5. M. S. Plesset and A. T. Ellis. On the mechanism of cavitation damage. Trans. ASME, 1955, Vol. 77, No. 7.

6. Ch. Parsons and St. Cook. Investigations into the causes of corrosion or erosion of propellers. Engineering, 1919, Vol. 107.

7. S. L. Kerr. Determination of the relative resistance to cavitation erosion by the vibratory method. Trans. ASME, 1937, Vol. 59, No. 5.

8. J. M. Mousson. Pitting resistance of metals under cavitation. Trans. ASME, 1937, Vol. 59, No. 5.

9. V. V. Gavranek. Study of cavitational erosion of metallic substances on a magnetostrictive vibrator. Khar'kov Polytechnic Inst. im. V. I. Lenin, 1957, Vol. IX, 1.

10. R. T. Knapp. Recent investigation of the mechanics of cavitation damage. Trans. ASME, 1955, Vol. 77, No. 7.

11. J. Noskievic. Beitrag zur Ähnlichkeit bei Kavitation. Bergakademie, 1956, Bd. 8, No. 2.

12. S. K. Kerr and K. Rosenberg. An index of cavitation erosion by means of radioisotopes. Trans. ASME, 1958, Vol. 80, No. 6.

13. H. Schröter. Korrosion durch kavitation in einem diffusor. Z. veraines dtsch. Ingr., 1932, Bd. 76, No. 21.

14. J. M. Rata. Erosion de cavitation. Meaure de l'erosion par jauges resistantes. Symposium Recherche sur les Turbines Hydrauliques de Nice. 16-20 September 1960.

15. P. S. Gowinda Rao and A. Thiruvengadam. Production of cavitation damage. J. Hydraul. Div. Proc. Amer. Soc. Civil Engrs, 1961, Vol. 87, No. Hy 5.

16. L. Gillemot and F. Sinay. Die Brucharbeit als Werkstoffkenngrösse. Acta techn. Acad. Scient. Hung., 1958, Vol. XXII,

Fasc. 1-2.

17. R. T. Knapp. Accelerated field tests of cavitation intensity. Trans. ASME, 1958, Vol. 80, No. 1.

18. W. S. Gowinda Rao. Cavitation – its inception and damage. Irrigat. and Power, 1961, Vol. 18, No. 1.

19. Fáy Csaba. A Vizgépek Transzekenek Kavitációs Csatornája Magyar tud. akad. Müsz. tud. oszt. közl. 1958, Vol. 22, Kötet 1-3 számából.

20. L. Prandtl. Herstellung einwandfreier Lufströme. Handb. Exptl phys., 1932, Bd. 4, Teil 2.

21. E. Witoszinski. Über Strahlerweiterung and Strahlablenkung. Vorträge aus dem Gebiete der Hydro-und aerodynamik. Berlin, 1924.

22. K. K. Shal'nev. Cavitation of irregularities of a surface of a triangular profile. PMTF, 1962, No. 6.

23. H. Nowotny. Werkstoffzerstörung durch Kavitation. Berlin, VDI – Verlag, 1942.

24. M. P. Frank. Elementary approximate calculations. Moscow, 1932.

GENERALIZATION OF CERTAIN EXPERIMENTS ON CRISIS OF BOILING OF LIQUID DURING FORCED MOTION ON BASIS OF THERMODYNAMIC SIMILARITY

L. Ye. Mikhaylov

(Moscow)

There are presented results of processing experimental data on crisis of boiling under conditions of forced motion of three alcohols and water by means of an approximate thermodynamic similarity. There is proposed a calculation formula.

Empirical functions for crisis of boiling during a forced motion of liquid have the form

$$q_* = f(p, w, \Delta t)$$

where q_* is the critical density of the heat flux, p is the pressure, w is the speed of liquid, $\Delta t = T - T_s$ is the underheating up to the saturation temperature.

On the basis of data in the work of I. I. Novikov [1] there may be proposed the function universal for similar substances

$$\frac{q_*}{c_{v_0}} = f\left(\frac{p}{p_*}, \frac{w}{c_0}, \frac{\Delta t}{T_*}, \frac{c_{v_0}}{R}\right) \quad \left(c_0 = \sqrt{\frac{gRT_0}{p}}\right)$$

where P_* is the critical pressure, c_{v_0} is the molar heat capacity of substance during an infinite expansion, R is a gas constant, c_0 is

*a.a = atm (Abs) [Tr. Ed. Note]

the speed of sound in substance as found in an ideal gas state, at the critical temperature T_*.

In practice there is used a simpler function in which the latter two parameters are combined in the form of a product

$$\frac{\Delta i}{r}\frac{c_{p_0}}{\mu} = \frac{\Delta i}{r}\frac{c_{p_0}}{\mu}$$

where r is the latent heat of vaporization.

Magnitude c_{v_0}/μ in this expression may be replaced by heat capacity $c_p = c_p(t)$ [2], and be written out

$$\frac{\Delta i}{r}\frac{c_{p_0}}{\mu} \to \frac{\Delta i_2}{r} = \frac{\Delta i}{r}$$

Thus, the generalized function between the given magnitudes essential for the crisis of boiling during forced motion acquires the form

$$\frac{q_0}{c_{p_0}\rho_0} = f\left(\frac{p}{p_0}, \frac{w}{w_0}, \frac{\Delta i}{r}\right)$$

A number of works has been devoted to an investigation of the crisis of boiling during forced motion of water (for example, [3-10]). For other liquids few experimental data have been published (see, for example, [11]). Data for a generalization on the basis of thermodynamic similarity have to be obtained in an experiment with different, chiefly organic liquids.

The experimental installation for investigating the boiling of organic liquids (Fig. 1) is a closed circulation contour through which liquid is pumped by a glandless rotary pump with shielded drive 1. The flow rate of liquid in contour is measured by means of an assembly double diaphragms 2 by the instrument EPID-02. Pressure in the contour is created by means of boiler 3 with an automatic control. The contour includes an active sector 4, auxiliary

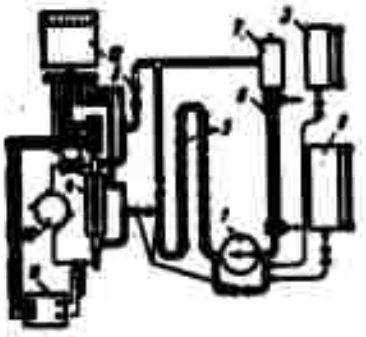

Fig. 1. Diagram of experimental installation.

heaters 5, refrigerator 6 and gas separator 7. The flow rate of liquid through active sector and regrigerator is regulated by means of valves 8. The contour is filled with liquid from reservoir 9 The active sector is supplied with direct current of low voltage from generator 10 type AND 1500/750. The registration of the advent of crisis is realized automatically by an electronic instrument 11, which disconnects the power supply of the active sector.

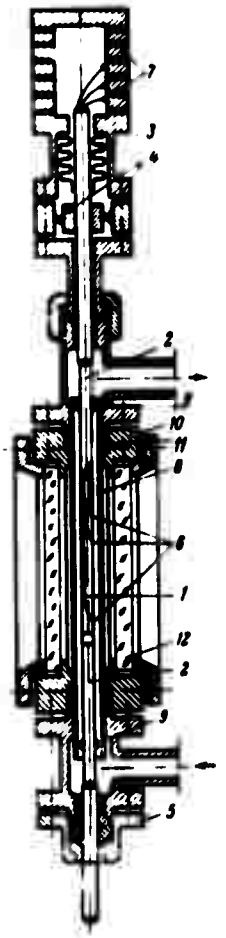

Fig. 2. Active sector.

Automatically, by a potentiometer 12 type EPP-09 there are registered also basic magnitudes being measured – current and voltage drop in fuel element, and also temperature of liquid at entry and outlet of active sector.

The active sector (Fig. 2) makes it possible to conduct experiment with an external circumflow by liquid of fuel element 1. This element is made of a thin-walled rust-resistant or nickel tube. It is heated by direct current which is delivered to it through copper bus lines 2. The upper bus is tightened by means of a bellows 3, which compensates thermal expansions of fuel element, and the electrical contact is realized by means of the flexible copper conductors 4. The upper bus is found under a zero potential and is combined with chassis of installation. The lower

bus is led through a teflon insulating stuffing box 5.

The ring slot through which the liquid flows is made up of fuel element and glass tube 8. The displacement of fuel element from central position is prevented by the registers 9. The glass tube is fastened to chassis of active sector 10 by means of stuffing boxes 11 of special rubber. The chassis has window with 100 x 10 mm flat glass 12 which makes it possible to conduct the observation of process.

Fuel element is unloaded within the gas. The glass tube is unloaded outside the liquid.

Within the fuel element there are welded potential leads 6 from Nichrome 0.2 mm in diameter, insulated by glass stocking. They are led out by a drilling in upper bus and are soldered to the insulated contact rings 7. Potential leads serve for registering the advent of crisis. The recorder of crisis reacts to change in drag of tube at place of formation of crisis and does not sense change in drag during a uniform heating of fuel element. This is attained by connecting two sectors of fuel element as two arms of the bridge (Fig. 3). An initial moment the bridge is balanced by means of potentiometer R_1 and signal, taken from its diagonal, will be equal to zero. During a change of resistance of one of sectors of fuel element the balancing of bridge is disturbed and in its diagonal there appears signal which is amplified by amplifier UE-109 (used in instrument EPP-09) and it governs the electronic relay standing at outlet of automatic machine. Relay disconnects the excitation of direct-current machines supplying the active sector. The duration of

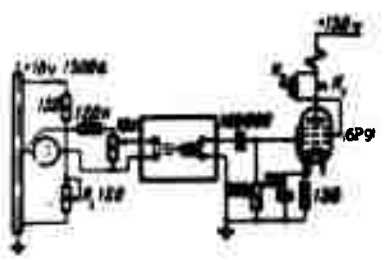

Fig. 3. [Boiling] Crisis Recorder.

disconnecting process was measured by means of a loop oscillograph and was found to be equal to 0.02 to 0.03 sec. The experiment of the operation in the installation showed that the use of an automatic recorder of the crisis is very useful. In a single fuel element is makes it possible to obtain up to fifty points.

Experiments always were begun with the adjustment of sensitivity of recorders of the crisis. The sensitivity was considered fixed correctly, if at moment of advent of crisis in upper part of fuel element there was observed dim brief flash, or in the boiling layer of liquid on surface of element there was formed distinctly visible zone of film boiling. Especially well the film boiling was observed on nickel fuel elements in a frontal illumination. Furthermore, during a large underheating the boiling is accompanied by sound phenomena. With increase in the load the tube will issue sharp sound, which rapidly abates only in direct proximity of the crisis.

In the installation a total of three series of experiments was made, in water, ethyl alcohol and butyl alcohol.

Experiments in water were conducted for calibrating the installation. There was obtained a total of about one hundred experimental points, in which a portion are prior to work on alcohol, and a portion – after work on alcohol.

The agreement of the obtained results with results obtained by L. D. Dodonov [4] and P. I. Povarnin [8] is satisfactory.

In experiments on ethyl alcohol there was encompassed a speed range of 1.5 to 12 m/sec at pressures of 5, 10, 20, 30, 40 and 50 a.a. The experiments were made in fuel elements of stainless steel with the width of radial clearance δ = 2.6 mm and length of heated section $l_0/2\delta$ = 15. The total length of channel $l/2\delta$ = 44. The entire series contains about 700 experimental points (Fig. 4).

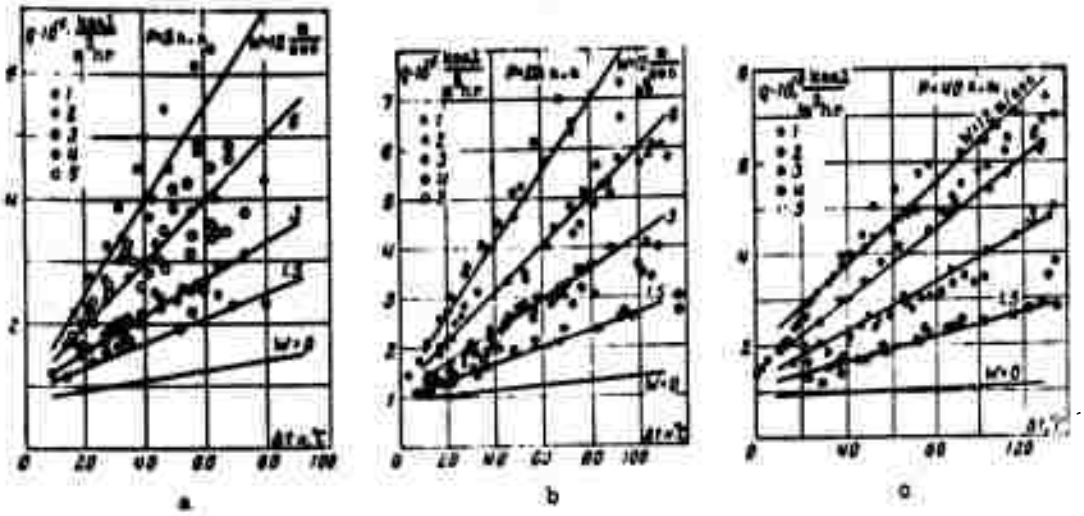

Fig. 4. Graphs of second series of experiments: 1) w = 12 m/sec, 2) w = 6 m/sec, 3) w = 3 m/sec, 4) w = 1.5 m/sec, 5) points, taken on a clean nonworked-in sector.

In experiments there was ascertained influence of working in of surface of fuel elements. By virtue of fact that the alcohol in the installation was very pure (distillate in contact with stainless steel, copper and teflon), an incrustation of deposits on fuel element was not observed up to a pressure of 20 a.a.

At higher pressures on fuel element there was deposited an incrustation of reddish brown color which in time darkened. It was found at the same time that points obtained in the pure brilliant sector lie 20 to 30% lower than points obtained in active sector covered by an incrustation. In the graphs of Fig. 4 points obtained on pure fuel elements are not colored.

There was made a comparison of the obtained results with experimental data of P. I. Povarnin [17] on ethyl alcohol.

At pressures of 5, 10 and 20 a.a I. P. Povarnin's points lie within the limits of the range of our experiments. There deviate downwards only the points at p = 20 a.a, w = 10 m/sec. At 40 a.a P. I. Povarnin and S. T. Semenov's points lie much lower than ours

and they have a wide range. As P. I. Povarnin suggests, this occurs from the effect of incrustation of products of decomposition of alcohol on walls of fuel element. The crisis in experiments of work [17] was registered on basis of bend in the course of recording the wall temperature of fuel element. But such bend will take place not only at the advent of the crisis, but also with an abrupt beginning of incrustation of deposits, i.e., prior to advent of crisis. Furthermore, in experiments of work [17] there was observed a spalling of incrustations from wall with the formation of crisis at place of chipping. This results in an "underswing" of points downwards.

Experiments in butyl alcohol were conducted in the same speed range and pressures as experiments of preceding series. The qualitative picture obtained as a result of these experiments, is analogous to picture, obtained in ethyl alcohol. Therefore, experimental points and graphs are not presented in the article.

It must be mentioned that influence of working in of surface of fuel element on results being obtained could not be recorded. Obviously, this is connected with small thermal stability of butyl alcohol.

It is obvious that for a generalization there must be selected a group of similar liquids. The dimensionless number may serve as critical coefficient [12]

$$K_0 = \frac{\sigma \rho_0 V_0^2}{\pi T_0}$$

A more graphic idea as to degree of similarity of liquids can be given by a comparison of their physical parameters in relative coordinates [13, 14].

It is obvious also that absolute properties of liquids must differ possibly more. As a criterion of distinction of liquids there

may be considered complexes which are combined from critical parameters and universal constants and have a dimensionality of magnitudes essential for the process under study [1, 2].

For generalization there were selected results of experiments, made in water and methyl, ethyl and butyl alcohols. Critical coefficients and dimensional complexes for them are given in the table ($(c_p/r)0{\cdot}01$ signifies that c_p and r were selected at $p/p_* = 0.01$).

Name	p	K_*	q_*	$c_0 p_*$	$(q_p/r)_{0.01}$
Water	18	4.15	340	10.4	2
Methyl alcohol	32	4.50	225	2.5	2.2
Ethyl alcohol	46	4.07	208	1.07	2.37
Butyl alcohol	74	3.8	250	1.085	3.9

From a review of the table there can be made the following conclusions.

1. Selected substances have close values of the critical coefficients. (Deviations from mean value ±12%.)

2. Measured complexes continuously depend on the molecular weight μ.

3. The difference between measured complexes for selected substances is significant. In particular, values of magnitude $c_0 p_*$, which is scale of q_*, differ for water and butyl alcohol by almost ten times.

Such large scale difference is a favorable fact since it will make it possible to establish with complete proof the presence or absence of similarity of phenomena in the crisis of boiling in different liquids.

Furthermore, as a result of a comparison of physical parameters of selected liquids in the given coordinates it happens that maximum

difference is observed for latent heat of vaporization r (up to 15%), and difference of remaining parameters – density, surface tension, temperature of saturation – does not exceed 5 to 10%.

For the generalization there were used following experimental data.

In water – the data of A. P. Ornatskiy [15, 16], P. I. Povarnin and S. T. Semenov [8].

In methyl alcohol – data of P. I. Povarnin and S. T. Semenov.

In ethyl alcohol – data of P. I. Povarnin, S. T. Semenov and the author's data.

In butyl alcohol – the author's data.

The processing of experimental data was conducted in two stages. First, experimental data were recalculated in system of given magnitudes

$$\frac{q_0}{c_0 p_0} = f\left(\frac{p}{p_*}, \frac{w}{c_0}, \frac{\Delta i}{r}\right)$$

and were plotted on graphs, analogous to Fig. 5.

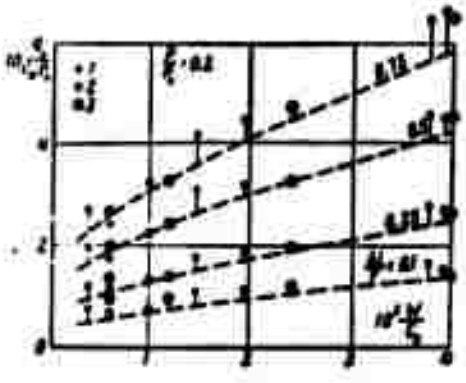

Fig. 5. 1) water, 2) ethyl alcohol, 3) butyl alcohol.

For obtained curves there was selected the formula

$$\frac{q_0}{c_0 p_0} = 3 \cdot 10^{-4}\left(1 - \frac{p}{p_*}\right)\left(1 + 6.7\frac{\Delta i}{r}\right) \times \left[1 - 0.8\left(10^{-\frac{w}{c_0}}\right)^{0.8}\right] \qquad (1)$$

This formula approximates curves with accuracy up to ±5% for values $0.1 < p/p_* < 0.6$, $0.1 < \Delta i/r < 1$, $0.5 < w/c_0 < 5$. The character of dependence for values $p/p_* < 0.1$ and $p/p_* > 0.6$ will differ from formula being given, where chiefly there will vary value of coefficient at $(w/c_0)^{0.8}$. This coefficient will increase by

few times and will depend greatly on p/p_*.

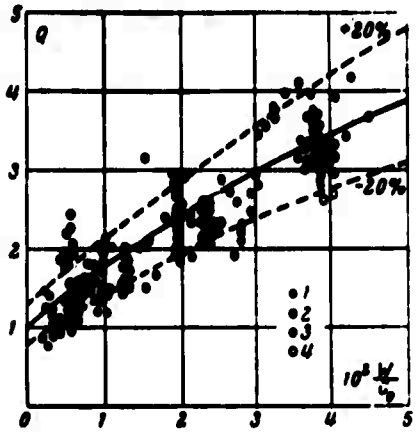

Fig. 6. 1) water, data of [8], 2) methyl alcohol, 3) ethyl alcohol, 4) butyl alcohol.

In Fig. 6 there is shown, how they are fitted on curve constructed on basis of formula (1), and experimental points are used for the generalization.

Here, along the axis of ordinates there is marked off the magnitude

$$Q = q_0 \left[3 \cdot 10^{-4} c_0 p_0 \left(1 - \frac{p}{p_0}\right)\left(1 + 0.7 \frac{\Delta \rho}{\rho}\right)\right]^{-1}$$

In Fig. 6 there are plotted the following points: in water — P. I. Povarnin and S. T. Semenov [8], in methyl alcohol — data of P. I. Povarnin and S. T. Semenov, in ethyl alcohol — the author's data, obtained on clean fuel elements, in butyl alcohol — the author's data. The scattering of experimental points in Fig. 6 does not exceed in most cases ±30%.

In Fig. 6 there are not plotted A. P. Ornatskiy's [15, 16] experimental points in water and in ethyl alcohol — the author's data obtained on the contaminated fuel elements. The dispersion of points here is the same, but all the points are higher than the formula by 20 to 25%.

This deviation can be explained obviously by the difference of surface properties in the experiments, in particular the difference in magnitude of the surface tension.

We note that an analysis of phenomenon of crisis of boiling from thermodynamic assumptions makes it possible to associate peculiarities of process with such characteristics of substances, as critical parameters and the molecular weight and to exclude from consideration many other physical paramters, such as viscosity, surface tension et cetera.

Submitted
24 October 1962

Literature

1. I. I. Novikov. Condition of similarity of processes of heat transfer with variable properties of a liquid. Application of theory of thermodynamic similarity to phenomenon of crisis during boiling of a liquid. State Power Engineering Publishing House. Collection. "Questions of heat emission and hydraulics of a two-phase media," 1961.

2. M. P. Vukalovich and I. I. Novikov. Technical thermodynamics. State Power Engineering Publishing House, 1952.

3. V. S. Chirkin and V. P. Yukin. Crisis of heat removal in the flow of some nonboiling water for a radial clearance. Journal of Technical Physics, 1956, No. 7.

4. I. T. Alad'yev, L. D. Dodonov, and V. S. Udalov. Critical thermal loads during flow of water in tubes. Atomic energy, 1959, Vol. 6, No. 1.

5. B. A. Zenkevich and V. I. Subbotin. Critical thermal loads during forced motion of water not yet heated to boiling. Atomic energy, 1957, Vol. 4, No. 8.

6. B. A. Zenkevich. Critical thermal loads during forced motion of water in pipes with the core, not het heated up to saturation temperature in interval of pressures of 100 to 210 atm. Atomic energy, 1958, Vol. 4, No. 1.

7. B. A. Zenkevich, V. I. Subbotin and M. F. Troyanov. Critical thermal loads during a longitudinal circumflow of beams of pipes by water, not yet heated up to saturation temperature. Atomic energy, 1958, Vol. 4, No. 4.

8. P. I. Povarnin and S. T. Semenov. Investigation of crisis of boiling during flow of underheated water in pipes of small diameters at high pressures. Heat-power Engineering, 1959, No. 4.

9. V. Ye. Doroshchuk and F. P. Frid. Investigation of critical thermal loads from wall for water and humid water vapor at a pressure of 170 a.a. Collection edited by N. A. Dollezhal. Atomizdat, 1958.

10. Z. L. Miropol'skiy and M. Ye. Shitsman. Investigation of temperature conditions of a vertical steam generating pipe at high pressures. Collection edited by N. A. Dollezhal. Atomizdat, 1958.

11. L. S. Sterman and N. G. Styushin. Investigation of dependence of critical heat flux on the circulation. Journal of Technical Physics, 1952, Vol. 22, No. 3.

12. I. I. Novikov. Conditions of thermodynamic similarity of real substances. Certain questions in engineering physics. Collection of transactions of MIFI. M., 1957.

13. V. M. Borishanskiy. Calculation of influence of pressure on heat emission and critical loads during boiling on the basis of theory of thermodynamic similarity. State Power Engineering Publishing House. Collection "Questions of heat emission and hydraulics of two-phase media," 1961.

14. P. I. Povarnin. Calculation of certain physical parameters of heat-transfer agent by method of thermodynamic similarity. Heat-power Engineering, 1962, No. 6.

15. A. P. Ornatskiy. Influence of length and diameter of pipe on magnitude of critical heat flux during forced motion of water not yet heated up to saturation temperature. Heat-power Engineering, 1960, No. 6.

16. A. P. Ornatskiy and A. M. Kichigin. Critical thermal loads during boiling of underheated water in pipes of small diameter in region of high pressures. Heat-power Engineering, 1962, No. 6.

17. P. I. Povarnin. Investigation of crisis of boiling during flow of 96% ethyl alcohol under conditions of underheating. Heat-power Engineering, 1962, No. 12.

INVESTIGATION OF MECHANISM OF BOILING DURING LARGE HEAT FLOWS BY MEANS OF PHOTOGRAPHY

N. N. Mamontova

(Novosibirsk)

The first investigations of mechanism of boiling by means of photography were made 25 to 30 years ago [1, 2] for heat a flux with small densities (from the contemporary point of view).

In one of the recent works by Westwater [3] by means of high-speed photography at atmospheric pressure there was investigated bubbling of methanol in case of a heat flux with the intensity $q[kcal/m^2hr]$, approximately up to the critical value $q = q_*$, at which there occurs a replacement of a nucleate regime of boiling by a film regime. It was revealed that in this case magnitude of the break-away diameter of vapor bubble D_0 [mm], the frequency of break-away of vapor bubbles $u[sec^{-1}]$ and rate of increase of vapor bubbles D_0u[mm/sec] depend on density of the heat flux.

A detailed investigation of mechanism of the boiling process in a moving underheated fluid was made by G. G. Treshchev [4]. There were obtained distribution curves of magnitudes of maximum diameters D, periods of bubble formation τ and number of centers of vaporization with a change of regime of boiling. However, to apply these, data

for boiling of completely saturated liquid it appears to be impossible.

Below there are discussed the results of first stage of investigation of mechanism of boiling of saturated liquid with free convection.

The experiments were made in experimental installation, whose fundamental diagram and description are given in [5].

The working sector was made of foil of stainless steel with a thickness of 0.1 mm; width of working sector 2 mm, length about 40 mm. Lower side of working sector was heat-insulated by textolite which excluded possibility of formation of bubbles on it. For the packing between textolite and lower side of working sector there was used a thermoresistant rubber. Rubber and textolite were clamped to lower side of foil by means of special screws. Upper exothermal surface of sector was polished with a paste from the State Optical Institute.

The heating was realized by means of transmission of an electrical current through the foil. Filming of boiling process was made in a transmitting light on a scale M 1:2. Inspection windows were made of quartz. Speeds of photographings were between 1000 and 4000 frames/sec. There were used high-speed cameras: 16 mm – TsL-16 and 35 mm – Pentatset-35.

For determining the value of break away diameter D_0 the appropriate frames of filming were examined in a measuring microscope and there was made a measurement of the bubble diameter. The frequency of the breaking away u was determined by directly establishing the interval of time between breaking away of one bubble and breaking away of the next at the same place.

There was studied the boiling process in water and ethyl alcohol. With the nucleate boiling of water at atmospheric pressure with an increase of density of heat flux approximately to q = 100,000 kcal/m^{2}hr ($\sim$0.1 q_*) a gradual increase in number of centers of vaporization

occurs as long as the entire surface will not be covered by bubbles. With further increase of heat flux there begins the coalescence of neighboring bubbles, expanding in individual centers of vaporization. A similar influence of heat flows on picture of nucleate boiling of water is observed during all investigated pressures from 1 to 52 kg/cm^2.

In the region close to critical heat flux there is observed an intense and random motion of vapor and liquid near heating surface. The characteristic photography of the transient regime during boiling of ethyl alcohol is shown in Fig. 1. The heating surface is separated from liquid by unstable film of vapor; the vapor bubbles form as a result of the rupture of the film in scattered places.

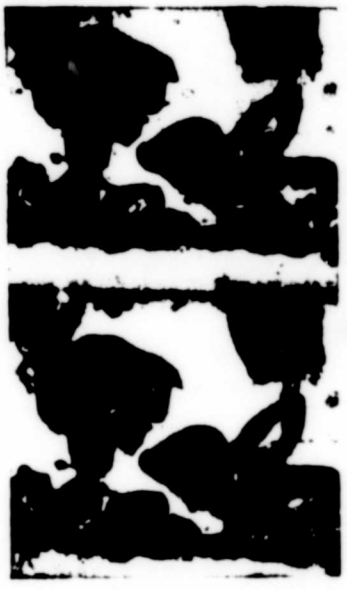

Fig. 1. Transient regime during boiling of ethyl alcohol. Thermal load is close to the critical, p = = 1 atm.

Fig. 2. Film boiling of ethyl alcohol: q ≈ ≈ 600,000 $kcal/m^2hr$, p = = 1 atm.

With a further increase of heat flux there developes a stable film

boiling. In Fig. 2 there is presented a photograph of the film boiling of ethyl alcohol: there is evident the wave character of the motion of the vaopr film. In each wave length there are formed two series of vapor bubbles, which break away with a specific frequency.

The quantitative study was made for the purpose of determining the statistical magnitudes of the break-away diameters of vapor bubbles D_0, their frequency of breaking away from surface u and rate of increment of D_0u during nucleate boiling of water and film boiling of ethyl alcohol. For determining the avarage statistical magnitudes of D_0 and u there were constructed distribution curves for eacn regime. Experimental distribution curves of diameter D_0 are close to a symmetric curve, and the frequency distribution curves of u differ from normal distribution curve – mean value of the frequency of u differs from the most probable value by approximately 20%.

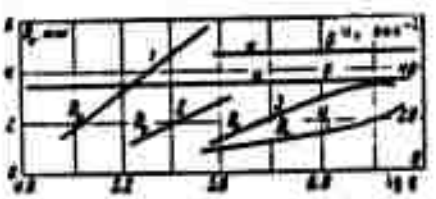

Fig. 3. Curves 1, 2, 3, 4, 5 correspond to pressures p = 1, 11, 20, 52, 52 kg/cm^2; curve at p = 1-20 kg/cm^2.

In Fig. 3 there is given influence of heat flux and pressure on the average-statistical magnitudes of D_0 and u during nucleate boiling of water; an increment in the heat flux results in an increase of break away diameters D_0 during all investigated pressures: frequency of breaking away u does not vary either from the heat flux or from pressure and is approximately equal to 35 sec^{-1} up to 20 kg/cm^2. At p = 52 kg/cm^2 frequency increased to 45 sec^{-1}.

In Fig. 4 there are presented results of processing of photos with the film boiling of ethyl alcohol with a change in pressure from 1 to 54 kg/cm^2 ($\sim$0.75 P_*) with densities of the heat flux $q \approx 1.2q_*$.

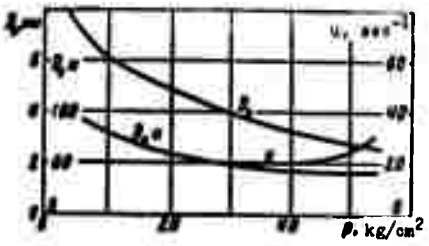

Fig. 4. Dependence of average-statistical values of D_0, u and D_0u on pressure during a film boiling of ethyl alcohol.

As can be seen from the graph, diameter D_0 decreases with a rise in pressure, the frequency of u does not change and remains approximately equal to 20 sec^{-1} up to a pressure of p = 42 kg/cm^2, then it increases somewhat; magnitude D_0u correspondingly decreases.

From obtained data it becomes evident that character of motion of vapor phase during nucleate boiling of water heated up to saturation temperature, with large heat fluxes greatly differes from that which was observed during heat fluxes smaller than $\sim 0.1q_*$. There occurs a coalescence and formation of huge bubbles, "vapor clubs."

During regimes close to the critical conditions of boiling of liquids there is revealed the complex and unstable hydrodynamics in two-phase boundary layer. Much more orderly is the hydrodynamics in region of stable film boiling.

With a rise in pressure there decreases the rate in increment of vapor bubbles of D_0u, i.e., qualitatively there takes place the same dependence as during a low heat flux. However, in this case the frequency of formation of bubbles at $q < q_*$ either does not depend on the pressure or it depends so slightly and the break-away diameter of the bubbles varies greatly.

The frequency of formation and break-away diameters of vapor bubbles from surface of the vapor film ($q > q_*$) also depend on the pressure and density of the heat flux.

Submitted
25 December 1962

Literature

1. W. Fritz and W. Ende. Verdampfungsvorgang nach Kinematographischen Aufnahmen und Dampfblasen. Phys. Z., 1936, No. 11.

2. L. M. Zysina-Molozhen and S. S. Kutateladze. On questions about influence of pressure on mechanism of vaporization in a boiling liquid. Journal of Technical Physics, 1950, Vol. 20, No. 1.

3. A. S. Perkins and J. W. Westwater. Measurements of bubbles formed in boiling methanol. A. I. Ch. E. Journal, 1956, Vol. 2, No. 4.

4. G. G. Treshchev. Experimental investigation of mechanism of the surface boiling process. Heat-power Engineering, 1957, No. 5.

5. G. I. Bobrovich, I. I. Gogonin, S. S. Kutateladze and V. N. Moskvichev. Critical heat flow during boiling of binary mixtures. PMTF, 1962, No. 4.

METHOD OF BOUNDARY CONDITIONS IN PROBLEMS OF STATIONARY THERMAL CONDUCTIVITY

V. I. Van'ko

(Novosibirsk)

In work [1] there is considered stationary temperature field in rotor of multistage turbine (cylindrical drum with series of blades located on lateral surface). For the solution of this problem thermal interaction between rotor and the blades is replaced by certain fictitious coefficient of the heat exchange from the working gas to rotor. Below a certain generalization of this concept is presented.

Let us assume that in thermal contact there are several one-dimensional bodies, for example, rods (Fig. 1). At points x_1, x_2,..., x_{n-1} there are observed conditions of an ideal thermal contact (for the sake of simplicity), i.e.,

Fig. 1.

$$T_i(x_i) = T_{i+1}(x_i), \quad \lambda_i T_i'(x_i) = \lambda_{i+1} T_{i+1}'(x_i)$$

Conditions at initial and final points of the systems are determined

$$\lambda_1 T_1'(x_0) = h_1 (T^{(1)} - T_1(x_0)) \text{ when } x = x_0, \quad \lambda_n T_n'(x_n) = h_2 (T^{(2)} - T_n(x_n)) \text{ when } x = x_n \qquad (1)$$

where h_1 and $T^{(1)}$, $T^{(2)}$ are coefficients of the heat emission and temperature of media, λ_1 are coefficients of thermal conductivity. Conditions of the heat exchange of each rod with the environment are arbitrary, but there are known the common solutions of each heat-conductivity equation adopted in the form

$$T_i(x) = c_1^i u_1^i(x) + c_2^i u_2^i(x)$$

If from system of rods certain ones are rejected then their influence on remaining can be replaced by condition of heat exchange with any one medium for which coefficient of heat exchange and temperature are determined explicitly, i.e., at plact of contact with rejected rod (i + 1-m)

$$T_i'(x_i) = \gamma^i [T_i(x_i) + T^i] \tag{2}$$

We shall analyze in detail the case of two rods

$$\begin{aligned} T_1(x) &= c_1^1 u_1^1(x) + c_2^1 u_2^1(x) \quad (x_0 \leq x \leq x_1) \\ T_2(x) &= c_1^2 u_1^2(x) + c_2^2 u_2^2(x) \quad (x_1 \leq x \leq x_2) \end{aligned}$$

Using condition (1) and at point of contact, we shall set up four equations

$$\begin{aligned} a_{11}c_1 + a_{12}c_2 &= b_1 \\ a_{21}c_1 + a_{22}c_2 + a_{23}c_3 + a_{24}c_4 &= 0 \\ a_{31}c_1 + a_{32}c_2 + a_{33}c_3 + a_{34}c_4 &= 0 \\ a_{43}c_3 + a_{44}c_4 &= b_2 \end{aligned} \tag{3}$$

Here

$$\begin{aligned} &a_{11} = u_1^{1\prime}(x_0) + \gamma_1 u_1^1(x_0), \quad a_{12} = u_2^{1\prime}(x_0) + \gamma_1 u_2^1(x_0), \quad b_1 = \gamma_1 T^{(1)} \\ &a_{21} = u_1^1(x_1), \quad a_{22} = u_2^1(x_1), \quad a_{23} = -u_1^2(x_1), \quad a_{24} = -u_2^2(x_1) \\ &a_{31} = u_1^{1\prime}(x_1), \quad a_{32} = u_2^{1\prime}(x_1), \quad a_{33} = -u_1^{2\prime}(x_1), \quad a_{34} = -u_2^{2\prime}(x_1) \\ &a_{43} = u_1^{2\prime}(x_2) - \gamma_2 u_1^2(x_2), \quad a_{44} = u_2^{2\prime}(x_2) + \gamma_2 u_2^2(x_2), \quad b_2 = \gamma_2 T^{(2)} \\ &\gamma_1 = h_1/\lambda_1, \quad \gamma_2 = h_2/\lambda_2, \quad y_1 = c_1^1, \quad y_2 = c_2^1, \ldots \end{aligned} \tag{4}$$

It is readily seen that if the temperature in rods are not identical zeroes, then determinant Δ of system (3) is different from zero and, as usually, the solution will be

$$y_1 = \Delta_1/\Delta, \qquad y_2 = \Delta_2/\Delta \tag{5}$$

We shall show that values of the constants of integrations determined by the solution of system (3) and the proposed method are identical. Let us assume that the second rod is excluded from the analysis; then we shall define boundary condition for the remaining rod at point of contact. For this purpose we shall determine temperature field in the excluded rod, i.e., we shall find $T_2(x)$ from the contitions

$$T_2'(x_2) = \gamma_2(T^{(2)} - T_2(x_2)) \quad \text{when } x = x_2$$

at $x = x_1$ we assume $T_2(x_1) = T_1(x_1)$, where $T_1(x)$ is the unknown temperature of the first rod. We have (in designations of the system (3))

$$-a_{21}y_2 - a_{22}y_2 = T_1(x_1), \qquad a_{21}y_2 + a_{22}y_2 = b_2$$

Hence

$$y_2 = \frac{T_1(x_1)\,a_{21} + b_2 a_{21}}{a_{22}a_{21} - a_{22}a_{21}}, \quad y_2 = \frac{-a_{22}b_2 - a_{22}T_1(x_1)}{a_{22}a_{21} - a_{22}a_{21}}, \quad T_2(x) = y_2 u_2^2(x) + y_2 u_2^2(x)$$

The condition at point x_1 for remaining rod will be found from equality of the heat fluxes

$$T_1'(x_1) = \gamma^*[T_1(x_1) + T^*]; \quad \gamma^* = \frac{a_{22}a_{21} - a_{22}a_{21}}{a_{22}a_{21} - a_{22}a_{21}}, \quad T^* = \frac{a_{22}b_2 a_{21} - a_{22}b_2 a_{21}}{a_{22}a_{21} - a_{22}a_{21}}$$

Constants y_1, y_2 are sought under the conditions

$$T_1'(x_1) = \gamma_1(T^{(1)} - T_1(x_1)), \qquad T_1(x_1) = \gamma^*(T_1(x_1) + T^*)$$

from the system

$$a_{11}y_1 + a_{12}y_2 = b_1, \qquad [a_{21} - \gamma^* a_{21}]y_1 + [a_{22} - \gamma^* a_{22}]y_2 = \gamma^* T^* \tag{6}$$

Having solved system (6) and substituting the expressions for γ^* and T^*, we shall obtain for y_1 and y_2 values identically coinciding with expressions (5), which of course will determine the solution of the system (3).

The result is readily generalized for an arbitrary number of bodies, in which the propagation of heat is described by one-dimensional equation. Actually, system of n bodies we shall consider as two bodies: the first $x_0 \leq x \leq x_{n-1}$, the second $x_{n-1} \leq x \leq x_n$. On basis of what has been proven, rejecting the second, we shall find at point of contact the condition of heat exchange in the form (2). Remaining system we again shall consider as two bodies etc. Finally, in a similar manner it is possible from the entire system to isolate a certain k-th body by means of removing others to the right and to the left.

Submitted
7 January 1963

Literature

1. V. I. Danilovskaya. Concerning the question of determining the temperature fields in rotors of multistage turbines. Engineering collection, 1954, Vol. 18.

ON THE CONVECTIVE INSTABILITY OF A COMPRESSIBLE FLUID IN MAGNETOHYDRODYNAMICS

A. A. Rukhadze

(Moscow)

In an approximation of the method of geometric optics there is solved the problem about convective instability of a compressible ideally conducting fluid located in the field of gravity. The obtained dispersion equation is analyzed in region of high and low frequencies of oscillations of liquid. It is shown that a conducting fluid in field of gravity may be unstable only with respect to low-frequency oscillations, and there is obtained a condition of instability generalizing well-known criteria of convective instability, obtained earlier.

1. Stability of a compressible conducting fluid located in external magnetic and gravitational fields, under conditions, when for the description of small oscillations of liquids there are applicable equations of magnetohydrodynamics, in which the dissipative terms may be ignored, has been investigated in works [1, 2]. In obtaining the spectrum of oscillations of liquid in these works there were used methods essentially coinciding with that applied for description of oscillations of a homogeneous medium, when the fluid

in field of gravity is essentially inhomogeneous. Such inconsistency results in dependence of spectrum of eigen values on the point of space. Furthermore, in works [1, 2] as equation of state of fluid there is used equation of Poisson's adiabat which limits the generality of the analysis.

In this work, for the purpose of eliminating the indicated deficiences, for the problem of convective instability of fluid in field of gravity there is applied method of geometric optics, where equation of state of liquid has not been specified. Method of geometric optics successfully was applied in works [3-5] for problem of stability of a slightly inhomogeneous plasma being retained by the magnetic field. This method is associated with theory of asymptotic solutions of equations of the type

$$y'' + q(\omega, x)y = 0 \tag{1}$$

where $q(\omega, x)$ is a gradually varying function in region of variation x, and namely

$$\frac{d}{dx}\frac{1}{\sqrt{q(\omega, x)}} < 1 \tag{2}$$

The spectrum of eigen values of equation (1) in case of real $q(\omega, x)$ (below we shall consider such a case) is determined by the relationship

$$\int dx \sqrt{q(\omega, x)} = \pi n \tag{3}$$

where the n are integers significantly exceeding unity. Integration in this relationship must be made over regions of transparency ($q(\omega, x) \geq 0$), located between transition points at which $q(\omega,x) = 0$. If in region of variation of x, points of the transition are absent and $q(\omega, x) > 0$, then integration is made over entire region of

variation of x. The latter is valid under any nondissipative boundary conditions for the function y(x).

2. System of equations of magnetohydrodynamics for an ideally conducting fluid under the condition of ignoring the dissipative processes, has the form [5]:

$$\frac{\partial \mathbf{H}}{\partial t} = \operatorname{rot}[\mathbf{v} \times \mathbf{H}], \qquad \operatorname{div} \mathbf{H} = 0$$
$$\rho\left(\frac{\partial \mathbf{v}}{\partial t} + (\mathbf{v}\cdot\nabla)\mathbf{v}\right) = -\nabla\left(P + \frac{H^2}{8\pi}\right) + \frac{1}{4\pi}(\mathbf{H}\cdot\nabla)\mathbf{H} + \rho\mathbf{g} \tag{4}$$
$$\frac{\partial \rho}{\partial t} + \operatorname{div}\rho\mathbf{v} = 0, \qquad \frac{\partial S}{\partial t} + (\mathbf{v}\cdot\nabla)S = 0, \qquad \rho = \rho(P, S)\ .$$

The latter of these equations represents equation of state of the fluid, which associates among themselves the pressure P, density ρ and entropy S (or the temperature T). Here we shall be limited by consideration of case of plane geometry when external magnetic field H_0, whose lines of force are not distorted is directed along z-axis, i.e., $\mathbf{H}_0 = H_0\mathbf{e}_z$, field of gravity $\mathbf{g}$ is directed along the x-axis, i.e., $\mathbf{g} = g\mathbf{e}_x$, and all the equilibrium magnitudes characterizing the fluid, depend only on one coordinate x. The equilibrium state of fluid in which $\mathbf{v}_0 = 0$, is determined by equation of equilibrium

$$\nabla\left(P_0 + \frac{H_0^2}{8\pi}\right) = \rho_0\mathbf{g} \tag{5}$$

We shall investigate stability of the equilibrium state of fluid in field of gravity by imparting the small perturbations

$$P \to P_0 + P_1, \quad \rho \to \rho_0 + \rho_1, \quad S \to S_0 + S_1, \quad \mathbf{H} \to \mathbf{H}_0 + \mathbf{H}_1, \quad \mathbf{v}$$

For magnitudes characterizing the perturbation of the equilibrium state of fluid, the dependence on time and coordinates can be taken in the form $f(x) \exp(-i\omega t + ik_y y + ik_z z)$. System of equations (4) for perturbed magnitudes here can be reduced to one second order differential equation for function $u = \rho_0 v_x$:

$$u'' + u'\left(\ln\frac{a_1}{\rho_0}\right)' + u\left\{\frac{a_0'}{a_1} - g\frac{a_0}{a_1}\frac{k_x^2+k_z^2}{\omega^2} + \frac{\omega^2}{a_1}\left[1 - K^2\left(1 + \frac{g}{\omega^2}\frac{\rho_0'}{\rho_0}\right)\right]\right\} = 0 \qquad (6)$$

where

$$a_1 = \frac{\omega^2(1-K^2)(v_0^2+u_0^2(1-K^2))}{\omega^2-(k_x^2+k_z^2)(v_0^2+u_0^2(1-K^2))}, \qquad u_0^2 = \left(\frac{\partial P_0}{\partial\rho_0}\right)_S, \qquad K^2 = \frac{k_x^2 v_a^2}{\omega^2}$$

$$a_0 = \frac{\rho\omega^2(1-K^2)}{\omega^2-(k_x^2+k_z^2)(v_0^2+u_0^2(1-K^2))} - \frac{\rho_0'}{\rho_0}a_1, \qquad v_a^2 = \frac{H_0^2}{4\pi\rho_0} \qquad (7)$$

Here v_a is the Alfvén velocity, u_0 is the speed of sound in a liquid,* and the prime signifies differentiation in x.

By means of substituting

$$u = y\exp\left(-\frac{1}{2}\int^x A(x)\,dx\right)$$

where A(x) is the coefficient at u', equation (6) reduces to an equation of form (1). If here we take into consideration the condition of applicability of approximation of geometric optics (2), then for determining the spectrum of oscillations of a weak-nonhomogeneous fluid in the field of gravity we obtain the following dispersion equation:

$$\int dx\left\{\frac{1}{v_0^2+u_0^2(1-K^2)}\left[\omega^2-(k_y^2+k_z^2)\left(v_0^2+u_0^2(1-K^2)+\frac{g\rho_0'}{\omega^2}\right)+\right.\right.$$
$$\left.\left.+g\frac{\rho_0'}{\rho_0}\frac{(k_y^2+k_z^2)(v_0^2+u_0^2(1-K^2))-k_y^2v_0^2}{\omega^2(1-K^2)}\right]\right\}' = \pi n \qquad (8)$$

---

*For a fluid, in which equation of Poisson state is valid

$$P\rho_0^{-\gamma} = \text{const}, \text{we have } u_0 = \sqrt{\gamma P_0/\rho_0}.$$

We note also that equations of monoliquid hydrodynamics (4) are applicable and in case of a nonisothermal plasma, in which $T_e \gg T_i$ (see [6]). Here the speed of sound is equal to

$$u_0 = \sqrt{T_e/M}$$

3. To analyze dispersion equation (8) in the general case it is difficult. There is no necessity of this. For an investigation of the stability of a fluid in field of gravity it is sufficient to be limited to the analysis of equation (8) in limiting cases of high and low frequencies of oscillations of a nonhomogeneous fluid.

In region of high frequencies of oscillations, when $\omega^2 \gtrsim (k_y^2 + k_z^2)(v_a^2 + u_0^2)$, the components containing gravitational field g, in dispersion equation (8) within the framework of approximation of geometric optics can be ignored. As a result we obtain a dispersion equation for determining the spectrum of magnetohydrodynamic oscillations of a nonhomogeneous fluid *

$$\int dx \left\{ \frac{\omega^2}{v_a^2 + u_0^2 (1 - k^2)} - k_y^2 - k_z^2 \right\}^{1/2} = \text{const} \qquad (9)$$

It is readily seen that with respect to such high-frequency oscillations a nonhomogeneous fluid is stable, i.e., always $\omega^2 > 0$.

Another situation takes place in region of low frequencies of oscillations of a nonhomogeneous fluid when there are fulfilled the conditions

$$\omega^2, k_z^2 v_a^2 \ll (k_y^2 + k_z^2)(v_a^2 + u_0^2)$$

---

*The dispersion equation (9) does not contain that branch of the Alfvén waves which describes oscillation of components of speed and magnetic field perpendicular to the plant of vectors H_0 and k. Equations for these components are detached from remaining equations in system (4), and in case of a nonhomogeneous fluid, just as in a homogeneous are found to be algebraic. Equality to zero of determinant of these equations results in the following expression for frequency of oscillations $\omega^2 = k_z^2 v_a^2$. Dependence of frequency of oscillations on the x-coordinate in this case should not cause any perplexity, because these oscillations are not natural oscillations of a nonhomogeneous fluid. They characterize only development in time of initial perturbations of components of speed and magnetic field perpendicular to the plane of the vectors H_0 and k.

The dispersion equation (8) in this case takes the form:

$$\int d\omega \left\{ -1 - \frac{g}{\omega^2 (v_0^2 + v_{0z}^2) - k_z^2 v_0^2 v_{0z}^2} + g \frac{\rho_0'}{\rho_0} \frac{1}{\omega^2 - k_z^2 v_{0z}^2} \right\}^{1/2} = \frac{\pi n}{\sqrt{k_x^2 + k_z^2}} \qquad (10)$$

From this equation it follows that a nonhomogeneous fluid in the field of gravity the fluid may be unstable with respect to the low-frequency oscillations (i.e., $\omega^2 < 0$) only under the conditions

$$A = \left(k_x^2 v_0^2 + g \frac{\rho_0'}{\rho_0} \right) \omega^2 - g^2 < 0$$
$$B = \left(k_x^2 v_0^2 + g \frac{\rho_0'}{\rho_0} \right) (v_0^2 + v_{0z}^2) - g^2 + k_x^2 v_0^2 v_{0z}^2 < 0 \qquad (11)$$

Fulfillment of at least one of these local conditions in region of transparency of fluid is necessary, but is not a sufficient condition of the instability. On the other hand, the fulfillment of either of these conditions in entire region of transparency knowingly is sufficient for instability of the fluid. Condition (11) generalize well known criteria of convective instability of conducting fluids obtained in works [1, 2, 7, 8], where there were considered different particular cases of the oscillations.

For an incompressible fluid ($U_0 \to \infty$) conditions (11) take the form

$$k_x^2 v_0^2 + g \frac{\rho_0'}{\rho_0} < 0$$

Such a condition is obtained in work [8] for a "cold" fluid ($u_0 \to 0$). Conditions of instability (11) correspond to those obtained in work [7] and are always fulfilled. Finally, the conditions

$$\frac{\rho_0'}{\rho_0} > \frac{f'}{g}, \quad \frac{f}{v_0^2 + v_{0z}^2}$$

obtained in works [1, 2] follow from (11) at $k_z = 0$. In works [1, 2] (see also [7]), as already was noted above, during investigation of

convective instability of a nonhomogeneous fluid there were used the same methods which are used for the description of oscillations of a homogeneous medium. And precisely, the solution of equations for perturbed magnitudes were sought for in the form exp ($-i\omega t + ik_y y + ik_z z + ik_x x$). Thus, it is possible to proceed, if the spectrum of oscillations of a nonhomogeneous medium is found to be independent of the point of space. From dispersion equation (10) it is evident that this takes place in the case when integrand in equation (10) in entire plasma is constant. Here, the spectrum of oscillations of fluid is determined by expression:

$$\omega^2 = \frac{B_1 \pm \sqrt{B_1^2 - 4k_z^2 v_a^2 A_1}}{2\xi(v_a^2 + \omega_g^2)} \qquad (12)$$

where

$$A_1 = \left(k_z^2 v_a^2 + g\frac{d\rho'}{\rho_0}\right)\omega^2 - g^2 k_z^2, \qquad \xi = 1 + \frac{g^2 \omega^2}{\omega^2 (k_y^2 + k_z^2)}$$
$$B_1 = \left(k_z^2 v_a^2 + g\frac{d\rho'}{\rho_0}\right)(v_a^2 + \omega_g^2) - g^2 k_z^2 + k_z^2 v_a^2 \omega_g^2$$

Here d is the linear dimension of fluid along the x-axis where magnitude $\pi n/d$ plays role of wave number k_x. From expression (12) it follows that the fluid is unstable during fulfillment of one of the conditions

$$A_1 < 0, \qquad B_1 < 0 \qquad (13)$$

Within the limit $\xi \to 1$ (i.e., $k_x \to 0$) these conditions transform to (11). These conditions, however, have a narrower sense than condition (11), since they were obtained just as expression (12), on the assumption that A_1 and B_1 are constant in the entire fluid.

From the analysis made of dispersion equation (8) it follows that conducting nonhomogeneous fluid in field of gravity may be unstable only with respect to low-frequency oscillations. Oscillations of an unstable fluid bear an aperiodic character. In case

$B^2 \gg k_z^2 v_a^2 (u_0^2 + v_a^2)A$, increment of increase of oscillations

$$\gamma \sim k_z \rho_0 \sqrt{|A|/|B|} \quad \text{when } A<0, \quad \text{or} \quad \gamma \sim \sqrt{|B|/v_0^2 + \omega^2} \quad \text{when } B<0$$

For the case $B^2 \ll k_z^2 v_a^2 (u_0^2 + v_a)A$, increment of increase of oscillations

$$\gamma \sim k_z \rho_0 \sqrt{|A|/v_0^2 + \omega^2}$$

In conclusion I thank V. P. Silin for his discussion of the work.

Submitted
25 December 1962

Literature

1. Yu. A. Tserkovnikov. Concerning the question of convection instability of plasma. Reports. Academy of Sciences of USSR, 1960, Vol. 130, No. 2, p. 295.

2. W. A. Newcomb. Convective instability induced by gravity in a plasma with a frozen – in magnetic field, Phys. fluids, 1961, Vol. 4, No. 3, p. 391.

3. V. P. Silin. Oscillations of a weak-nonhomogeneous plasma. Journal of Experimental and Theoretical Physics, 1963, Vol. 44, No. 4, p. 1271.

4. Ye. Ye. Lovetskiy, L. M. Kovrizhnykh, A. A. Rukhadze and V. P. Silin. Hydrodynamic oscillations of a nonhomogeneous plasma of low pressure in a magnetic field. Reports of Academy of Sciences of USSR, 1963, Vol. 149, No. 5, p. 1052.

5. Ye. Ye. Lovetskiy and A. A. Rukhadze. On the convective instability of a nonhomogeneous plasma in the field of gravity. News of Higher Educational Institutions, Radio Physics, 1963, Vol. 6, No. 6.

6. Yu. L. Klimontovich and V. P. Silin. On magnetohydrodynamics of nonisothermal plasma without collisions. Journal of Experimental and Theoretical Physics, 1961, Vo.. 40, No. 6, p. 1213.

7. Ye. Ye. Lovetskiy and A. A. Rukhadze. Hydrodynamic oscillations in field of gravity. Hournal of Technical Physics, 1963, Vol. 33, No. 6, p. 652.

8. Ye. P. Velikhov. Stability of the boundary plasma – vacuum. Journal of Technical Physics, 1961, Vol. 31, No. 2, p. 180.

INVESTIGATION OF CRISIS OF BOILING DURING THE FLOW OF UNDERHEATED METHYL ALCOHOL

P. I. Povarnin

(Moscow)

At present there are known many works on study of crisis of boiling during forced flow of underheated water in wide range of the variation of pressures [1-3].

The use in technology of other heat-transfer agents, mainly organic compounds, and expansion of concepts on character of phenomenon require new investigations. At the same time there are few works of this type. In particular, in alcohols there are known the articles by L. S. Sterman and N. G. Styushin [4] in which there are described experiments on the crisis for isopropyl and ethyl alcohols. Here these experiments encompass comparatively narrow interval of variation of speed of flow from 0.2 to 7.0 m/sec with the pressure at 2 atm and zero underheating.

Below there are described investigations of crisis of boiling during forced flow of methyl alcohol on the bases of the All-Union Government Standard No. 6995-54 in pipes of small diameter at pressures from 5 to 70 atm, the speed of liquid up to 45 m/sec and underheating up to a temperature of saturation from 8 to 200°C.

Description of experiment. Experimental installation was a closed contour with circulating pump, a flow-rate meter, devices for maintaining the pressure, preliminary preheating ahead experimental sector and cooling of liquid in front of pump, analogous to the installation in our experiments with water [1].

Experiments were made in machined and seamless tubes of stainless steel and bronze with an internal diameter of 2.0 to 3.5 mm, with the thickness of wall 0.2-0.3 mm and length of tube from 40 to 210 mm. The method of conducting the experiment, measurement and calculation of the experimental magnitudes remained the same as in experiments with water. The possible accuracy of measurements was evaluated in following limits [1]: determination of heat flux with an accuracy of ±12%, determination of speed of flow ±5%, determination of temperature of fluid ±5°C, determination of temperature of internal surface of tube depending upon magnitude of heat flux q from ±5 to ±30°C.

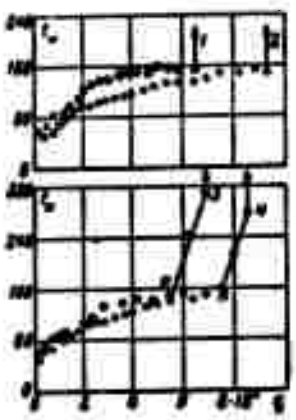

Fig. 1. Graph of model experimental dependences $t_w = f(q)$: 1-st type (above) — sudden temperature jump, accompanied by an overheating 1 or detachment 2; 2-nd type (below) — crisis is complicated by a carbon-deposit formation, at point of bend n there is observed spontaneous increment t_w as a result of which there occurs the detachment 3 on overheating 4.

In distinction from experiments with water the phenomenon of crisis of boiling during flow of methyl alcohol was complicated by the thermal decomposition of working fluid with the formation of a layer of carbon scale on internal surface of tube. In accordance with this all experiments were divided into two groups. Experiments of first type proceeded according to the well known diagram characteristic for water, when in process of

experiment the heat flux q gradually increases with the maintenance of constancy of all the remaining parameters. Here in sequence there were observed stages of convective heat exchange of surface boiling and crisis with sudden surge of temperature and frequent overheating of tube (Fig. 1, upper graph).

Experiments of second type. Passing through the stages of convective heat exchange and surface boiling, on internal surface of tube there began to be deposited layer of carbon scale which resulted in a spontaneous rise in temperature of external surface of wall measured by a thermocouple. In this case there could be recorded during a certain time the wall temperature in a recalculation for the internal surface which exceeded the saturation temperature by several hundred degrees (see Fig. 1, lower graph). The opening of tubes showed that layer of carbon scale in certain cases attained a thickness 50 μ. It must be noted that the formation of similar scales was observed also for other investigators during work with organic liquids, for example for Bailey and Dean [5] during work with the rocket fuel JP-4. It may be assumed that the marked difference between temperatures of internal surface of tube and boundary layer of liquid occurs as the result of temperature differential in layer of carbon scale. Calculations showed that thermal conduction of carbon scale material in this case should be of an order of 0.1 kcal/m$^{\circ}$C·hr.

Thus, the genesis of a vapor film during the crisis occurs not on metallic surface of wall of tube, but on surface of carbon scale layer and crisis in certain cases is prolonged. For the critical thermal load in these experiments there was taken the magnitude q_*, corresponding to point of beginning of spontaneous rise t_w.

Table 1. Experimental Data in Methyl Alcohol

t, °C	G, $\frac{kg}{m^2 \cdot sec}$	q_w, $\frac{kcal}{m^2 \cdot hr}$	Metal	$\frac{l}{d}$
$P = 5$ atm, $B = 0.0162$, $A = 0.96 \cdot 10^6$, $C = 0.217$				
109	1582	$1.53 \cdot 10^6$	EYa — 1T	60
85	3980	2.96	»	»
48	»	3.02	BR	5.0
45	1592	1.9	»	3.28
30	3960	4.3	»	3.28
$P = 10$ atm, $B = 0.0152$, $A = 1.15 \cdot 10^6$, $C = 0.184$				
60	1592	3.5	EYa — 1T	10
60	1592	3.9	»	10
65	2388	4.9	»	10
65	2388	4.0	»	10
50	3960	6.3	»	10
50	3960	5.05	»	10
40	7960	7.5	»	10
21	31840	16.0	»	10
56	»	5.75	»	16.7
56	»	4.9	»	12.5
55	7960	6.4	»	»
50	1592	3.4	»	10
60	2388	4.45	»	10
115	1592	2.75	BR	10
85	3960	4.3	»	10
80	»	4.8	»	10
60	7960	6.65	»	10
40	31840	14.80	»	12.5
40	23880	13.80	»	»
40	15920	8.0	»	»
102	3980	3.85	»	10
108	7960	4.3	»	10
80	15920	5.45	»	22.5
80	23880	8.35	»	»
25	7960	9.3	»	»
78	31840	9.2	»	»
32	15920	11.0	»	»
32	7960	8.8	»	»
70	3980	3.05	EYa — 1T	64
72	11940	6.70	»	»
22	»	8.2	»	»
68	3980	4.18	»	»
78	1592	3.25	»	»
82	2388	3.43	»	»
110	1592	1.85	»	»
120	»	1.94	»	12.5
130	15920	2.84	»	»
38	23880	8.6	»	»
38	15920	5.65	»	»
35	7960	4.40	BR	5.0
48	3960	3.60	»	»
55	1592	3.76	»	»
$P = 30$ atm, $B = 0.01365$, $A = 1.03 \cdot 10^6$, $B = 0.185$				
110	1592	2.6	BR	10
60	3980	3.3	»	»
60	7960	6.3	»	»
40	31840	12.1	»	12.5
»	23880	9.7	»	»
»	15920	6.85	»	»
105	»	7.9	»	»
120	7960	3.6	»	»
140	3980	2.45	»	»
130	1592	1.68	»	10.0
28	15920	8.4	»	12.5
»	»	7.95	»	»
40	7960	6.5	»	»
80	11940	8.1	EYa - 1T	64
»	3980	4.4	»	»
»	2388	4.36	»	65
110	»	2.94	»	64
150	1592	2.6	»	»
142	»	1.38	»	60
82	3980	2.6	»	»
155	7960	3.8	»	»
148	11940	4.25	»	»
45	7960	7.43	»	»
»	15920	8.7	BR	12.5
40	23880	8.42	»	»
»	31840	9.5	»	»
84	»	12.6	»	»
112	»	9.0	»	»
170	15920	3.86	»	»
36	31840	10.4	»	5.0
43	23880	9.0	BR	5.0
40	7960	5.55	»	»
83	»	3.6	»	»
45	3980	3.06	»	»
119	1592	1.63	»	»
$P = 50$ atm, $B = 0.0128$, $A = 0.59 \cdot 10^6$, $C = 0.29$				
20	6368	17.4	EYa — 1T	10.0
60	1592	2.2	BR	»
120	796	1.2	»	»
105	3980	2.1	»	»
80	7960	6.3	»	»
100	3980	2.0	»	»
»	»	2.1	»	»
»	1592	1.6	»	»
»	»	1.66	»	»
48	15920	7.5	»	12.5
40	39800	19.0	»	»
»	31840	9.2	»	»
»	23880	7.6	»	»
»	31840	13.0	»	»
20	5920	8.0	»	»
50	7960	5.5	»	»
100	11940	7.5	EYa — 1T	65
85	3980	3.52	»	64
100	»	4.06	»	65
135	1592	1.7	»	60
158	3980	2.56	»	»
185	15922	1.55	»	»
125	7960	5.12	»	»
178	»	3.72	»	»
50	31840	14.9	BR	12.5
45	23880	11.3	»	»
»	15920	9.0	»	»
120	31840	10.5	»	»
180	39800	6.42	»	»
185	15920	4.8	»	»
38	31840	10.5	»	5.0
40	23880	9.15	»	»
45	15920	7.0	»	»
40	7960	5.05	»	»
50	3980	4.25	»	»
40	1592	2.6	»	3.28
$P = 70$ atm, $B = 0.0123$, $A = 0.21 \cdot 10^6$, $C = 1.2$				
40	15920	9.5	BR	12.5
»	»	10.5	»	»
66	23880	10.4	»	»
»	31840	14.0	»	»
»	»	12.0	»	»
50	»	16.1	»	»
55	7960	3.8	»	»
»	»	5.2	»	10.0
50	3980	2.3	»	»
45	1592	1.8	»	12.5
32	15920	8.6	»	»
»	»	10.8	»	»
35	7960	5.0	»	65
100	15920	7.7	EYa — 1T	»
»	»	8.9	»	»
85	3980	2.7	»	»
»	»	3.92	»	»
»	»	2.93	»	»
»	»	3.5	»	»
95	1592	1.42	»	»
135	»	1.04	»	60
145	»	1.2	»	»
135	3980	1.8	»	»
122	7960	5.1	»	»
168	»	3.8	»	»
50	31840	15.2	BR	12.5
45	23880	13.5	»	»
50	15920	9.6	»	»
120	31840	12.7	»	»
180	39800	9.8	»	»
190	15920	3.8	»	»
38	31840	16.4	»	5.0
40	23880	10.5	»	»
38	15920	8.05	»	»
50	3980	3.9	»	»
40	1592	2.2	»	»
»	»	2.88	»	»

Cleaning the tube of carbon scale made it possible to make repeated experiments where there was observed a good frequency of the results. In a prolonged circulation the alcohol was altered, there was observed an increase in acidity, contents of water, manifestation of suspended particles et cetera. Therefore, after 10 experiments the alcohol in the contour was completely replaced.

Results of the experiments. In all there were conducted 156 experiments, data on which are presented in Table 1. Experiments were conducted in separate series with maintenance of constant pressure in each series. Experiments during small underheating at $8\text{-}10^{\circ}$ were very few and pulsational conditions recorded for water in work [6], were not observed. Given below calculating dependences pertain to region of large underheatings $\Delta t > 20$ and nonoscillating regimes of the flow.

In Table 2 there is given the number of experiments N, conducted at various pressures p and there are indicated the number N_1 and N_2 of crises of first and second type $N = N_1 + N_2$. From table it is evident that at low pressures p = 5 and 10 atm the crisis more frequently generated according to 1st type, i.e., in pure form, although with these pressures there were observed cases of carbon scale formation. In proportion to the rise in pressure to 30, 50 and 70 atm the number of crises of 2nd type complicated by thermal decomposition continuously increased and at 70 atm crises of 1st type amounted to 8% of the total. A decrease in percentage of crises of 1st type was observed also with an increase in speed of flow.

In Table 2 there are indicated also the wall temperatures at which were recorded, respectively the beginning of thermal decomposition of alcohol T_0 and moment of genesis of a crisis in pure form T_*. As is evident, these temperatures overlap each other and at all

pressures there is possible the genesis of a crisis of both types.

Table 2

p atm	N	N_1	N_1, %	N_2	N_2, %	T_1, °C	T_2, °C
5	5	4	80	1	20	115—135	145—175
10	43	22	51	21	49	150—180	140—205
20	35	17	48.5	18	51.5	170—195	185—220
50	36	4	11	32	89	180—220	220—225
70	37	3	8	34	92	195—200	215—230
Total	156	50	32	106	68	—	—

Discussion of results. In work [1] it is shown that for water within a wide range of pressures of underheating and of speeds of flow of liquid there is valid the empirical formula

$$q_0 = A(1 + B\Delta t)(1 + CW)\rho^{0.6} \tag{1}$$

where A, B, C are coefficients depending only on the pressure.

The use of equation (1) for methyl alcohol during processing of data of described experiments made it possible to establish that character of change of coefficients A, B, C for both liquids is identical at identical given pressures $\pi = p/p_*$ or given temperatures $\tau = T/T_*$, corresponding to them where p_*, T_* are respectively the pressure and temperature at the critical point of a given substance.

The recorded fact makes it possible to express coefficients of equation (1) in criterial form. In this case magnitude A represents that hypothetical value q_*, which should take place during a zero underheating and a zero speed of flow

$$q_0 = 1.55 \cdot 10^9 \frac{K_2^{0.65} K_3^{0.3}}{(K_1)^{0.3}} \tag{2}$$

$$K_1 = \frac{\sigma^{0.5} \gamma_2 r^{0.5}}{\mu^{0.3} \lambda^{0.6} (T_1 - T_0)^{0.6}}, \quad K_2 = \frac{r^{0.5} (T_1 - T_0)^{0.5}}{\lambda^{0.5} T_0}, \quad K_3 = \frac{\gamma_2 r^{0.5}}{\sigma^{0.5} (T_1 - T_0)^{0.5}} \tag{3}$$

Here γ_1, γ_2 are specific gravities of liquid and vapor on the line of saturation; c_p, r, σ, μ, λ are respectively the heat capacity,

latent heat of vaporization, surface tension, viscosity and thermal conductivity of liquid under the same conditions; $g = 9.81$ msec^{-2} is the acceleration due to gravity; 427 is the mechanical heat equivalent [kgm/kcal]; $(K_1)_1$ is the value at $q = 1$.

Influence of underheating on crisis of boiling, coefficient B in equation (1), is obtained from following considerations. S. S. Kutateladze [7] showed that influence of underheating on crisis under conditions of free convection is expressed by relationship

$$q_0/q_* = 1 - D\left(\frac{T_1}{T_s}\right)^n \frac{\Delta i}{r}, \qquad \Delta i = i_l - i' \tag{4}$$

Here Δi is negative during underheating, and q_0 corresponds to q_* during a zero underheating. The processing of experimental data in water, alcohols and other organic liquids made it possible to replace in case of a forced flow equation (4) by a simpler relationship on the basis of equation (1). It was found that for all investigated heat-transfer agents the coefficient B in this equation is inversely proportional to the absolute boiling point T_s at a given pressure.

For water

$$B = 9.5/T_s,$$

for methyl alcohol

$$B = 6.25/T_s.$$

In order to take into account the influence of speed of flow on crisis of boiling (coefficient C in equation (1)) there was used work [8], in which it is shown that difference between stability of a vapor bubble on surface of heating during free convection and during compulsory flow may be calculated by the Weber number

$$W = \frac{w\rho_1}{\rho''}, \quad \text{or} \quad W = \frac{w^{0.6}\gamma_1}{\rho''^{0.6}(\gamma_1 - \gamma_2)^{0.4}} \tag{5}$$

if for the geometric dimension l we take a magnitude, proportional to the break-away diameter of vapor bubble during free convection. Under these conditions for coefficient C there was obtained the expression (P – Prandtl number)

$$C = 0.0205 \frac{W^{0.4}\rho^{0.1}}{K_1^{0.5}K_2^{0.25}}\left(\frac{\gamma_1}{\gamma_2}\right)^{0.65}, \quad P = 3600\eta\frac{c_p}{\lambda} \quad \left(K_2 = \frac{r}{T_s\vartheta_p}\right)$$

Thus, magnitude of heat flow during a crisis of boiling under conditions of forced flow and underheating of main mass of liquid up to saturation temperature is determined in a general form by the criterial equation

$$K_1 = f(K_2, K_3, K_4, P, W, \gamma_1/\gamma_2, \Delta t/T_s) \tag{6}$$

or by its concrete form of the heat-transfer agent under consideration – methyl alcohol

$$q_s = 1.55 \cdot 10^3 \frac{K_2^{0.65}K_3^{0.5}}{(K_4)^n}\left(1 + \frac{6.25}{T_s}\Delta t\right)\left[1 + 0.0205\frac{W^{0.4}\rho^{0.1}}{K_2^{0.5}K_3^{0.25}}\left(\frac{\gamma_1}{\gamma_2}\right)^{0.65}\right] \tag{7}$$

A comparison of coefficients A, B, C with experimental data showed that difference between the calculated and experimental values of A at pressures, remote from critical point does not exceed 2% and in region near the critical 8.5%. For coefficient B such deviations in general were not observed. For the coefficient C there are recorded larger deviations where they increase in proportion with increasing proximity to critical region; this can be explained by the inaccuracy in determining the physical properties of substance and indistinctness of phenomenon of crisis of boiling in this region.

In Fig. 2 there is given a comparison of experimental and calculated values of q_* at all operating pressures. From graph it is evident that over 60% of all experiments is concentrated in band ±20% from the calculated curve and remaining points deviate not more than by 40%.

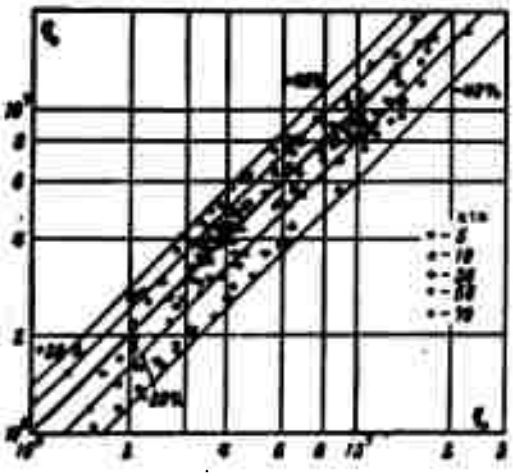

Fig. 2. Comparison of experimental data for q_* by calculation on basis of equations (2) and (14).

The investigation of crisis of boiling of methyl alcohol made in a forced flow in tubes of small diameter within wide range in variation of pressure the contour, of speed of flow and underheating up to the saturation temperature showed a lack of influence if dimension of the tube on crisis of boiling of given liquid. At all pressures there are recorded cases of complication of crisis of boiling by thermal decomposition of alcohol on surface of heating, where with increase of pressure the probability of decomposition increases. The conducted treatment of experiments makes it possible to propose criterial equation (7) for determination of q_*, useful for water, methyl alcohol and other liquids.

Submitted
18 June 1962

Literature

1. P. I. Povarnin and S. T. Semenov. Investigation of crisis of boiling during flow of underheated water in tubes of small diameters at high pressures. Heat-power engineering, 1959, No. 4, 1960, No. 1.

2. I. T. Alad'yev, L. D. Dodonov and V. S. Udalov. Heat emission and critical heat flow during boiling of underheated water in pipes.

Atomic energy, 1959, Vol. 6, Issue 1.

3. B. A. Zenkevich and V. I. Subbotin. Critical thermal loads during forced flow of water, not heated up to boiling. Atomic energy, 1957, Vol. 2, Issue 8.

4. L. S. Sterman and N. G. Styushin. Influence of circulation on crisis of the heat exchange during boiling of isopropyl alcohol. Journal of Technical Physics, 1952, No. 3.

5. S. Bailey and L. Dean. Investigation of heat exchange for fuel of rocket motor JP-4. Problems of rocket technology. Collection of translations and resumes of foreign periodicals literature, 1955, No. 4.

6. I. T.Alad'yev,V. Ye. Doroshchuk, Z. L. Miropol'skiy and M. A. Styrikovich. Crisis of boiling in pipes. Reports on 2nd International Conference on Heat Exchange, Colorado, USA, 1961.

7. S. S. Kutateladze. Critical heat flux during flow of a wetting liquid with core, not yet heated to saturation temperature. Scientific Reports of Higher Schools. Collections "Power Engineering," 1959, No. 2.

8. S. G. Teletov. On the maximum dimension of vapor bubble. Publishing House of Academy of Sciences of USSR. News of G. M. Krzhizhanovskiy, Institute of Power Engineering, 1940, Vol. 11.

DETERMINING THE SHAPE OF A GAS BUBBLE IN AN AXIALLY SYMMETRIC FLUID FLOW

O. M. Kiselev

(Kazan')

There are known only a few works devoted to the determination of shape of free boundaries of flow which take into account the effect of forces of surface tension. The problem on finding the shape of two-dimensional bubble in a two-dimensional potential flow of an incompressible fluid inside a rectilinear channel was solved be N. Ye. Zhukovskiy [1]. In 1955 McLeod [2] by another method solved particular case of Zhukovskiy's problem (the flow is unlimited, the pressure inside bubble is equal to pressure of stagnation). Finally M. I. Gurevich [3] investigated the effect of forces of surface tension on compressibility factor of stream. Lower is offered method of approximation of determining the shape of a gas bubble in an axially symmetric potential flow of an incompressible fluid. It is shown that the sought shape differs little from an oblate ellipsoid of revolution. There are determined basic dimensions of bubble depending upon physical parameters of the flow.

Designations

V is the speed of flow,
V_∞ is the speed of undisturbed flow,
v is the dimensionless speed, $v = V/V_\infty$
p is the pressure in liquid,
p_0 is the pressure of stagnated flow,
p_i is the pressure of gas in bubble (p_i = = const, $p_i \geq p_0$),
T is the force of surface tension (T = = const),
R_1, R_2 are the major radii of curvature of bubble,
2a is the length of bubble (diameter, parallel to x-axis),
2b is the thickness of bubble (diameter, perpendicular to x-axis),
c is the aspect ratio $c = a/b$
ρ is the density of liquid.

The flow around of a gas bubble by an axially symmetrical potential flow of an ideal incompressible fluid (Fig. 1) is examined in cylindrical coordinates x, r.

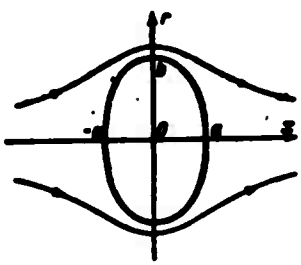

Fig. 1.

On the boundary of liquid and gas there must be fulfilled Laplace equation

$$T\left(\frac{1}{R_1}+\frac{1}{R_2}\right)=p_i-p \qquad (1)$$

(its conclusion can be found, for example, in work [4]). By means of the Bernoulli equation we shall transform (1) to the form

$$\tau\left(\frac{1}{R_1}+\frac{1}{R_2}\right)=1+cv^2$$
$$\left(\tau=\frac{T}{a(p_i-p_\infty)},\quad c=\frac{\rho V_\infty^2}{2(p_i-p_\infty)}\right) \qquad (2)$$

Let us assume that x = x(t), r = r(t) are the parametric equations of surface of revolution; then, designating differentiation with respect to the point t, we have

$$\frac{1}{R_1}=-\frac{r''_{xx}}{(1+r'^2_x)^{3/2}}=-\frac{(\dot{x}\ddot{r}-\ddot{x}\dot{r})\dot{x}/|\dot{x}|}{(\dot{x}^2+\dot{r}^2)^{3/2}} \qquad \frac{1}{R_2}=\frac{1}{r(1+r'^2_x)^{1/2}}=\frac{|\dot{x}|}{r(\dot{x}^2+\dot{r}^2)^{1/2}}$$

Thus, equation (1) can be presented in the form

$$\gamma\alpha\frac{|\dot{x}|(\dot{x}^2+\dot{r}^2)-r(\dot{x}\ddot{r}-\ddot{x}\dot{r})\dot{x}/|\dot{x}|}{r(\dot{x}^2+\dot{r}^2)^{3/2}}=1+\alpha v^2 \qquad (3)$$

We shall show that in a definite interval of variation of parameter α equation (3) will be satisfied with a fairly high degree of accuracy, if bubble has form of ellipsoid of revolution oblate in direction of x-axis.

For such ellipsoid

$$x=a\cos t,\quad r=b\sin t\quad (0\leqslant t\leqslant\pi,\ a/b=c\leqslant 1)$$

$$\gamma\alpha\frac{|\dot{x}|(\dot{x}^2+\dot{r}^2)-r(\dot{x}\ddot{r}-\dot{r}\ddot{x})\dot{x}/|\dot{x}|}{r(\dot{x}^2+\dot{r}^2)^{3/2}}=$$

$$=\gamma\frac{c^2[2-(1-c^2)\sin^2 t]}{[1-(1-c^2)\sin^2 t]^{3/2}}\equiv A(\gamma, c; t)$$

The flow around oblate ellipsoid of revolution has been investigated (see, for example, in work [5]). Using given formulas there, we shall have

$$1+\alpha v^2=1+\beta\frac{c^2\sin^2 t}{1-(1-c^2)\sin^2 t}\equiv B(\beta, c; t)$$

$$\alpha=\beta\frac{c^2}{(1-c^2)^{3/2}}\left(\frac{1}{\sqrt{1-c^2}}\arcsin\sqrt{1-c^2}-c\right)^2 \qquad (4)$$

With the fixed value c we shall determine the parameters γ and β in wuch a way so that the functional

$$I(\gamma,\beta)=\int_0^{\pi/2}(A-B)^2dt$$

acquires a minimum value. Having required a vanishing of the partial derivatives from I through γ and β, we shall obtain the system of equations

$$\gamma\left[\frac{2}{3}\frac{1+c^2}{c^2}E(\sqrt{1-c^2})-\frac{1+3c^2}{3}K(\sqrt{1-c^2})\right]-\beta\alpha\frac{1+c-2c^2}{4c(1+c)}=\alpha\frac{1-c}{2c}$$

$$\gamma\alpha\frac{3+10c^2+15c^4}{15c^2}-\beta\frac{1}{1-c^2}\left[\frac{2}{3}\frac{1+c^2}{c^2}E(\sqrt{1-c^2})-\right.$$

$$\left.-\frac{1+2c^2}{3}K(\sqrt{1-c^2})\right]=\frac{1}{c^2}E(\sqrt{1-c^2})+K(\sqrt{1-c^2})$$

where $K(\sqrt{1 - c^2})$, $E(\sqrt{1 - c^2})$ are the total elliptical integrals of first and second kind. The solution of this system at different values of $c(0.5 \leq c \leq 1)$ are given in Table 1. The magnitude of α is determined by formula (4).

Table 1

c	γ	β	α
1.0	0.5	0	0
0.9	0.6175	0.2405	0.0985
0.8	0.7849	0.6040	0.2211
0.7	1.0352	1.1853	0.3821
0.6	1.4334	2.1909	0.6020
0.5	2.1480	4.1948	0.9375

Table 2

α	t = 0			t = π/4			t = π/2		
	A	B	100 δ	A	B	100 δ	A	B	100 δ
1.0	1	1	0	1	1	0	1	1	0
0.9	1.0004	1	0.04	1.1088	1.1076	−0.07	1.2419	1.2405	0.13
0.8	1.0047	1	0.37	1.2315	1.2357	−0.35	1.6080	1.6040	0.39
0.7	1.0145	1	0.97	1.3788	1.3898	−0.87	2.2034	2.1853	1.22
0.6	1.0320	1	1.80	1.5461	1.5799	−1.91	3.2490	3.1919	3.28
0.5	1.0730	1	3.04	1.7644	1.8390	−3.11	5.3650	5.1948	7.10

In Table 2 there are given the magnitudes of A and B calculated at the points t = 0, 1/4π, 1/2π at corresponding values of parameters c, γ, β. Character of change of indicated magnitudes is shown in Fig. 2. The magnitude

$$\delta = \frac{A - B}{B_0}$$

$$\left(B_0 = \frac{2}{\pi}\int_0^{\pi/2} B\,dt = 1 + \beta\frac{e}{1+e}\right)$$

characterizes the accuracy of equality (3).

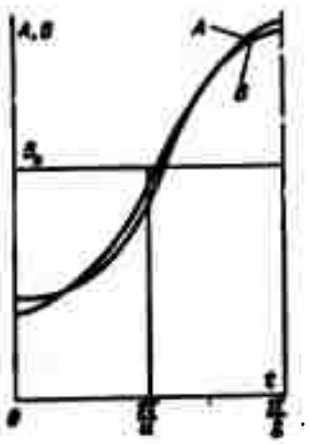

Fig. 2.

The obtained data indicate that at $0 \leq \alpha < 1$ the shape of the bubble actually is close to the shape of an oblate ellipsoid of revolution. With an increase in α the difference between them increases (magnitude of error δ increases).

In setting up the physical parameters of the flow basic dimensions of bubble a, b can be found from the graphs of Figures

3, 4 and taking into account formulas (2).

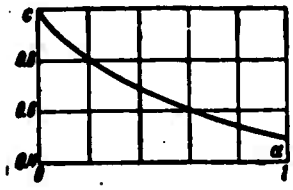

Fig. 3.

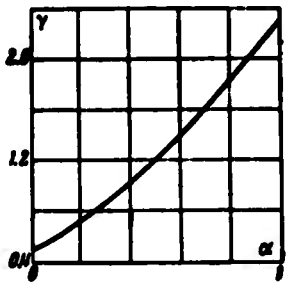

Fig. 4.

Submitted
10 October 1962

Literature

1. N. Ye. Zhukovskiy. Determination of motion of liquid under any condition given on line of flow. Complete collection of works, Moscow-Leningrad, ONTI, 1936, Vol. 3.

2. E. B. McLeod. The explicit solution of a free boundary problem involving surface tension. Journal of Rational Mechanics and Analysis, 1955, Vol. 4, No. 4.

3. M. I. Gurevich. Influence of capillary forces on the compressibility factor of a jet. PMM, 1961, Vol. 25, Issue 6.

4. L. Prandtl'. Hydroaeromechanics. Foreign Literature Press, 1949.

5. N. Ye. Kochin, I. A. Kibel' and N. V. Roze. Theoretical hydromechanics. Vol. 1, State Press for Technical and Theoretical Literature, 1948.

ON THE RESISTANCE OF A FLAT PLATE PERPENDICULAR TO A HYPERSONIC FLOW OF A RAREFIED GAS

O. G. Fridlender

(Moscow)

There is considered an almost free molecule flow with the primary collisions of the reflected and incident molecules taken into account. The formula for the distribution of pressure along flat plates of arbitrary form in plan is obtained in the form of simple integral and for round and polygonal plates – in explicit form. By numerical integration there is found the value C_x for a round plate.

The calculation of primary collisions of reflected and incident molecules in almost free-molecule flows, is found in works [1-4] and others devoted to this subject. Proceeding from assumptions taken in these works, we shall use the method proposed in work [5].

We shall consider in an almost free-molecule flow (Knudsen number $K \geq 1$) at high speeds (Mach number $M \geq 1$) the influence of primary collisions on aerodynamic properties of plates having one characteristic linear dimension. We shall assume the temperature of wall of an order of temperature in an undisturbed flow and constant ($T_w \sim T_\infty$, $T_w = \text{const}$), and coefficient of accommodation $\alpha \approx 1$, then it may be assumed that the incoming molecules with a speed V_∞ collide

with the stationary reflected molecules (since $V_w \ll V_\infty$); collisions between the reflected molecules may be ignored. Owing to the collisions part of molecules previously which had encountered any element ds_1 of the surface now will not encounter it, and conversely, the part which earlier had not encountered it will be scattered and will encounter this element.

Let us consider influence of element ds_2 of flat plate on its other element ds_1. Let us assume that these elements are encountered by a flow perpendicular to plate. Assuming that the reflected molecules have a Maxwellian distribution we shall obtain density of reflected molecules for the plate equal to

$$n = n_\infty V_\infty \pi^{1/2} \beta, \qquad \beta = (2RT_w)^{-1/2}$$

This follows from law of conservation of mass

$$n_\infty V_\infty = 2n \int_{-\infty}^{\infty}\int_{-\infty}^{\infty}\int_{0}^{\infty} \pi^{-3/2}\beta^3 \times$$
$$\times \exp\left[-\beta^2 (V_x^2 + V_y^2 + V_z^2)\right] V_z \, dV_x \, dV_z \, dV_y$$

On the assumption the Knudsen K >> 1 and, consequently, in determining the number of collisions it can be assumed the number of incident and reflected molecules at any point of space is the same as in a free-molecule flow.

For determining the influence of several elements of the surface on element ds_1 it is possible to add the influence of each of them, calculated independently. Number of molecules not encountering per unit of time the element ds_1 owing to collisions with molecules reflected from element ds_2 is equal to

$$dN_{ds} = \int_0^\infty n\sigma^2 n_\infty \rho_1 V_\infty \, dx_2 \, dz, \qquad n_1 = \frac{n}{2\pi} d\omega, \qquad d\omega = \frac{\cos\chi}{R_1^2} dx_2$$
$$R_1^2 = (x_1 - x_2)^2 + (y_1 - y_2)^2 + z^2$$

Here $\pi\sigma^2$ is the cross section of collision of equivalent solid

spheres; ds_1 has the coordinates (x_1, y_1); n_2 is the density of molecules at point (x_1, y_1, z) reflected by element ds_2; $d\omega$ is the solid angle at which there is seen the element ds_2 from point (x_1, y_1, z); χ is the angle between z-axis and direction (Fig. 1) to element ds_2 with coordinates (x_2, y_2) from the point (x_1, y_1, z). Then

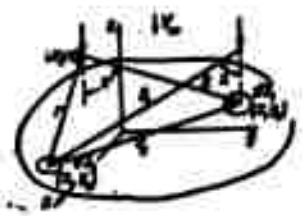

Fig. 1.

$$dN_{12}^{-} = A d\omega_2 ds_2 \int_0^{\infty} \frac{e^{-\beta r}}{r_2^2} dz = \frac{A}{r_2^2} e^{-\beta r_2} d\omega_2 ds_2 \qquad \left(A = 0.5\pi^{1/2} n_{\infty}^2 V_{m\infty}^2 \beta,\ r_2^2 = (x_1 - x_2)^2 + (y_1 - y_2)^2\right)$$

The pulse which carried these molecules is equal to

$$dP_{12}^{-} = A m V_{m\infty} r_2^{-1} e^{-\beta r_2} d\omega_2 ds_2$$

We shall determine number of molecules, which, in being dispersed in molecules reflected by element ds_2, encounter per unit of time the element ds_1. It is equal

$$dN_{12}^{+} = 2 \int_0^{\infty} \int_{-\infty}^{\infty} \int_{-\infty}^{\infty} V_{m\infty} n_{\infty} n_2 z^2 \cos\chi' d\omega' dx dy dz = \frac{2A}{\pi} ds_1 ds_2 \int_{-\infty}^{\infty} \int_{-\infty}^{\infty} \int_0^{\infty} \frac{z^2 dx dy dz}{r^2 R^4}$$
$$(R^2 = (x - x_1)^2 + (y - y_1)^2 + z^2,\ r^2 = (x - x_2)^2 + (y - y_2)^2 + z^2)$$

Here χ' is the angle between direction to element ds_1 and the z-axis and $d\omega'$ is the solid angle, at which there is seen element ds_1 from the point (xyz).

The determination directly of dN_{12}^{+} results in cumbersome calculations. They are essentially simplified if we operate now with function dN_{12}^{+}, but with $dN_{12,21}^{+} = dN_{12}^{+} + dN_{21}^{+}$ where dN_{21} is the number of molecules encountering element ds_2 per unit of time owing to scattering in molecules reflected from ds_1. (Let us note that by virtue of symmetry $dN_{12}^{+} = dN_{21}^{+}$ and, consequently, $dN_{12,21} = 2dN_{12}^{+}$.) Then

$$dP_{12,21}^{+} = \frac{2AmV_{\infty}}{\pi} d\omega_2 ds_2 \int_{-\infty}^{\infty} \int_{-\infty}^{\infty} \int_0^{\infty} \left(\frac{z^2}{r^2 R^4} + \frac{z^2}{r^4 R^2}\right) dx dy dz$$

We shall introduce the spherical coordinates

$$x - x_1 = r\sin\Phi\cos\varphi, \qquad y - y_1 = r\sin\Phi\sin\varphi, \qquad z = r\cos\Phi$$
$$x_1 - x_0 = r_0\cos\varphi_0, \qquad y_1 - y_0 = r_0\sin\varphi_0$$

Here i is equal to 1 or 2 for first and second integral, respectively. Integrating over r and over φ, we shall obtain

$$dP_{12}^{+}{}_{21} = 0.4\pi m V_\infty \frac{dx_1 dz_1}{r_0}\int_0^{\pi/2}\cos^4\Phi\sin\Phi\,d\Phi = 1.6\pi m V_\infty \frac{dx_1 dz_1}{r_0}$$

Since $dP_{12}{}^{+}{}_{21} = 2dP_{12}^{+}$, then

$$dP_{12}^{+} = 0.4\pi^{1/2}\sigma^2 m n_\infty^1 V_\infty^2 \beta \frac{dx_1 dz_1}{r_0}$$

Thus, the pulse being obtained by element ds_1 per unit of time will decrease from collision with molecules scattered by the element ds_2 by a magnitude $dP_{12}^{-} - dP_{12}^{+}$. The total decrease in pressure in comparison to pressure in free-molecule flow at any point of arbitrary flat plate being flowed-around by a flow perpendicular to its plane, owing to the primary collisions is

$$\Delta P = k_p\iint_D \frac{dx_1}{r_0} = k_p\int_0^{2\pi} R_1(\varphi)\,d\varphi, \quad k_p = 0.1\pi^{1/2}\sigma^2 m n_\infty V_\infty \beta = \tag{1}$$
$$= 0.0787\,\frac{m n_\infty V_\infty^2}{2}\,\frac{S}{\lambda}\left(\frac{T_\infty}{T_w}\right)^{1/2}, \quad S = \beta V_\infty = M\left(\frac{\pi}{2}\right)^{1/2}, \quad \lambda = \frac{1}{\sqrt{2}\,\pi\sigma^2 n_\infty}$$

Here φ is the angle of polar system of coordinates with center at point, where we calculate the correction, $R_1 = R_1(\varphi)$ – equation of boundary of plate in the same system of coordinates. We note that in the calculation of correction for the energy yielded per unit of surface per unit of time, we shall

$$\Delta E = 0.5\,V_\infty \Delta P$$

Proceeding in (1) to the system of coordinates r_1, φ_1 independent of the fact where we calculate correction, we shall obtain

$$\Delta P = k_p\int_0^{2\pi} R_1(\varphi(\varphi_1))\frac{d\varphi}{d\varphi_1}\,d\varphi_1 \tag{2}$$

Fig. 2.

The relationship between R_1, φ and φ_1 is given by the expressions (Fig. 2)

$$R_1^2(\varphi(\varphi_1)) = r_1^2(\varphi_1) + r_0^2 - 2r_1(\varphi_1) r_0 \cos(\varphi - \varphi_0) \qquad \operatorname{tg}\varphi = \frac{r_1(\varphi_1)\sin\varphi_1 - r_0\sin\varphi_0}{r_1(\varphi_1)\cos\varphi_1 - r_0\cos\varphi_0}$$

Here $(r_0\varphi_0)$ are coordinates of the point at which there are calculated the correction, and $r_1(\varphi_1)$ is the boundary of plate in the new system of coordinates. Let us consider examples.

1. After taking for the round plate with radius a for a stationary system of coordinates the system with origin at center of circle, we shall transform expression (2) to the form

$$\Delta P(r_0) = k_p \int_0^{2\pi} \frac{a^2 - a r_0 \cos\varphi_1}{\sqrt{r_0^2 + a^2 - 2ar_0\cos\varphi_1}}\, d\varphi_1$$

At the points $r_0 = 0$ and $r_0 = a$ respectively we have

$$\Delta P(0) = 2\pi a k_p, \qquad \Delta P(a) = 4ak_p$$

In the remaining by substitution $\varphi_1 = 2\$ - \pi$ we shall reduce it to well-known standard forms of Legendre elliptical integrals

$$\Delta P(r_0) = 2k_p\left[(a - r_0)K(b^2/_0) + (a + r_0)E(b^2/_0)\right]. \qquad \left(b^2 = \frac{4ar_0}{(a + r_0)^2}\right)$$

For C_x of the plate the calculations give

$$C_x = C_{x0} - 0.220\,\frac{M}{K}\sqrt{\frac{\pi T_w}{2T_\infty}} \qquad \left(K = \frac{\lambda}{a}\right)$$

Here C_{x0} is the drag coefficient in a free-molecule flow. This agrees with results which earlier were obtained in work [6] with the same assumptions but by a somewhat different method.

2. In case of polygon plates expression (1) is integrated in explicit form.

Since equation of a side of a polygon or of its extension is

$$R_i(\varphi) = \left|\frac{h_i}{\sin(\varphi - \alpha_i)}\right| \qquad (3)$$

where $|h_i|$ is the distance from origin of coordinates to the side or its extension and the vector h_i is directed from the origin of coordinates to boundary and α_i is the angle of slope of edges, then for an n-square we have

$$\Delta P = k_p \sum_{s=1}^{s'} |h_s| [\ln \operatorname{tg} 0.5(\varphi_{s+1} - \alpha_s) - \ln \operatorname{tg} 0.5(\varphi_s - \alpha_s)] - k_p \sum_{q=s'}^{n} |h_q| [\ln \operatorname{tg} 0.5(\varphi_{q+1} - \alpha_q) - \ln \operatorname{tg} 0.5(\varphi_q - \alpha_q)] \quad (4)$$

where the subscript s pertains to edges, for which $1/2\pi \leq \arg h_s < 3/2\pi$, and the subscript q – to edges for which $3/2\pi \leq \arg h_q < 5/2\pi$, furthermore, we assume that $0 \leq \varphi_s, \varphi_q < 2\pi$ (here φ_i is the argument of the radius-vector, directed to points of n-square) and $0 \leq \alpha_s, \alpha_q < 2\pi$.

The author is grateful to M. N. Kogan for his constant direction and numerous advices and to A. V. Zhbakovoy who made most of the calculations.

Submitted
23 October 1962

Literature

1. M. Heineman. Theory of drag in highly rarefied gases. Comm. Appl. Math., 1948, Vol. 1, No. 3. (Russian Translation: Foreign Literature Press. Collection of Articles "Mechanics," 1951, Issue 2).

2. M. Lunc and I. Lubonski. La perturbation de lecoulement moleculaire libre, produite par un obstacle. Bull, Acad. Polon. sci., Cl. IV, 1957, Vol. 5, No. 1. (Russian Translation: Collection "Mechanics," 1958, Issue 2.)

3. V. C. Liu. On pitot pressure in an almost free molecule flow. A physical theory for rarefied gas flow. J. Aero-Space Sci., 1958, Vol. 25, No. 2. (Russian Translation: Collection "Mechanics," 1959, Issue 4.)

4. V. C. Liu. On the drag of a flat plate at zero incidence in an almost free molecule flow. J. Fluid Mec., 1959, Vol. 5, No. 3. (Russian Translation: Collection "Mechanics," 1960, Issue 1.)

5. M. N. Kogan. Theorem of reversibility for almost free molecule flows. DAN SSSR, 1962, Vol. 144, No. 6.

6. V. A. Perepukhov. On drag of flat plate in a flow of strongly rarefied gas. ZhVM and MF, 1961, Vol. 1, No. 4.

ON THE INTERACTION OF PERTURBATIONS WITH SHOCK WAVE IN A ONE-DIMENSIONAL TRANSIENT MOTION OF GAS

Zh. S. Sislyan

(Moscow)

We shall consider one-dimensional transient flow of gas caused by motion of a piston moving in a long cylindrical tube with variable speed. We shall assume that speed of piston in considered interval of motion differs little from certain constant value u_p, i.e., we shall assume that

$$\dot{x}(t) = u_p[1 + \varepsilon X'(t)] \tag{1}$$

Here $x = x(t)$ is the law of motion of piston (point signifies differentiation with respect to time), ε is a small magnitude characterizing deviation of value of speed of piston from the constant, and function $X'(t)$ has in the considered interval of motion an order of unity. By virtue of the made assumption the speed $D(t)$ of shock wave developing immediately after beginning of motion of piston also moving away piston at a variable speed will also differ little from a certain constant value U (corresponding to motion of piston with constant speed u_p)

$$D(t) = U + \varepsilon D'(t) \qquad (2)$$

For determining a perturbed motion of gas being found between piston and shock wave, we shall use differential equations of one-dimensional nonisentropic flow of the gas

$$\frac{\partial p}{\partial t} + u\frac{\partial p}{\partial x} + \rho\frac{\partial u}{\partial x} = 0, \quad \rho\frac{\partial u}{\partial t} + \rho u\frac{\partial u}{\partial x} + \frac{\partial p}{\partial x} = 0, \quad \frac{\partial}{\partial t}\frac{p}{\rho^\gamma} + u\frac{\partial}{\partial x}\frac{p}{\rho^\gamma} = 0 \qquad (3)$$

and conditions by which there are associated parameters of gas from both sides of shock wave

$$\rho_1(D-u_1) = \rho_2(D-u_2), \quad p_1(D-u_1)^2 + p_1 = p_2(D-u_2)^2 + p_2 \qquad (4)$$
$$\frac{(D-u_1)^2}{2} + \frac{\gamma}{\gamma-1}\frac{p_1}{\rho_1} = \frac{(D-u_2)^2}{2} + \frac{\gamma}{\gamma-1}\frac{p_2}{\rho_2}$$

The subscripts 1 and 2 designate parameters of gas ahead of and behind the shock wave. The magnitudes u, p and ρ are respectively the speed, pressure and density of gas, and γ is the ratio of the heat capacities. The gas ahead shock wave is at rest ($u_1 = 0$). The functions u_2, p_2 and ρ_2, characterizing motion behind shock wave we shall seek in the form:

$$u_2 = u_2^\circ(1 + \varepsilon u + \ldots), \quad p_2 = p_2^\circ(1 + \varepsilon p + \ldots), \quad \rho_2 = \rho_2^\circ(1 + \varepsilon\rho + \ldots) \qquad (5)$$

Here u_2°, p_2° and ρ_2° are constant and correspond to the state of gas behind shock wave during motion of piston with a constant speed.

Substituting expressions (5) in equations (3) and ignoring terms higher than first order in ε, we shall obtain the following system of linear equations for determining the functions u, p and ρ

$$\frac{\partial p}{\partial t} + u_2^\circ\left(\frac{\partial p}{\partial x} + \frac{\partial u}{\partial x}\right) = 0, \quad u_2^\circ\frac{\partial u}{\partial t} + u_2^{\circ 2}\frac{\partial u}{\partial x} + \frac{a_2^{\circ 2}}{\gamma}\frac{\partial \rho}{\partial x} = 0 \qquad (6)$$
$$\frac{\partial \rho}{\partial t} + u_2^\circ\frac{\partial \rho}{\partial x} - \gamma\left(\frac{\partial p}{\partial t} + u_2^\circ\frac{\partial p}{\partial x}\right) = 0 \quad \left(a_2^{\circ 2} = \frac{\gamma p_2^\circ}{\rho_2^\circ}\right)$$

The common solution of this system containing three arbitrary functions has the form

$$p = \gamma (F_1[(u_0^\circ + a_0^\circ)t - x] + F_2[x - (u_0^\circ - a_0^\circ)t])$$
$$\rho = F_1[(u_0^\circ + a_0^\circ)t - x] + F_2[x - (u_0^\circ - a_0^\circ)t] + F_3(x - u_0^\circ t) \qquad (7)$$
$$u = \frac{1}{M_0^\circ}(F_1[(u_0^\circ + a_0^\circ)t - x] - F_2[x - (u_0^\circ - a_0^\circ)t]) \quad \left(M_0^\circ = \frac{u_0^\circ}{a_0^\circ}\right)$$

We shall linearize boundary conditions at the shock wave, substituting in (4) expressions (2) and (5), we shall obtain

$$D'\left(1 - \frac{\rho_1}{\rho_0^\circ}\right) - u_0^\circ u + p(U - u_0^\circ) = 0$$
$$p_0^\circ p + \rho_0^\circ p (U - u_0^\circ)^2 - 2\rho_0^\circ u_0^\circ u (U - u_0^\circ) = 0 \qquad (8)$$
$$-u_0^\circ D' - u_0^\circ u (U - u_0^\circ) + \frac{\gamma}{\gamma - 1}\frac{p_0^\circ}{\rho_0^\circ}(p - \rho) = 0$$

where in the adopted approximation it suffices, that these conditions took place on the straight line x = Ut. Substituting under conditions (8) expressions for p, ρ and u from (7), we have

$$\left(1 - \frac{\rho_1}{\rho_0^\circ}\right) D' + (U - u_0^\circ - a_0^\circ) F_1 + (U - u_0^\circ + a_0^\circ) F_2 + (U - u_0^\circ) F_3 = 0$$
$$(U - u_0^\circ - a_0^\circ)^2 F_1 + (U - u_0^\circ + a_0^\circ)^2 F_2 + (U - u_0^\circ)^2 F_3 = 0 \qquad (9)$$
$$\left(\frac{p_0^\circ}{\rho_0^\circ} - 1\right)(U - u_0^\circ) D' + a_0^\circ (U - u_0^\circ - a_0^\circ) F_1 - a_0^\circ (U - u_0^\circ + a_0^\circ) F_2 + \frac{a_0^{\circ 2}}{\gamma - 1} F_3 = 0$$

Eliminating D' and F_3, we shall obtain

$$\lambda F_1 - F_2 = 0, \qquad \lambda = \frac{M_1^\circ(\beta M_0 - 1) - 1}{M_1^\circ(\beta M_0 + 1) + 1} \qquad (10)$$
$$\left(M_1 = \frac{U}{a_0^\circ}, M_0 = \frac{U - u_0^\circ}{a_0^\circ} = \left[\frac{\mu^2 M_1^2 + (1 - \mu^2)}{M_1^2(1 + \mu^2) - \mu^2}\right]^{\frac{1}{2}}, \mu^2 = \frac{\gamma - 1}{\gamma + 1}\right)$$

From (10) and the first equation (7) it is evident that magnitude λ is the reflecting of perturbations from shock wave equal to ratio of amplitude of perturbation reflected from shock wave, to amplitude of perturbation overtaking it. In Figures 1 and 2 there are given curves of variation of λ for different values of γ and M_1. From an analysis of the curves it is evident that λ is negative, i.e., reflection always occurs with change in the sign of the perturbation. Furthermore the magnitude $|\lambda|$ is small, especially at small M_1 and γ is not very close to unity, and for a given value of γ asymptotically

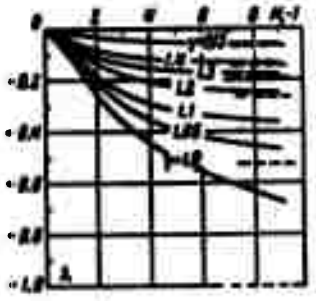

Fig. 1.

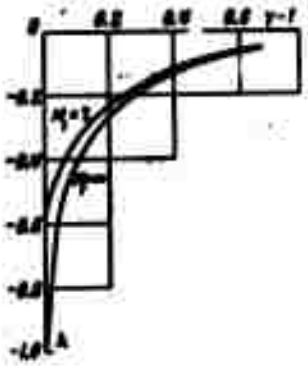

Fig. 2.

tends to a certain constant value when $M_1 \to \infty$. It is important to note also that the coefficient λ is fairly sensitive to change of magnitude γ; in absolute value λ increases with decrease of γ especially for values of γ, close to unity. At $M_1 = \infty$ and $\gamma = 1$ coefficient λ reverts to -1, i.e., the perturbation are reflected, changing the sign and maintaining its own magnitude. At small values of M_1 for λ there takes place the following formula

$$\lambda = -\frac{1-4\varphi^2}{4}(M_1-1)^2$$

i.e., magnitude λ has an order $(M_1 - 1)^2$. The curves for λ are tangent to axis of abscissas at origin of coordinates.

We shall determine the functions F_1, F_2, F_3 and D'. From (1) and third equation (7) we have

$$\varepsilon = \frac{1}{M_2^2}[F_1(t) - F_1(0)] = X'(t) \tag{11}$$

Eliminating F_2 from relationships (10) and (11), we shall obtain one equation for determining the function F_1

$$[F_1(\tau) - \lambda F_1(k\tau) = M_2^2 X'(\tau) \tag{12}$$

where there are introduced the designations

$$\tau = (1+M_2)t, \quad k = \frac{1-M_2}{1+M_2}, \quad 0 < k < 1$$

The unique limited solution of equation (12) is following series [1]

$$F_1(\tau) = M_0^2 \sum_{n=0}^{\infty} \lambda^n X^n(k^n\tau) \tag{13}$$

For functions F_2, F_3 and D' we have

$$F_0(\tau) = M_0^2 \sum_{n=1}^{\infty} \lambda^n X^n(k^n\tau) \tag{14}$$

$$F_0\left(\frac{1-k}{2}\tau\right) = -\left(\frac{1+M_0}{M_0}\right)^2 M_0^2 \left(1+\frac{k}{2}\right)^2 \sum_{n=1}^{\infty} \lambda^n X^n(k^n\tau) \tag{15}$$

$$\left(1-\frac{\rho_0}{\rho_1}\right) D' = u_p \frac{1+M_0}{M_0}\left(1+\frac{k}{2}\right) \sum_{n=1}^{\infty} \lambda^n X^n(k^n\tau) \tag{16}$$

By virtue of smallness of reflection λ at approximate determination of field of flow between piston and shock wave it is possible to ignore the influence of the reflected perturbations. In this method of approximation the flow behind a curvilinear compression wave is assumed approximately a simple wave (Riemann wave) in which entropy and one of characteristic parameters have constant values equal to their values at initial point of path of piston. A generalization of this method considering the variability of entropy in flow and its vorticity after curvilinear shock wave in a one-dimensional transient motion is given, for example by Yu. S. Zav'yalov [2].

The author thanks S. S. Grigoryan for valuable advice.

Submitted
3 January 1963

Literature

1. G. G. Chernyy. Gas flows with a high supersonic speed. Fizmatgiz, 1959.

2. Yu. S. Zav'yalov. On possible generalizations of method of compression wave and flow of rarefaction. Scientific conference on theoretical and applied question of mathematics and mechanics. Tomsk, Tomsk Univ. Press, 1960, p. 93-95.

ABOUT ESTABLISHED MOTION OF ELECTROCONDUCTING FLUID IN A RECTILINEAR CHANNEL DURING PRESENCE OF TRANSVERSE MAGNETIC FIELD

O. A. Berezin

(Leningrad)

We consider established motion of electroconducting fluid in a rectilinear channel whole lateral walls ($y = \pm a$) are ideally conducting, and the upper and lower ($z = \pm b$) are nonconducting. There is perpendicular to upper and lower walls of channel the applied constant transverse magnetic field $B_z = B_0$, and through lateral walls of channel there is passed the direct current $i_y = i_0$, relating to unit of length of the electrodes. This problem at $i_0 = 0$ also of ideally conducting walls of channel has been solved by Ya. S. Uflyand [1], and for nonconducting walls by Shercliff [2]. In work by G. A. Grinberg [3] the solution of indicated problem is reduced to the solution of integral equation containing double series in MacDonald functions.

Below the solution of problem reduces to the solution of one infinite system of algebraic equations, which may be solved by method of successive approximations, and also there is given an approximate solution at large values of Hartman number.

Assuming the induced magnetic field and speed of flow having only one component along the x-axis the equation of magnetohydrodynamics may be presented in the form

$$\frac{c^2}{4\pi\sigma\mu}\left(\frac{\partial^2 B_z}{\partial x^2}+\frac{\partial^2 B_z}{\partial y^2}\right)+B_0\frac{\partial v_z}{\partial x}=0,\qquad \eta\left(\frac{\partial^2 v_z}{\partial x^2}+\frac{\partial^2 v_z}{\partial y^2}\right)+\frac{B_0}{4\pi\mu}\frac{\partial B_z}{\partial x}=-q,\qquad p+\frac{B_z^2}{8\pi\mu}=p_0-qx \tag{1}$$

Here p is the pressure, σ is the conductivity of medium, η is the coefficient of viscosity, c is the velocity of light, μ is the magnetic permeability.

Here electric field strength has the components

$$E_x=0,\qquad E_y=-\frac{c}{4\pi\sigma\mu}\frac{\partial B_z}{\partial x}+\frac{B_0 v_z}{c},\qquad E_z=-\frac{c}{4\pi\sigma\mu}\frac{\partial B_z}{\partial y} \tag{2}$$

We shall introduce the dimensionless magnitudes

$$v=\frac{v_z}{v_0},\qquad B=\frac{B_z}{B_0\mu_m},\qquad R_m=\frac{4\pi\sigma\mu v_0 b}{c^2}$$
$$M=\frac{B_0 b}{c}\sqrt{\frac{\sigma}{\eta}},\qquad Q=\frac{qb^2}{2\eta v_0},\qquad \xi=\frac{x}{b},\qquad \eta=\frac{y}{b},\qquad k=\frac{a}{b} \tag{3}$$

System (1) can be reduced to the form

$$\frac{\partial^2 B}{\partial\xi^2}+\frac{\partial^2 B}{\partial\eta^2}+\frac{\partial v}{\partial\xi}=0,\qquad \frac{\partial^2 v}{\partial\xi^2}+\frac{\partial^2 v}{\partial\eta^2}+M^2\frac{\partial B}{\partial\xi}=-Q \tag{4}$$

The boundary conditions for considered problem will have following form:

$$v=0,\quad \frac{\partial B}{\partial\eta}=0 \text{ when } \begin{cases}\xi=\pm 1\\ \eta=\pm k\end{cases}$$
$$B=\tfrac{1}{2}J \text{ when } \xi=1,\qquad B=-\tfrac{1}{2}J \text{ when } \xi=-1,\qquad \left(J=\frac{4\pi\mu_0}{B_0\mu_m}\right) \tag{5}$$

The solution of problem will be sought in the form

$$v=\left(\frac{Q}{M^2}+\frac{J}{2}\right)M\frac{\operatorname{ch}M-\operatorname{ch}M\xi}{\operatorname{sh}M}+\operatorname{ch}\frac{M}{2}\xi V(\xi,\eta)+\operatorname{sh}\frac{M}{2}\xi W(\xi,\eta)$$
$$B=\left(\frac{Q}{M^2}+\frac{J}{2}\right)\frac{\operatorname{ch}M\xi}{\operatorname{sh}M}-\frac{Q}{M^2}\xi-\frac{1}{M}\operatorname{sh}\frac{M}{2}\xi V(\xi,\eta)-\frac{1}{M}\operatorname{ch}\frac{M}{2}\xi W(\xi,\eta) \tag{6}$$

Substituting (6) in (4), for V and W we shall obtain two separate equations

$$\frac{\partial^2 V}{\partial \xi^2} + \frac{\partial^2 V}{\partial \eta^2} - \frac{M^2}{4} V = 0, \qquad \frac{\partial^2 W}{\partial \xi^2} + \frac{\partial^2 W}{\partial \eta^2} - \frac{M^2}{4} W = 0 \tag{7}$$

Solution of system (7) we take in the form

$$V = \left(\frac{Q}{M^2} + \frac{J}{2}\right)\frac{M}{\operatorname{sh} M}\sum_{n=1}^{\infty} c_n \frac{\operatorname{ch} \lambda_n \eta}{\operatorname{ch} \lambda_n b} \cos\frac{(2n-1)\pi\xi}{2}, \qquad \lambda_n = \frac{\gamma (2n-1)^2 \pi^2 + M^2}{2}$$

$$W = \left(\frac{Q}{M^2} + \frac{J}{2}\right)\frac{M}{\operatorname{sh} M}\sum_{n=1}^{\infty} b_n \frac{\operatorname{ch} \mu_n \eta}{\operatorname{ch} \mu_n b} \sin n\pi\xi, \qquad \mu_n = \frac{\gamma 4n^2 \pi^2 + M^2}{2} \tag{8}$$

The constants c_n and b_n were determined from conditions (5); we have

$$\operatorname{sh} M\xi - \operatorname{sh} M = \operatorname{sh}\frac{M}{2}\xi \sum_{n=1}^{\infty} c_n \cos\frac{(2n-1)\pi\xi}{2} + \operatorname{ch}\frac{M}{2}\xi \sum_{n=1}^{\infty} b_n \sin n\pi\xi \tag{9}$$

$$\operatorname{sh}\frac{M}{2}\xi \sum_{n=1}^{\infty} c_n \lambda_n \operatorname{th} \lambda_n b \cos\frac{(2n-1)\pi\xi}{2} + \operatorname{ch}\frac{M}{2}\xi \sum_{n=1}^{\infty} b_n \mu_n \operatorname{th} \mu_n b \sin n\pi\xi = 0 \tag{10}$$

Multiplying each of equations (9) and (10) respectively by

$$\cos\frac{(2j-1)\pi\xi}{2} \operatorname{sch}\frac{M\xi}{2}, \qquad \cos\frac{(2j-1)\pi\xi}{2} \operatorname{cosech}\frac{M\xi}{2}$$

and integrating results in ξ from -1 to +1, we shall obtain

$$\varphi_{0j} = c_j + \sum_{n=1}^{\infty} b_n \varphi_{nj}, \qquad c_j \lambda_j \operatorname{th} \lambda_j b + \sum_{n=1}^{\infty} b_n \mu_n \operatorname{th} \mu_n b \varphi_{nj} = 0 \tag{11}$$

Here

$$\varphi_{0j} = \int_{-1}^{1} \frac{\operatorname{ch} M\xi - \operatorname{ch} M}{\operatorname{ch}(M\xi/2)} \cos\frac{(2j-1)\pi\xi}{2} d\xi$$

$$\varphi_{nj} = \int_{-1}^{1} \operatorname{th}\frac{M}{2}\xi \sin n\pi\xi \cos\frac{(2j-1)\pi\xi}{2} d\xi, \qquad \varphi_{nj} = \int_{-1}^{1} \operatorname{cth}\frac{M}{2}\xi \sin n\pi\xi \cos\frac{(2j-1)\pi\xi}{2} d\xi$$

Excluding c_j from (11), for determining the unknown constants b_j we shall obtain one infinite system of algebraic equations

$$\varphi_{0j} = \sum_{n=1}^{\infty} b_n \left(\varphi_{nj} - \frac{\mu_n \operatorname{th} \mu_n b}{\lambda_j \operatorname{th} \lambda_j b} \varphi_{nj}\right) \tag{12}$$

The determining of coefficients c_n and b_n may be reduced to the solution of one integral equation as follows.

Equality (10) may be satisfied after assuming

$$\sum_{n=1}^{\infty} c_n \lambda_n \operatorname{th} \lambda_n k \cos \frac{(2n-1)\pi\xi}{2} = \varphi(\xi) \operatorname{ch} \frac{M}{2}\xi$$
$$\sum_{n=1}^{\infty} b_n \mu_n \operatorname{th} \mu_n k \sin n\pi\xi = -\varphi(\xi) \operatorname{sh} \frac{M}{2}\xi \qquad (13)$$

Here $\varphi(\xi)$ is an arbitrary even function, vanishing at $\xi = \pm 1$. Hence

$$c_n = \frac{1}{\lambda_n \operatorname{th} \lambda_n k} \int_{-1}^{1} \varphi(t) \operatorname{ch} \frac{M}{2} t \cos \frac{(2n-1)\pi t}{2} dt$$
$$b_n = -\frac{1}{\mu_n \operatorname{th} \mu_n k} \int_{-1}^{1} \varphi(t) \operatorname{sh} \frac{M}{2} t \sin n\pi t \, dt \qquad (14)$$

Substituting (14) in (9), for determining the unknown function $\varphi(t)$ we shall obtain the integral equation

$$\operatorname{ch} M\xi - \operatorname{ch} M = \operatorname{ch} \frac{M}{2}\xi \sum_{n=1}^{\infty} \int_{-1}^{1} \frac{\operatorname{ch}(Mt/2)\varphi(t)}{\lambda_n \operatorname{th} \lambda_n k} \cos \frac{(2n-1)\pi\xi}{2} \cos \frac{(2n-1)\pi t}{2} dt -$$
$$- \operatorname{sh} \frac{M}{2}\xi \sum_{n=1}^{\infty} \int_{-1}^{1} \frac{\operatorname{sh}(Mt/2)\varphi(t)}{\mu_n \operatorname{th} \mu_n k} \sin n\pi\xi \sin n\pi t \, dt \qquad (15)$$

Let us consider case of larger values of Hartman number M. In this case $\operatorname{th} \lambda_n k \approx \operatorname{th} \mu_n k \approx 1$. We shall assume

$$\int_{-1}^{1} \varphi(t) \operatorname{ch} \frac{Mt}{2} \sum_{n=1}^{\infty} \frac{1}{\lambda_n} \cos \frac{(2n-1)\pi\xi}{2} \cos \frac{(2n-1)\pi t}{2} dt = (\operatorname{ch} M\xi - \operatorname{ch} M) \operatorname{ch} \frac{M}{2}\xi \qquad (16)$$

$$\int_{-1}^{1} \varphi(t) \operatorname{sh} \frac{Mt}{2} \sum_{n=1}^{\infty} \frac{1}{\mu_n} \sin n\pi\xi \sin n\pi t \, dt = (\operatorname{ch} M\xi - \operatorname{ch} M) \operatorname{sh} \frac{M}{2}\xi \qquad (17)$$

In the fulfillment of conditions (16) and (17) equation (15) is identically satisfied. Multiplying equation (16) by $\cos[(2j - 1)\pi\xi/2]$, and equation (17) by $\sin j\pi\xi$ and integrating in ξ from -1 to +1, we shall obtain

$$\frac{2(2j-1)\operatorname{ch}{}^{1}/_{2}M(-1)^{j+1}}{8M^{3}+(2j-1)^{3}\pi^{3}}-\frac{4(\operatorname{ch}M-{}^{1}/_{2})(2j-1)\pi\operatorname{ch}{}^{1}/_{2}M(-1)^{j+1}}{M^{4}+(2j-1)^{4}\pi^{4}}=$$

$$=\frac{1}{I_{j}}\int_{-1}^{1}\varphi(t)\operatorname{ch}\frac{Mt}{2}\cos\frac{(2j-1)\pi t}{2}\,dt \qquad (18)$$

$$\frac{4j\pi\operatorname{ch}{}^{1}/_{2}M(-1)^{j+1}}{8M^{3}+4j^{3}\pi^{3}}-\frac{8(\operatorname{ch}M+{}^{1}/_{2})j\pi\operatorname{ch}{}^{1}/_{2}M(-1)^{j+1}}{M^{4}+4j^{4}\pi^{4}}=$$

$$=\frac{1}{I_{j}}\int_{-1}^{1}\varphi(t)\operatorname{ch}\frac{Mt}{2}\sin j\pi t\,dt \qquad \left(\varphi(t)=8M^{3}\operatorname{ch}\frac{3M}{2}f(t)\right)$$

At large M approximately we have

$$\int_{-1}^{1}f(t)\operatorname{ch}\frac{Mt}{2}\cos\frac{(2j-1)\pi t}{2}\,dt=\frac{(2j-1)\pi(-1)^{j}}{[8M^{3}+(2j-1)^{3}\pi^{3}]\sqrt{M^{2}+(2j-1)^{2}\pi^{2}}} \qquad (19)$$

and also

$$\int_{-1}^{1}f(t)\operatorname{ch}\frac{Mt}{2}\sin j\pi t\,dt=\frac{2j\pi(-1)^{j}}{(8M^{3}+4j^{3}\pi^{3})\sqrt{M^{2}+4j^{2}\pi^{2}}} \qquad (20)$$

We assume

$$f(t)=\operatorname{ch}\frac{Mt}{2}\sum_{m=1}^{\infty}A_{m}\cos\frac{(2m-1)\pi t}{2}$$

From equation (19) we find coefficients A_m, we have

$$A_{m}=\frac{(2m-1)\pi(-1)^{m}}{[8M^{3}+(2m-1)^{3}\pi^{3}]\sqrt{M^{2}+(2m-1)^{2}\pi^{2}}} \qquad (21)$$

We shall show that the function f(t) found in this manner at large M also satisfies equation (20). Using relationships

$$\frac{1}{\sqrt{M^{2}+(2m-1)^{2}\pi^{2}}}=\frac{2}{\pi}\int_{0}^{\infty}\frac{d\sigma}{\sigma^{2}+M^{2}+(2m-1)^{2}\pi^{2}} \qquad (22)$$

$$\sum_{m=1}^{\infty}\frac{(2m-1)(-1)^{m}}{8M^{3}+(2m-1)^{3}\pi^{3}}\cos\frac{(2m-1)\pi t}{2}-\sum_{m=1}^{\infty}\frac{(2m-1)(-1)^{m}}{\sigma^{2}+M^{2}+(2m-1)^{2}\pi^{2}}\times$$

$$\times\cos\frac{(2m-1)\pi t}{2}=\frac{1}{4\pi}\left[\frac{\operatorname{ch}({}^{1}/_{2}\sqrt{M^{2}+\sigma^{2}}t)}{\operatorname{ch}({}^{1}/_{2}\sqrt{M^{2}+\sigma^{2}})}-\frac{\operatorname{ch}{}^{1}/_{2}Mt}{\operatorname{ch}{}^{1}/_{2}M}\right]$$

equation (20) may be transformed to the form

$$\frac{1}{\pi}\int_{0}^{\infty}\frac{d\sigma}{\sigma^{2}-8M^{3}}\int_{0}^{1}\operatorname{ch}\frac{Mt}{2}\sin j\pi t\left\{\frac{\operatorname{ch}({}^{1}/_{2}\sqrt{M^{2}+\sigma^{2}}t)}{\operatorname{ch}({}^{1}/_{2}\sqrt{M^{2}+\sigma^{2}})}-\frac{\operatorname{ch}{}^{1}/_{2}Mt}{\operatorname{ch}{}^{1}/_{2}M}\right\}dt=$$

$$=\frac{2j\pi(-1)^{j}}{[8M^{3}+4j^{3}\pi^{3}]\sqrt{M^{2}+4j^{2}\pi^{2}}} \qquad (23)$$

Using the concept

$$\text{th}\,\frac{Mt}{2} = 1 + 2\sum_{\nu=1}^{\infty}(-1)^{\nu}e^{-\nu Mt};$$

we shall obtain

$$\int_0^1 \text{th}\,\frac{Mt}{2}\sin j\pi t\left\{\frac{\text{ch}\,(1/2\sqrt{M^2+\sigma^2}\,t)}{\text{ch}\,(1/2\sqrt{M^2+\sigma^2})} - \frac{\text{ch}\,1/2\,Mt}{\text{ch}\,1/2\,M}\right\}dt = \tag{24}$$
$$= 4j\pi(-1)^j\left[\frac{1}{9M^2+4j^2\pi^2} - \frac{1}{M^2+\sigma^2+4j^2\pi^2}\right] + \varepsilon_j$$

Here (25)

$$\varepsilon_j = \frac{4j\pi}{\text{ch}\,1/2\sqrt{M^2+\sigma^2}}\frac{1}{M^2+\sigma^2+4j^2\pi^2} - \frac{4j\pi}{\text{ch}\,1/2\,M}\frac{1}{9M^2+4j^2\pi^2} +$$
$$+ j\pi\left\{\frac{1}{\text{ch}\,(1/2\sqrt{M^2+\sigma^2})}\sum_{\nu=1}^{\infty}(-1)^{\nu}\left[\frac{1-(-1)^j\exp(1/2\sqrt{M^2+\sigma^2})-\nu M}{(1/2\sqrt{M^2+\sigma^2}-\nu M)^2+j^2\pi^2}+\right.\right.$$
$$\left.+\frac{1-(-1)^j\exp(-1/2\sqrt{M^2+\sigma^2}-\nu M)}{(1/2\sqrt{M^2+\sigma^2}+\nu M)^2+j^2\pi^2}\right]-$$
$$\left.-\text{ch}\,\frac{3M}{2}\sum_{\nu=1}^{\infty}(-1)^{\nu}\left[\frac{1-(-1)^j\exp[M(1/2-\nu)]}{(1/2-\nu)^2M^2+j^2\pi^2}+\frac{1-(-1)^j\exp[-M(1/2+\nu)]}{(1/2+\nu)^2M^2+j^2\pi^2}\right]\right\}$$

It follows from this that ε_j has the order of first term of right-hand side of equality (24), divided by ch (1/2)M. Since M is large, then, by ignoring ε_j and substituting (24) in (23), we shall obtain the identity which had to be proved. Thus, at large M expressions for coefficients c_j and b_j in solution (8) may be written out as

$$c_j = \frac{16M^2(2j-1)\pi(-1)^j}{[9M^2+(2j-1)^2\pi^2][M^2+(2j-1)^2\pi^2]}\text{ch}\,\frac{3M}{2}$$
$$b_j = -\frac{16M^2 2j\pi(-1)^j}{(9M^2+4j^2\pi^2)(M^2+4j^2\pi^2)}\text{ch}\,\frac{3M}{2}$$

The obtained values of the coefficients c_j and b_j attest to the fact that approximately $j = 1/2(M+1)$ of the first coefficients increase linearly with the number j. A decrease of these coefficients begins from the values j, comparable with $1/2(M+1)$. This property of the series is characteristic in general, for boundary value problems, setup for equations having a small parameter with higher derivatives which is accompanied by certain calculating difficulties.

The indicated difficulties to a significant degree can be surmounted by means of G. A. Grinberg's [4] method.

Submitted
26 June 1962

Literature

1. Ya. S. Uflyand. Established flow of a conducting fluid in a rectilinear channel in the presence of transverse magnetic field. Journal of Technical Physics, 1960, No. 10, p. 1256.

2. J. A. Shercliff. Steady motion of conducting fluids in pipes under transverse magnetic fields. Proc. Cambridge Philos. Soc., 1953, No. 1, p. 49.

3. G. A. Grinberg. On established flow of conducting fluid in rectilinear tube with two nonconducting walls and two conducting, parallel to external magnetic field. PMM, 1961, Vol. 25, Issue 6.

4. G. A. Grinberg. On certain cases of the flow of conducting fluid in tubes of rectilinear cross-section located in a magnetic field. PMM, 1961, Vol. 26, Issue 1.

EXPERIMENTAL INVESTIGATION OF SPEED OF SOUND IN ARGON ON LINE OF SATURATION

I. S. Radovskiy

(Moscow)

Measurements of speed of sound in liquified argon at low temperatures have been covered in several works dedicated to this subject. However, for curve of phase equilibrium "liquid-vapor" in literature there are only a few values of speed of sound obtained experimentally near the point of hardening [1, 2].

Practically data on speed of sound in argon on line of saturation up to present are lacking.

The author made systematic measurements of speed of sound in vapor and liquid phases of argon on curve of phase equilibrium at temperatures from 83.94 to 150.65°K, i.e., from triple point to the critical. For realization of these measurements there was created experimental installation on basis of which there is assumed the method of acoustic interferometer with variable distance between radiator of ultrasonics and the reflector. Theory of method in detail is described in the literature [3, 4].

The diagram of interferometer being used is presented in Fig. 1. Basic parts of interferometer are: radiator of ultrasonics 1 (quartz

plate of X-cut with natural frequency of oscillations of about 500 kilocycles), quartzholder 2, directing glass 3, reflector 4, nut 5 and micrometric screw 6 with pitch of thread 0.5 mm, during rotation of which there is realized a vertical displacement of the reflector. Transmission of torque to micrometric screw from reversible motor is realized by glandless magnetic clutch consisting of constant magnet 7 and armature 8. The chassis of interferometer 9 is made in the form of thick-walled copper block which contributes to a rapid levelling of temperature in interferometer.

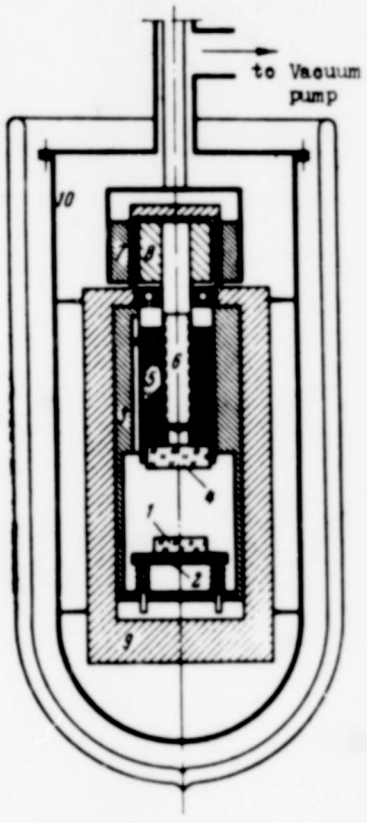

Fig. 1.

The design of installation provides for a reduction to a minimum of the heat exchange between interferometer and environment. Inside vacuum jacket 10 placed in open Dewar flask with liquid nitrogen, there is created a vacuum of an order 10^{-5} mm mercury column. Therefore, the losses of heat by interferometer reduce basically to radiation and constitute an insignificant magnitude. For their compensation there serve two constantan heaters (the main and the regulating), wound directly onto chassis of interferometer. By calculating and then experimentally there was ascertained that even with significant temperature differentials between interferometer and boiling nitrogen (order of $100^{\circ}C$) the total power of heaters does not exceed 5 w. This made it possible to conduct comparatively simply and fairly accurately the automatic regulating of the interferometer.

The temperature was measured by standard platinum resistance

thermometer on potentiometer PMS-48 with an accuracy of 0.02°C. The temperature regulation was realized by means of turning on and turning off the heater. Here a large part of thermal loss is compensated by main heater turned on constantly, and for the regulating heater there is necessary 5 to 10% of total power. The automatic turning on and turning off of heater is realized by sensitive relay RP-5 onto whose winding there is supplied the noncompensated part of voltage drop in resistance thermometer augmented by photocompensational amplifier F-16. The thermal inertia of such a regulator as a consequence of small power of heaters is insignificant, and high amplification factor of amplifier F-16 makes it possible to close and release relay contacts during a change of measured voltage drop by not more than 0.05-0.1 μv. Therefore, despite the simplicity of regulator, relative changes of temperature during experiments did not exceed ±0.005°C.

Pressure in interferometer was measured by loadpiston manometer MP-60 of class 0.05.

For the excitation of ultrasonic oscillations of the quartz there were used signals of frequency meter 121a, amplified by resonance amplifier by which simultaneously there was measured the frequency of oscillations.

The reaction of interferometer during displacement of reflector was recorded by a photocompensational amplitier F-16 and automatically was recorded by the self recorder N-16. Method of recording of reaction is presented in work [5].

Results of measurement of speed of sound are given in the table, and also in Fig. 2. In saturated vapor the speed of sound with increase of temperature of first increases and at 124.5°K passes through a maximum. With approximation to the critical temperature the

speed of sound sharply decreases attaining minimum value at the critical point.

Table

T, °K	P, kg/cm²	c, m/sec	T, °K	P, kg/cm²	c, m/sec	T, °K	P, kg/cm²	c, m/sec
				Vapor phase				
83.94	0.00	188.4	122.00	13.55	185.8	148.72	45.91	167.1
84.11	0.00	188.7	124.24	15.09	186.1	149.12	46.67	164.5
84.40	0.73	188.9	124.48	15.36	186.0	149.36	47.08	162.9
84.86	0.79	189.2	125.16	16.06	185.9	149.61	47.56	160.5
85.36	0.83	189.6	128.40	18.74	185.7	149.84	48.17	156.9
87.37	1.03	171.2	130.00	20.22	185.5	150.07	48.62	153.0
91.81	1.63	174.3	134.44	24.97	184.7	150.20	48.77	148.2
95.24	2.22	176.7	138.39	30.05	183.0	150.25	48.89	146.9
98.92	3.02	178.6	142.97	36.44	180.2	150.43	49.25	138.3
104.98	4.77	181.4	143.20	36.80	179.9	150.48	49.30	136.5
109.85	6.26	182.8	146.40	41.80	175.7	150.56	49.41	129.1
113.87	8.64	184.5	147.40	43.48	173.2	150.59	49.50	124.8
118.29	11.15	185.2	148.04	44.68	170.6	150.62	49.55	120.2
				Liquid phase				
83.94	—	865.9	93.62	—	788.5	146.40	41.56	268.6
84.12	—	864.9	95.19	—	786.1	146.62	42.02	265.0
84.39	—	863.1	97.16	—	772.5	147.78	44.20	239.8
84.78	—	860.7	97.96	2.77	768.1	148.36	45.30	227.3
85.16	—	858.2	100.16	—	750.8	149.15	46.71	201.5
85.30	—	857.1	103.96	4.40	721.5	149.63	47.79	184.4
85.44	—	856.0	112.75	8.10	647.5	150.05	48.53	169.5
85.62	—	855.9	118.49	11.27	586.6	150.38	49.12	141.5
85.84	—	853.2	125.69	16.30	531.4	150.45	49.30	134.3
85.98	—	850.2	132.03	22.[illegible]	486.9			
87.14	—	842.1	135.36	26.08	428.8	150.57	—	122.6
88.53	—	833.4	140.07	32.33	369.9	150.61	—	121.7
90.41	—	821.4	143.57	37.25	318.3	150.63	49.60	120.2

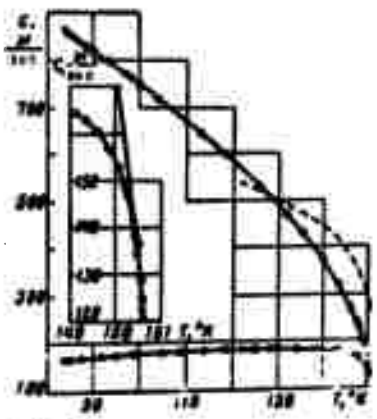

Fig. 2.

In liquid phase the speed of sound monotonically decreases from triple point to the critical. Deceleration of sound intensifies with increasing proximity to critical temperature. In interval of temperatures from 103 to 121.5°K there is ascertained a linear dependence of speed of sound in liquid phase on the temperature

$$c = c_0(1 - \alpha\Delta T) \qquad (c_0 = 748\ m/sec, \alpha = 0.0114)$$

A linear dependence c(t) was obtained also by other authors for many liquids [4, 6]. A deviation from linearity was ascertained only

in critical region and in approaching the temperature of hardening. For argon the linear dependence c(t) was found to be valid in a comparatively small interval of temperatures.

In conducting the experiments special attention was given to critical region and temperatures close to temperature of hardening.

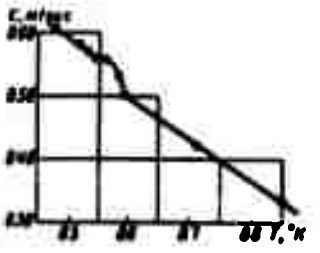

Fig. 3.

In these regions there is obtained large number of experimental points. In region close to temperature of hardening there is revealed an anomalous behavior of curve of speed of sound in liquid phase in the interval of temperatures 85.6-85.9°K (Fig. 3). The causes of anomaly are, obviously, the structural changes associated with transition from liquid state into the solid and which are accompanied, possibly by the dispersion of speed of sound.

In critical region there is ascertained the mutual location of curves of speed of sound in liquid and vapor phases. Interest toward this question is caused by the fact that in a number of works with other substances [5, 7] these curves happened to be intersecting, i.e., speed of sound in liquid phase in interval of about 0.5°C from critical point was found to be lower than speed of sound in the vapor. Yu. S. Trelin [5] explains this phenomenon by influence of admixtures of external gases, because even insignificant amount of the latter markedly decreases the speed of sound in the liquid phase.

In described experiments there was used a chemically pure argon with contents of admixtures not more than 0.02%. As can be seen in Fig. 2 an intersection of curves is not detected. In interval 0.3°C from critical point they practically coincide, but then diverge. The obtained results to a certain extent corroborate the assumption

of Yu. S. Trelin about influence of admixtures.

Total error in a major part of experiments did not exceed 0.2%.

In Fig. 2 there is plotted also curve of speed of sound in liquid phase obtained in dissertation by Adkhamov (Moscow State University, 1954) by means of calculation with the use of molecular-kinetic theory Bogolyubov. A comparison of theoretical and experimental curves shows that results of Adkhamov's calculations qualitatively correctly reflect temperature dependence of speed of sound in liquid phase of argon. However, quantitatively discrepancy between calculated and experimental data reaches more than 100%.

Submitted
11 January 1963

Literature

1. A. Itterbeek and L. Verhaegen. Measurement of the sound velocity in liquified argon and methan. Proc. Phis. Soc. B, 1949, Vol. 62, p. 800.

2. A. Itterbeek, W. Grevendonk, W. Dael and G. Forrez. The velocity of the sound in the liquid argon at high pressures. Physica, 1959, Vol. 25, No. 12, p. 1255.

3. L. Bergman. Ultrasonics and its application in science and technology. Foreign Literature Press, 1957.

4. B. B. Kudryavtsev. Application of ultraacoustic methods in the practice of physico-chemical investigations. State Press for Technical and Theoretical Literature, 1952.

5. Yu. S. Trelin. Investigation of speed of propagation of ultrasonic waves in carbon dioxide in region of liquid and gaseous state. Collection "Application of ultrasonics for investigation of matter." Edition MOPI, 1961, Issue 13.

6. V. F. Nozdrev. Application of ultrasonics in molecular physics. Fizmatgiz, 1958.

7. H. Tanneberger. Eine untersuchung des kritischen zustandes mit ultraschall. Z. Phys., 1959, Bd. 153, S. 445.

INFLUENCE OF MAGNETIC FIELD ON OPTIMUM COMPOSITION OF AN ELECTROCONDUCTIVE GAS MIXTURE

E. P. Zimin and V. A. Popov

(Moscow)

In presence of a magnetic field the electrical conductivity becomes a function of magnetic field strength and, furthermore, acquires an anisotropic character.

For a Lorentz gas, according to Spitzer [1], Ohm's law takes the following form:

$$\frac{\mathbf{j}}{\sigma_0} = \mathbf{E}_0 + \mu_0 \mathbf{W} \times \mathbf{H} - \frac{\mu_0}{n_e e} \mathbf{j} \times \mathbf{H} + \frac{1}{n_e e} \nabla p_e \qquad (1)$$

where n_e is the concentration of electrons, e is the charge of electron, p_e is the electron pressure.

Introducing Larmor frequency of electrons ω and assuming gradient of electron pressure equal to zero, equation (1) may be transformed to the form

$$\mathbf{j} + \frac{\omega\tau}{|H|} \mathbf{j} \times \mathbf{H} = \sigma_0 \mathbf{E}$$
$$\left(\omega = \frac{|e|\mu_0 H}{m}, \quad \sigma_0 = \frac{n_e e^2 \tau}{m} \right) \qquad (2)$$
$$\mathbf{E} = \mathbf{E}_0 + \mu_0 \mathbf{W} \times \mathbf{H}$$

where m is the mass of the electron, τ is the time of the free path.

The second term of left-hand side of this equation corresponds to the Hall effect.

We shall solve equation (2) with respect to j. For this purpose we shall multiply it vectorially by H

$$\mathbf{j}\times\mathbf{H}+\frac{\omega\tau}{|H|}[(\mathbf{j}\cdot\mathbf{H})\cdot\mathbf{H}-H^2\mathbf{j}]=\sigma_0\mathbf{E}_\perp\times\mathbf{H} \qquad (3)$$

Here there is used the expansion of vector of electric field strength into two components: $E_{\parallel}$ – parallel to vector of magnetic field strength H and $E_{\perp}$ – normal to it. The two terms in brackets are obtained as a result of opening of double vector product $(j \times \times H) \times H$. Further, multiplying equation (2) scalarly by H, we find

$$\mathbf{j}\cdot\mathbf{H}=\sigma_0\mathbf{H}\cdot\mathbf{E}_\parallel-\frac{\omega\tau}{|H|}(\mathbf{j}\times\mathbf{H})\cdot\mathbf{H}$$

It is obvious that mixed product is equal to zero, so that

$$(\mathbf{j}\cdot\mathbf{H})\mathbf{H}=\sigma_0 H^2\mathbf{E}_\parallel \qquad (4)$$

Substituting (3) and (4) in (2), we finally obtain

$$\mathbf{j}=\sigma_0\mathbf{E}_\parallel+\frac{\sigma_0}{1+\omega^2\tau^2}\mathbf{E}_\perp-\frac{\omega\tau\sigma_0}{1+\omega^2\tau^2}\frac{\mathbf{E}_\perp\times\mathbf{H}}{|H|}$$

The electric conductivity along magnetic field remains constant, whereas electric conductivity in transverse direction depends on magnetic field $(\sim(1+\omega^2\tau^2)^{-1})$.

It is of interest to determine condition of maximum of transverse electric conductivity of a mixture of a practically nonionizing gas (diluent) with gas having a low ionization potential admixture in the presence of a magnetic field. The problem reduces to seeking the dependence of optimum admixture from magnetic field strength.

The transverse electrical conductivity of mixture is equal to

$$\sigma_\perp = 3.85\cdot 10^{-10}\frac{\varepsilon}{(1+\omega^2\tau^2)\,Q\sqrt{T}}\frac{m_0}{cm}, \qquad \varepsilon = n_e/(n_1+n_2) \tag{5}$$

Here α is the degree of ionization of mixture, n_2 and n_1 are concentrations of the admixture and diluent, Q is the effective cross section of collisions of electrons with neutral atoms of mixture. In the case of small degrees of ionization of admixture ($x = n_e/n_2 \ll 1$), ignoring the Coulomb interaction of electron with ion, we shall obtain

$$Q = \frac{Q_1 n_1 + Q_2 n_2}{n_1+n_2} = Q_1[\varepsilon(\beta-1)+1], \qquad (\varepsilon = p_2/p,\ \beta = Q_2/Q_1)$$

where Q_1 and Q_2 are the cross sections of collisions of electron with neutral atoms of diluent and admixture respectively, p_2 is the partial pressure of admixture, p is the total pressure of the mixture. The magnitude x is determined in accordance with the Saha equation

$$x^2 = \frac{K(T)}{p}, \quad K(T) = A\left(\frac{2\pi m}{h^2}\right)^{3/2} k^{3/2}\frac{g_i g_e}{g_0}\,T^{\frac{i+3}{2}}\exp\left(-\frac{eu_i}{kT}\right)$$

Here u_i is the ionization potential of the admixture, k and h are the Boltzmann and Planck constants, i is the number of degrees of freedom, g_i g_e and g_0 are the statistical weights of the ion, electron and neutral, A is a constant depending on the selection of units of measurement of pressure. Finally we obtain

$$\sigma_\perp = \frac{3.85\cdot 10^{-10}}{Q_1\sqrt{T}}\sqrt{\frac{K(T)}{p}}\frac{\sqrt{\varepsilon[\varepsilon(\beta-1)+1]}}{[\varepsilon(\beta-1)+1]^2+\tau}, \qquad \tau = \left(\frac{\omega kT}{Q_1 vp}\right)^2$$

Here v is the mean square velocity of electrons, T is the temperature.

For determining the optimum value $\varepsilon = \varepsilon_*$ it is sufficient to find root of equation $\partial\sigma_\perp/\partial\varepsilon = 0$, which reduces to the cubic equation:

$$y^3 + 3ay + 2b = 0, \quad y = t + 1/3, \quad a = -[\tau + (\beta/3)^2], \quad b = -(\beta/3)^3, \quad t = \varepsilon_*(\beta-1) \tag{6}$$

The discriminant of this equation $D = a^3 + b^2 = -(\gamma^3 + 4/3\gamma^2 + 16/27\gamma) < 0$; therefore, it has three different real roots

$$y_n = 2\sqrt{|a|}\cos[1/3(\alpha + 2\pi n)], \quad \alpha = \arccos(-b|a|^{-3/2}) \quad (n = 1, 2, 3)$$

It is possible to show that at any γ the solution at $n = 3$ has the physical sense

$$\varepsilon = \varepsilon_*(\beta - 1) = 2\sqrt{\gamma + 4/3}\cos 1/3\alpha - 1/3$$

At relatively small and large γ we obtain the asymptotic expressions:

$$\varepsilon \sim 1 \text{ at } \gamma \ll 4/3, \quad \varepsilon \sim \sqrt{3\gamma} \text{ at } \gamma \gg 4/3$$

The limiting composition of mixture corresponds to $\varepsilon_* = 1$; using the second asymptotic expression, we can determine maximum value $\gamma_m = 1/3(\beta - 1)^2$.

In Figures 1 and 2 there are given the dependences of ε_* on γ and magnetic field strength H for mixtures of a number of gases with Cs (at pressures – 0.1, 1, 2, 5 and 10.0 atm and T = 3000°K in Fig. 2).

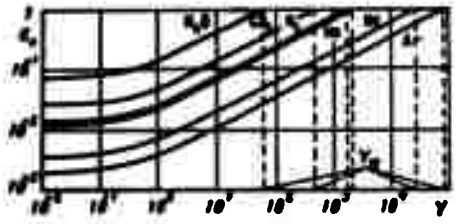

Fig. 1.

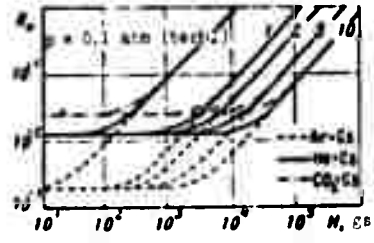

Fig. 2.

At a fixed pressure value beginning from a certain value H at which optimum concentration of a readily ionized admixture is still relatively small, the latter practically ceases to depend on nature of diluent. With a decrease in pressure marked peculiarity begins to manifest itself at smaller values of magnetic field strength. At specific values of magnetic field strength H_m optimum value of relative concentration of the readily ionized admixture becomes equal to unity

i.e., at $H > H_m$ question about determining the optimum composition of mixture loses sense. Under these conditions the pure vapors of the readily ionized admixture possess maximum electric conductivity.

The dependence of the ratio of maximum transverse electric conductivity (corresponding to optimum composition of mixture) (σ_m) to maximum electric conductivity at $H = 0(\sigma_{0m})$ on the magnetic field strength is determined by expression (the subscript 1 is omitted):

$$\chi = \frac{\sigma_m}{\sigma_{0m}} = \frac{2(1+\varepsilon)\sqrt{\gamma}}{(1+\varepsilon)^2+\gamma}$$

We note that σ_{0m} is determined by value $\varepsilon_* = (\beta - 1)^{-1}$, corresponding to equation [2]

$$\frac{\partial \sigma_0}{\partial \varepsilon} = 0 \qquad \left(\varepsilon_* \sim \frac{\sqrt{\gamma}}{1+\varepsilon(\beta-1)}\right)$$

Obviously, at large γ

$$\chi = 1.14\gamma^{-1/4} \qquad (\chi_m = 1.5(\beta-1)^{1/2})$$

At during $\gamma > \gamma_m$, as was shown above, maximum electric conductivity is possessed by the pure vapors of the admixture, for which

$$\chi_2 = \frac{\sigma_2}{\sigma_{0m}} = \frac{2\beta\sqrt{\beta-1}}{\beta^2+\gamma}$$

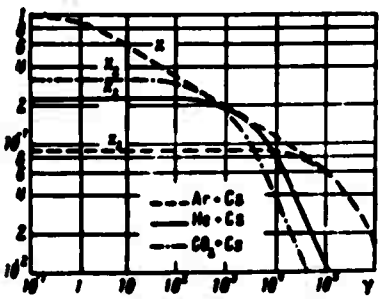

Fig. 3.

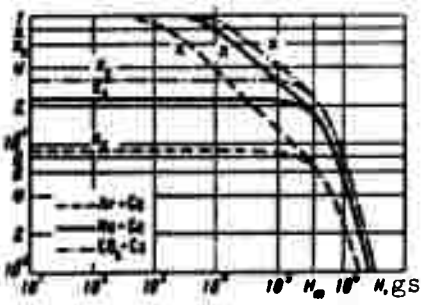

Fig. 4.

Here σ_2 is the conductivity of pure vapors of the admixture. Dependences χ and χ_2 on γ and H for mixtures Cs with Ar, He and CO_2 are presented respectively in Figures 3 and 4 (for Fig. 4, T = 3000°K,

p = 3 atm).

As one should have expected, an anisotropic electric conductivity occurs in mixtures at smaller H values, than in pure cesium. However, at $H < H_m$ the electric conductivity of any considered mixture is higher than electric conductivity of pure cesium.

From approximate formula for γ_m it is evident that

$$H_m = (\beta - 1) Q_{12}(p/e)\sqrt{m/kT}$$

At $\beta \gg 1$, which corresponds to mixtures being considered here, H_m does not depend on nature of diluent

$$H_m \approx Q_{12}(p/e)\sqrt{m/kT}$$

For example, $H_m = 3.45 \cdot 10^5$ gs. in case of admixture of Cs at $T = 3000^\circ K$ and p = 3 atm.

Submitted
5 March 1963

Literature

1. L. Spitzer. Physics of a completely ionized gas. Fizmatgiz, 1957.

2. E. P. Zimin and V. A. Popov. Determination of optimum compositions of gas mixtures in the presence of a readily ionized admixture. PMTF, No. 3, 1962.

CERTAIN METHODS OF INVESTIGATING THE DYNAMIC STRUCTURE OF PLASMA FLOWS

A. M. Trokhan

(Novosibirsk)

Multislot attachment for a photoregister. The basic instrument for measurement of speed of plasma containing optical heterogeneities is at present the photoregister. The chief merits of use of photoregisters together with their high reliability, peculiar to an overwhelming majority of kinematic methods of measurement [1], are: continuity of registration during a certain interval of time, an extermely high time resolving and simplicity of utilized equipment. A defect in the use of phototiming is a possibility of measuring speed of plasma only along one straight line isolated in image of flow by slot of the photoregister. For measurement of field of speeds of plasma usually there are used exposure photographings. However, use of exposure photographings in view of the difficulty of identification of heterogeneities in the photographs is found to be limited, being used mainly for investigating shock waves and fluxes containing sharply nonhomogeneous regions or particles.

The author used a very simple device, making it possible to use photoregister for measurement of the velocity fields of a plasma.

The principle of operation of device is evident from Fig. 1. Close to the plasma flux under investigation containing a certain heterogeneity 1, there is placed a opaque diaphragm 2, having a number of parallel slots located at different height across flow section. The beams of light passing through these slots are scattered by means of a periscope in direction parallel to velocity of flux and emerge through slots in diaphragm 3. As a result of the scanning of image of the outlet slots which are made by usual method we obtain a multichannel phototracing which makes it possible to determine field of speeds of flux in the investigated section and its change during period of scanning.

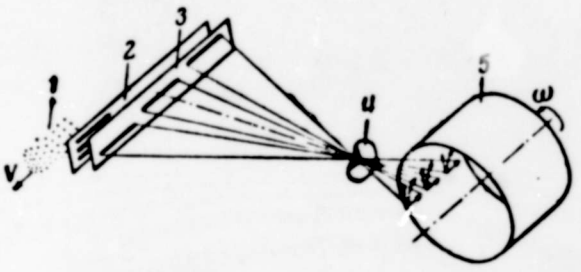

Fig. 1. Diagram of measurements for multislot periscope.

The design of a 5-slot periscope, assembled of mirrors is presented in Fig. 2, and an example of the result, obtained during its use, is shown in Fig. 3. In this phototracing there is fixed the propagation of reflected wave in shock tube.

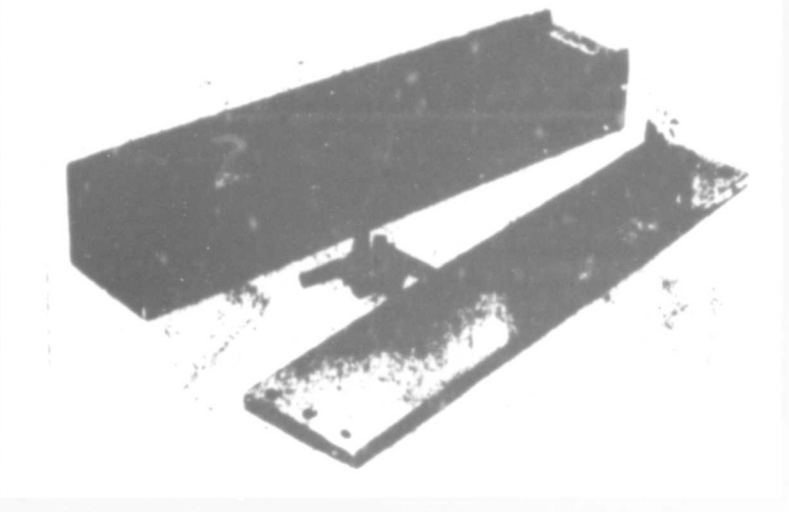

Fig. 2. Five-slot mirror periscope.

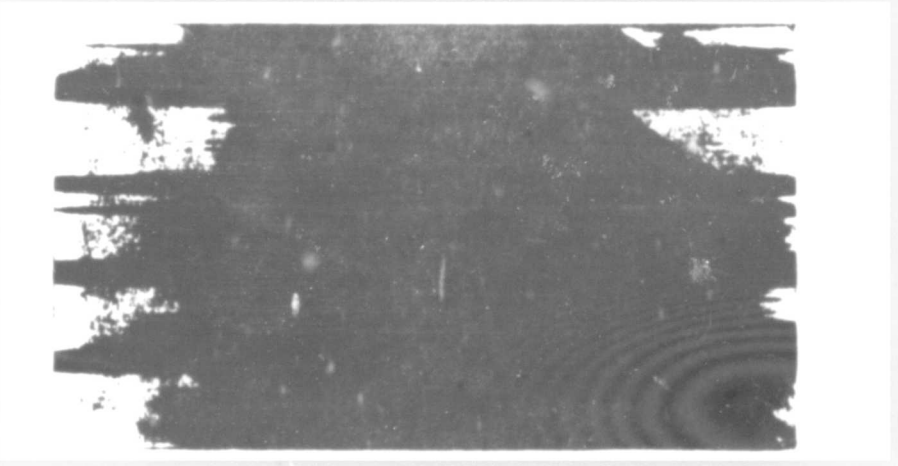

Fig. 3. Five-channel phototracing of propagation of shock wave.

A consequence of presence of the difference of the variation of the beams in periscope is a necessity of sufficient diaphragming of objective for obtaining the required depth of sharpness. For example, maximum difference of the variation of the beams in periscope shown in Fig. 2, amounts to 220 mm. Taking maximum magnitude of the small circle of aberration equal to 0.1 mm, and scale of image equal to 1:10, we find maximum relative aperature of the objective equal to 1:10.

Another consequence of presence of difference of the variation of beams is a certain difference of image scale for recording channels on the phototracing. Most conveniently for determining the scale of images we apply the measurement of the channels of the recording trace. Width of the channel is equal length of corresponding inlet slot in scale of image, and true dimensions of slots are known, therefore, the determination of scale with sufficient accuracy presents no difficulty.

The photoelectric registration of time of passage of optical heterogeneities. Use of photoregister, especially the multislot, makes it possible to obtain very extensive information about dynamic structure of the investigated fluxes. However, it not always is

found to be convenient to obtain results in the form of photograph. Thus, for example, if there is required statistical treatment of results of measurement in time, the use of photographic recording results in very great time-consuming work. Furthermore, photographic recording is difficult, if the luminosity of the flux is weak. In such cases a photoelectric recording is more convenient.

At present photoelectric recording is fairly widely used for investigating shock processes.

In present work the registration of time of the transit of optical heterogeneities by means of photomultipliers was used for measuring speed of a gas flow in plasmatron of alternating current. There was used the following measuring scheme. At a certain distance along flux near investigated region of flux there were placed two photomultipliers with corresponding diaphragming devices, separating narrow beams of light. The passage of heterogeneities (peaks of brightness) past the first of multipliers caused the starting of driven sweep of oscillograph, and the signals in second multiplier caused vertical deflection of the beam. Measurement of time between moment of starting of sweep and passage of heterogeneity which had caused the starting past second multiplier, makes it possible to determine the speed of plasma average on a given basis. In the given measuring scheme there is possible both a single registration and also one averaged by time. In Fig. 4 there is presented the result of measurement obtained by means of superposing of oscillograms for approximately two hundred transits of

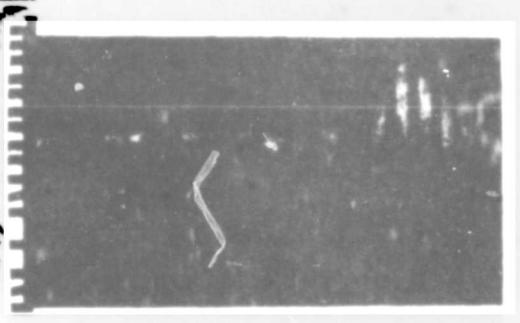

Fig. 4. Typical result of recording during photoelectric registration of times of transit.

heterogeneities. By regulating the time of exposure of screen of oscillograph, there can be obtained in any manner a large time-averaging of the results, and by using the photographing of screen on a continuously moving film, it is possible to fix the variation of speed of flux in time.

Coincidence circuit. The most general method of obtaining statistical characteristics of the flux is the differential analysis of probability of times of transits of optical heterogeneities. The diagram of an installation for such an analysis is is given in Fig. 5.

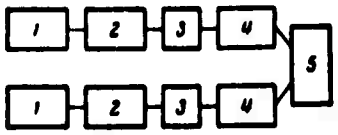

Fig. 5. Diagram of measurements by method of coincidences.

Signals from two investigated points of the flux proceed to photomultipliers 1, and then to the cathode repeaters 2 and divisors 3. The divisors are used so that even with a significant difference in level of signal from investigated points of flux at the output we obtain signals of approximately identical amplitude. Signals of both channels are delivered to identical delay lines 4, and then to coincidence counter 5.

Principle of measurement consists in the following: optical heterogeneities (for example, brighter regions or particle), passing through investigated points, cause a corresponding series of pulses. If the manifestation of pulses in first and second channels is independent and bears a random character, then the circuit will record only random coincidences. The average number of randon coincidences, recorded in unit of time is equal to

$$N = 2\tau n_1 n_2 \qquad (1)$$

Here N is the number of recorded random coincidences, n_1, n_2 is

the average number of pulses per unit of time in the channels, τ is the resolving time of coincidence counter.

Let us assume that investigated flow of gas is directed along x-axis. We shall consider elementary areas normal to the flux, located at points 1 and 2, displaced one with respect to the other by certain distance L along x-axis. Let us assume also that the number of pulses being recorded by the first and second channels per unit of time is equal to the number of heterogeneities passing through the corresponding elementary areas.

The number of particles which have passed through first area and which are passing after this through second area per unit of time may be determined as follows:

$$N_{12} = n_1 \int_{F_2} p(y,z)\, dF \qquad (2)$$

Here n_1 is the number of heterogeneities passing through first area per unit of time; $p(y, z)$ is the probability frequency of passage of heterogeneities which have passed through first area and are passing through points of plane of second area; F_2 is the area of second area.

If the heterogeneities which have passed through first area pass also through the second, then between the pulses being caused by their passage in first and second channels, there occurs a time shift equal to time of the transit.

Thus, if at least part of heterogeneities which has passed through first area, passes also through the second then during delay of pulses of first channel by a magnitude of the transit time there will take place coincidences caused by the passage of the same heterogeneity.

Number of coincidences per unit of time during the delay t in

first channel is equal to

$$(N_{12})_t = N_{12} \int_{t-\tau}^{t+\tau} p_2(t)\,dt \qquad (3)$$

Here τ is the resolving time of coincidence counter, p(t) is the probability frequency of time of transit of base L along the x-axis.

System N_{12} - N is consistent, i.e., at the same moment of time through second area there may pass both the "true" heterogeneity (i.e., which has passed preliminarily through first area), so also the random, and at the same time they will be recorded as one, therefore, the total number of coincidences in system at a given magnitude of delay in first channel will be equal to

$$N_t = N + (N_{12})_t - N_t \qquad (4)$$

Here N_t is the number of random coincidences occurring simultaneously with the ture.

Assuming the probabilities of the manifestation of signal and noise independent, we find

$$N_t = 2n_1n_2\tau \int_{S_1} p(y, z)\,dF \int_{t-\tau}^{t+\tau} p_2(t)\,dt$$

Using (1)-(4), we shall find the signal to noise ratio, i.e., the ratio of total number of coincidences during a given time of delay in first channel to the number of random coincidences

$$\frac{N_t}{N} = 1 + \frac{1 - 2n_2\tau}{2n_2\tau} \int_{S_1} p(y, z)\,dF \int_{t-\tau}^{t+\tau} p_2(t)\,dt \qquad (5)$$

Having assumed for simplicity $n_1 = n_2 = n$ and taking into consideration the position of the areas and flux regimes as constant, it is possible to write

$$\frac{N_t}{N} = 1 + \cos\varphi \frac{1 - 2n\tau}{2n\tau} \qquad (6)$$

From (6) it is evident that if magnitude $n\tau$ is fairly small, the signal-to-noise ratio may be as large as desired. On the other hand, if magnitude $n\tau$ approaches 0.5, the signal-to-noise ratio approaches 1, i.e., signal is indistinguishable from the noise. This also is understood. At $n\tau = 0.5$ within any interval of time 2τ, solvable by a counter, is found to be, on an average, according to the pulse and counter must count continuously independently of the fact whether the signal is true or not.

Regulating by the divisors 3 (Fig. 5) the levels of signals, proceeding through the channels, it is possible to attain that which system will consider only the sharpest expressed heterogeneities, and thus magnitude n will be found to be fairly small. Resolving time of counters amounts to usually $\tau = 10^{-6}$ to 10^{-8} sec; thus, n may be fairly large.

It must be noted that the discussion above is valid for statistical distribution of the heterogeneities. If in distribution of the heterogeneities there are any periodicities, then for obtaining of unique solutions by indicated method it is necessary that linear scale of these periodicities is larter than the base of measurement being utilized. This requirement is equivalent to requirement of absence of corresponding harmonics in the results of measurements.

By varying the position of second area relative to the first and measuring dependence of frequency of count from time of delay, there can be found differential function of probability of transit of heterogeneities; this fully determines the statistical position of vector of speed of flux at the first point. This method is convenient for study of characteristics of turbulence and may be applied for investigating both the plasma and also a cold gas. The heterogeneities being utilized for measurements can have the most diverse

nature (hotter clusters of plasma, drops of burning fuel, artificially introduced solid or liquid particles etc.). Furthermore, given method may be used for study of structure of the flux. Thus, in Fig. 6 there are given results of measurements of time of transit of heterogeneities on a base of 12 mm in a complex flow including relatively large particles. As can be seen from Fig. 6, time of transit in this case has a large dispersion and is grouped near two values t = 14 and 31 microseconds. The first corresponds to particles, moving with an average speed of 850 m/sec and the second to a motion of purely gas heterogeneities with a speed of 390 m/sec.

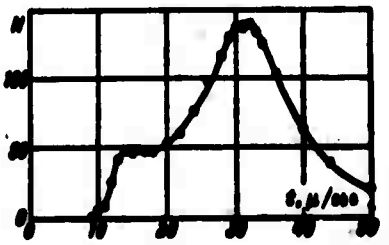

Fig. 6. Result of measurements of transit times by means of the method of coincidences.

In these measurements there was used photoelectric transducer, assembled in multipliers of type FEU-29.

For selecting the base of measurement there was used the optical system. There were used delay lines and a counter from installation for registration of coincidences and anticoincidences – SSA.

Submitted
27 November 1962

Literature

1. A. M. Trokhan. Measurement of the speed of gas flows by kinematic methods. PMTF, 1962, No. 2, p. 112-121.